10th Human Amyloid Imaging

January 13-15, 2016
Miami, Florida

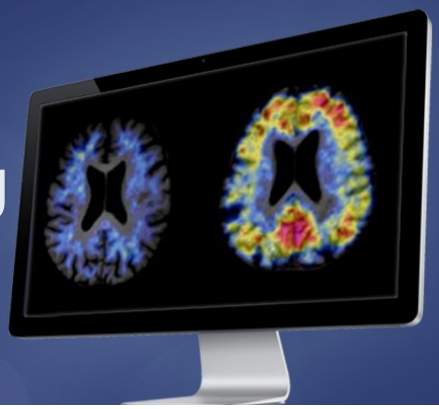

Co-Organizers:
Keith A. Johnson, MD ● William J. Jagust, MD ● William E. Klunk, MD, PhD ● Chester A. Mathis, PhD

Conference Program and Abstracts

www.worldeventsforum.com/hai

TABLE OF CONTENTS

PRESENTER INDEX

S# = Session # (S1-S2 Wed, S3-6 Thu, S7-10 Fri)
PP# = Podium Presentation
KL# = Keynote Lecture (1 Thursday, 2 Friday)
PE# = Poster Session Even-Numbered (Thu)
PO# = Poster Session Odd-Numbered (Fri)

HAI2016 PROGRAM

Podium presentations will be held in the Grande Promenade Ballroom at the Miami Beach Resort; the overflow room will be set up in the Spanish Suite (mezzanine); the poster sessions will be held in the Regency Ballroom.

Wednesday, January 13, 2016

11:30 am	Check-in	
1:00	Welcome Notes	Keith Johnson, Massachusetts General Hospital
1:15-2:30	SESSION 1: NEW PET LIGANDS; CENTILOIDS; KINETIC STUDIES	CHAIRS: Robert Koeppe, University of Michigan Chester Mathis, University of Pittsburgh
1:15-1:30	Quantification, test-retest and dosimetry of the novel Genentech Tau Probe 1, [18F]GTP1	**Sandra Sanabria Bohorquez**, Genentech Research and Early Development, Genentech
1:30-1:45	Clinical evaluation of [18F]RO6958948, a new radioligand for imaging tau pathology in AD	**Dean Wong**, Johns Hopkins University
1:45-2:00	Implementation and validation of the Centiloid transformation for 18F-NAV4694	**Christopher Rowe**, The University of Melbourne
2:00-2:15	Quantification of the tau PET tracer [18F]AV-1451 with kinetic modeling	**Olivier Barret**, Molecular NeuroImaging LLC
2:15-2:30	Comparing tau measurements, within tracers and between	**Suzanne Baker**, Lawrence Berkeley National Lab
2:30-3:10	Discussion	
3:10-3:40	Coffee break *(Regency Ballroom)*	
3:40-4:40	SESSION 2: PET DATA ANALYTICS: TIME SERIES, DATA REDUCTION, AND THK5351	CHAIRS: Suzanne Baker, Lawrence Berkeley National Lab Julie Price, University of Pittsburgh
3:40-3:55	Longitudinal changes in [18F]AV-1451 PET tau signal: Interim analysis of a Phase 2 study	**Mark Mintun**, Avid Radiopharmaceuticals, Inc.
3:55-4:10	Optimizing Florbetapir SUVR change-over-time measurement	**Christopher Schwarz**, Mayo Clinic and Foundation
4:10-4:25	Principal component analysis of [18F]-AV-1451 Tau PET in sporadic AD and frontotemporal dementia	**Shruti Mishra**, Washington University School of Medicine
4:25-4:40	Distinct patterns of [18F]THK-5351 retention in AD and non-AD tauopathies	**Nobuyuki Okamura**, Tohoku University
4:40-5:20	Discussion	
5:20-7:30	Welcome Reception *(Poolside/Oceanview)*	

Thursday, January 14, 2016

7:00am-8:00	Check-in and Breakfast *(Starlight Ballroom)*	
8:00-9:00	SESSION 3: PATHOLOGY	CHAIRS: William Klunk, University of Pittsburgh Melissa Murray, Mayo Clinic, Jacksonville
8:00-8:15	Differences between lateral and medial PET image intensity for equivalent levels of Aβ pathology	**Chris Buckley**, GE Healthcare Life Sciences
8:15-8:30	Centiloid thresholds for amyloid positivity derived from autopsy-proven cases	**Nagehan Ayakta**, University of California, San Francisco
8:30-8:45	In vitro binding and histology analyses of a putative tau ligand T807 in AD and non-AD tauopathy cases	**Milos Ikonomovic**, University of Pittsburgh
8:45-9:00	Neuropathologic maturity of neurofibrillary tangles: implications for Tau PET Imaging	**Melissa Murray**, Mayo Clinic, Jacksonville
9:00-9:40	Discussion	
9:40-10:25	Poster Session (Even-Numbered)/Coffee Break	
10:25-11:25	SESSION 4: NON-AD TAUOPATHIES	CHAIRS: Agneta Nordberg, Karolinska Institutet

		Gil Rabinovici, University of California, San Francisco
10:25-10:40	18F-AV-1451 binding corresponds to disease severity and laterality in non-AD tauopathy syndromes with distinct tau filament strains	**Richard Tsai**, University of California, San Francisco
10:40-10:55	Elevated [18F]AV-1451 binding matches the distribution of Tau pathology in Progressive Supranuclear Palsy	**Daniel Schonhaut**, University of California, San Francisco
10:55-11:10	Binding characteristics of Tau PET tracer [18F]AV-1451	**Giorgio Attardo**, Avid Radiopharmaceuticals Inc.
11:10-11:25	In vivo [F-18]-AV-1451 (T807) PET imaging in the first two autopsy-confirmed non-Alzheimer tauopathy cases studied at MGH	**Marta Marquie**, MassGeneral Institute for Neurodegenerative Disease
11:25-12:05pm	Discussion	
12:05-1:30	Lunch *(Starlight Ballroom)*	
1:30-2:30	SESSION 5: ANATOMIC CORRELATIONS	CHAIRS: Clifford Jack, Jr., Mayo Clinic, Rochester Susan Resnick, National Institutes of Health, National Institute on Aging
1:30-1:45	PET tau imaging with AV-1451 in FTD with suspected underlying tauopathies and non-tauopathies relative to Alzheimer's and controls	**David Jones**, Mayo Clinic, Rochester
1:45-2:00	Specific hippocampal subfield volumes mediate tau-related memory performance in amyloid positive individuals	**Heidi Jacobs**, Massachusetts General Hospital/Harvard Medical School
2:00-2:15	Association between T807 and retrospective cortical thinning in cognitively normal elderly	**Molly LaPoint**, Massachusetts General Hospital/Harvard Medical School
2:15-2:30	Identifying cortical areas of change in longitudinal 18F-T807 PET	**J. Alex Becker**, Massachusetts General Hospital/Harvard Medical School
2:30-3:10	Discussion	
3:10-3:55	Poster Session (Even-Numbered)/Coffee Break	
3:55-4:25	**Keynote Lecture:** New CSF and plasma biomarkers for neurodegenerative diseases	**Henrik Zetterberg**, University of Gothenburg
4:25-4:40	Keynote Discussion	
4:40-5:25	SESSION 6: TAU PET: CLINICAL AND COGNITIVE CORRELATIONS	CHAIRS: William Jagust, University of California, Berkeley Reisa Sperling, Massachusetts General Hospital/Harvard Medical School
4:40-4:55	Aβ+ clinically normal participants with elevated Tau show greatest decline in the preclinical AD cognitive composite	**Elizabeth Mormino**, Massachusetts General Hospital, Harvard Medical School
4:55-5:10	Association between in vivo tau deposition and concomitant cognition mediated by metabolic dysfunction in AD	**Laure Saint-Aubert**, Karolinska Institutet
5:10-5:25	Tau-PET imaging with AV-1451 in Alzheimer's disease	**Val Lowe**, Mayo Clinic, Rochester
5:25-5:55	Discussion	
6:00-8:00	Networking Reception *(Starlight Ballroom)*	
Friday, January 15, 2016		
7:00-8:00am	Check-in and Breakfast *(Starlight Ballroom)*	
8:00-8:45	SESSION 7: TAU PET: CONNECTIVITY AND PS1	CHAIRS: Tammie Benzinger, Washington University Trey Hedden, Massachusetts General Hospital
8:00-8:15	Tau covariance patterns in AD patients resemble intrinsic connectivity networks in young adults	**Rik Ossenkoppele**, University of California, San Francisco

8:15-8:30	Amyloid, Tau, and functional connectivity MRI	**Aaron Schultz**, Massachusetts General Hospital/Harvard Medical School
8:30-8:45	Patterns of Tau deposition using [18F]-AV-1451 in autosomal dominant Alzheimer's disease: Results from the DIAN	**Tammie Benzinger**, Washington University in St. Louis
8:45-9:15	Discussion	
9:15-10:00	Poster Session (Odd-Numbered)/Coffee Break	
10:00-11:00	SESSION 8: TAU AND AMYLOID BIOMARKER CORRELATIONS	CHAIRS: Charles Duyckaerts, Hôpital La Pitié Salpêtrière Victor Villemagne, The University of Melbourne
10:00-10:15	The Tau MeTeR scale for the generation of continuous and categorical measures of tau deposits in the brain: Results from 18F-AV1451 and 18F-THK5351 tau imaging studies	**Victor Villemagne**, The University of Melbourne
10:15-10:30	Amyloid and tau demonstrate region-specific associations in normal older people	**Samuel Lockhart**, University of California, Berkeley
10:30-10:45	Relating cerebrospinal fluid and positron emission tomography measures of tau pathology	**Brian Gordon**, Washington University in St. Louis
10:45-11:00	Metabolic efficiency predicts the spatial pattern of Amyloid-β in late life	**Katelyn Arnemann**, University of California, Berkeley
11:00-11:40	Discussion	
11:40-12:10pm	**Keynote Lecture:** Synergy of Aβ and tau pathologies, neuropathological data	**Charles Duyckaerts**, Hôpital La Pitié Salpêtrière
12:10-12:25	Keynote Discussion	
12:25-1:50	Lunch *(Starlight Ballroom)*	
1:50-2:50	SESSION 9: TRANSLATION TO CLINICAL POPULATIONS AND GENETIC FACTORS	CHAIRS: Christopher Rowe, The University of Melbourne Andrew Saykin, Indiana University
1:50-2:05	Appraisal of the utility of the AIT appropriate use criteria of the Amyloid-PET	**Marina Boccardi**, IRCCS Centro San Giovanni di Dio Fatebenefratelli
2:05-2:20	[11C]PiB imaging in the Down syndrome population: A closer investigation of amyloid burden in the striatum	**Patrick Lao**, University of Wisconsin-Madison
2:20-2:35	APOE epsilon 2 genotype associates with reduced amyloid load but does not affect brain structure or function in non-demented older individuals	**Michel Grothe**, German Center for Neurodegenerative Diseases
2:35-2:50	Association between [11C]PIB PET and CSF Aβ1-42 in a multicentre European memory clinic population	**Antoine Leuzy**, Karolinska Institutet
2:50-3:30	Discussion	
3:30-4:15	Poster Session (Odd-Numbered)/Coffee Break	
4:15-4:25	Awards Ceremony	
4:25-5:10	SESSION 10: MULTIPLE MOLECULAR IMAGING BIOMARKERS	CHAIRS: Gaël Chételat, INSERM, Université de Caen Susan Landau, University of California, Berkeley
4:25-4:40	Rates of transition between amyloid and neurodegeneration biomarker states and to dementia among non-demented individuals in a longitudinal population-based cohort study	**Clifford Jack**, Jr., Mayo Clinic, Rochester
4:40-4:55	Do midlife vascular risk factors contribute to brain amyloid? The ARIC-PET Amyloid Imaging Study	**Rebecca Gottesman**, Johns Hopkins University
4:55-5:10	The clinical significance of increasing amyloid in cognitively normal, amyloid negative individuals	**Susan Landau**, University of California, Berkeley
5:10-5:40	Discussion	
5:40-6:00	Closing Notes	

Wednesday, January 13, 2016 – 1:15pm-2:30

Podium Presentations
SESSION 1: New Pet Ligands; Centiloids; Kinetic Studies

CHAIRS: ***Robert Koeppe, University of Michigan***
Chester Mathis, University of Pittsburgh

1:15-2:30	**SESSION 1: NEW PET LIGANDS; CENTILOIDS; KINETIC STUDIES**	**CHAIRS: Robert Koeppe** University of Michigan **Chester Mathis** University of Pittsburgh
1:15-1:30	Quantification, test-retest and dosimetry of the novel Genentech Tau Probe 1, [18F]GTP1	**Sandra Sanabria Bohorquez** Genentech Research and Early Development, Genentech, Inc.
1:30-1:45	Clinical evaluation of [18F]RO6958948, a new radioligand for imaging tau pathology in AD	**Dean Wong** Johns Hopkins University
1:45-2:00	Implementation and validation of the Centiloid transformation for 18F-NAV4694	**Christopher Rowe** The University of Melbourne
2:00-2:15	Quantification of the tau PET tracer [18F]AV-1451 with kinetic modeling	**Olivier Barret** Molecular NeuroImaging, LLC
2:15-2:30	Comparing tau measurements within tracers and between	**Suzanne Baker** Lawrence Berkeley National Lab
2:30-3:10	Discussion	

Quantification, test-retest and dosimetry of the novel Genentech Tau Probe 1, [18F]GTP1

Sandra Sanabria Bohorquez[1], Olivier Barret[2], Gilles Tamagnan[2], David Alagille[2], Simon Williams[1], Alex de Crespigny[1], Gai Ayalon[1], Geoffrey Kerchner[1], William Cho[1], Danna Jennings[2], John Seibyl[2], Ken Marek[2], Robby Weimer[1], Jan Marik[1]

[1]gRED, Genentech Research and Early Development, Genentech, Inc., South San Francisco, CA, United States
[2]Molecular NeuroImaging LLC, New Haven, CT, United States

PET imaging utilizing radiotracers specific for tau pathology could enable cross-sectional and longitudinal assessment of tau pathology. Here, we present the preliminary [^{18}F]GTP1 characterization and dosimetry.

Test-retest: [^{18}F]GTP1 imaging was performed in 3 AD subjects (65-77y, MMSE 26-27) and 2 healthy volunteers (HV; 51-58y). Dynamic scans were acquired and the arterial input function (AIF) was measured. Compartmental modeling and Logan graphical analyses were applied to calculate the total volume of distribution. The distribution volume ratio (DVR) was calculated using cerebellum gray (CBL) as reference: $DVR_{AIF}=V_T(\text{target-ROI})/V_T(\text{CBL})$. SRTM was also applied; $DVR_{SRTM}=BP_{ND}+1$. The use of SUVR as a surrogate for GTP1 specific binding was evaluated.

Dosimetry: Whole body (WB) images were acquired over ~6h in 5 HV (ages 18-53y). The individual absorbed doses and the effective dose (ED) were calculated using OLINDA.

Results: AIF modeling showed that the 1-tissue model is sufficient to describe the cerebellum gray (CBL) tracer kinetics. DVR_{AIF} and DVR_{SRTM} were highly correlated suggesting tracer kinetics is well described using the CBL curve. %T-RT [100% (day2-day1)/(day1+day2)/2] variability for DVR_{SRTM} and SUVR was ±10%. A linear relationship between DVR_{SRTM}(120min) vs. SUVR(90-120min) and DVR_{SRTM}(120min) vs. SUVR(60-90min) shows SUVRs in both time intervals are appropriate surrogates of GTP1 specific binding to tau.

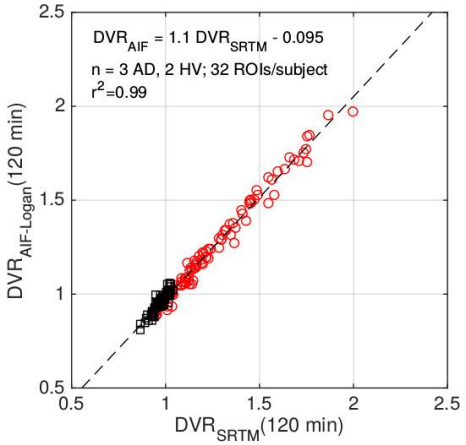

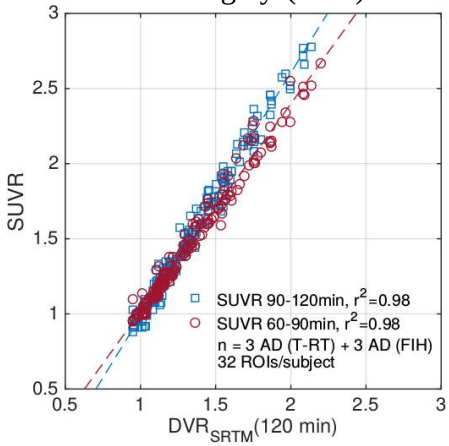

The average ED per 185MBq were 6.4 mSv (F, n=3) and 4.9mSv (M, n=3) with no UB voiding and 6.0mSv (F, n=3) and 4.6mSv (M, n=3) with 2h UB voiding interval.

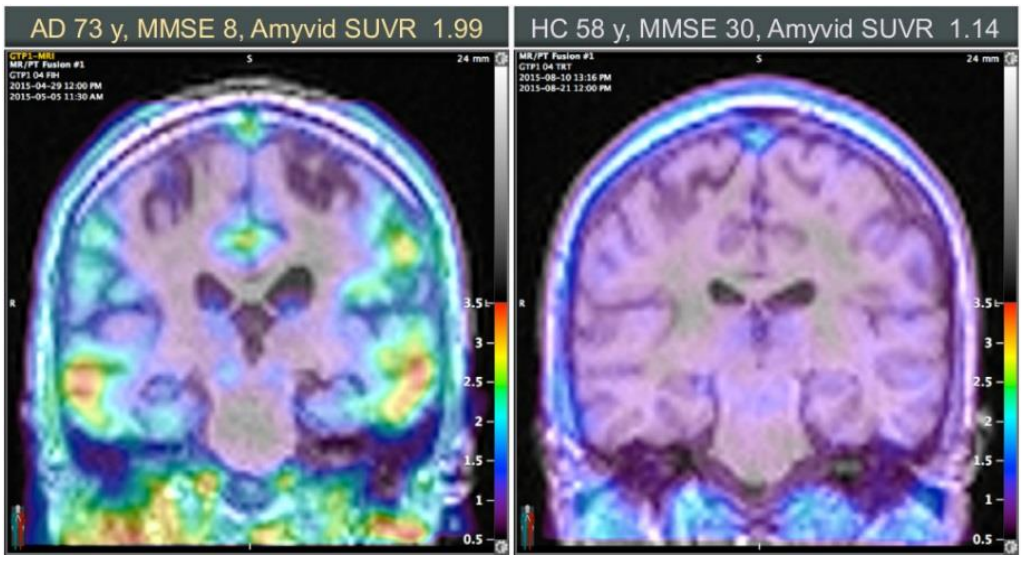

GTP1 has favorable radiation dosimetry profile, displays excellent kinetics that allows SUVR estimates of target binding and provides a large dynamic range between regions of low and high tau accumulation and between HV and AD. We are currently conducting an 18-month natural history study in AD to assess the performance of GTP1 in reporting longitudinal change of tau pathology.

Clinical evaluation of [18F]RO6958948, a new radioligand for imaging tau pathology in AD

Dean Wong[1, 2, 3], Robert Comley[4], Hiroto Kuwabara[1], Noble George[1], Paul Rosenberg[2], Constantine Lyketsos[2], Madhav Thambisetty[5], Henner Knust[4], Michael Honer[4], Frank Boess[4], Susanne Ostrowitzki[4], Robert Dannals[1], Edilio Borroni[4]

[1]Russell H. Morgan Department of Radiology, Nuclear Medicine – PET Center, The Johns Hopkins University School of Medicine, Maryland, United States
[2]Department of Psychiatry and Behavioral Sciences, The Johns Hopkins University School of Medicine, Maryland, United States
[3]Solomon H. Snyder Department of Neuroscience, The Johns Hopkins University School of Medicine, Maryland, United States
[4]Roche Pharmaceutical Research and Early Development, Roche Innovation Center, Basel, Switzerland
[5]National Institute of Aging, Maryland, United States

Background: We provide an update on the evaluation of [18F]RO6958948, a new radioligand for imaging tau pathology in AD.

Methods: Five Aβ+ AD patients (3M: 2F; 67-86y; MMSE: 18-24) and 5 young controls (YC) (4M: 1F; 25-38y) received a [18F]RO6958948 scan to evaluate tracer kinetics. Five additional Aβ+ AD patients (4M: 1F; 55-66y; MMSE: 16-25) and 5 Aβ- older controls (OC) (5M: 0F; 51-73y) received two scans (approximately 6 weeks apart) to assess reproducibility. A third group of 6 controls (3M:3F) had whole-body scans for dosimetry. After bolus injection of [18F]RO6958948 dynamic emission data were collected (for the first group from 0-90 min and out to 200 min in the reproducibility cohort). Arterial blood sampling was performed in 12/15 AD and 11/15 controls. ROIs were defined by MRI, and PET data were quantified by kinetic analysis.

Results: In controls washout was fast, with very little retention. Metabolism was rapid: 10% parent in plasma at 60 min. There was no evidence of brain penetrant radiometabolites. In AD tracer distribution was broadly consistent with post-mortem literature, cortical SUV (60-90 min) is ~ 2, white matter retention was low, and off-target binding minimal. SUVR values (60-90 min using Cb grey reference) showed a strong correlation with VT, R2 =0 .92 The dynamic range for the detection of tau pathology is approximately 1 - 3 (cortical SUVR in OC vs. AD). Test-retest variability for SUVR 60-90 min (Cb grey) across a range of ROIs was 1.8-8.9 %. Preliminary whole body dosimetry suggests at least 3- 4 PET scans could be performed annually based on local radiation guidelines.

Conclusion: [18F]RO6958948 is a promising tracer that can be used to assess the degree of tau pathology in the AD brain.

Implementation and validation of the Centiloid transformation for ^{18}F-NAV4694

Christopher C. Rowe[1, 2], Gareth Jones[1], Svetlana Pejoska[1], Vincent Doré[3, 4], Laura Margison[1], Rachel Mulligan[1], Pierrick Bourgeat[4], J. Gordon Chan[1], Olivier Salvado[4], Colin L. Masters[3], Victor L. Villemagne[1, 2, 3]

[1]*Department of Molecular Imaging & Therapy & Centre for PET, Melbourne, Australia*
[2]*Department of Medicine, The University of Melbourne, Australia*
[3]*The Florey Institute of Neuroscience and Mental Health, The University of Melbourne, Australia*
[4]*CSIRO Digital Productivity Flagship, The Australian e-Health Research Centre, Brisbane, Australia*

Background: A common quantitative output value for Aβ imaging across tracers and methods will improve clinical and research use. A method has recently been developed by an international team of Aβ imaging experts for this purpose that produces a unit of measurement called the Centiloid (Klunk et al, Alzheimers Dement, 2015). This approach was implemented on Aβ imaging studies performed with ^{18}F-NAV4694 (NAV) and ^{11}C-PiB (PiB).

Methods: Fifty-five participants underwent PET imaging between 50-70 min after injection of PiB and NAV: 10 healthy young controls (33±7 yo), 25 healthy elderly controls (74±8 yo, MMSE 29±1), 10 mild cognitive impairment (75±9 yo, MMSE 27±3), 3 frontotemporal dementia (68±5 yo, MMSE 27±1), and 7 Alzheimer's disease (73±11 yo, MMSE 24±2) patients. Spatially normalized images were analyzed using the standard Centiloid regions (cortex and whole cerebellum reference region) downloaded from the Global Alzheimer's Association Interactive Network website (GAAIN; http://www.gaain.org). The non-standard reference regions, cerebellar cortex, pons, and whole cerebellum+pons were also investigated.

Results: Both radiotracers presented an almost identical dynamic range of neocortical SUVR (linear slopes=1.09±0.01) and Centiloid values, the latter ranging from -30 to 130 Centiloids. Both tracers were highly correlated (R2>0.97), irrespective of the reference region used for the scaling. We further validated the Centiloid transformation by comparing the results from the standard approach and our own imaging analysis software, while using the same cortical and whole cerebellum masks from GAAIN. Our software yielded results that differed by 1-2% from the standard SPM approach. A correction was implemented to adjust for this small discrepancy.

Conclusions: Both ^{11}C-PiB and ^{18}F-NAV4694 results can now be calculated in the common language of Centiloids by centers across the world using the data supplied through the GAAIN website. This is an important step towards better use of the clinical and research potential of Aβ imaging.

Quantification of the tau PET tracer [18F]AV-1451 with kinetic modeling

Olivier Barret[1], David Alagille[1], Sandra Sanabria[2], Robert Comley[3], Robby Weimer[2], Edilio Borroni[3], Nicholas Seneca[4], Abhinay D. Joshi[5], Michael D. Devous[5], Mark A. Mintun[5], Danna Jennings[1], Ken Marek[1], John P. Seibyl[1], Gilles D. Tamagnan[1]

[1]*Molecular NeuroImaging, LLC, New Haven, CT, United States*
[2]*Genentech Research and Early Development, Genentech, Inc., South San Francisco, CA, United States*
[3]*Pharma Research and Early Development, F. Hoffmann-La Roche, Konzern-Hauptsitz, Basel, Switzerland*
[4]*Product Development, F. Hoffmann-La Roche, Konzern-Hauptsitz, Basel, Switzerland*
[5]*Avid Radiopharmaceuticals, Inc., Philadelphia, PA, United States*

Background: The study objective was to perform kinetic analysis of [18F] AV-1451 with arterial input function, and compare SUVr at different time intervals to the more quantitative Binding Potential (BPND).

Methods: 16 subjects (4 young healthy controls (YHC) (26-37y), 4 aged HC (OHC; 52-73y) and 8 Alzheimer's Disease subjects (AD) (57-85y)) were administered 9.0 ± 0.7 mCi [18F] AV-1451 and imaged for 3.5 hours (0-50, 80-130 and 160-210 min). [18F] AV-1451 data were analyzed using plasma and reference-tissue-based methods to estimate distribution volume VT and binding potential BPND. SUVr and BPND were derived using cerebellar cortex as the reference region. SUVr curves were calculated over 210 min and compared at various times (80-100, 110-130, 160-180 and 190-210 min) to BPND. BPND and SUVr were also compared between groups.

Results: BPND dropped by ~15% on truncation of acquisition time from 210 to 130 min. VT (130 min) ranged from 5.5±1.1 (across all subjects) to up to ~20 mL/cm3 in cortical regions of AD subjects. Good correlation (R2>0.93) was found between BPND (130 min or 210 min) and SUVr-1 from all time intervals, but best agreement occurred between BPND (130 min) and SUVr-1 (110-130 min), and between BPND (210 min) and SUVr-1 (160-180 min). Cortical SUVr curves reached a relative plateau around 1.0-1.2 for YCH and OHC, but increased for AD subjects by up to ~15%, ~30% and ~40% at 110-130 min, 160-180min and 190-210 min relative to 80-100min, respectively.

Conclusions: The 80-100 min interval provides SUVr in good correlation with BPND (130 min) in AD subjects despite the increasing curves, although later time intervals gave better agreement. Linearity should be confirmed in more subjects. Likely influence of disease progression and treatment on tracer kinetics and SUVr should be considered in studies designed to detect tau load changes.

Comparing tau measurements within tracers and between

Suzanne Baker[1], Mark He[2], Sam Lockhart[2], Gil Rabinovici[3], Nobuyuki Okamura[4], William Jagust[1, 2]

[1]*Lawrence Berkeley National Lab, CA, United States*
[2]*Helen Wills Neuroscience Institute, UC Berkeley, CA, United States*
[3]*Memory and Aging Center, UC San Francisco, CA, United States*
[4]*Tohoku University School of Medicine, Miyagi Prefecture, Japan*

Objectives: We explored the optimal quantification method within and between tau PET tracers.

Methods: 38 subjects (23 older healthy controls (HCs), 15 ADs) were scanned using AV1451 on a Biograph PET/CT 0-100 minutes post-injection and 120-150 minutes. Different subjects (10 ADs, 6 HCs) were scanned using THK5351 on an Eminence Stargate PET scanner from 0-90 min post-injection (shorter for 4 ADs). MRIs were segmented using Freesurfer; ROIs for analysis were hippocampus, anterior and posterior cingulate, brainstem, caudate, pallidum, thalamus, putamen, frontal, parietal, occipital, temporal, and entorhinal cortices (reference region=cerebellar gray). SRTM2 BP_{ND} was calculated as the standard for comparison; median k'_2 from SRTM2 was used for DVR quantification. DVRs and SUVRs were calculated for various start times with 20-30 minute durations.

Results: Figure 1 shows correlations between BP_{ND} and DVR and SUVR measurements.

In figure 2, imaging intervals that resulted in the highest r^2 between SUVR and BP_{ND} were plotted. Linear and non-linear fits were tested, the fit with lowest SSE was used; this relationship was non-linear for AV1451 and linear for THK5351. The SUVR dynamic range was wider for AV1451 (0.47–3.47) than for THK5351 (0.98-3.49). By dividing the SUVR range into 0.2 intervals (blue lines) and calculating corresponding BP_{ND} (green lines) it is clear that the nonlinear relationships result in unequally spaced BP_{ND} values for AV1451 compared to equally spaced BP_{ND} values for THK5351. The nonlinear relationship between SUVR and BP_{ND} means that differences in AV1451 SUVRs reflect small changes in BP_{ND} at the low end of the scale but larger changes in BP_{ND} at the high end.

Conclusion: SUVRs for AV1451 provide better estimates of BP_{ND} at low levels of tracer binding than at high levels. SUVRs for THK5351 are linear throughout the range of binding with respect to BP_{ND}.

Figure 1: Correlation of SRTM2 BP_{ND} with DVR and SUVR (AV1451 & THK5351)

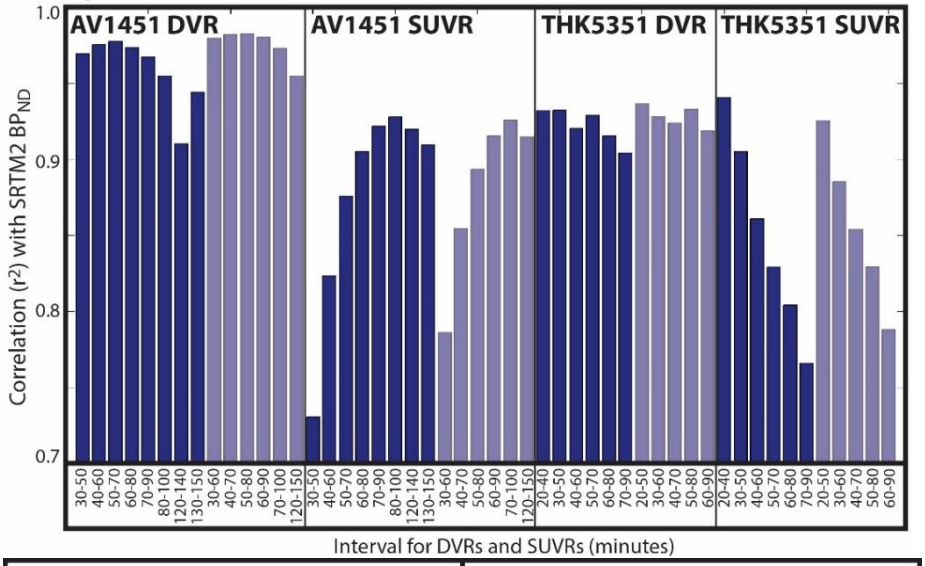

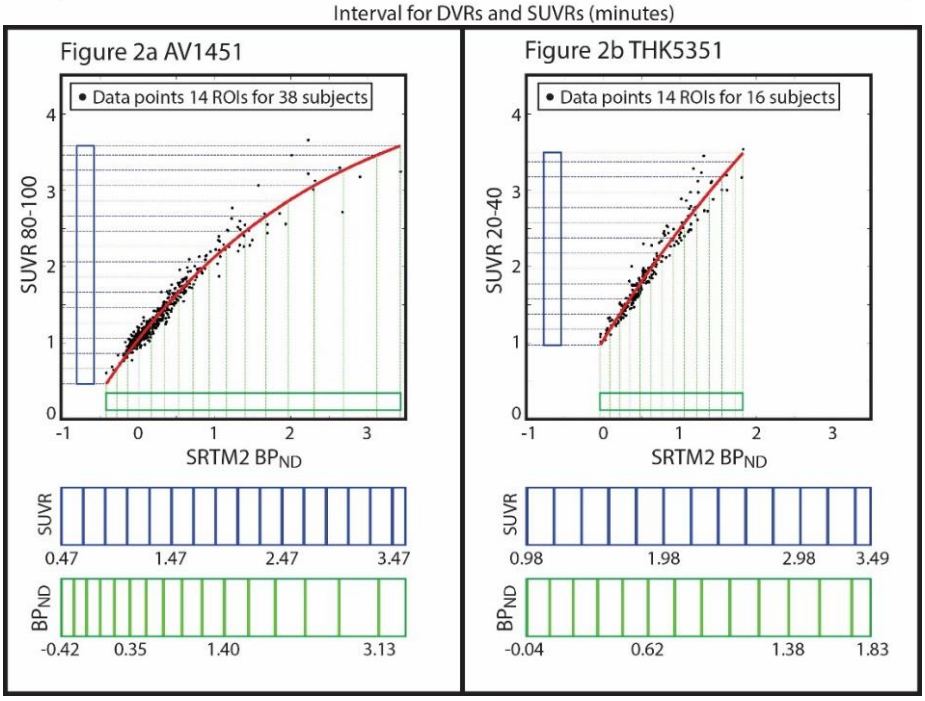

Wednesday, January 13, 2016 - 3:40 - 4:40pm

Podium Presentations

SESSION 2: PET Data Analytics: Time Series, Data Reduction, and THK5351

CHAIRS: *Suzanne Baker, Lawrence Berkeley National Lab*
Julie Price, University of Pittsburgh

3:40-4:40	**SESSION 2:** **PET DATA ANALYTICS: TIME SERIES, DATA REDUCTION, AND THK5351**	**CHAIRS:** **Suzanne Baker** Lawrence Berkeley National Lab **Julie Price** University of Pittsburgh
3:40-3:55	Longitudinal changes in [18F]AV-1451 PET tau signal: Interim analysis of a Phase 2 study	**Mark Mintun** Avid Radiopharmaceuticals, Inc.
3:55-4:10	Optimizing Florbetapir SUVR change-over-time measurement	**Christopher Schwarz** Mayo Clinic and Foundation
4:10-4:25	Principal component analysis of [18F]-AV-1451 Tau PET in sporadic AD and frontotemporal dementia	**Shruti Mishra** Washington University in St. Louis
4:25-4:40	Distinct patterns of [18F]THK-5351 retention in AD and non-AD tauopathies	**Nobuyuki Okamura** Tohoku University
4:40-5:20	Discussion	

Longitudinal changes in [18F]AV-1451 PET tau signal: Interim analysis of a Phase 2 study

Mark Mintun, Michael Devous, Sr, Abhinay Joshi, Ian Kennedy, Michael Navitsky, Ming Lu, Andrew Siderowf, Michael Pontecorvo

Avid Radiopharmaceuticals, Inc., PA, United States

Background: [18F]AV-1451 is a PET ligand developed for imaging of aggregated tau in Alzheimer's Disease (AD). As the neurodegeneration of AD is typically considered relentlessly progressive, we hypothesized that longitudinal 18F-AV-1451 PET imaging of patients suspected of AD pathology will demonstrate a significant increase in PET tau signal over time.

Methods: 160 subjects clinically diagnosed as healthy controls, Mild Cognitive Impairment or AD underwent [18F]AV-1451PET imaging (~370 MBq iv; scanning 80-100 min post injection) at baseline and ~9 months later). Images were co-registered and resampled into MNI atlas space. Activity in a single large atlas-based cortical region was normalized by cerebellum to create an SUV ratio (SUVr) for each scan. Amyloid imaging (~370 MBq i.v. florbetapir) was done at baseline and reviewed using published methods.

Results: 63/160 subjects were Aβ+. These subjects demonstrated a significant increase (paired t-test p=0.0007) in [18F]AV-1451 SUVr (Mean ± S.D were 1.44±0.37 at baseline and 1.48±0.43 at 9 months). Across subjects the change in SUVr averaged 0.038 ± 0.085. The change in SUVr was inversely correlated to age (r = -0.51), not correlated to baseline cognitive performance by MMSE (r=-0.01) but was correlated positively to baseline tau signal by SUVr (r=+0.64).

Aβ- subjects had significantly lower SUVr values compared with Aβ+ subjects ($p < 0.0001$) and no significant change (p=0.80) at follow up (SUVr: 1.08±0.07 at baseline and 1.08±0.08 at 9 months).

Conclusions: Although the follow-up time of 9 months is relatively short these data strongly suggest that in subjects likely having AD pathology the 18F-AV-1451 PET tau signal significantly increases over time, consistent with the predicted progression of AD neurodegeneration. The observations that the change in SUVr correlates to both age and to baseline SUVr is preliminary but could indicate that these factors are related to differences in aggressiveness and underlying stage of the disease.

Optimizing Florbetapir SUVR change over time measurement

Christopher Schwarz[1], Matthew Senjem[1, 2], Jeffrey Gunter[1, 2], Nirubol Tosakulwong[3], Heather Wiste[3], Stephen Weigand[3], Bradley Kemp[1], Anthony Spychalla[1], Prashanthi Vemuri[1], Ronald Petersen[4], Val Lowe[1], Clifford Jack[1]

[1]*Department of Radiology, Mayo Clinic and Foundation, Rochester, MN, United States*
[2]*Department of Information Technology, Mayo Clinic and Foundation, Rochester, MN, United States*
[3]*Department of Health Sciences Research, Division of Biostatistics, Mayo Clinic and Foundation, Rochester, MN, United States*
[4]*Department of Neurology, Mayo Clinic and Foundation, Rochester, MN, United States*

Background: Accurate measurement of intra-subject B-amyloid change from serial PET scans is critical for clinical trials and longitudinal studies of Alzheimer's disease. Many software pipelines exist, varying in choices of reference region, partial volume correction (PVC), target region segmentations, analysis voxel space, etc. Previously, we presented a comparison of pipelines for measuring change in amyloid using serial PiB scans, which favored using PVC and reference regions including both supratentorial white matter and whole cerebellum together. Here, we present a comparison of the same pipelines for longitudinal florbetapir analysis.

Methods: We studied 81 subjects, ages 55-90 (median 75), from the Alzheimer's Disease Neuroimaging Initiative with each having three serial scans of 3T T1-w MRI and florbetapir scans with baseline SUVR < 1.05. Florbetapir scans were registered to corresponding MRI using SPM12. SPM12 and Longitudinal Freesurfer 5.3 were each used to segment cortical gray matter. PVC was optionally applied. An in-house atlas was registered using ANTs to locate regions of interest. SUVRs using 1,040 combinations of reference region, target segmentation, PVC type, and analysis space (MRI or PET) were calculated and their longitudinal trajectories were analyzed. Pipelines were compared using three distinct longitudinal criteria: trajectory straightness, trajectory plausibility (lack of apparently-decreasing trajectories), and correlation between change in SUVR and change in MMSE. We also created a combined, weighted score from these criteria.

Conclusions: In the combined score, top-performing pipelines mostly used PVC, and mostly used reference regions including a combination of both supratentorial WM and whole cerebellum, with or without brainstem. Both of these results were consistent with our previous analysis of longitudinal PiB. An exception was the corpus callosum reference, which here performed well for longitudinal florbetapir, but only average in PiB. We stress that our findings are applicable only to longitudinal studies; cross-sectional criteria were not examined.

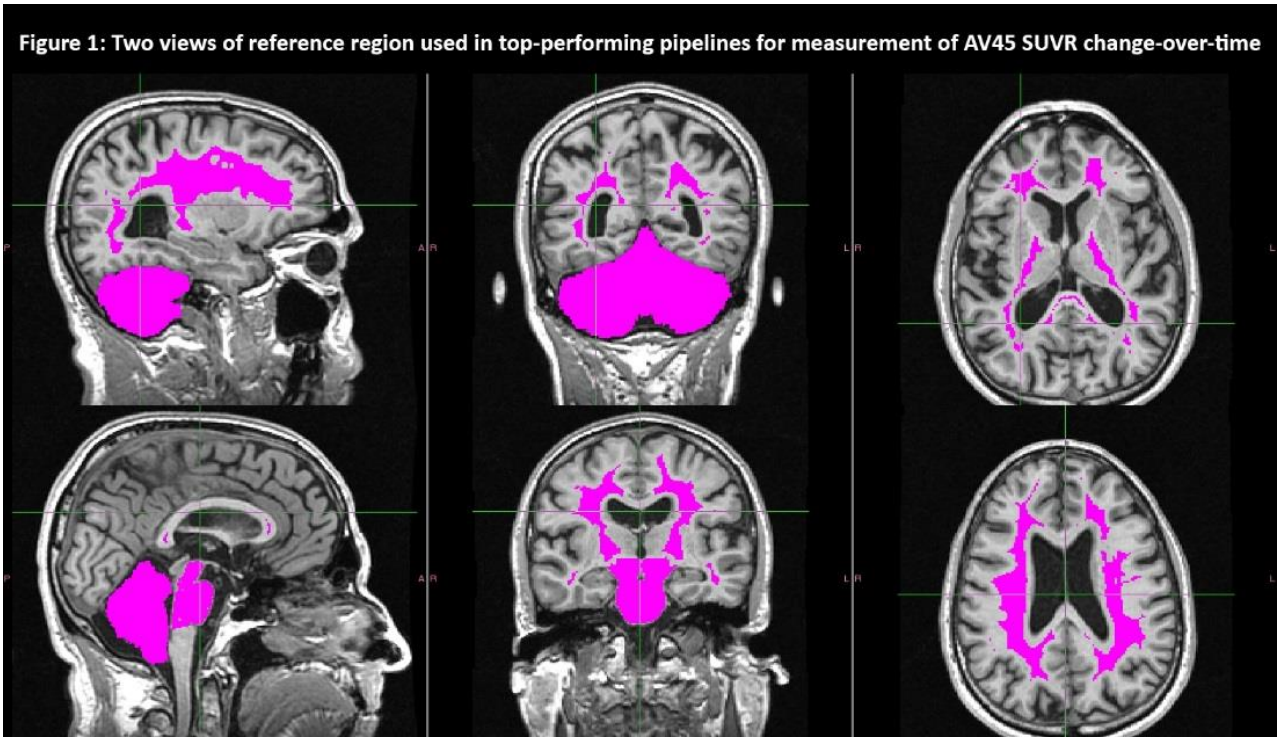

Principal component analysis of [18F]-AV-1451 tau PET in sporadic Alzheimer's disease and frontotemporal dementia

Karl Friedrichsen[1, 6], Shruti Mishra[1, 6], Brian Gordon[1, 2, 6], Tyler Blazey[1], Nelly Joseph-Mathurin[1, 6], Nupur Ghoshal[1, 2, 3], Yi Su[1, 6], Jon Christensen[1, 6], Russ Hornbeck[1, 6], Patricia Aldea[1], Jonathan McConathy[1, 6], Beau Ances[1, 2, 3], Nigel Cairns[1, 2, 3, 5], John Morris[1, 2, 3], Tammie Benzinger[1, 2, 4, 6]

[1]*Washington University in Saint Louis, MO, United States*
[2]*Knight Alzheimer's Disease Research Center, MO, United States*
[3]*Department of Neurology - Washington University School of Medicine, MO, United States*
[4]*Department of Neurological Surgery - Washington University School of Medicine, MO, United States*
[5]*Department of Neuropathology - Washington University School of Medicine, MO, United States*
[6]*Department of Radiology - Washington University School of Medicine, MO, United States*

Background: Development of radiotracers for imaging tau protein in vivo holds potential for identifying biomarkers for diseases featuring tauopathy, such as Alzheimer's disease (AD) and Frontotemporal Dementia (FTD), even prior to clinical presentation. Our aim is to identify tau binding topographies and relate them to disease and aging processes.

Methods: Sixty-nine adults (12 with global Clinical Dementia Ratings (CDR) above zero) underwent [F-18]-AV-1451 positron emission tomography (PET). Six were from an FTD cohort. Data were processed using a region of interest (ROI) approach with FreeSurfer. Regional data were partial volume corrected and converted to Standardized Uptake Value Ratios (SUVRs) normalized to whole cerebellum. Data from 58 ROIs were entered into a principal component analysis. Sixty-two participants also underwent beta-amyloid PET scans using either Pittsburgh Compound B (PiB) or Florbetapir (AV45), and were categorized as beta-amyloid positive or negative by a mean cortical SUVR cutoff.

Results: Three components were identified (fig. 1), explaining 80% of the binding variance. The first component (60% total variance) had positive loadings in the temporal, parietal, and occipital lobes, both lateral and medial surfaces. The second component almost entirely comprised the choroid plexus. The third component had positive loadings for the medial temporal lobes and negative for the posterior areas noted in component 1. The first component was higher in beta-amyloid positive participants. The second component correlated with age. The third component was higher in the FTD cohort compared to the AD cohort.

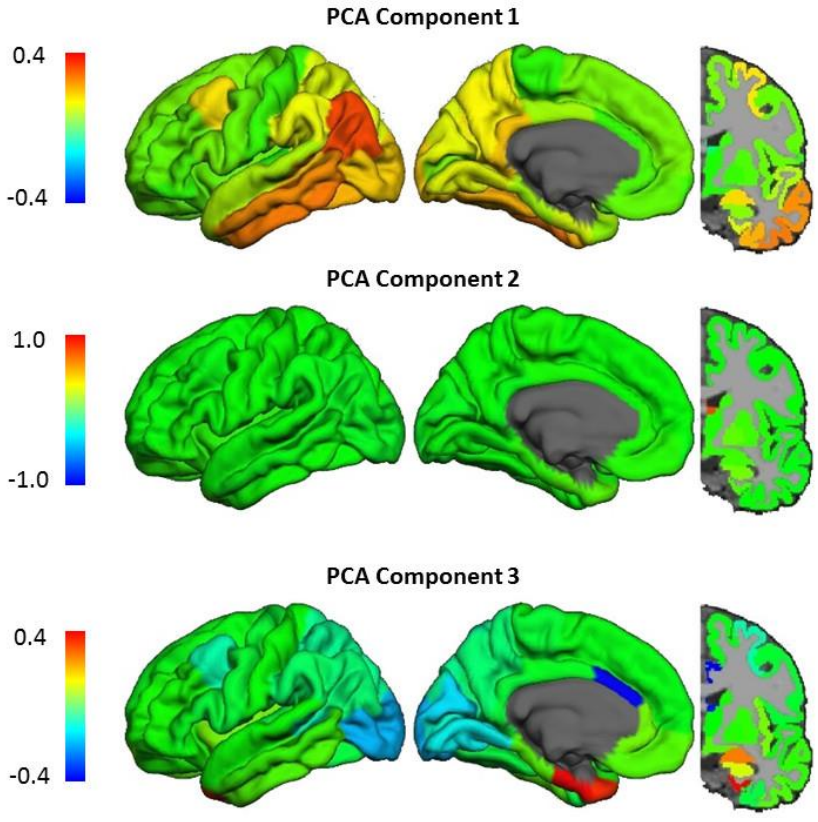

Conclusions: Our analysis showed three separate tau deposition processes (fig. 2). The first component was similar to the tau topography associated with preclinical AD. Component two was associated with age. The third component was higher in the FTD cohort than either cognitively normal or demented persons not in the FTD group, though a larger number of participants is required for validation.

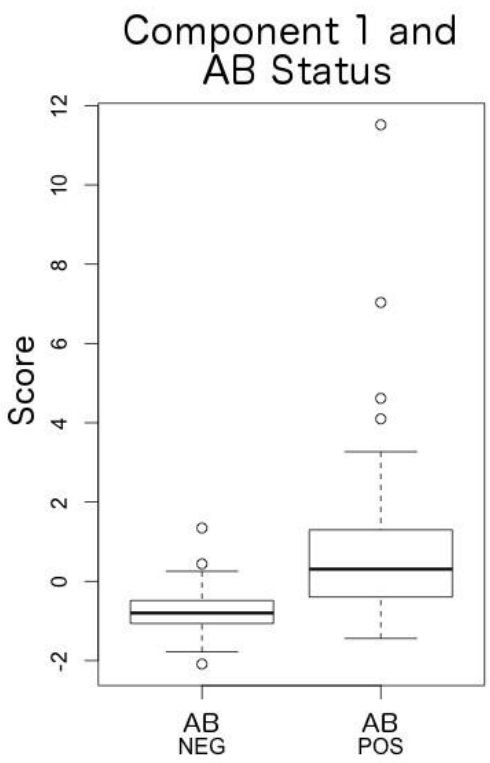
Component 1 and AB Status
Score
12
10
8
6
4
2
0
-2
AB NEG
AB POS

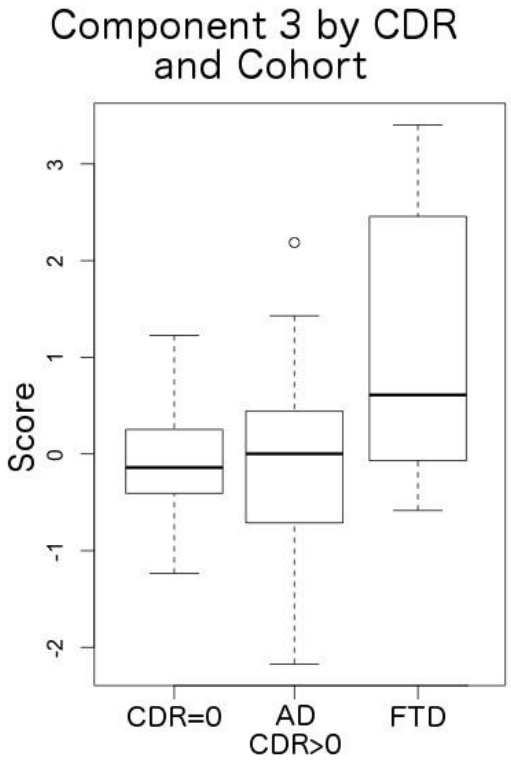
Component 3 by CDR and Cohort
Score
3
2
1
0
-1
-2
CDR=0
AD CDR>0
FTD

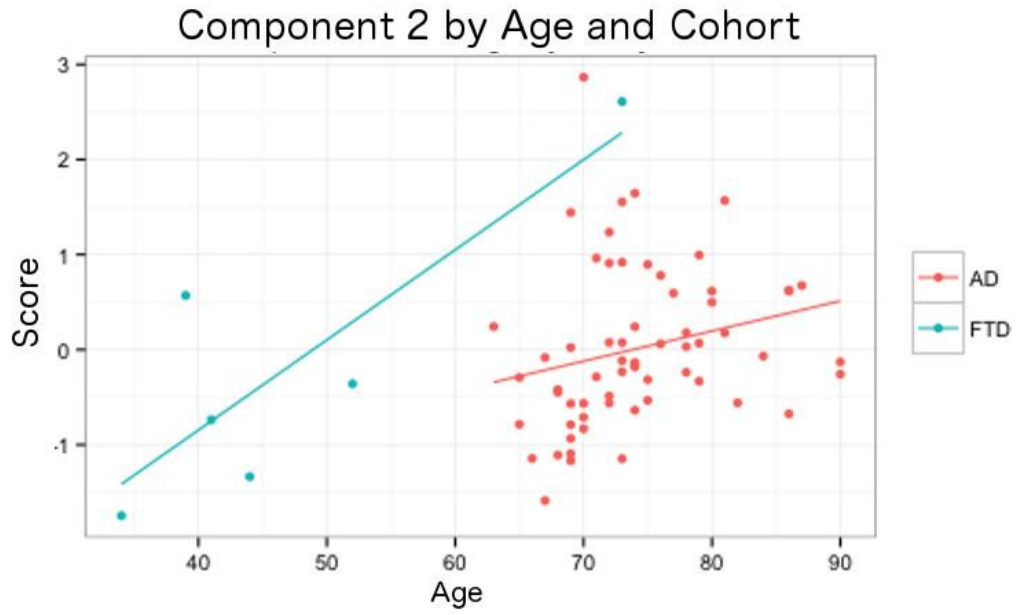
Component 2 by Age and Cohort
Score
3
2
1
0
-1
40
50
60
70
80
90
Age
AD
FTD

Distinct patterns of [^{18}F]THK-5351 retention in AD and non-AD tauopathies

Nobuyuki Okamura[1, 2, 3], Akio Kikuchi[4], Katsutoshi Furukawa[5], Aiko Ishiki[5], Ryuichi Harada[1], Takafumi Hasegawa[4], Atsushi Takeda[6], Shozo Furumoto[3], Ren Iwata[3], Manabu Tashiro[3], Kazuhiko Yanai[2, 3], Masashi Aoki[4], Hiroyuki Arai[5], Yukitsuka Kudo[1]

[1]*Division of Neuro-imaging, Institute of Development, Aging and Cancer, Tohoku University, Japan*
[2]*Department of Pharmacology, Tohoku University School of Medicine, Japan*
[3]*Cyclotron and Radioisotope Center, Tohoku University, Japan*
[4]*Department of Neurology, Tohoku University School of Medicine, Japan*
[5]*Department of Geriatrics and Gerontology, Institute of Development, Aging and Cancer, Tohoku University, Japan*
[6]*Department of Neurology, Sendai Nishitaga Hospital, Japan*

Background: [^{18}F]THK-5351 is a pyridine derivative of [^{18}F]THK-5117, and shows higher binding affinity for tau-rich brain homogenates, lower affinity for white matter homogenates, and faster clearance from normal brain tissue than [^{18}F]THK-5117. In addition to PHF-tau in AD brain, [^{18}F]THK-5351 has been suggested to bind to tau deposits in non-AD tauopathies including progressive supuranuclear palsy (PSP) and corticobasal degeneration. The aim of this study was to evaluate the clinical usefulness of [^{18}F]THK-5351 PET for imaging tau pathology in various kinds of tauopathies.

Methods: [^{18}F]THK-5351 PET scans were performed in 14 elderly healthy controls, 11 patients with AD and 10 patients with non-AD tauopathies including 3 patients with PSP and 5 patients with corticobasal syndrome (CBS). Regional SUVR values at 50-60 min post injection were calculated using cerebellar cortex as a reference region. Volumes of interest were automatically delineated using PNEURO module of PMOD software (Ver.3.6). Hammers maximum probability atlas was applied for this analysis. Voxel-based comparison of PET images was additionally performed using statistical parametric mapping (SPM) 8 software.

Results: AD patients showed THK-5351 retention in the common sites of tau pathology (mainly in the medial and lateral temporal cortex). Patients with advanced dementia showed greater and more extensive neocortical THK-5351 retention than patients with mild dementia. PSP and CBS cases exhibited significant THK-5351 retention in the midbrain and globus pallidus. CBS cases additionally showed asymmetric THK-5351 retention in the precentral and postcentral gyri, and the laterality of tracer retention was consistent with clinical symptom in these patients. Temporal THK-5351 retention with brain atrophy was observed in PiB-PET negative cases.

Conclusion: Significant [^{18}F]THK-5351 signals were detected in expected brain regions of AD, PSP and CBS patients, suggesting the usefulness of this tracer for PET imaging in a variety of tauopathies.

Thursday, January 14, 2016 - 08:00am - 09:00

Podium Presentations

SESSION 3: Pathology

CHAIRS: ***William Klunk, University of Pittsburgh***
Melissa Murray, Mayo Clinic, Jacksonville

8:00-9:00	**SESSION 3: PATHOLOGY**	**CHAIRS:** **William Klunk** University of Pittsburgh **Melissa Murray** Mayo Clinic, Jacksonville
8:00-8:15	Differences between lateral and medial PET image intensity for equivalent levels of Aβ pathology	**Chris Buckley** GE Healthcare Life Sciences
8:15-8:30	Centiloid thresholds for amyloid positivity derived from autopsy-proven cases	**Nagehan Ayakta** University of California, San Francisco
8:30-8:45	In vitro binding and histology analyses of a putative tau ligand T807 in AD and non-AD tauopathy cases	**Milos Ikonomovic** University of Pittsburgh
8:45-9:00	Neuropathologic maturity of neurofibrillary tangles: Implications for tau PET Imaging	**Melissa Murray** Mayo Clinic, Jacksonville
9:00-9:40	Discussion	

Differences between lateral and medial PET image intensity for equivalent levels of Aβ pathology

Adrian Smith, Chris Buckley

GE Healthcare Life Sciences, Buckinghamshire, United Kingdom

A notable feature in amyloid positron emission tomography (PET) imaging is that in subjects where the overall level of amyloid is moderate, the medial cortical regions (particularly the anterior-cingulate and posterior-cingulate and precuneus) are often as, or more, visually intense than the lateral regions. Images are often reviewed in the para-sagittal plane to show these medial surfaces.

Pathology measurements at autopsy, however, show that the earliest involvement of sparse and moderate levels of Ab plaques predominantly affect the lateral aspects of the temporal, frontal and parietal lobes. This apparent difference in moderate Ab pathology levels and image intensity has been assessed using data from GE Healthcare's autopsy Study GE067-026, where 106 autopsy subjects were imaged with [18F]flutemetamol in-life.

The regions where there was a direct spatial concordance between tissue sampling and blinded image evaluation were the lateral temporal, inferior parietal and posterior cingulate and precuneus regions. To assess the PET image representation of moderate levels of pathology in these regions, we compared the percentage of positive visual reads for the three regions where pathology levels were just above the threshold for positivity by tissue-based standard of truth (figure 1).

Figure 1. Aβ pathology range considered for analysis

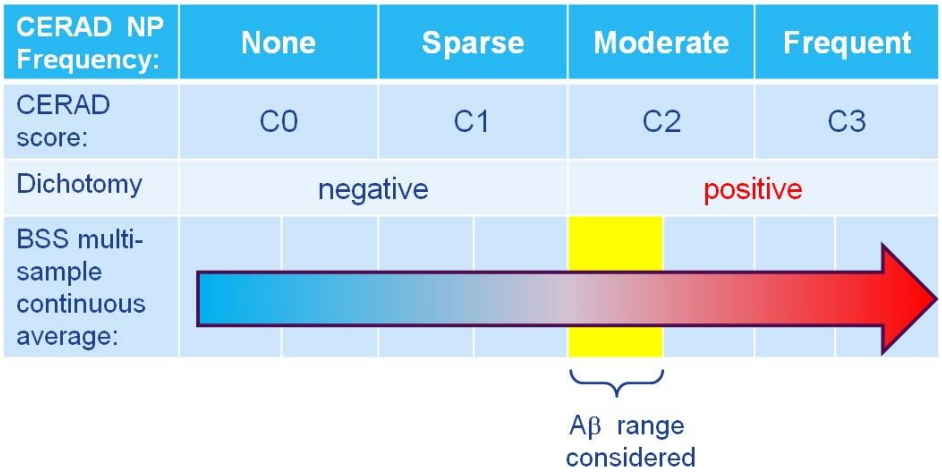

Figure 2. Positive regional PET image interpretation

	Medial surface	Lateral surfaces	
			
	Post. Cing. / Precuneus	**Lat. Temporal**	**Inf. Parietal**
Positive reads	94.5 %	72.3 %	72.0 %
95% Conf. Int.	(88.5 - 100)	(61.4 - 83.2)	(61.8 - 82.1)
N	55	65	75

N = Subset of cases where region is moderate for neuritic plaque assessment – each with 5 readers.

The percentages of reads with a positive assessment for this level of pathology were: posterior-cingulate and precuneus 94.5%, lateral temporal 72.3% and parietal 72.0% (figure 2).

Similar trends were observed for SUVR analysis. The primary reason for this difference is partial volume effects - resulting in either leaching or bridging of intensity in PET images. The magnitude of these effects and their consequences are discussed in this presentation. They are likely to be relevant for all amyloid PET tracers.

Centiloid thresholds for amyloid positivity derived from autopsy-proven cases

Nagehan Ayakta[1, 2], Samuel Lockhart[2], James O'Neill[2], Rik Ossenkoppele[1], Bruce Reed[1], John Olichney[3], Adam Boxer[1], Bruce Miller[1], Ewa Borys[4], Lee-Way Jin[5], Eric Huang[1], Lea Grinberg[1], Charles DeCarli[3], William Seeley[1], William Jagust[2], Gil Rabinovici[1, 2]

[1]*Memory and Aging Center, University of California, San Francisco, Department of Neurology, CA, United States*
[2]*Helen Wills Neuroscience Institute, University of California, Berkeley, CA, United States*
[3]*University of California, Davis, Neurology, CA, United States*
[4]*Stritch School of Medicine, Loyola University, IL, United States*
[5]*Alzheimer's Disease Center, University of California, Davis, CA, United States*

Objective: To establish thresholds for amyloid positivity applying the Centiloid method to patients studied with [11C]PiB-PET and autopsy.

Methods: We first validated methodology by processing the core Centiloid image dataset available at GAAIN.org. The regression between UCSF/Berkeley and Pittsburgh derived Centiloids yielded R2 = 0.99943. Then a cohort of 60 diagnostically diverse subjects with PiB-PET and autopsy data (Table1) was processed with the Centiloid method and our internal pipeline (50-70 min SUVRs, gray cerebellum reference) to generate Centiloids and a conversion regression. The relationship between Centiloids versus CERAD and Thal stages was investigated. Finally, we assessed the performance of two a priori thresholds previously introduced by our group (liberal –SUVR 1.21 = 7.47 Centolids; conservative –SUVR 1.40 = 27.48 Centiloids) as well as an empirically derived threshold from an ROC analysis of the current dataset, using CERAD moderate-frequent plaques as the standard of truth.

	Total	AD	FTLD	Vascular	Mixed	Other
N	60	14	30	6	8	2
Gender (M/F)	37/23	11/3	18/12	4/2	2/6	2/0
Education	15.7 (2.8)	17.5 (2.5)	15.7 (2.6)	14 (2.5)	14.5 (2.8)	16.0
Age at PET	67.8 (9.6)	69.4 (11.6)	65.2 (6.7)	81.2 (5.0)	68.6 (4.5)	58.5
$T_{autopsy}$ - T_{PET} (years)	3.2 (2.0)	3.9 (1.8)	2.9 (1.9)	2.4 (1.5)	4.5 (2.8)	1.3
Avg SUVR (STD)	1.3 (0.5)	2 (0.5)	0.97 (0.13)	1.2 (0.29)	1.6 (0.45)	0.96
Avg Centiloid	28.5 (50.4)	91.6 (46.7)	-5.6 (15.2)	13.8 (27)	47.7 (51.9)	-4.6
Avg Thal phase	2.2 (1.9)	4.9 (0.4)	1.0 (1.06)	1.0	4.3 (0.95)	n/a
Avg Braak phase	2.9 (2.3)	5.9 (0.3)	1.2 (1.2)	1.8 (0.7)	5.0 (0.93)	2.0
MMSE at PET	21.4 (7.2)	19.4 (6.0)	21.4 (8.2)	25.0 (6.4)	23 (6.2)	26.0
CDR at PET	1.09 (0.8)	1.1 (0.5)	1.2 (0.88)	0.38 (0.5)	0.88 (0.92)	0.75
ApoE E4 positive	16	7	5	0	4	0
C9ORF72	2	0	1	0	1	0

Table 1: Summary of the autopsy cohort organized by the primary diagnosis at autopsy. AD, Alzheimer's Disease, includes both AD and AD+DLB at autopsy, FTLD, Frontotemporal Lobar Degeneration, includes PSP, CBD, Pick's Disease, and TDP-43, Mixed includes autopsy cases with 2 primary diagnoses, Other, includes prion disease and argyrophillic grain disease.

Results: CERAD none-sparse patients had a mean of -4.85±6.88 Centiloids; the moderate-frequent group had 66.02±50.45 Centiloids (t-test, p <0.001). The ROC analysis identified 9.50 Centiloids as the optimal threshold with 0.89 sensitivity (0.71-0.97), 1.00 specificity (0.86 – 1.00); AUC 0.91, 95% CI 0.808-1.000 (Figure1).

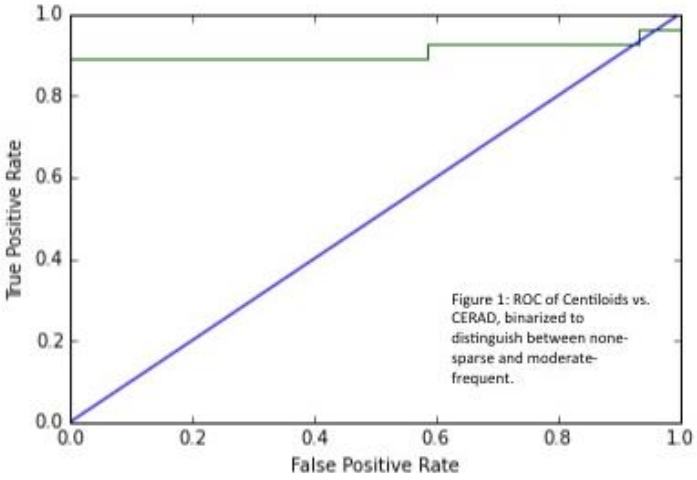

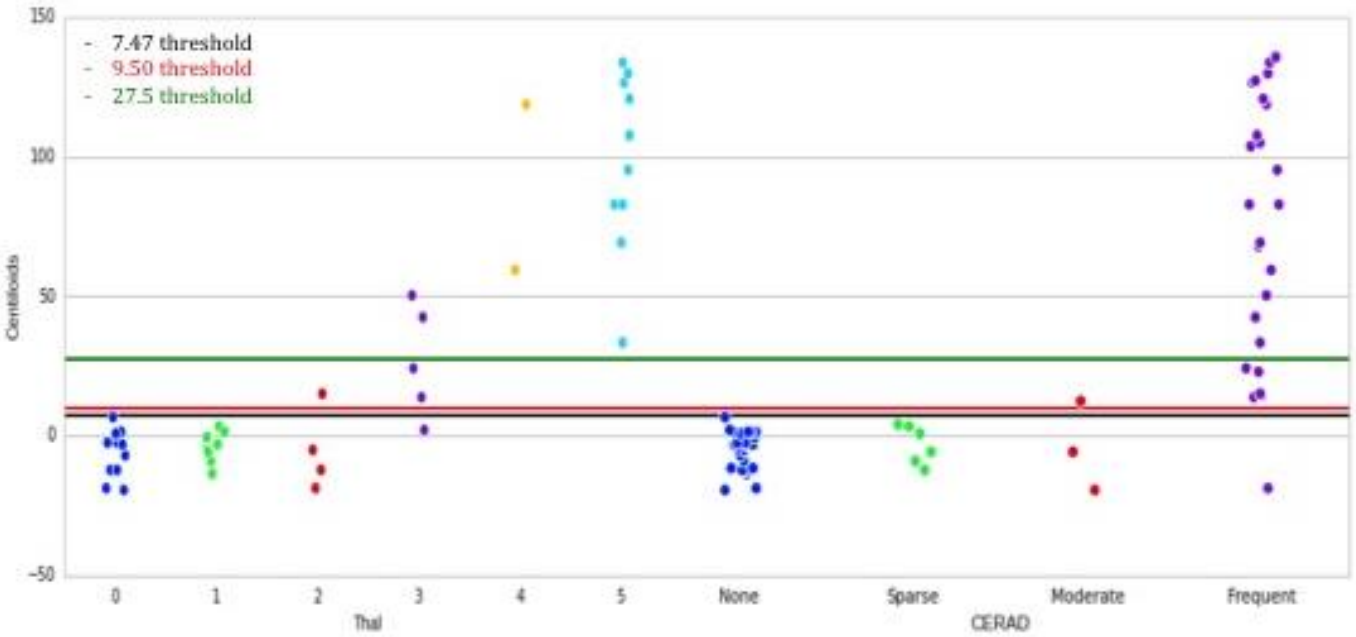

Figure 2: Distribution of Centiloids across Thal phases and CERAD scores. Thresholds 7.47 and 9.50 create a distinct divide between Thal phases 0-2 and 3-5 and identifies a majority of frequent CERAD as positive.

The a priori liberal threshold had identical sensitivity and specificity as the ROC-derived threshold. These thresholds also distinguished between Thal phases 0-2 and 3-5 (Figure2). The a priori conservative threshold had sensitivity of 0.68 (0.48-0.83) and specificity of 1.00 (0.86-1.0).

Discussion: This project has shown the feasibility of applying the Centiloid scale across centers to overcome differences in tracers, scanners, and methods of processing. The a priori liberal threshold (7.47 Centiloids) and the ROC-derived threshold (9.50 Centiloids) showed excellent sensitivity/specificity, and did not differ significantly. Thus, a Centiloid threshold between 7.47-9.50 may be considered for detection of early amyloid signal.

In vitro binding and histology analyses of a putative tau ligand T807 in AD and non-AD tauopathy cases

Milos Ikonomovic[1], Eric Abrahamson[1], Manik Debnath[1], William Paljug[1], Lan Shao[1], William Seeley[2], Chester Mathis[1], Gil Rabinovici[2], William Klunk[1]

[1]*University of Pittsburgh, PA, United States*
[2]*University of California, San Francisco, CA, United States*

Background: Developing a tau-selective PET imaging ligand would facilitate clinical diagnosis of tauopathies. [F-18]T807 has become a widely used tau imaging agent in clinical research studies, but its selectivity for tau over other pathological protein aggregates is poorly understood. We investigated the pathological substrates for T807 in autopsy brain samples from cases with Alzheimer's disease (AD) and non-AD tauopathies.

Methods: Frontal cortex (FC) tissues were obtained from brain banks at University of California, San Francisco and University of Pittsburgh ADRC. Neuropathology screening demonstrated absence of FC Aβ deposits in seven non-AD tauopathy cases with a primary neuropathological diagnosis of progressive supranuclear palsy (PSP, n=3), corticobasal degeneration (CBD, n=2), and Pick's disease (PD, n=2). Controls included frontotemporal lobe dementia cases with TDP inclusions (FTLD-TDP-A, n=3; no Aβ or tau pathology), AD (n=2, positive for Aβ and tau), tau-only dementia (TauD, n=1), and normal controls (NC, n=2, no Aβ or tau pathology). Assays included [H-3]T807, [F-18]T807, and [H-3]PiB radiometric binding, histology using a fluorescent T807 analogue CN-T807, tau and Aβ immunohistochemistry.

Results: CN-T807 fluorescence labeled tau-immunoreactive structures in AD (tangles and neuritic Aβ plaques), PD (Pick bodies), PSP (tufted astrocytes), and CBD (astrocytic plaques). [H-3]T807 and [H-3]PiB binding values were comparably high in AD FC, and low in all non-AD cases regardless of tau pathology load. Similarly, [F-18]T807 binding was high in AD FC but comparable or below control levels in FC from other cases. Significant [F-18]T807 binding was also observed in TauD FC and in a sample of meninges from an AD case.

Conclusion: T807 binding is high in AD, but relative contributions of tau in neurofibrillary tangles and neuritic plaques remain to be elucidated. In non-AD tauopathy cases, low T807 binding contrasts positive CN-T807 histology results and positive [F-18]T807 PET reports in PSP subjects, and requires further investigation.

Neuropathologic maturity of neurofibrillary tangles: Implications for tau PET imaging

Melissa Murray[1], Geoffry Curran[2], Amanda Liesinger[1], Mukesh Pandey[2], Ping Fang[2], Kejal Kantarci[2], Bradley Boeve[2], David Knopman[2], Leonard Petrucelli[1], Dennis Dickson[1], Ronald Petersen[2], Neill Graff-Radford[1], Clifford Jack, Jr.[2], Val Lowe[2]

[1]*Mayo Clinic, Jacksonville, FL, United States*
[2]*Mayo Clinic, Rochester, MN, United States*

Background: Neurofibrillary pathology underlying Alzheimer's disease (AD) develops progressively in the intracellular space of the neuron. Maturity of a neurofibrillary tangle (NFT) is strongly associated with cognitive decline. Our goal was to investigate the relationship between tau maturity and tau PET utilizing autoradiographic and immunohistochemical methods.

Methods: Representative neuropathologically-confirmed normal and AD cases were selected from the Mayo Clinic Jacksonville brain bank to undergo autoradiographic tau binding using AV1451. The hippocampal section was immunohistochemically examined for initial and mature tau with hyperphosphorylated tau antibodies, and advanced tau with a conformational epitope to NFTs. To examine the range of neurofibrillary tau pathology, primary age-related tauopathy cases and tangle-predominant dementia cases were also selected. Groupwise quantitative comparisons of autoradiographic binding and subsequent correlation analyses between autoradiographic data and tau burden were performed.

Results: Visually, autoradiographic tau binding patterns were closely related to the initial tau antibody pattern and to a subtler extent with mature tau. Advanced tau pathology was difficult to visualize at the same resolution as autoradiography images and not considered to associate. Autoradiographic binding in the CA1 significantly differed, but only initial and mature tau showed an association. Subiculum did not differ across groups, but was strongly associated with all tau. Occipitotemporal cortex significantly differed, and was strongly associated with all tau. When AD cases were removed from association studies, only initial and mature tau was found to associate with autoradiographic binding.

Conclusions: Visual comparison of autoradiographic images and tau supports the hypothesis that AV1451 labels early and mature tau, but may not label advanced tau pathology. Autoradiographic labeling of AV1451 was quantitatively associated with tau species, but AD cases acted as an anchor interfering with interpretation of association. Our preliminary findings suggest that AV1451 labels early tau pathology, which should be considered when evaluating tau PET ligands as a biomarker in preclinical AD.

Poster Session (even-numbered)

Joshi, Aniket – PE02

Determination of smallest detectable difference for amyloid PET tracers using test-retest data

Aniket Joshi[1], Dai Feng[2], Richard Baumgartner[2]

[1]Novartis Institute for Biomedical Research, Cambridge, MA, United States
[2]Biometrics Research, Biostatistics and Research Decision Sciences, Merck & Co, Rahway, NJ, United States

Several studies with amyloid PET tracers have been performed to investigate the longitudinal change in amyloid deposition due to disease progression or response to therapy. These studies are typically designed to measure mean difference between two samples (Beckett et al, 2010); e.g. tracer uptake at baseline and at follow-up, or uptake pre- and post-dosing in a drug trial. However, there is no methodology in use to determine if the longitudinal change in the SUVR of an AD subject is due to change in amyloid density or simply due to test-retest variability. We propose the application of the smallest detectable difference (SDD) concept by leveraging test-retest data in AD subjects to determine if the change measured in a repeated PET scan in an individual may be attributed to change in target density or to the test-retest variability. The proposed approach would also provide a useful cutoff for time-to-event analysis which has been proposed to be a more suitable model for AD progression (Vemuri et al, 2011).

Methods: We modeled the test-retest data in AD subjects using one-way random analysis of variance with two mutually independent, normally distributed random components (subject random effect and measurement error). From this model, it is straightforward to calculate the SDD and the corresponding confidence intervals.

Results and Conclusion: To illustrate the methodology, it was applied to published test-retest data of cortical standard uptake value ratio (SUVR) of two tracers in AD subjects: [^{18}F]florbetapir (Joshi et al, 2013; Bland-Altman plot in Fig. 1): SDD in SUVR = 0.07 (95% CI:0.05-0.12) and [^{18}F]flutemetamol (Vandenberghe et al, 2010; Bland-Altman plot in Fig 2): SDD in SUVR = 0.08 (95% CI: 0.05-0.17). To account for uncertainty in estimation of SDD, upper confidence limit of SDD should be used as the threshold for attributing the change in the SUVR in an AD subject to change in amyloid density or test-retest variability.

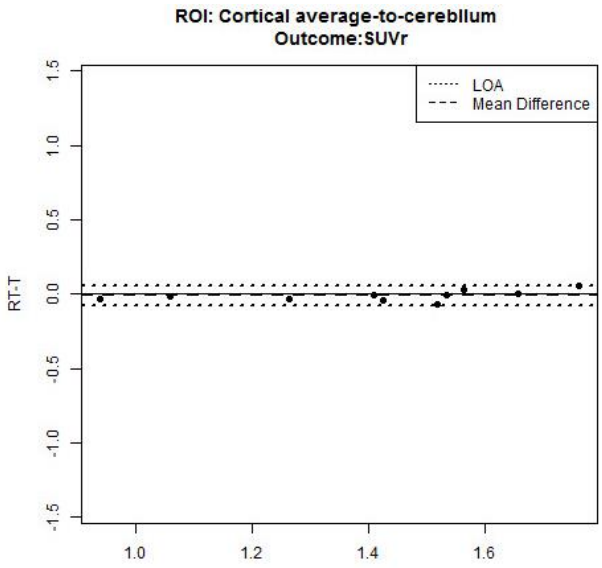

Figure 1: Bland-Altman plot for test-retest data for [^{18}F]Florbetapir (Joshi et al, 2013). The dotted lines represent Limits of Agreement (LOA) and the dashed lines denotes the mean difference.

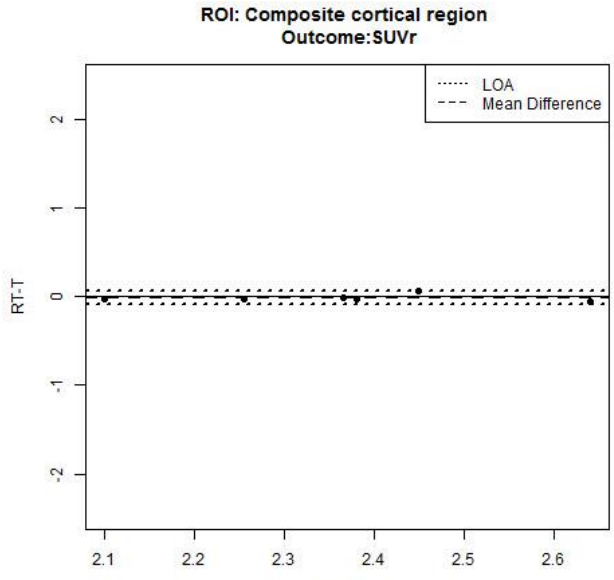

Figure 2: Bland-Altman plot for test-retest data for [^{18}F]flutemetamol (Vandenberghe et al, 2010). The dotted lines represent Limits of Agreement (LOA) and the dashed line denotes the mean difference.

Serum adiponectin levels and neuroimaging outcomes in the Mayo Clinic Study of Aging

Alexandra Wennberg[1], Deborah Gustafson[2], Clinton Hagen[1], Rosebud Roberts[1, 4], David Knopman[4], Clifford Jack[3], Ronald Petersen[1, 4], Michelle Mielke[1, 4]

[1]*Department of Health Sciences Research, Mayo Clinic, Rochester, MN, United States*
[2]*Department of Neurology, State University of New York Downstate Medical Center, NY, United States*
[3]*Department of Radiology, Mayo Clinic, Rochester, MN, United States*
[4]*Department of Neurology, Mayo Clinic, Rochester, MN, United States*

Adiponectin, an adipose tissue protein involved in inflammatory, energy, appetite, and other metabolic pathways, may impact the development and progression of Alzheimer's disease (AD). Cerebrospinal fluid and plasma adiponectin levels are associated with mild cognitive impairment (MCI) and AD, but the association between adiponectin and Alzheimer-associated neuropathology is unknown.

We investigated the cross-sectional association between plasma adiponectin and continuous measures of amyloid PET, FDG PET, hippocampal volume (HVa), cortical thickness, global and domain specific cognitive z-scores, and presence of MCI among 535 non-demented participants aged 70 and older in the Mayo Clinic Study of Aging (MCSA). Adiponectin was higher in women than men (12,631 ng/mL vs. 8,908 ng/mL, $p<0.001$) thus models were stratified by sex. Regression models were adjusted for age, education, waist-to-hip ratio, diabetes, hypertension, and APOE ε4. Among men, higher adiponectin was associated with lower cerebral glucose uptake in AD-associated regions (B=-0.087; 95% CI -0.166, -0.008). Among women, higher adiponectin was associated with smaller HVa (B=-0.595; 95% CI -1.19, -0.005); poorer performance on tests of language (B=-0.777; 95 % CI -1.42, -0.138) and global cognition (B=-0.729; 95% CI -1.40, -0.053); and greater odds of MCI (OR=6.23; 95% CI 1.20, 32.43). Notably, in analyses stratified by sex and elevated amyloid (PiB-PET>1.4) results remained significant only among women with elevated amyloid, such that higher adiponectin was associated with smaller HVa (B=-0.723; 95% CI -1.43, -0.014); poorer performance in memory (B=-1.40; 95% CI -2.38, -0.422), language (B=-1.03; 95% CI -1.82, -0.244) and global (B=-1.07; 95% CI -1.85, -0.288) cognition; and greater odds of MCI (OR=19.34; 95% CI 2.72, 137.34).

Longitudinal analyses are necessary to determine whether high plasma adiponectin predicts neurodegeneration and cognitive decline among women with elevated amyloid.

The loss of functional and effective connectivity in mild cognitive impairment is linked to amyloid deposition and ApoE4

Lars Michels[1], Muthuraman Muthuraman[2], Abdul Rauf Anwar[2], Spyros Kollias[1], Sandra Leh[3], Florian Riese[3], Paul Unschuld[3], Michael Siniatchkin[4], Anton Gietl[3], Christoph Hock[3]

[1]*Institute of Neuroradiology, University Hospital of Zurich, Switzerland*
[2]*Clinic for Neurology, University of Kiel, Germany*
[3]*Division of Psychiatry Research and Psychogeriatric Medicine, University of Zurich, Switzerland*
[4]*Institute of Medical Psychology and Medical Sociology, Christian-Albrechts-University of Kiel, Germany*

The assessment of effects associated with cognitive impairment with electroencephalography (EEG) power mapping allows the assessment of frequency-band specific local changes in oscillatory activity. In contrast, measures of coherence and dynamic source synchronization allow studying functional and effective connectivity, respectively. Yet, these measures have been rarely assessed in parallel in the context of mild cognitive impairment (MCI) and furthermore it has not been examined if they are related to risk factors of Alzheimer's disease such as amyloid deposition and apolipoprotein ε4 allele occurrence.

We investigated functional and directed connectivities with Renormalized Partial Directed Coherence (RPDC) in 17 healthy controls (HC) and 17 participants with MCI. Participants underwent ApoE-genotyping and PiB-PET to assess the amyloid deposition. We observed lower spectral source power in MCI in the alpha and beta bands. Coherence was stronger in HC than MCI across different neuronal sources in the delta, theta, alpha, beta and gamma band. The directed coherence analysis indicated lower information flow between fronto-temporal (including the hippocampus) sources and unidirectional connectivity in MCI. Global amyloid deposition inversely correlated to alpha coherence and RPDC, and beta and gamma coherence. The ApoE status was negatively correlated to alpha coherence and RPDC, beta RPDC, and gamma coherence. A classification analysis of cognitive state revealed the highest accuracy using EEG power, coherence, and RPDC as input. We verified by Bayesian power analyses that our sample size was large enough to call the classification results reliable.

Our results suggest that resting EEG related functional and directed connectivities are sensitive to the cognitive state and are linked to ApoE and amyloid burden.

Early AD detection: Performance of a new fast hippocampus volumetry in comparison with automated voxel-based [^{11}C]PiB PET quantitation

Arthur Mikhno[1], Janos Redei[1], J John Mann[2, 3], Ramin Parsey[4]

[1]*i2Dx, Inc., CA, United States*
[2]*Columbia University, NY, United States*
[3]*New York State Psychiatric Institute, NY, United States*
[4]*Stony Brook University, NY, United States*

Background: Recent advances in disease-modifying AD therapies have highlighted the need to target the early phase of disease for successful intervention. Even though quantitative hippocampus volumetry has clinical utility, it is not typically part of the MRI assessment because accurate volume measurement is time consuming. The objective of this study was to evaluate the utility of a new fast automated hippocampus volumetry, ~1 minute with a T1 MRI scan, and compare to automated voxel-based [^{11}C]PiB PET quantitation in an early AD population (~50% prodromal and 50% mild AD) as studied in recent intervention trials.

Methods: [^{11}C]PiB PET and T1 MRI scans for independent testing were obtained from previously described early AD data (Mikhno *et al.*, AAIC 2015): (1) a prodromal dataset (n=29) from the ADNI database that included 29 MCI subjects divided into 16 converters (PET 1 to 3.5 years prior to conversion to AD) and 13 non-converters (4 to 8 years of MCI follow-up); (2) and a mild-AD dataset (n=26) that included 10 mild-AD patients and 16 age-matched healthy controls. A voxel-based-SUVR (Mikhno *et al.*, JNM 2008) was calculated for each [^{11}C]PiB PET scan and hippocampal volume (HCV) was calculated for each corresponding T1 MRI with a novel GPU-accelerated software for hippocampus segmentation that was validated against EADC/ADNI harmonized protocol (HarP).

Results: Receiver operating characteristic (ROC) area under the curve for early AD was 0.75 and 0.96 for HCV and voxel-based-SUVR, respectively. Performance (sensitivity% / specificity% / accuracy%) for identifying early AD was (72/73/73) for HCV and (92/93/93) for voxel-based-SUVR. Combining HCV with voxel-based-SUVR did not improve results.

Conclusions: Rapid quantitative hippocampus volume measurement is possible and provides utility for initial assessment of early AD. When a PET scan is ordered, voxel-based-SUVR can detect the early phase of AD with high accuracy that outperforms other approaches.

Prodromal AD: Utility of a new fast hippocampus volumetry, in combination with APOE vs. MR-less- and voxel-based [^{18}F]florbetapir PET quantitation

Arthur Mikhno[1], Janos Redei[1], J John Mann[2, 3], Ramin Parsey[4]

[1]*i2DX, Inc., CA, United States*
[2]*Columbia University, NY, United States*
[3]*New York State Psychiatric Institute, NY, United States*
[4]*Stony Brook University, NY, United States*

Background: Accurately identifying prodromal disease is a key challenge in AD. While quantitative hippocampus volumetry has clinical utility, it is not typically part of the MRI assessment due to time constraints. It is further unclear whether current Amyloid PET approaches are cost-effective over less expensive MRI. The objective of this study was to evaluate the utility of a new fast automated hippocampus volumetry, that can be completed in as little as 1 minute with a T1 MRI scan, combined with APOE genotype, and compare to PET-only (MR-less) and voxel-based PET quantitation approaches.

Methods: Subjects with MCI at the time of their earliest [^{18}F]florbetapir PET, and their corresponding T1 MRI scans, were selected from a previously described ADNI MCI population (Mikhno *et al.*, HAI 2015). Subjects with APOE genotype and semi-automated regional PET-only-SUVR (Syngo/SPAP) data available were divided into converters (to AD) and non-converters; 25 converters (PET 1 to 3 years prior to conversion) and 25 non-converters (5 to 7 years of MCI follow-up) were included. Voxel-based-SUVR was calculated from each PET/MRI scan pair (Mikhno *et al.*, JNM 2008). Hippocampal volume (HCV) was calculated with a novel GPU-accelerated software for hippocampus segmentation of the MRI that was validated against EADC/ADNI harmonized protocol (HarP). Performance of the combination of HCV and APOE was assessed with a logistic regression model in a leave-one-out analysis.

Results: For converters vs. non-converters, the receiver operating characteristic (ROC) area under the curve was 0.78, 0.75 and 0.91 for HCV+APOE, PET-only-SUVR, and voxel-based-SUVR, respectively. Performance (sensitivity% / specificity% / accuracy%) was (92/68/80), (96/52/74) and (88/84/86), respectively.

Conclusions: Rapid hippocampus volumetry is possible and combined with APOE genotype provides utility for initial MRI-based assessment of prodromal AD that is comparable to PET-only-SUVR. When a subsequent PET is included in the sequence, voxel-based-SUVR can identify prodromal AD with high certainty.

The quest for a robust and reliable reference region (RR): Exploring RR stability across clinical categories, across Aβ status and across time for five different Aβ radiotracers

Victor L. Villemagne[1, 2], Pierrick Bourgeat[3], Vincent Doré[1, 3], Lance Macaulay[3], Robert Williams[2], Ralph Martins[4], David Ames[5], Olivier Salvado[3], Kewei Chen[6], Eric Reiman[6], Colin L. Masters[2], Christopher C Rowe[1]

[1]*Department of Molecular Imaging & Therapy & Centre for PET, Melbourne, Australia*
[2]*The Florey Institute of Neuroscience and Mental Health, The University of Melbourne, Melbourne, Australia*
[3]*CSIRO, Digital Productivity Flagship, The Australian e-Health Research Centre, Brisbane, Australia*
[4]*Edith Cowan University, Perth, Australia*
[5]*National Ageing Research Institute, Melbourne, Australia*
[6]*Banner Alzheimer's Institute, Phoenix, AZ, United States*

Background: The reference region (RR) was defined as having similar cellular and blood flow as target regions (TR) but lacking specific binding, assuming that both nonspecific binding and the volume of distribution of the free compartment are the same as in TR. On account semiquantitative standard uptake value (SUV) ratio (SUVR) being used as outcome measure in anti-Aβ therapeutic trials we assessed the stability of different RR with five Aβ imaging tracers and then evaluated the variance in TR derived with the stable RRs. While several studies have focused on such variance by using different RR, none has focused on assessing if a given RR is truly stable, and if its performance is tracer specific or not.

Methods: 1066 participants were evaluated (327-PiB; 256-flutemetamol -FLUTE-; 189-florbetapir -FBP-; 212-florbetaben -FBB-, and 82-NAV4694), where 496 had longitudinal scans. SUV of either gray matter (GM) or white matter (WM) RR, and their combinations across clinical conditions, Aβ status, and time was examined. Variance of global Aβ burden estimates were assessed for stable RR.

Results: Cerebellar GM (CbGM) was the most stable RR for PiB, FBB and NAV. SMM_{KCER}* was the most stable performing RR for FBP, while performing almost identically to SWM-Pons for FLUTE. SMM_{KCER} and SWM+Pons yielded the lowest variance for longitudinal FBP and FLUTE, respectively. Despite smaller variances in target regions, SWM+WCb+pons was not stable for PiB and FBB across clinical diagnoses, nor for PiB, FLUTE and FBP across Aβ status. Aβ burden variances obtained with the stable RR were similar for all tracers.

Conclusions: SWM+pons and SWM_{KCER} for FLUTE, CbGM for PiB, FBB and NAV, and SWMKCER for FBP remained stable across the examined conditions, yielding low variances of the Aβ burden estimates. To optimize outcomes in ongoing therapeutic trials, a tracer-specific RR should be applied.

Comparison of *in vitro* binding characteristics of PET ligands, PBB3 and T807, for tau lesion in AD and non-AD tauopathy

Maiko Ono[1, 5], Naruhiko Sahara[1], Mari Yoshida[2], Shunsuke Koga[3], Dennis Dickson[3], John Trojanowski[4], Virginia Lee[4], Tetsuya Suhara[1], Ming-Rong Zhang[1], Makoto Higuchi[1]

[1]*National Institute of Radiological Sciences, Chiba, Japan*
[2]*Aichi Medical University, Aichi, Japan*
[3]*Mayo Clinic, Jacksonville, FL, United States*
[4]*University of Pennsylvania, PA, United States*
[5]*Tohoku University, Miyagi, Japan*

Conformational diversities of tau assemblies, known as fibril strains, result from distinct isoform compositions and posttranslational processing of tau proteins. A number of positron emission tomography (PET) imaging agents targeting fibrillary tau pathologies have been recently developed in recent years, whereas common and/or distinct features of their binding to various tau fibril strains are largely unknown.

Here, we compared binding characteristics of tau PET tracers, PBB3 and T807, by performing fluorescence and autoradiographic labeling of brain slices derived from patients with AD and non-AD tauopathies. T807 and its radiosynthesis precursor were prepared by in-house generation. In AD, tau fibrils are composed of all six tau isoforms, and both PBB3 and T807 similarly bound to ghost and non-ghost tangles without overt reactivity with pre-tangles. Meanwhile, PBB3 labeled neuropil threads and plaque neurites more intensely than T807. All tau isoforms are also incorporated in tau tangles in a rare presenile dementia termed diffuse neurofibrillary tangles with calcification, and PBB3 and T807 strongly bound to a subset of ghost tangles, seemingly in a manner dependent on packing density of tau fibrils. In the brain of a patient with the N279K FTDP-17-*MAPT* mutation, tau deposits are composed of 4-repeat tau isoforms (4RTs) only, and PBB3 intensely labeled neuritic and oligodendrocytic tau lesions in whiter matter regions including the alveus, in contrast with no specific binding of T807 to these samples. Moreover, 4RT aggregates in neurites, astrocytes and oligoodendrocytes were clearly illuminated by PBB3 but relatively weakly by T807 in progressive supranuclear palsy and corticobasal degeneration brains.

Our data indicate distinct selectivities of PBB3 and T807 for tau assemblies among diverse fibril strains, highlighting the detectability of a broad spectrum of tau lesions by PBB3.

Structural MRI and molecular PET imaging in the diagnosis of chronic traumatic encephalopathy: Study of a retired NFL player

Dara Dickstein[1], Mariel Pullman[1], Corey Fernandez[1], Jennifer Short[1], Lale Kostakoglu[1], Karin Knesaurek[1], Barry Jordan[2], Wayne Gordon[1], Kristen Dams-O'Connor[1], Bradley Delman[1], Cheuk Tang[1], Steven DeKosky[3], James Stone[3], Robert Cantu[4], Patrick Hof[1], Samuel Gandy[1], et al.

[1]Icahn School of Medicine at Mount Sinai, NY, United States
[2]Weill Medical College of Cornell University, NY, United States
[3]University of Virginia, VA, United States
[4]Boston University School of Medicine, MA, United States
[5]Emerson Hospital, MA, United States

Chronic traumatic encephalopathy (CTE) is a neurodegenerative disorder resulting from repetitive mild brain trauma. Currently, the definite diagnosis of CTE is established postmortem, and studies are needed to facilitate detection during life.

Here, we describe the clinical case of a 39-year-old retired National Football League player with a history of 22 concussions and cognitive complaints. Evaluation included neurologic and neuropsychological assessment, structural MRI, [18F]florbetapir amyloid positron emission tomography (PET) imaging, and experimental tau PET imaging with [18F]T807. Additional neuropsychological data from 2010 and a structural MRI from 2011 enabled us to perform longitudinal analyses of neuropsychological performance, cortical thickness, and subcortical volumes. Cognitive performance as assessed by neuropsychological testing, declined over the 5-year period from 2010 to 2015, especially in the domains of executive functioning, verbal fluency, and fine motor skills. Overall performance was below average on tests of narrative memory and naming but was average or higher in other memory and language tests. In longitudinal structural analysis, left frontal areas (Broca's area, medial orbitofrontal cortex), the lateral temporal areas, and the basal ganglia showed greatest volume losses, with apparent sparing of medial temporal lobe structures. PET imaging was negative for amyloid but revealed possible multifocal [18F]T807 retention, consistent with postmortem patterns of tau deposition in CTE at the junction of cortical grey matter and white matter.

Although the definitive identification of the neuropathological retention of [18F]T807 requires postmortem correlation, our data suggests that [18F]T807 may inform future diagnostic criteria for CTE in living patients.

Florbetapir-binding increase from 20 to 60 years old in the temporal lobe: What does it mean?

Julie Gonneaud, Eider M. Arenaza-Urquijo, Miranka Wirth, Géraldine Poisnel, Florence Mézenge, Brigitte Landeau, Alexandre Bejanin, Robin de Flores, Malo Gaubert, Béatrice Desgranges, Gaëlle Chételat

Inserm-EPHE-UCBN U1077, Caen, France

Alzheimer's disease (AD) is characterized by accumulation of cortical beta-amyloid (Aβ), mainly in medial frontal and posterior cingulate regions. Aβ accumulation is thought to start about 15 years before symptoms but studies on healthy controls focused on participants older than 50 yrs. The present study aimed at assessing Aβ deposition across the adult lifespan, from 20 to 60 yrs old.

Fifty-three cognitively normal individuals aged 20 to 60 underwent a florbetapir-PET scan. Florbetapir-PET images were spatially normalized using MRI parameters and scaled using the cerebellum gray matter (GM) values. Voxelwise correlations were performed between florbetapir-PET images and age.

A significant linear age-related Aβ increase was found in the bilateral temporal neocortex (Figure 1). Complementary analyses were conducted to assess the validity and robustness of these findings including normalization on a PET template, extraction of the values from native space images, extraction from the native space images removing the extreme 10%-values that may reflect white matter (WM) or cerebrospinal fluid spillover, application of a thin GM band to avoid contamination by WM fixation, correction for GM volume, replication in the 20-50 yrs old. The same findings were recovered in all these analyses.

Our results revealed that florbetapir-binding increases linearly in the temporal lobe from 20 to 60 yrs old. This increase is unlikely to be explained by methodological bias due to spatial normalization, voxelwise analyses, WM spillover or age-related changes in GM volume. It suggests that Aβ starts accumulating earlier and elsewhere than usually thought. This may be surprising considering that neuropathological studies indicate a low frequency of Aβ plaques before 50. Alternatively, it might reflect the binding of florbetapir to another process, itself linearly related with age. Further studies are needed, with other tracers and including neuropathological analyses, to understand this specific binding in the temporal neocortex.

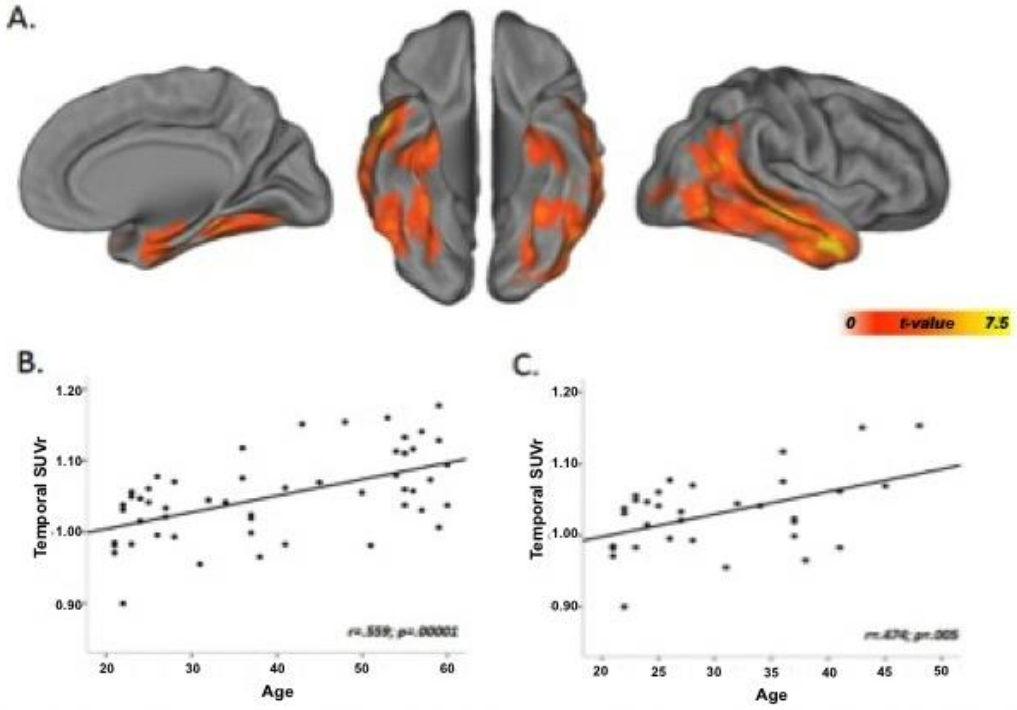

Figure 1. Results of the voxelwise correlation analysis showing an age-related increase in Aβ depositions in the bilateral temporal neocortex, including the lateral temporal noecortex, the temporal pole and the parahippocampal cortex, at $p < .05$ (family-wise error-corrected) and superimposed onto an inflated reconstruction of the MNI template brain (A). Plots illustrate the positive correlations between age and Aβ deposition values in the temporal cortex within the whole sample (20-60 yrs old) (B) and within individuals aged 20 to 50 yrs old (C).

Imaging aggregates of amyloid and tau in dementia with Lewy bodies and Parkinson's disease

Stephen Gomperts, Joseph Locascio, Sara Makaretz, Aaron Schultz, Brad Dickerson, John Growdon, Keith Johnson

Massachusetts General Hospital, MA, United States

Background: Deposits of beta-amyloid and tau are common in dementia with Lewy bodies and Parkinson's disease and may contribute to their course. PET radioligands that label paired helical filaments of tau (PHF-tau), such as [F18]T807, have recently been developed. Together, amyloid and PHF-tau imaging provide a means to evaluate, antemortem, the contribution of these co-pathologies to DLB and PD. We hypothesized that beta-amyloid would accelerate cognitive decline in DLB and PD dementia (PDD) and that PHF-tau deposition would be elevated in DLB and in PD-associated cognitive impairment.

Methods: 16 DLB and 17 PDD subjects underwent [C11]PiB PET and underwent annual neurologic and neuropsychological assessments for an average of 3.3 visits. 7 DLB, 9 PD with normal cognition (PDnl), and 8 PD with either PDD or PDMCI (PDimpaired) underwent [F18]T807 PET and were compared with 29 healthy control subjects (HCS) with negligible PiB retention. [C11]PiB retention was expressed as the distribution volume ratio with cerebellar reference. [F18]T807 retention was expressed as the SUVR using cerebellar gray matter as reference. Groups were similar in age.

Results: Greater baseline cortical PiB retention in DLB and PDD was associated with faster decline in the CDR sum of boxes score ($p=0.026$, mixed random/fixed effects longitudinal model). Cortical T807 retention was prominent in the inferior temporal region, where it differed across the diagnostic groups ($p=0.013$, Kruskall-Wallis test for a main effect of group). Post hoc tests indicated that T807 binding was higher in DLB than in HCS ($p=0.005$, Wilcoxin test) or PDnl ($p=0.034$). In addition, T807 binding in the PDimpaired group trended higher than HCS ($p=0.053$). We are exploring the relation of T807 retention to cognitive function and PiB retention.

Conclusions: These results suggest that amyloid deposition accelerates cognitive decline in DLB and PDD. In addition, our early experience with T807 suggests that PHF-tau deposition may contribute to DLB.

Metabolite analysis of tau PET tracer [18F]THK-5351

Ryuichi Harada[1], Nobuyuki Okamura[1, 2], Shozo Furumoto[3], Tetsuro Tago[3], Katsutoshi Furukawa[4], Aiko Ishiki[4], Ren Iwata[4], Manabu Tashiro[3], Hiroyuki Arai[4], Kazuhiko Yanai[2, 3], Yukitsuka Kudo[1]

[1]*Division of Neuro-imaging, Institute of Development, Aging and Cancer, Tohoku University, Japan*
[2]*Department of Pharmacology, Tohoku University School of Medicine, Japan*
[3]*Cyclotron and Radioisotope Center, Tohoku University, Japan*
[4]*Department of Geriatrics and Gerontology, Institute of Development, Aging and Cancer, Tohoku University, Japan*

Objectives: For the quantitative measurement of tau in the brain, it is ideal that the radioactive metabolites do not enter into the brain and not bind to specific target in the brain. In this study, we investigated the metabolism of [18F]THK-5351 in human and characterized the pharmacological properties of radiolabeled metabolites.

Methods: Venous blood samples were taken from 3 human subjects after injection of [18F]THK-5351 and the extracted plasma was analyzed by high performance thin layer chromatography. The metabolite was isolated from mouse plasma following injection of 1 mg/kg cold THK-5351, and MALDI-TOF MS spectrometry was used to determine identity. Enzymatic assay was additionally performed to confirm this metabolite. The suspected metabolite was chemically synthesized. Furthermore, the radiolabeled metabolite was isolated from mouse liver after intravenous injection of [18F]THK-5351. The brain uptake of radiolabeled metabolite was evaluated in mice and the binding ability of radiolabeled metabolite to tau aggregates was also evaluated by the autoradiography of human brain sections.

Results: About 13% of unmetabolized fraction remained detectable in human plasma at 60 min following injection of [18F]THK-5351. The sulfoconjugate of [18F]THK-5351 was identified as the major metabolite by MALDI-TOF MS spectrometry. Chemically synthesized sulfated THK-5351 were chromatographically identical to those of the metabolite extracted from mouse and human plasma. This metabolite was produced by the incubation with liver homogenates, but not with brain homogenates. The radiolabeled metabolite of [18F]THK-5351 did not enter into mouse brain after intravenous administration. Furthermore, the radiolabeled metabolite did not bind to tau and other protein deposits in human brain sections.

Conclusions: Sulfoconjugate was identified as the major metabolite of [18F]THK-5351. This metabolite does not cross the blood-brain barrier to a significant extent. These results suggest that the radioactivity in the brain after intravenous administration of [18F]THK-5351 is entirely comprised of unchanged [18F]THK-5351.

Tau imaging relationships with amyloid-beta imaging, CSF tau/Aβ42, and cognition in Alzheimer's disease

Beau Ances[1], Matthew Brier[1], Brian Gordon[2], Karl Friedrichsen[2], John McCarthy[3], Ari Stern[3], Yi Su[2], Jason Hassenstab[1], Nigel Cairns[1], David Holtzman[1], Anne Fagan[1], John Morris[1], Tammie Benzinger[2]

[1]*Department of Neurology Washington University in Saint Louis, MO, United States*
[2]*Department of Radiology Washington University in Saint Louis, MO, United States*
[3]*Department of Mathematics Washington University in Saint Louis, MO, United States*

Alzheimer's disease (AD) is characterized by two molecular pathologies: cerebral beta-amyloidosis (amyloid-beta [Ab] plaques) and tauopathy (neurofibrillary tangles, neuritic plaques and neuropil threads). Until recently, only Ab topographies could be studied in vivo in humans owing to a lack of tau positron emission tomography (PET) imaging agents. Current clinic-pathological studies link tau pathology closely to the onset and progression of cognitive symptoms AD. This study reports on PET tau and Ab imaging results in a cohort of cognitively normal older adults and those with very mild AD (Figure 1).

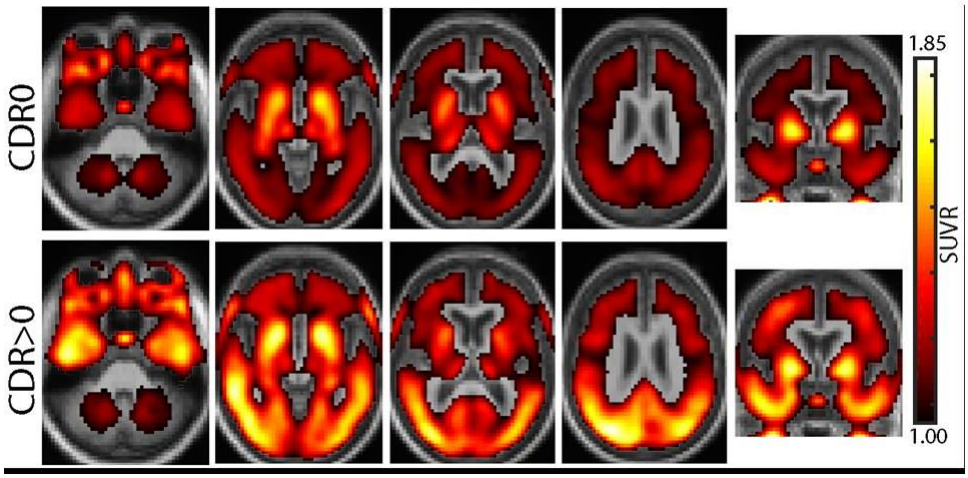

Figure 1. Tau topographies in participants with and without clinical AD.

Multivariate analyses identified unique disease-related spatial topographies in both tau and Ab deposition. These PET tau and Aβ topographies were spatially unique but strongly related (Figure 2).

Cerebrospinal fluid measures of tau, often used to stage preclinical AD, were strongly correlated with tau deposition in the temporal lobe. Tau deposition in the temporal lobe more closely tracked dementia status and was a better predictor of cognitive performance than Ab deposition in any region of the brain (Figure 3). These data support models of AD where tau pathology closely tracks changes in brain function responsible for the onset of early symptoms.

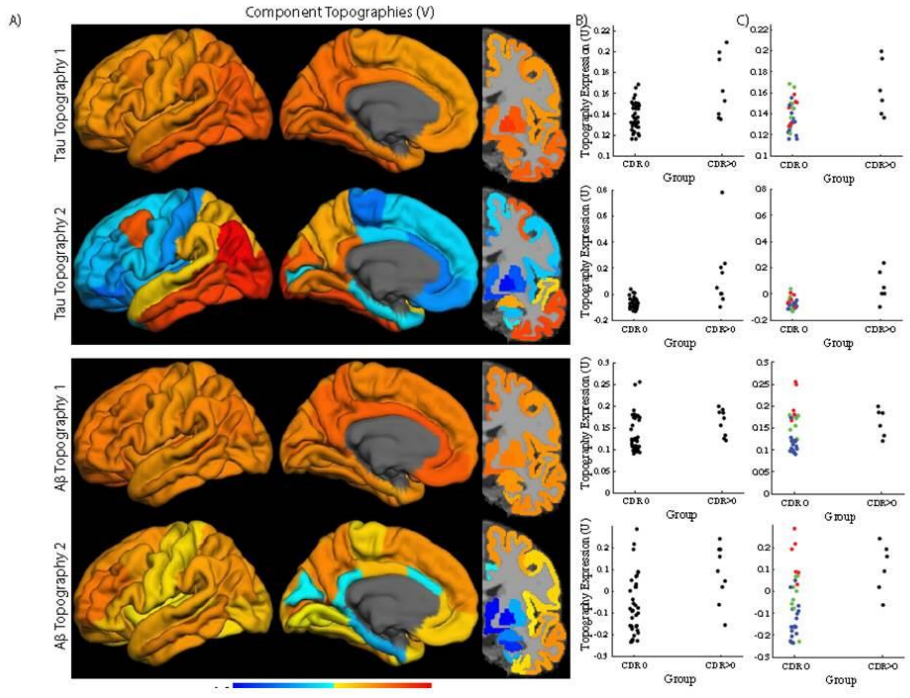

Figure 2. PET tau and Aβ topographies are associated with disease severity. A: Singular value decomposition (SVD) of tau and Aβ represented as topographies. B: The representations of these topographies varies with CDR for both PET tau topographies and the second PET Aβ topography. C: Similar graphs as (B) but only participants with CSF are included.

Figure 3: CSF and Neuropsychological Performance are predicted by the total weight of the tau and Aβ topographies. A: Penalized regression models that predict CSF tau and Aβ42. B: Penalized regression models that predict neuropsychological performance.

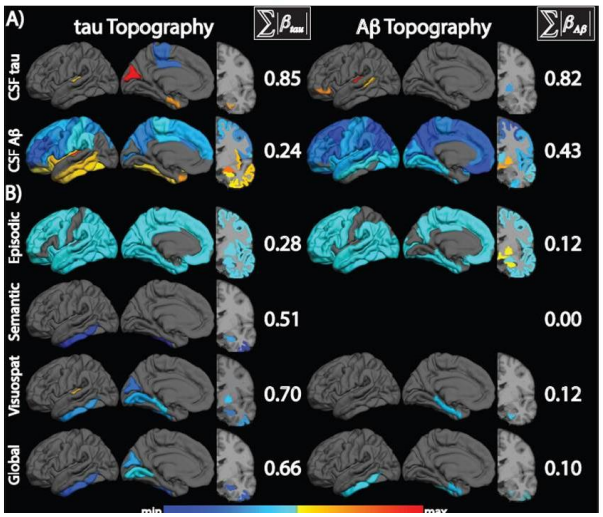

Higher cortical amyloid is associated with loneliness in cognitively normal older adults

Nancy Donovan[1], Victoria Jonas[2], Patrizia Vannini[1, 2], Aaron Schultz[2], Elizabeth Mormino[2], Rebecca Amariglio[1, 2], Dorene Rentz[1, 2], Olivia Okereke[1, 2], Gad Marshall[1, 2], Keith Johnson[1, 2], Reisa Sperling[1, 2]

[1]*Brigham and Women's Hospital, MA, United States*
[2]*Massachusetts General Hospital, MA, United States*

Background: Loneliness is a perceived state of social and emotional isolation that is distinct from depression and has been associated with cognitive decline and risk of Alzheimer's disease (AD) dementia. Loneliness may be a sensitive symptom of brain changes related to preclinical AD in older people.

Objective: To determine whether in vivo measures of cortical amyloid and entorhinal tau, are associated with greater loneliness in cognitively normal (CN) older adults.

Methods: We performed cross-sectional analyses using data from 89 CN, community-dwelling men and women, age 69-89, participating in the Harvard Aging Brain Study. Loneliness was assessed using the 3-item UCLA loneliness scale, an instrument well-validated for elderly samples. A continuous, aggregate measure of amyloid, determined by Pittsburgh Compound B-PET was used as a predictor of loneliness in regression models adjusting for age, sex, APOE4 carrier status, socioeconomic status, depression, anxiety and social network. A second model included the interaction of amyloid with APOE4 as a predictor. The primary analysis was repeated using entorhinal tau, measured by T807 (AV1451) PET, as the predictor for loneliness, using the same covariates, without and with amyloid.

Results: Higher amyloid significantly predicted greater loneliness (β=0.4, p=0.002; for the model R2=0.3, p=0.001). Furthermore, the interaction of high amyloid burden and the presence of the APOE4 allele was associated with greater loneliness (β= 0.6, p<0.0001; for the model R2=0.3, p<0.0001). Entorhinal tau also predicted loneliness in the analogous model (β=0.2, p=0.04; for the model R2=0.21, p=0.015) but not when controlling for amyloid.

Conclusions: We report novel associations of loneliness with cortical amyloid and entorhinal tau and present loneliness as a neuropsychiatric symptom relevant to preclinical AD in CN older people. This work will inform new research into the neural underpinnings and disease mechanisms involved in loneliness and may enhance early detection and intervention research in AD.

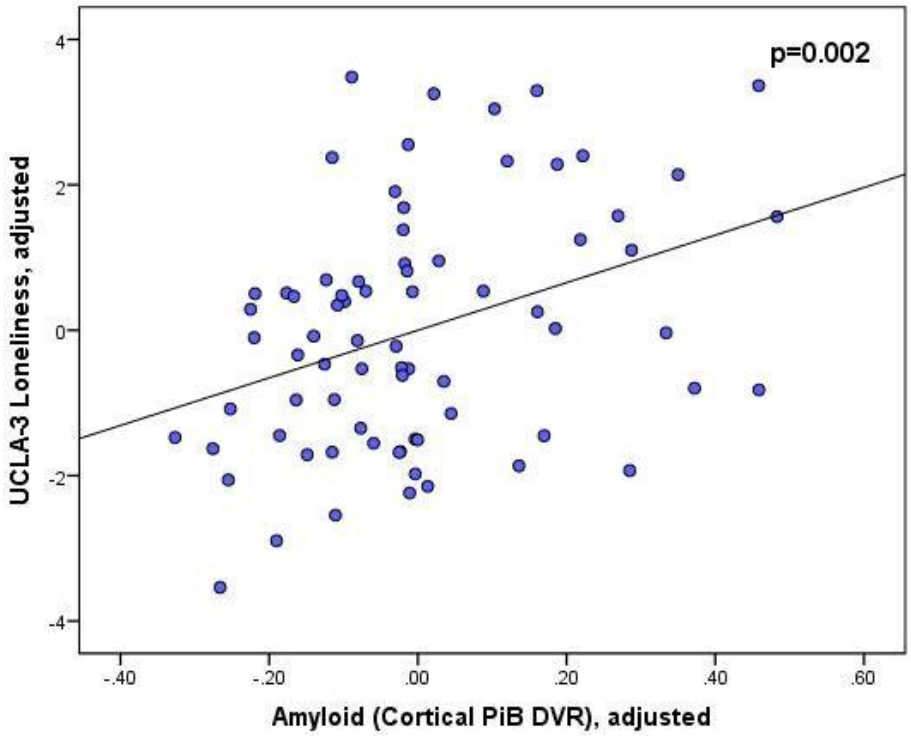

Tau PET imaging in relation to amyloid β and neurodegeneration biomarkers in aging and AD

Liang Wang, Tammie Benzinger, Yi Su, Jon Christensen, Karl Friedrichsen, Jon McConathy, Nigel Cairns, Anne Fagan, John Morris, Beau Ances

Washington University in St. Louis, MO, United States

Objective: 1) To assess whether tau accumulation is associated with brain volume loss, and 2) to determine whether the presence of amyloid b (Ab) plaques modulates tau accumulation and its association with volume loss.

Methods: Cognitively normal individuals (N=50) or participants with symptomatic AD (N=12) were imaged by positron emission tomography using [F-18]-AV-1451 and structural MRI. Brain amyloid burden was measured by cerebrospinal fluid (CSF) Ab42 in a subset of the cohort. [F-18]-AV-1451 binding (i.e., standardized uptake value ratio, SUVR) was assessed with respect to brain volumes (i.e., the hippocampus and AD signature) as well as CSF Ab42 status [positive (i.e., low Ab42 levels) vs. negative (i.e., high Ab42 levels)].

Results: An inverse association of regional SUVR and volume was seen in both the hippocampus and AD signature (Figure 1). CSF Ab42 status affected regional SUVR and its association with volume differentially. Specifically, hippocampal SUVR was not different according to CSF Ab42 status but its relationship with hippocampal volume was, with such relationship seen in CSF Ab42 positive but not CSF Ab42 negative individuals. In contrast, AD signature SUVR was elevated in CSF Ab42 positive compared to CSF Ab42 negative participants. However, the relationship between AD signature SUVR and thickness was not different with respect to CSF Ab42 status. Interestingly, across 6 AD signature regions, the magnitude of observed relationship was decreased in an order that was consistent with the hypothetic sequence of tau spreading (i.e., entorhinal cortex to temporal and to parietal neocortices) (Figure 2). In the vertex-wise analysis, the association of increased [F-18]-AV-1451 binding and reduced cortical thickness was observed in the topography of areas similar to AD signature (Figure 3).

Conclusion: [F-18]-AV-1451 has potential for tracking tau pathology and related neurodegenerative changes in AD. [F-18]-AV-1451 PET in combination with Ab markers may provide new insight into the pathophysiology of AD.

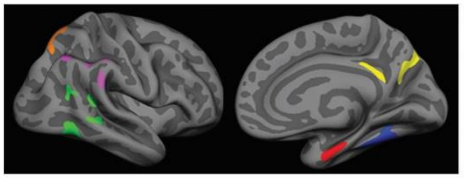

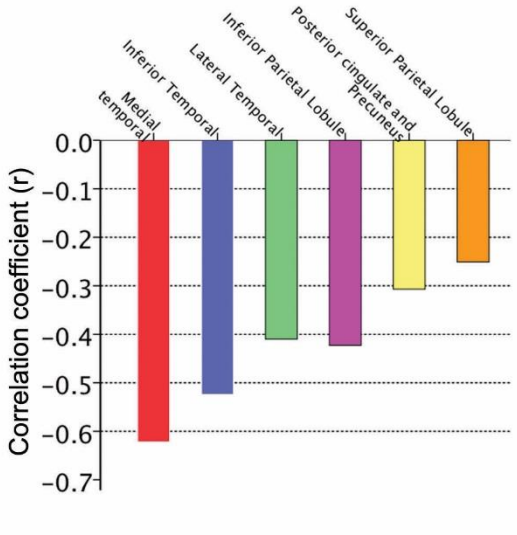

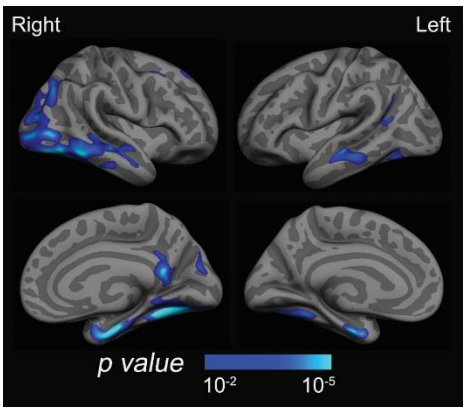

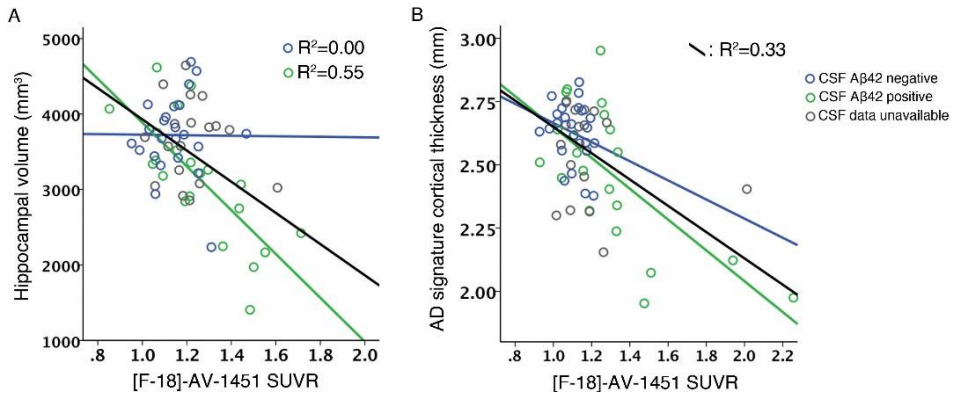

Contributions of age and Alzheimer's pathology to hippocampal memory network function in healthy elderly

Shawn Marks[1], Samuel Lockhart[1], Katelyn Arnemann[1], Jacob Vogel[1], Henry Schwimmer[1], William Jagust[1, 2]

[1]Helen Wills Neuroscience Institute, University of California, Berkeley, CA, United States
[2]Life Sciences Division, Lawrence Berkeley National Laboratory, CA, United States

Hippocampal function during memory encoding can be conceptualized as engaging in pattern separation in order to orthogonalize similar events into distinct memories. Episodic memory deficits are common in aging and Alzheimer's disease (AD). We sought to investigate whether age and AD pathology affect the memory network by imaging neural function, tau accumulation, and beta-amyloid (Ab).

Thirty cognitively normal older adults and 11 young controls participated in a functional MRI paradigm designed to emphasize pattern separation. A subset of elderly participants underwent Pittsburgh Compound B and AV-1451 PET scans, as well as structural and resting-state MRI. Older adults performed worse on the memory task by demonstrating a bias towards pattern completion, not separation. They showed increased activation in left dentate gyrus/CA3 (DGCA3) during encoding of subsequent false alarms when compared to young controls. Increased DGCA3 activity was associated with worse task performance at trend levels, suggesting this activity is not a form of successful compensation. Elevated tau in a composite Braak 1-2 region was associated with increased DGCA3 activation. Unlike tau, Aβ was not directly related to task performance or hippocampal function; however, Aβ was modestly correlated with network connectivity, such that elevated Aβ was associated with decreased connectivity between retrosplenial cortex and parahippocampal gyrus. The same measure of connectivity was negatively associated with DGCA3 activation during subsequent false alarms.

These preliminary results suggest that age and AD pathology may influence memory in two distinct ways. First, medial temporal lobe tau accumulation leads to local changes in the hippocampus, altering its function. Second, Aβ reduces hippocampal-neocortical connectivity which also interferes with hippocampal function. These two pathologies together may have a clinical effect on episodic memory function.

[^{18}F]GTP1 - A tau specific tracer for imaging tau-pathology in AD

Jan Marik[1], Jeff Tinianow[1], Annie Ogasawara[1], Ning Liu[1], Simon Williams[1], Joseph Lyssikatos[1], Olivier Barret[2], Gilles Tamagnan[2], Danna Jennings[2], John Seibyl[2], Ken Marek[2], Robby Weimer[1], Sandra Sanabria Bohorquez[1]

[1]gRED, Genentech Research and Early Development, Genentech, Inc., South San Francisco, CA, United States
[2]Molecular NeuroImaging LLC, New Haven, CT, United States

[^{18}F]GTP1 was selected from a library of compounds by autoradiographic assay using human brain tissues containing various levels of tau and Aβ pathology. [^{18}F]GTP1 bound selectively to tau-positive tissues but did not bind to tau-negative yet Aβ-positive tissues; binding affinity to tau was 14.9±4.3nM, suggesting [^{18}F]GTP1 exhibits sufficient properties to enable its use as a tau PET probe. In mice and rhesus, [^{18}F]GTP1 exhibited good brain uptake and rapid clearance, however a low level of bone uptake was detected in mice 14.3±1.7%ID/g and rhesus (SUV 0.4). Susceptibility to enzymatic defluorination was further assessed by liver microsomes in-vitro. [^{18}F]GTP1 exhibited low levels of defluorination when incubated with mouse (13.8±2.4%) and rhesus (15.4±1.3%) liver microsomes, but no-defluorination (0%) was observed with human liver microsomes, suggesting defluorination should not impede the interpretation of [^{18}F]GTP1 human imaging data.

A first-in-human [^{18}F]GTP1 study was conducted in two healthy volunteers (HV; mean age 36y) and three probable AD subjects (mean age 72y, mean MMSE 16) to assess the tracer properties. Dynamic scans were acquired for up to 180min. Tracer uptake was quantified using SUVR (target to cerebellum gray ratio). [^{18}F]GTP1 exhibited high initial brain uptake, rapid washout and low non-specific binding, in particular in the white matter. No defluorination was observed during the scan duration. In the 90-120min interval, homogeneous uptake was observed in the HV in cortical areas (median SUVR=1.04), whereas elevated retention was observed in regions expected to contain tau pathology: temporal (SUVR up to 3), parietal (up to 2.4), fusiform (up to 2.7) cortices. The uptake pattern varied among AD patients and between hemispheres, consistent with known heterogeneity of tau pathology. Preliminary PET data suggest [^{18}F]GTP1 has both excellent signal to noise properties and good dynamic range making this a potentially superior agent for in-vivo assessment of tau pathology.

Imaging tau and beta amyloid using ^{11}C-PiB, ^{18}F-THK-5117, and ^{18}F-THK-5351 in Alzheimer's disease

Tobey Betthauser[1], Patrick Lao[1], Dhanabalan Murali[1], Todd Barnhart[1], Shozo Furumoto[3], Nobuyuki Okamura[3], Charles Stone[4], Sterling Johnson[2], Bradley Christian[1]

[1]*University of Wisconsin-Madison, Department of Medical Physics, WI, United States*
[2]*Univeristy of Wisconsin-Madison, Alzheimer's Disease Research Center, WI, United States*
[3]*Tohoku University, Sendai, Japan*
[4]*University of Wisconsin-Madison, School of Medicine and Public Health, WI, United States*

Introduction: Alzheimer's disease is characterized by accumulation of beta amyloid (Aβ) and hyperphosphorylated tau proteins, which neuropathology suggests follow distinct spatiotemporal patterns. ^{11}C-PiB, ^{18}F-THK-5117, and ^{18}F-THK-5351 are PET radioligands for fibrillar Aβ (PiB), and neurofibrillary tau (THK) aggregates. Tau, more so than Aβ, is thought to correlate with cognitive decline in AD. This cross-sectional study observes spatial patterns of aggregated tau and Aβ in individuals ranging in age, AD risk factors, and cognitive status.

Methods: N=16 subjects (4 cognitively normal, 5 cognitive declining, 4 MCI, 2 AD, 1 non-AD dementia) underwent T1-weighted MRI, ^{11}C-PiB (70min dynamic), and ^{18}F-THK-5117 (n=14) and/or ^{18}F-THK-5351 (n=3) (90min dynamic) scans. PET time series were coregistered to T1w MRI, and FreeSurfer segmented. Distribution volumes ratios were calculated (Logan 1996) using a cerebellar gray matter reference region. Subjects were grouped and rank ordered by disease severity based on longitudinal neuropsychological assessment and clinical diagnosis upon study enrollment. Spearman's rank analyses were performed to assess monotonic relationships between PiB, THK, and cognitive status. THK kinetics were also assessed.

Results: Significant spatial inter-correlation of PiB and THK DVRs and affected volumes were observed globally, and regionally in temporal, parietal, occipital and frontal cortices, and the fusiform gyrus, but not medial temporal lobe, independent of cognitive status. These regions also showed correlations between Aβ and tau measures and cognitive decline, though, only tau measures in the ventral and lateral temporal, lateral parietal, and occipital cortices survived multiple comparisons correction. In WM, THK compounds exhibited slow uptake and clearance, with THK-5351 showing a 1.5-fold reduction compared to THK-5117 at t>40 min. In GM, THK-5351 and THK-5117 demonstrated rapid kinetics and linearization of Logan plots (t*=30 min).

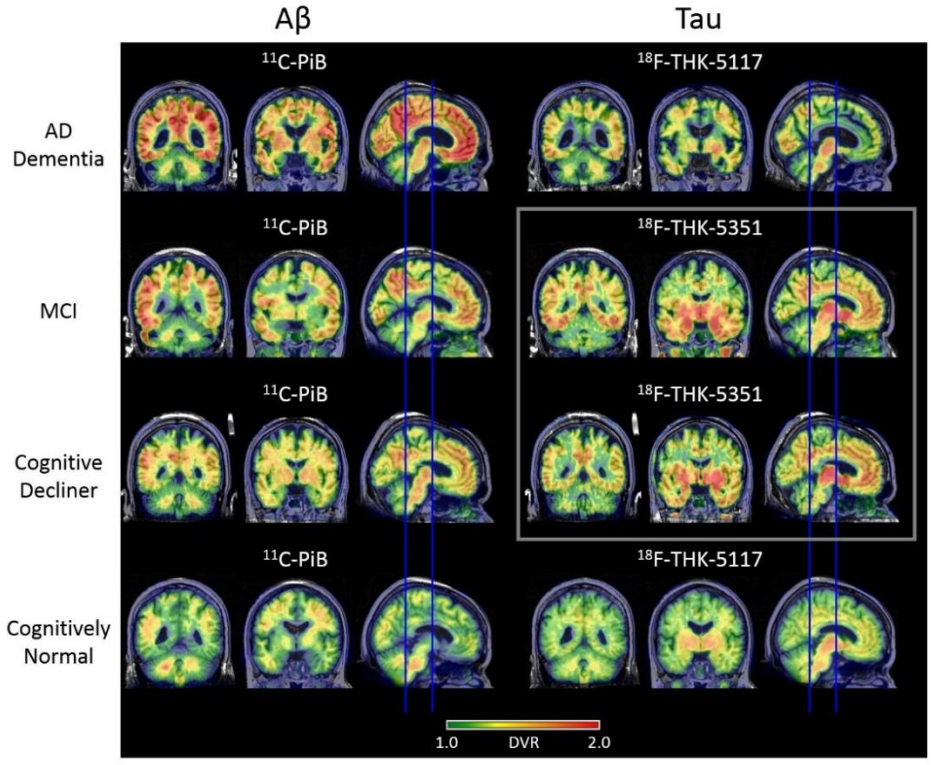

Figure 1: Paired PiB (left) and THK (right) parametric DVR images. All subjects had some degree of THK binding in the medial temporal lobe. Regions in the temporal, parietal, and occipital cortices and the fusiform gyrus correlated with cognitive decline. The gray box distinguishes between THK-5117 and THK-5351.

Conclusion: These data indicate combined regional Aβ and tau accumulation may play a role in cognitive dysfunction. Additional studies of paired PiB/THK-5351 are ongoing.

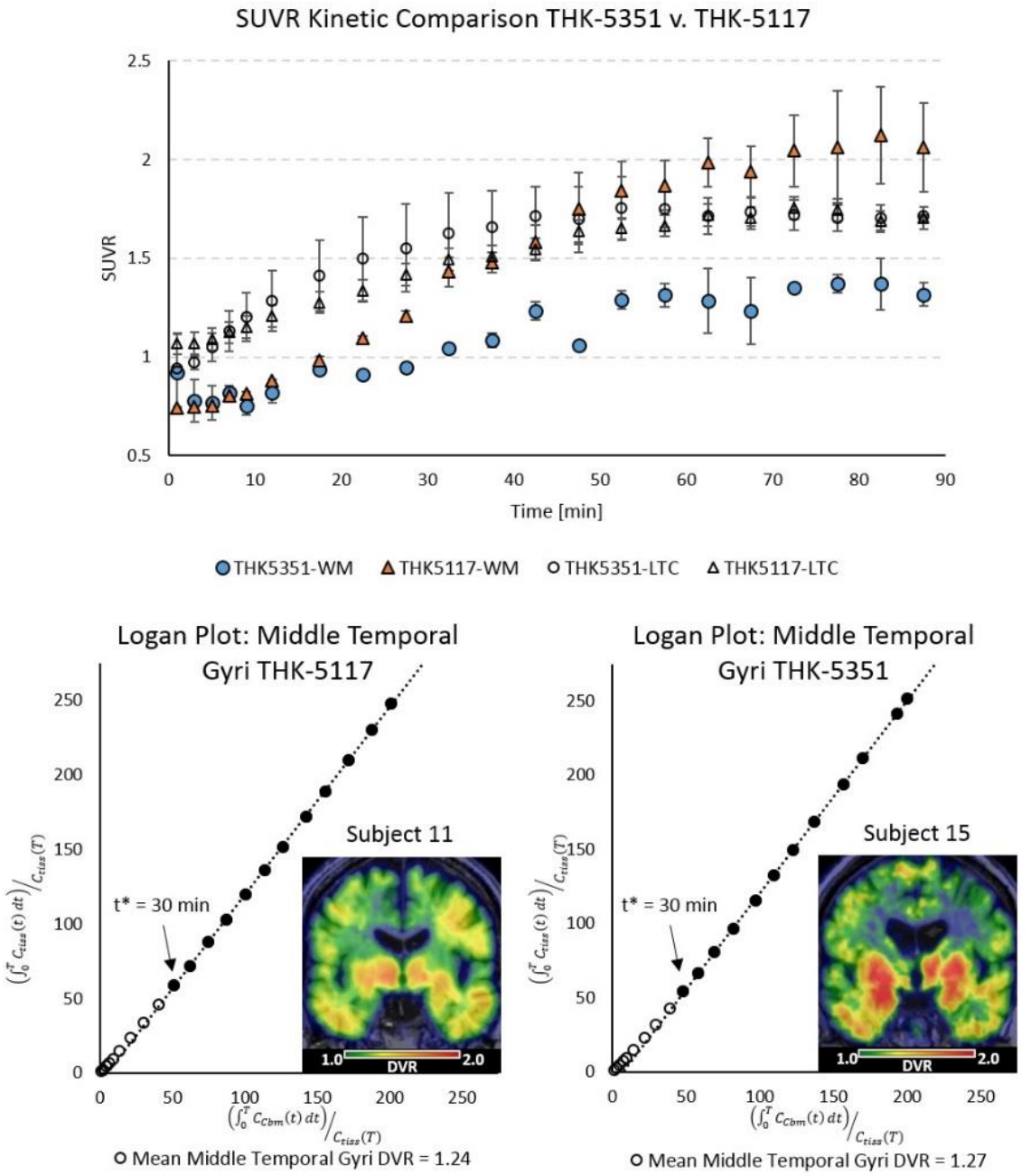

Figure 2: Comparison of THK-5117 and THK-5351 kinetics in cerebellar WM and lateral temporal GM (middle temporal gyrus) using cerebellar GM as a reference region (top). Data was taken from 4 MCI subjects (THK-5117x2, THK-5351x2). Temporal cortex was chosen based on similar mean DVR values for both tracers ($\overline{DVR}$ = 1.37 for THK-5351 and $\overline{DVR}$ = 1.36 for THK-5117). Logan plots of THK-5117 (bottom left) and THK-5351 (bottom right) showing linearization in the middle temporal gyrus in two MCI subjects. Inset images are coronal slices taken at the level of the uncus for each subject.

Association between years of education and Aβ deposition in cognitively normal adults, mild cognitive impairment and Alzheimer's disease: evidence for reserve

Eider Arenaza-Urquijo[1, 2, 3, 4], Alexandre Bejanin[1, 2, 3, 4], Miranka Wirth[1, 2, 3, 4], Julie Gonneaud[1, 2, 3, 4], Renaud La Joie[1, 2, 3, 4], Justine Mutlu[1, 2, 3, 4], Malo Gaubert[1], Vincent De la Sayette[1, 2, 3, 5], Francis Eustache[1, 2, 3, 4], Gaël Chételat[1, 2, 3, 4]

[1]*INSERM, U1077, Normandy, France*
[2]*University of Caen Lower-Normandy, UMR-S1077, Normandy, France*
[3]*Ecole Pratique des Hautes Etudes, UMR-S1077, Normandy, France*
[4]*CHU de Caen, U1077, Normandy, France*
[5]*CHU de Caen, Neurology Service, Normandy, France*

Background: In cognitively normal older adults, higher cognitive engagement (measured by lifespan cognitive activities or years of education) has been related to lower or slower Aβ deposition suggesting a neuroprotective effect of cognitive engagement on Aβ. In contrast, AD patients with higher cognitive engagement (measured by years of education) have shown higher Aβ deposition to reach a certain level of cognitive performance, suggesting compensation. We studied this crossover effect assessing the relation between Aβ deposition and years of education from cognitively normal older adults to AD, including MCI patients. In a second step, we investigated potential reserve mechanisms by taking advantage of a multimodal neuroimaging approach.

Methods: Fifty-six normal older adults, 29 MCI and 20 AD patients underwent florbetapir-PET, FDG-PET and MRI examinations. Voxel-wise correlations between years of education and florbetapir-PET were assessed within each group, including age, sex and global cognitive function as covariates ($p<0.05$ FDR corrected). When a significant relationship was found, further analyses were conducted with gray matter volume and FDG-PET metabolism.

Results: Higher years of education were related to increase Aβ deposition in frontal, parietal and temporal regions in MCI patients. Such association was not found in normal older adults and AD. Complementary analyses in MCI i) revealed increased FDG-PET metabolism related to higher years of education restricted to the areas where Aβ increases with education were found and ii) suggest a link between metabolism and Aβ in higher educated MCI patients.

Conclusions: Our results have different implications; first, considering normal older adults, MCI and AD, education-related compensation for Aβ appears to be maximal at MCI stage. Second, higher FDG-PET metabolism in higher educated MCI patients may protect against the deleterious effects of Aβ deposition such that more Aβ deposition would be needed in higher educated MCI patients to convert to AD.

MR imaging biomarkers of brain amyloid in cognitive impairment

Sara Shams[1], Mykol Larvie[2], Juha Martola[1], Tobias Granberg[1], Andreas Charidimou[4], Michael Lev[2], Maria Kristoffersen Wiberg[1], Lars-Olof Wahlund[3]

[1]*Department of Radiology, Karolinska University Hospital, Stockholm, Sweden*
[2]*Department of Radiology, Massachusetts General Hospital, MA, United States*
[3]*Department of clinical geriatrics, Karolinska University Hospital, Stockholm, Sweden*
[4]*Hemorrhagic Stroke Research, Massachusetts General Hospital, MA, United States*

Introduction: Cerebral small vessel disease (SVD) is the most common comorbidity with Alzheimer pathology and is an important determinant of cognitive impairment. SVD affects cerebral microvasculature that is too small for direct observation with routine clinical imaging, and so correlative imaging biomarkers of SVD are utilized as markers for the disease. Cerebral amyloid angiopathy (CAA) and hypertensive arteriopathy are among the most common etiologies of SVD, and SVD related to CAA may serve as imaging biomarkers of brain amyloid in cognitive impairment. We hypothesized that this was the case, and investigated MR SVD markers of amyloid in the brain.

Methods: Patients undergoing memory investigation (n=1039) underwent an MR scan and cerebrospinal fluid (CSF) sampling. CSF analysis was done for amyloid β (Aβ) 42, total tau (T-tau), and phosphorylated tau (P-tau). MR images were assessed for all proposed imaging markers of SVD: cerebral microbleeds, cortical superficial siderosis, white matter hyperintensities, lacunes, and cortical microinfarcts. CSF biomarkers were log-transformed, and findings were assessed with linear multivariate models, with independent analysis for each SVD marker, controlling for diagnostic group. Results are given as the standardized regression coefficient β.

Results: Increasing number of cerebral microbleeds was associated with brain amyloid deposition, low CSF Aβ 42: ($\beta = -0.15$, $P<0.001$), and this was especially true for lobar($\beta = -0.16$, $P<0.001$), but not for deep and infratentorial, microbleeds. Cortical superficial siderosis ($\beta = -0.13$, $P<0.001$) and cortical microinfarcts ($\beta = -0.12$, $P<0.001$), but not enlarged perivascular spaces, lacunes and white matter hyperintensities, were associated with increased brain amyloid, decreased CSF Aβ 42.

Conclusion: MR imaging biomarkers of SVD are associated with brain amyloid in our study. Our findings suggest that amyloid subtypes and the topographic amyloid distribution may be important determinants of SVD and this warrants further investigation.

[18F] T807 PET imaging in subcortical vascular cognitive impairment

Hee Jin Kim[1, 2], Hanna Cho[3], Young Kyoung Jang[1, 2], Yeo Jin Kim[1, 2], Jin San Lee[1, 2], Juyoun Lee[1, 2], Duk L. Na[1, 2], Chul Hyoung Lyoo[3], Sang Won Seo[1, 2]

[1]Department of Neurology, Samsung Medical Center, Sungkyunkwan University School of Medicine, Seoul, South Korea
[2]Neuroscience Center, Samsung Medical Center, Seoul, South Korea
[3]Department of Neurology, Gangnam Severance Hospital, Yonsei University College of Medicine, Seoul, South Korea

Background: Subcortical vascular cognitive impairment (SVCI) consisting of subcortical vascular mild cognitive impairment (svMCI) and subcortical vascular dementia (SVaD), is characterized by extensive small vessel disease (SVD) such as white matter hyperintensities (WMH) and lacunes in the white matter regions. Previous studies showed that 30% of SVCI patients have significant amyloid burden as measured by [11C]Pittsburgh compound B (PiB) PET. However, the distribution of tau in SVCI patients is largely unknown. Thus, we investigated the distribution of tau burden in SVCI patients.

Methods: 15 SVCI (7 svMCI and 8 SVaD) patients underwent [18F] T807 –PET to measure paired helical filament (PHF)-tau. Tau Braak stage (0, I/II, III/IV, and V/VI) was assessed based on the pattern of cortical [18F] T807 binding, visualized with surface projected SUVR>1.5.

Results: Among seven svMCI patients, five patients did not show significant T 807 binding in any region (Braak 0). Two svMCI patients showed [18F]T807 binding which does not correspond to the temporal ordering of tau distribution in Braak stage: One svMCI patient showed left hemispheric predominant deposition and the other patient showed high [18F]T807 binding in the right anterior temporal and occipital areas.

Among the 8 SVaD patients, five patients showed significant [18F] T807 binding, which corresponds to Braak stage I/II for two patients and Braak stage V/VI for three patients. One patient did not fit in the Braak stage as high [18F] T807 binding was observed only in the left anterior temporal and occipital cortices. Two patients did not show significant [18F] T807 binding in any region (Braak 0).

Conclusions: Our findings suggested that SVaD patients hand no significant tau deposition (Braak 0) or had Alzheimer's pattern of tau distribution with Braak stage ranging from I/II to V/VI. However, svMCI patients did not show tau deposition (Braak 0) or did not follow Alzheimer's pattern of tau distribution as they could not be classified into classic Braak stage.

Validation of the novel tau PET tracer RO6958948 on post mortem brain tissue

Michael Honer, Henner Knust, Luca Gobbi, Matthias Koerner, Dieter Muri, Robert Comley, Edilio Borroni

Roche Pharmaceutical Research and Early Development, Roche Innovation Center, Basel, Switzerland

Objectives: Tau aggregates represent a histopathological hallmark in Alzheimer's disease (AD) and a target for therapeutic intervention as well as PET imaging. Recently, [^{18}F]RO6958948 has been described as a promising PET tracer candidate for imaging aggregated tau in AD patients. This study presents a detailed *in vitro* characterization of this tracer candidate to examine its specificity as well as its region- and substrate-specific autoradiographic binding pattern in *post mortem* tissue sections.

Methods: Affinity of RO6958948 for tau and Aβ was assessed as displacement potency of [^{3}H]T808 and [^{3}H]florbetapir binding, respectively, using late stage AD cortex sections. Binding of tritiated RO6958948 to tissue sections of AD patients was analyzed by phosphor screen autoradiography and nuclear emulsion autoradiography, followed by co-staining of tau aggregates and Aβ plaques using specific antibodies. *In vitro* binding patterns were also examined in *post mortem* samples of striatum, cerebellum, pons and hippocampus of AD patients as well as cortical samples of Parkinson's disease and other neurodegenerative diseases.

Results: RO6958948 bound with high affinity and specificity to tau aggregates (IC_{50}=14.7±3.5nM), clearly lacking affinity for concomitant Aβ plaques in human AD Braak V cortical tissue sections (IC_{50}>10µM). Radioligand specificity for tau aggregates was confirmed by macroscopic and microscopic co-localization of radioligand binding and tau-antibody staining in AD brain sections. No significant binding was observed in brain regions devoid of tau aggregates such as striatum, pons and cerebellum of AD patients and healthy controls. Furthermore, no binding was detected to α-synuclein aggregates in Parkinson's disease tissue samples.

Conclusions: Our results indicate that RO6958948 binds specifically to tau aggregates in AD. Evaluation of this tracer candidate in healthy controls and AD patients is currently ongoing.

Low lifetime cognitive activity is associated with age-related tau pathology in normal elderly

Michael Schöll[1, 2], Eider Arenaza-Urquijo[1, 3], Samuel Lockhart[1], Daniel Schonhaut[4], Rik Ossenkoppele[4], Taylor Mellinger[1], Kaitlin Swinnerton[1], Rachel Bell[1], Suzanne Baker[5], William Jagust[1]

[1]Helen Wills Neuroscience Institute, University of California, Berkeley, CA, United States
[2]MedTech West and the Department of Clinical Neuroscience and Rehabilitation, University of Gothenburg, Sweden
[3]INSERM, U1077, Caen, France
[4]Memory and Aging Center, University of California, San Francisco, CA, United States
[5]Molecular Biophysics and Integrated Bioimaging, Lawrence Berkeley National Laboratory, Berkeley, CA, United States

We have previously shown that age is strongly linked to Alzheimer's disease (AD) related tau pathology in cognitively healthy elderly (Lockhart et al., AAIC 2015). Although age is a strong determinant for the development of AD, studies have shown that there are individual differences in the susceptibility to age-related pathological alterations.

In this study, we aimed to investigate whether lifetime participation in cognitively stimulating activities as a proxy of cognitive reserve (CR) modifies the effect of age on tau pathology measured with ^{18}F-AV-1451 tau positron emission tomography (PET). Thirty-three healthy elderly subjects (mean age 78.6 ± 5.1; MMSE 28.8 ± 1.2; 16.3 ± 1.9 years of education) underwent AV-1451 PET. Based on FreeSurfer parcellations of corresponding magnetic resonance images (MRI), we created regions of interest (ROI) corresponding to Braak stages I-VI and assessed AV-1451 retention in these ROIs. Information from the Wilson lifetime cognitive activity interview was used to rate CR. Using a median split of this measure, study participants were classified into low (n = 17) and high (n = 16) cognitive activity groups. These groups were included in a multivariate general linear model in order to test the interaction effect between age and cognitive activity group (low vs high) on AV-1451 uptake adjusted for sex and years of education.

We observed a significant age*cognitive activity group interaction effect on AV-1451 uptake in all examined ROIs (all $p < .05$). The interaction was such that older age was significantly associated with increase AV-1451 uptake exclusively in the low cognitive activity group.

These preliminary results suggest that tau accumulation in the aging brain may be influenced by lifetime cognitive activities, which may ultimately alter the risk of developing cognitive decline and dementia.

Imaging neuroinflammation, amyloid and tau in mild cognitive impairment and Alzheimer's disease

Melanie Dani[1], Melanie Wood[1], Zhen Fan[1], Grazia Femminella[1], Valeria Calsolaro[1], Adam Waldman[1], Rebecca Atkinson[1], Richard Morgan[1], David Brooks[1, 2], Paul Edison[1]

[1]Neurology Imaging Unit, Imperial College London, Hammersmith Hospital, London, United Kingdom
[2]Department of Nuclear Medicine, Aarhus University, Aarhus, Denmark

Introduction: Abnormal extracellular amyloid plaques, inflammation and tau are the pathological hallmarks of Alzheimer's disease (AD). The relationship between amyloid, tau and inflammation has not been evaluated before. Here, we evaluate the relationship between amyloid, tau and neuroinflammation in healthy controls, AD and Mild Cognitive Impairment (MCI) subjects using ^{18}F-flutemetamol, ^{18}F-AV1451 and ^{11}C-PBR28 PET.

Methods: 11 subjects (3 AD, 8 MCI) underwent PET imaging with ^{18}F-AV1451 (185MBq), ^{18}F-flutemetamol (185MBq), ^{11}C-PBR28 (370MBq) and T1/T2-weighted MRI scans. 13 healthy controls also had ^{11}C-PBR28, 17 controls had ^{18}F-flutemetamol and 4 controls had ^{18}F-AV1451 from a larger study.

^{11}C-PBR28 scans were analysed using a 2 tissue compartment model, with arterial input. Volume of distribution (V_T) of different cortical regions was estimated. ^{18}F-AV1451 and ^{18}F-flutemetamol were analysed using target to cerebellar ratio. Uptake more than 2 standard deviations of the mean of the controls was considered significant.

Results: Amyloid and Tau, No Inflammation: 2 MCI and 2 AD subjects had widespread deposition of amyloid and tau, but no evidence of inflammation

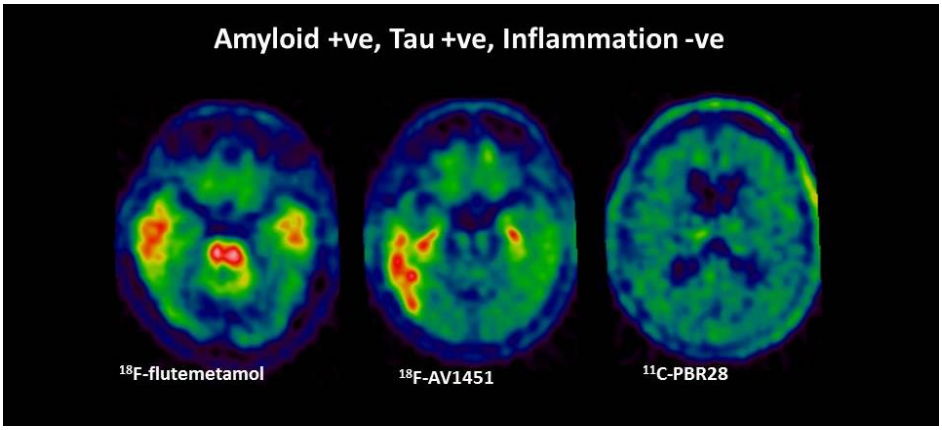

Amyloid and Inflammation, no Tau: 2 MCI subjects had widespread inflammation and amyloid deposition, but no evidence of tau deposition beyond the MTL.

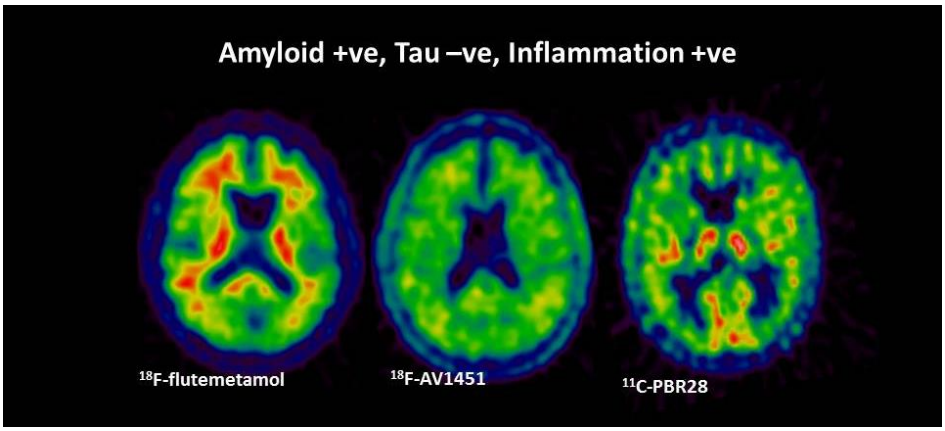

Inflammation, No Amyloid, No Tau: 1 MCI subject had widespread inflammation, but no evidence of amyloid or tau, and 1 MCI subject had inflammation limited to the thalamus, but with no evidence of amyloid or tau.

No Amyloid, No inflammation, No Tau: 1 AD and 1 MCI subject had no evidence of amyloid, inflammation or tau.

Conclusion: From this small cohort, inflammation appears to be independent of amyloid and tau in MCI and can occur in the early stages of disease. Cases with inflammation but without amyloid or tau could, however, represent an FTD variant and it is planned to extend and follow this cohort.

Relationship of tau deposition and hypometabolism in Alzheimer's disease: A multimodal imaging approach

Gérard Bischof[1, 2], Jochen Hammes[1], Julian Dronse[2, 3], Klaus Fliessbach[4, 5], Frank Jessen[5, 6], Bernd Neumaier[7], Özgür Onur[3], Juraj Kukolja[3], Alexander Drezga[1, 5], Thilo van Eimeren[1, 2, 3]

[1]*Multimodal Neuroimaging Group, Department of Nuclear Medicine, University Hospital Cologne, Germany*
[2]*Cognitive Neuroscience, Institute of Neuroscience and Medicine (INM-3), Research Center Jülich, Germany*
[3]*Department of Neurology, University Hospital Cologne, Germany*
[4]*Department of Psychiatry and Psychotherapy, University Hospital Bonn, Germany*
[5]*German Center for Neurodegenerative Diseases (DZNE), Germany*
[6]*Department of Psychiatry, University Hospital Cologne, Germany*
[7]*Institute of Radiochemistry and Experimental Molecular Imaging, University of Cologne, Germany*

In Alzheimer's Disease (AD), brain atrophy is preceded by gradual metabolic decline, as measured by [18F]FDG PET. Neuropathological hallmarks of the disease are beta-amyloid plaques (Aβ) and tau-based neurofibrillary tangles (Tau). While specific for AD, Aβ burden, as quantified by in vivo PET ligands, is largely unrelated to magnitude and topology of metabolic decline.

The very recent development of [18F]AV-1451 (T807) for the in vivo quantification of Tau, allows us to test if tau pathology is more intimately linked to metabolic decline than Aβ. To this end, we adopted a multimodal imaging approach to investigate the relationship of regional glucose hypometabolism (assessed by [18F]FDG PET) with regional measures of Tau ([18F]AV-1451 PET), and Aβ ([11C]PiB PET) in six AD patients. We created z-score deviation images of [18F]AV-1451 and [18F]FDG PET using healthy controls as reference samples (significance threshold: z-score >2). Regional cortical deviation of [18F]AV-1451 uptake correlated strongly with regional glucose hypometabolism (r =.77, p <.001), whereas PiB uptake did not (r = -.01, n.s.) (see Figure, panel A). Deviation of tangle pathology and hypometabolism was most pronounced in brain regions known to be affected by hypometabolism consistently in AD, even in early stages (i.e., parietal cortex, posterior cingulate and temporal cortex). Consistent with the notion that regional tau deposition may precede regional glucose hypometabolism, we found more regions exhibiting exclusive tau deviations (Tau+), than regions with isolated hypometabolism (FDG+; see Figure, panel B).

Overall, our results indicate a linear relationship of regional tau deposition and metabolic decline in AD and provide evidence for tau as a potential instigator of neuro-degeneration in AD.

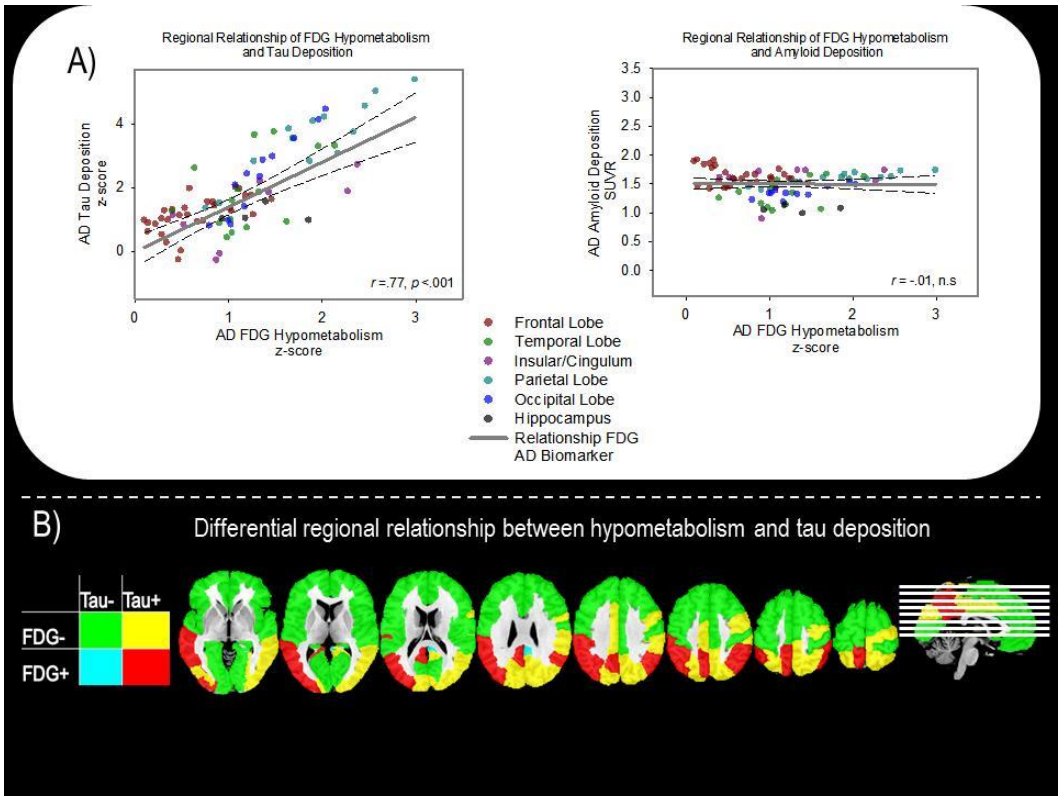

Impact of reference region and partial volume correction on PiB PET quantification in an autosomal dominant Alzheimer's disease cohort

Yi Su[1], Christopher Owen[1], Russ Hornbeck[1], Robert Koeppe[2], Karl Friedrichsen[1], Chengjie Xiong[3], Daniel Marcus[1], John Morris[4], Randall Bateman[4], Tammie Benzinger[1]

[1]*Mallinckrodt Institute of Radiology, Washington University School of Medicine, MO, United States*
[2]*Department of Radiology, University of Michigan, MI, United States*
[3]*Division of Biostatistics, Washington University School of Medicine, MO, United States*
[4]*Department of Neurology, Washington University School of Medicine, MO, United States*

Background: Amyloid imaging plays an important role in the research and diagnosis of dementing disorders. Substantial variation in quantitative methods to measure brain amyloid burden using PET exists in the field, including the choice of reference regions and the use of partial volume correction. Here, we investigate the impact of these methodological variations using cross-sectional and longitudinal PiB imaging data from the Dominantly Inherited Alzheimer Network (DIAN).

Methods: Quantification of PiB PET imaging data was performed using four reference regions: cerebellar cortex (CER), brainstem (BS), total white matter (TW), and core white matter (CW), with and without partial volume correction using a regional spread function (RSF) technique. The stability of the reference regions were assessed a cross-sectional subset from the overall DIAN cohort. In a longitudinal subset, the ability to detect longitudinal changes in amyloid burdens was assessed. We also estimated the number of participants per arm needed to detect a reduction in amyloid accumulation rate in placebo-controlled amyloid-targeting randomized clinical trials.

Results: Regional tracer uptake were not significantly different between mutation carriers and noncarriers for any of the reference regions regardless of partial volume correction except for TW, where the mutation carriers had higher uptake than noncarriers (p=0.01). Partial volume correction based analysis generated significantly (p<0.0005) larger percent change in SUVR regardless of the reference region used, and resulted in smaller sample size needed in clinical trials (Figure 1). Conflicting results were observed for using white matter as the reference region and warrants further investigation.

Conclusion: Partial volume correction consistently improves sensitivity to group differences and longitudinal changes over time, and reduces the sample size needed in clinical trials targeting amyloid.

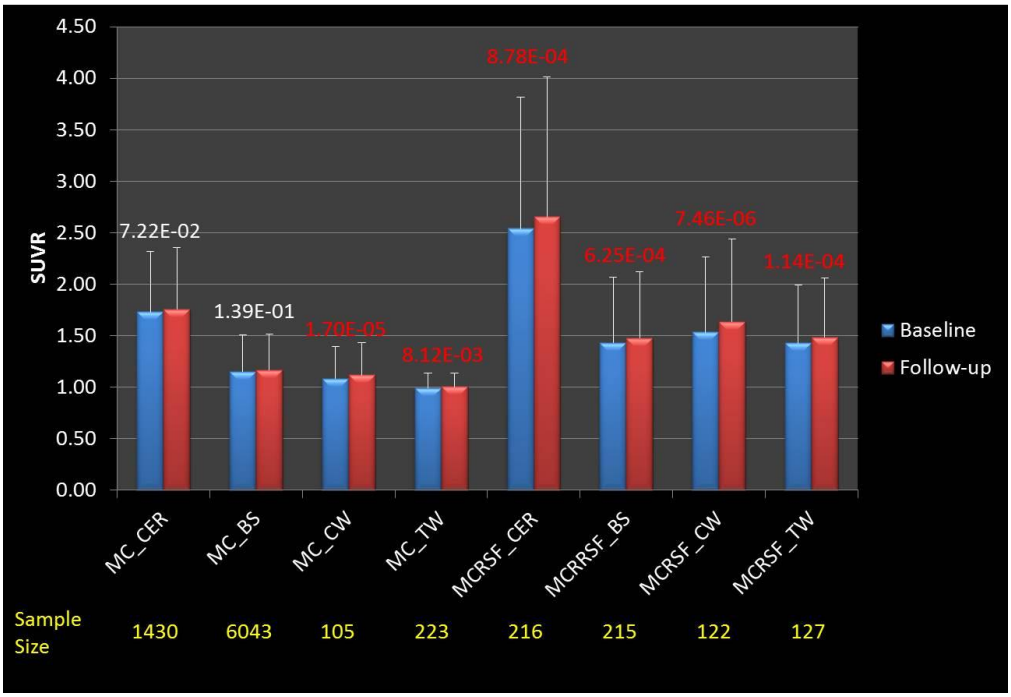

Quantification and reference optimization of tau PET imaging with [^{11}C]PBB3 in PSP patients

Hitoshi Shimada[1], Yasuyuki Kimura[1], Masanori Ichise[1], Hiroshi Ito[2, 3], Hironobu Endo[1, 4], Keisuke Takahata[1], Fumitoshi Niwa[1], Soichiro Kitamura[1], Shigeki Hirano[1, 5], Hitoshi Shinotoh[1, 6], Naruhiko Sahara[1], Makiko Yamada[1, 7], Ming-Rong Zhang[8], Makoto Higuchi[1], Tetsuya Suhara[1]

[1]*Molecular Neuroimaging Program, Molecular Imaging Center (MONI), National Institute of Radiological Sciences (NIRS), Chiba, Japan*
[2]*Biophysics Program, MONI, NIRS, Chiba, Japan*
[3]*Advanced Clinical Research Center, Fukushima Medical University, Fukushima, Japan*
[4]*Division of Neurology, Kobe University Graduate School of Medicine, Hyogo, Japan*
[5]*Department of Neurology, Graduate School of Medicine, Chiba University, Chiba, Japan*
[6]*Neurology Chiba Clinic, Chiba, Japan*
[7]*Precursory Research for Embryonic Science and Technology, Japan Science and Technology Agency, Tokyo, Japan*
[8]*Molecular Probe Program, MONI, NIRS, Chiba, Japan*

Background and aims: Since there was negligible tau pathology in the postmortem Alzheimer's disease (AD) cerebellum, cerebellar grey matter have been widely used as a reference region to estimate regional binding of tau PET ligands in AD. Meanwhile, some non-AD tauopathies such as progressive supranuclear palsy (PSP) and chronic traumatic brain encephalopathy tend to have tau accumulation in the cerebellar grey matter, leading to the fact that cerebellar grey matter couldn't be suitable as a reference region in these diseases. The aim of this study is to establish the optimized reference setting and investigate the utility of using optimized reference in tau PET imaging with [^{11}C]PBB3.

Methods: Participants were 14 patients with PSP and 11 cognitive healthy young control subjects (HC). We performed PET scans with [^{11}C]PBB3 and [^{11}C]Pittsburgh Compound B (PiB) for imaging of tau and Aβ deposition, respectively, along with MRI. A reference tissue model (MRTM $_{O}$) was used to estimate non-displaceable binding potential (BP_{ND}) of [^{11}C]PBB3 using reference regions defined with two ways; 1. manually-defined regions on the cerebellar grey matter and 2. optimized regions extracted from cerebral and cerebellar grey matter voxels that can be considered to have a low likelihood of tau accumulation (BP_{ND}[cb] and BP_{ND}[op], respectively). Aβ deposition was visually assessed with SUVR images of [^{11}C]PiB PET.

Results: All participants were PiB-negative. Compared with BP_{ND}[cb], BP_{ND}[op] values were increased in all participants (**Figure 1**), and differential diagnostic performance between PSP and HCs measured by the area under the ROC curve were also improved (**Table 1**).

Conclusions: Using optimized reference made BP_{ND} values increased in tau PET imaging in non-AD tauopathies, presumably reflecting improvement of underestimation of BP_{ND} due to involving tau accumulation in reference regions.

Figure 1 Representative BP_{ND} images in PSP

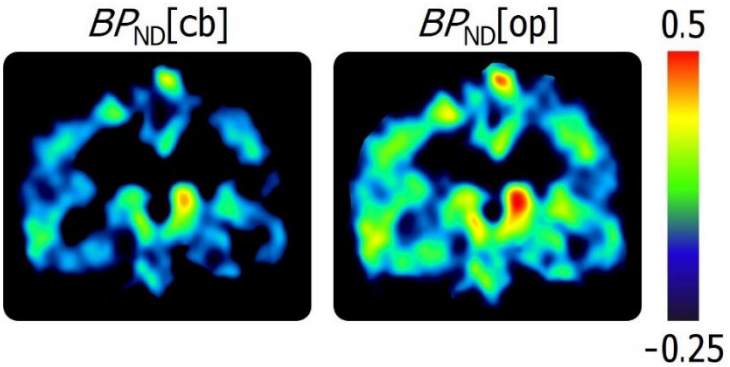

Table 1

		HC	PSP	AUC
Grey matter	BP_{ND}[cb]	-0.04 (0.17)	-0.04 (0.18)	0.474
	BP_{ND}[op]	0.07 (0.19)	0.11 (0.21)	0.656
White matter	BP_{ND}[cb]	-0.24 (0.16)	-0.18 (0.17)	0.805
	BP_{ND}[op]	-0.15 (0.17)	-0.05 (0.20)	0.981

HC: healthy control, PSP: progressive supranuclear palsy
AUC: Area under the ROC curve

Factors associated with negative amyloid PET for eligibility assessment in multicenter Alzheimer's therapeutic trials

John Seibyl[1, 2], Olivier Barret[1, 2], Gary Wisniewski[2], Kenneth Marek[1, 2]

[1]*Institute for Neurodegenerative Disorders, New Haven, CT, United States*
[2]*Molecular NeuroImaging, LLC, New Haven, CT, United States*

Objectives: Multicenter clinical treatment trials in Alzheimer disease (AD) commonly employ PET amyloid imaging for determining participant eligibility. There is intense interest in optimizing PET eligibility assessments using qualitative and quantitative interpretation, either alone or in combination, to accurately enroll appropriate AD participants. Previous multicenter studies showed highly variable rates of negative or ineligible scans (5% to 41%). Factors potentially associated with this variability include clinician diagnostic bias, reader bias, or other factors. This study systematically evaluated the factors associated with negative amyloid PET in a series of multicenter AD therapeutic trials.

Methods: 5,357 F18 Florbetapir PET scans were obtained at screening in preclinical, prodromal, and early Alzheimer's disease recruited in six Phase 2-3 therapeutic trials. Each scan was interpreted according to the florbetapir visual read method and required agreement by either two expert independent readers or a reader and an independent composite SUVr depending on the trial. A series of candidate clinical, technical, and methodological factors were identified and analyzed in a linear mixed discriminate function model for identifying factors strongly associated with a negative florbetapir PET scan.

Results: The most important individual factors associated with a negative amyloid PET scan were: cohort status with at risk>prodromal> early AD, enrolling site clinician, and scan interpretation methodology (visual vs visual + quantitation).

Conclusions: The clinical stage of the cohort is the most important factor predicting the number negative scans. In addition, enrolling centers and use of quantitation in eligibility are associated with negative scans rates, suggesting a role for additional diagnostic standardization and attention to how PET eligibility

Tau ligand PBB3 binds with broad range of tau lesions: Immunohistochemical and histochemical analyses in tauopathy patients

Shunsuke Koga[1], Naruhiko Sahara[2], Hitoshi Shimada[2, 3], Wenlang Lin[1], Makoto Higuchi[2], Tetsuya Suhara[2], Zbigniew Wszolek[4], Dennis Dickson[1]

[1]Department of Neuroscience, Mayo Clinic, Jacksonville, FL, United States
[2]Molecular Imaging Center, National Institute on Radiological Sciences (NIRS), Chiba, Japan
[3]Department of Neurology, Graduate School of Medicine, Chiba, Japan
[4]Department of Neurology, Mayo Clinic, Jacksonville, FL, United States

Background: Accumulating evidence has shown that pathological tau is a promising therapeutic target for Alzheimer disease (AD) and other tauopathies. To develop tau-targeted therapy, it is necessary to establish assay systems to visualize in vivo tau pathology for monitoring the efficacy of an anti-tau drug. Positron emission tomography (PET) imaging of tau pathologies is currently available using several tau PET ligands, including [11C]PBB3. Meanwhile, more compelling in vivo and neuropathological evidence supporting binding of PBB3 to tau lesions in diverse tauopathy is still required.

Method: We performed PBB3 fluorescence and immunohistochemistry with anti-tau antibodies in brain sections from AD, primary age-related tauopathy, progressive supranuclear palsy (PSP), corticobasal degeneration (CBD), Pick disease, globular glial tauopathy, frontotemporal dementia and parkinsonism linked to tau gene on chromosome 17 (FTDP-17-MAPT), and aged healthy subjects.

Results: PBB3 detected tau lesions composed of both and either of 3-repeat and 4-repeat isoforms, but the binding property of PBB3 varied among diseases. Extracellular tangles in AD or FTDP-17 with R406W mutation strongly bound to PBB3. In contrast, PBB3 less frequently detected coiled bodies and tau-positive threads in PSP and CBD, and Pick's bodies in Pick disease.

Conclusions: PBB3 binds with various types of tau lesions including 3-repeat and 4-repeat tau deposits not only in neuron, but also in glia. Further studies, including binding assay using brain homogenates and electron microscopic analysis, will clarify the differences in binding property among tau lesions.

AV-1451 tau-PET in progressive supranuclear palsy variants

Keith Josephs, Jennifer Whitwell, Nirubol Tosakulwong, Stephen Weigand, Ronald Petersen, Clifford Jack, Val Lowe

Mayo Clinic, Rochester, MN, United States

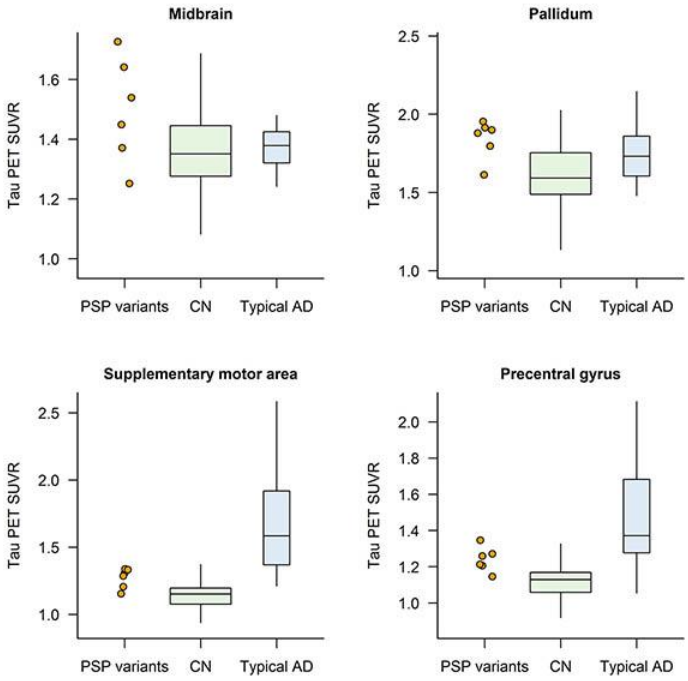

Background: Different clinical variants of progressive supranuclear palsy (PSP) have been described, the most common of which is Richardson syndrome. The relationship between these clinical variants and pathology is heterogeneous, with all variants associated with tau pathology but with varying patterns of tau deposition within, and across, brain regions. Tau-PET imaging using AV-1451 demonstrates striking uptake in Alzheimer's disease (AD), although it is unclear whether uptake is observed in the different variants of PSP.

Aim: To determine whether tau deposition can be identified on AV-1451 tau-PET in different clinical variants of PSP compared to cognitively normal (CN) subjects and to compare the degree of uptake with that observed in Alzheimer's disease (AD).

Methods: Six subjects representing four clinical variants of PSP underwent tau-PET imaging with AV-1451. These subjects were compared to 101 age-matched CN subjects and 19 subjects with AD. Regional tau-PET uptake was calculated for nine regions typically associated with tau deposition in PSP (midbrain, caudate, putamen, pallidum, supplementary motor area, superior frontal lobe, pre and post central cortex, and thalamus).

Results: The PSP subjects showed evidence for subtle elevated tau-PET uptake compared to CN subjects across all regions. Uptake was particularly evident in midbrain, pallidum, supplementary motor area and precentral cortex (Figure). The degree of tau-PET uptake in PSP was lower than AD across all regions except midbrain, pallidum and thalamus. Subtle regional differences were observed between the different clinical variants of PSP, with increased uptake in general being highest in those with Richardson's syndrome.

Conclusions: PET imaging using AV-1451 can detect a signal across the different clinical variants of PSP, although the degree of uptake is far less than that observed in AD. This ligand may be sensitive enough to detect regional differences across the clinical variants of PSP.

Modeling *in vivo* the pathology behind medial temporal atrophy in Alzheimer's disease: implications of amyloid and tau PET imaging

Konstantinos Chiotis[1], Laure Saint-Aubert[1], Elena Rodriguez-Vieitez[1], Antoine Leuzy[1], Lena Cavallin[2], Agneta Nordberg[1, 3]

[1]*Dept NVS, Center for Alzheimer Research, Translational Alzheimer Neurobiology, Karolinska Institutet, Stockholm, Sweden*
[2]*Department of Radiology, Karolinska University Hospital Huddinge, Stockholm, Sweden*
[3]*Department of Geriatric Medicine, Karolinska University Hospital Huddinge, Stockholm, Sweden*

Introduction: The development of amyloid- and tau-specific PET ligands has enabled the study of the *in vivo* relationship between cerebral atrophy and the two key pathologies (fibrillar amyloid-beta and tau deposits) of Alzheimer's disease (AD).

Methods: Nine patients with AD dementia and eleven with mild cognitive impairment, all positive for amyloid deposition ([^{11}C]PIB status), and four age-matched healthy controls, underwent structural MRI (T1 sequence) as well as PET imaging with an amyloid-specific and a tau-specific PET tracers: [^{11}C]PIB and *(S)*-[^{18}F]THK5117 (also know as [^{18}F]THK5317), respectively. An experienced neuroradiologist rated the MRI scans for Medial Temporal Atrophy (MTA), using the Scheltens scale. PIB $SUVR_{40\text{-}60}$ and *(S)*-THK5117 $DVR_{30\text{-}60}$ retention in the hippocampus was calculated with respect to the cerebellar grey matter, following the application of correction for partial volume effect. Cumulative link and linear mixed effects models were applied to investigate the relationship between imaging modalities, after correcting for diagnosis. The presence of a causal mediation (indirect) effect was tested with the use of Monte Carlo simulation.

Results: *(S)*-THK5117 DVR retention in the hippocampus was found to be positively correlated to MTA score (Likelihood-ratio=6.06, p=0.01), while no direct relationship was found between MTA score and PIB SUVR retention in the same region (Likelihood-ratio=0.08, p=0.77). A positive correlation was found between *(S)*-THK5117 DVR and PIB SUVR retention in the hippocampus (F-value=11.96, p<0.01). Mediation analysis identified a positive indirect effect of PIB SUVR retention on MTA score, through increasing *(S)*-THK5117 DVR retention (Indirect effect estimate=2.25, p<0.01).

Conclusion: Local tau pathology in the hippocampus is directly positively related to MTA and fibrillar amyloid pathology. Although no direct association was found between fibrillar amyloid pathology and MTA, evidence exists of an indirect neurotoxic effect of amyloid pathology through promoting the accumulation of tau pathology.

History of estrogen replacement therapy modulates the relationship of age and amyloid burden to hippocampal volume

Vaishnavi Rao[1, 2, 3], Aaron Schultz[3, 4, 6], Elizabeth Mormino[2, 4], Molly LaPoint[2, 3, 7], Keith Johnson[2, 4, 5, 6, 7], Reisa Sperling[2, 3, 4, 5], Jasmeer Chhatwal[2, 4, 5]

[1]*Department of Brain and Cognitive Sciences, Massachusetts Institute of Technology, MA, United States*
[2]*Department of Neurology, Massachusetts General Hospital, MA, United States*
[3]*Athinoula A. Martinos Center for Biomedical Imaging, MA, United States*
[4]*Center for Alzheimer Research and Treatment, Brigham and Women's Hospital, MA, United States*
[5]*Harvard Medical School, MA, United States*
[6]*Division of Nuclear Medicine and Molecular Imaging, Massachusetts General Hospital, MA, United States*
[7]*Department of Radiology, Massachusetts General Hospital, MA, United States*

Introduction: Several groups have shown elevated amyloid burden is associated with decreased hippocampal volume (HV), closely linking Alzheimer's pathology to hippocampal neurodegeneration and resultant memory loss. HV is also modulated by estrogen, though the effects of post-menopausal estrogen replacement therapy (ERT) on HV remain controversial. We thus examined whether history of ERT modulates the relationship between amyloid burden, age, and HV in 231 cognitively normal elderly participants in the Harvard Aging Brain Study.

Methods: 11C-Pittsburgh-compound B (PiB)-PET, structural MRI, and self-reported ERT history were used in linear regression models examining the cross-sectional relationship between age, amyloid burden and HV in women with (n=58) and without (n=77) a history of ERT, as well a comparison group of men (n=96).

Results: Average age and amyloid burden were similar across groups. We observed that women with a history of ERT had significantly greater HV for a given age than those without a history of ERT ($t_{(131)}$=-2.06, p=0.046). Higher amyloid burden significantly predicted decreased HV in the entire sample ($t_{(228)}$=-2.32, p=0.022). This relationship was driven by the subset of women with a history of ERT, in whom increased age and amyloid burden were similarly and significantly predictive of decreased HV (PiB: $t_{(55)}$=-2.74, p=0.008; Age: $t_{(55)}$=-3.11, p=0.003) . In contrast, amyloid burden was not a significant predictor of HV in women without a history of ERT or in men, after controlling for age (both p>0.2).

Conclusions: These results suggest that women with a history of ERT may be less sensitive to age-related decreases in HV than men and women with no history of ERT, but also that ERT-treated women may be more susceptible to amyloid-related hippocampal volume loss. Together, these results suggest that sex and ERT history may be relevant factors in interpreting relationships between HV, age and amyloid burden in clinical research settings.

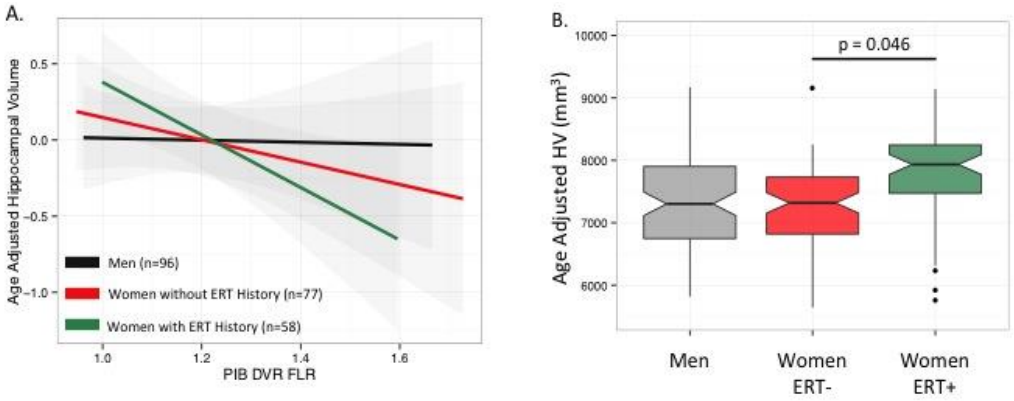

Figure 1: *ERT modulates the relationship of amyloid burden and age to hippocampal volume.* (A) After adjusting hippocampal volume for age, amyloid burden was a significant predictor of hippocampal volume in women with a history of ERT, but not in men or women without a history of ERT. (B) Women with a history of ERT had greater HV for age than women with no history of ERT.

Table 1: Age and Amyloid Burden as Predictors of Hippocampal Volume (HV ~ Age + PIB)

Group:	N	Avg Age	AMNART VIQ	Years of Education	Avg PIB DVR FLR	Effect of Age on HV			Effect of PiB DVR		
						Raw β	Std β	p-value	Raw β	Std β	p-value
Men	96	74.5	121.1	15.96	1.164	**-65.11**	**-0.44**	**< 0.0001**	-268.45	-0.05	0.597
Women ERT-	77	73.8	119.7	15.58	1.178	**-70.35**	**-0.58**	**< 0.0001**	-506.71	-0.11	0.239
Women ERT+	58	73.3	121.6	15.53	1.177	**-50.01**	**-0.36**	**0.003**	**-1463.90**	**-0.32**	**0.008**
Group Difference (p-value)		0.48	0.44	0.62	0.85						

(bold denotes significant at p < 0.01)

Absolute quantification of [18F]-AV45 PET using model-based kinetics with a metabolite corrected arterial input function

Julie Ottoy[1], Jeroen Verhaeghe[1], Ellis Niemantsverdriet[2], Leonie wyffels[3], Charisse Somers[2], Steven Deleye[1], Sarah Ceyssens[3], Sigrid Stroobants[3], Sebastiaan Engelborghs[2], Steven Staelens[1]

[1]*Molecular Imaging Center, Antwerp University, Wilrijk, Belgium*
[2]*Reference Center for Biological Markers of Dementia (BIODEM), Institute Born-Bunge, University of Antwerp, Belgium*
[3]*Nuclear Medicine, Antwerp University Hospital, Edegem, Belgium*

Here we report on the kinetic modeling for [18F]-AV45 data. Dynamic 60 min [18F]-AV45 PET (348±81 MBq) was acquired in 9 Alzheimer Diseased (AD; MMSE 22.0±0.9), 15 mild cognitively impaired (MCI; MMSE 26.5±2.0), and 5 (cognitively) healthy control (HC; MMSE 29.7±0.5) subjects. Arterial input was measured continuously over a detector complemented by manual samples for HPLC metabolite analysis. The two tissue compartmental model (2TCM) was required (lowest Akaike values) in all brain regions to describe the [18F]-AV45 tissue time activity curves (TACs) and to derive total volume of distribution (VT). Distribution volume ratios (DVR) with cerebellum (CB) as reference were derived from the 2TCM VT values. Static scan SUVr with CB as reference region were calculated from the 50-60 min p.i. data.

We measured a plasma free fraction of 11.24±4 % and only 32+14% of parent fraction remained at 10 min.

The mean VT was significantly increased in the precuneus only for AD (+38±8%, ANOVA, $p<0.05$) (Fig 1A) and equally the DVR was significantly increased for AD ($p<0.05$: parietal and posterior cingulate cortex +44±13% and +33±8%, respectively; and $p<0.01$: +47±11% precuneus). Moreover, also compared to MCI the DVR for AD was significantly increased (+24±9%, $p<0.05$) in the parietal cortex (Fig. 1B).

The SUVrs were significantly increased for AD in the anterior cingulate, the frontal and parietal cortices ($p<0.05$) and the precuneus ($p<0.01$), the latter for MCI as well ($p<0.05$) (Fig 1C). Further, SUVr was significantly but only moderately correlated with VT (r: 0.38-0.61; $p<0.05$) while stronger with DVR (r: 0.54-0.82; $p<0.05$). Importantly, compared to the DVR, average SUVr differences between MCI and HC were overestimated in all regions (+9±4%) while underestimated between the AD and MCI groups (-16±2%).

Absolute VT and relative DVR quantification determined from full kinetic modeling showed more discriminative power compared to simplified SUVr (Fig. 2).

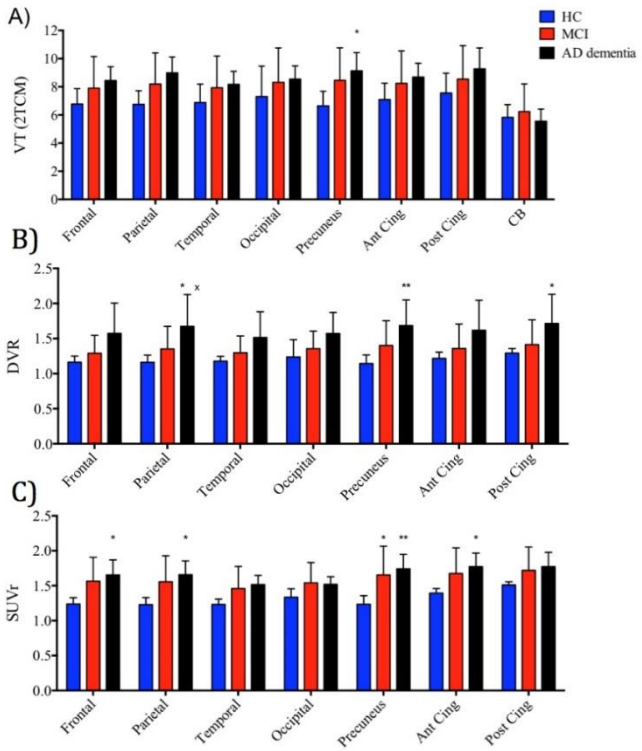

Figure 1 Regional V_T, DVR and SUVr (mean ± std) values for the three groups. Stars denote significant differences with the HC group and cross versus the MCI group (*,+ $p<0.05$; ** $p<0.01$). Note that DVR and SUVr do not show CB as this is the reference region.

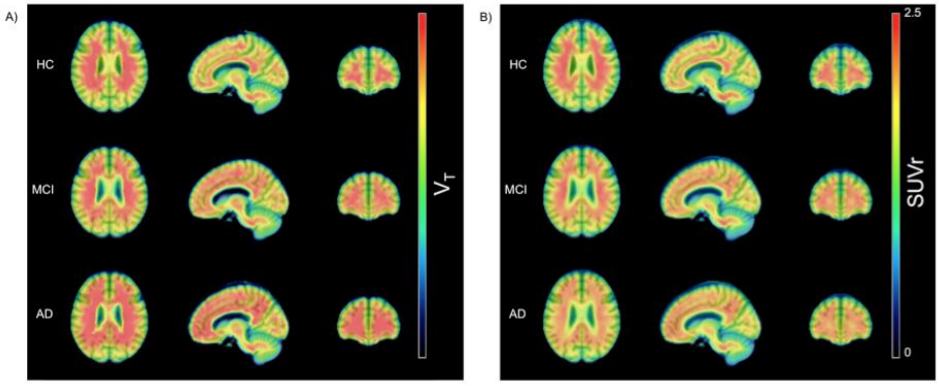

Figure 2 Average spatially normalized V_T and SUVr images for the three groups overlayed on the MR template. Parametric V_T images were obtained using Ichise's multilinear analysis and average V_T images were scaled to the mean cerebellar V_T value of the respective group.

Sex differences in the association between AD biomarkers and brain aging outcomes

Timothy Hohman

Vanderbilt University Medical Center, TN, United States

Women are disproportionately affected by Alzheimer's disease (AD) in terms of both disease prevalence and severity. Previous autopsy work has suggested that, in the presence of AD neuropathology, females are more susceptible to the clinical manifestation of AD. This manuscript extends that work by evaluating whether sex alters the established associations between cerebrospinal fluid (CSF) biomarker levels and brain aging outcomes (hippocampal volume, cognition). Participants were drawn from the Alzheimer's Disease Neuroimaging Initiative (ADNI) and included individuals with normal cognition (n=348), mild cognitive impairment (n=565), and AD (n=185). We leveraged mixed effects regression models to assess the interaction between sex and baseline cerebrospinal fluid biomarker levels of amyloid-β-42 (Aβ-42) and total tau on cross-sectional and longitudinal brain aging outcomes. We found a significant interaction between sex and Aβ-42 on longitudinal hippocampal atrophy (p=0.002), and longitudinal decline in memory (p=0.017) and executive function (p=0.025). Similarly, we observed an interaction between sex and total tau level on longitudinal hippocampal atrophy (p=0.008), and longitudinal decline in executive function (p=0.034). Women with Aβ-42 and total tau levels indicative of worse pathological changes showed more rapid hippocampal atrophy and cognitive decline. The sex difference was particularly pronounced among individuals with MCI, carrying an *APOE* ε4 allele, or with lower education. These results provide *in vivo* support that females may be more susceptible to the clinical manifestation of AD.

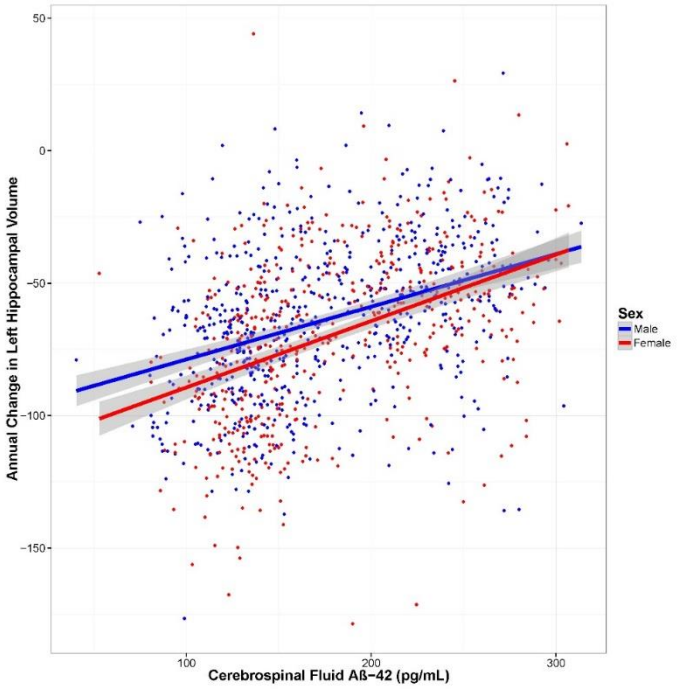

Figure 1: Females show a faster rate of hippocampal atrophy in the presence of enhanced (low levels) of CSF Aβ-42.

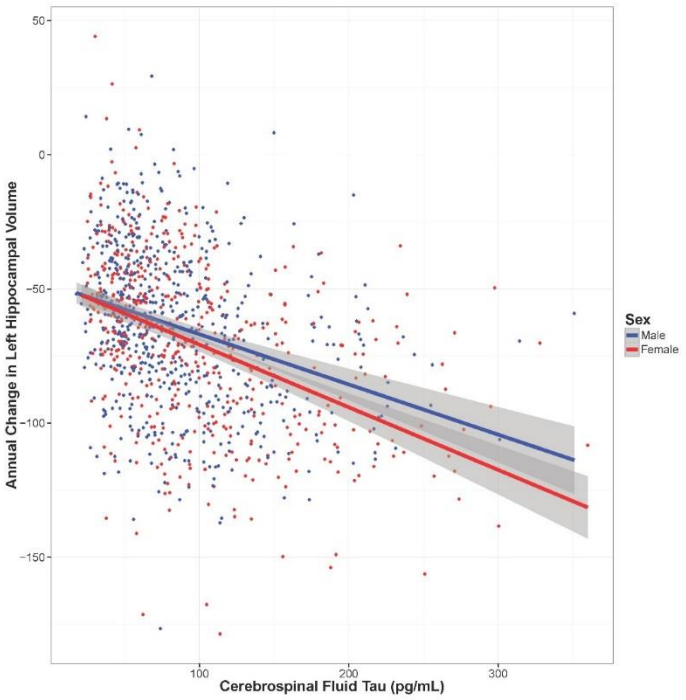

Figure 2: Females show a faster rate of hippocampal atrophy in the presence of enhanced CSF tau levels.

The utility of Aβ oligomers in the diagnosis and treatment of AD

Juliya Kalinina[1], Maria Michener[1], Brad Smith[1], Eric Parker[1], Julie Stone[1], Eline van Maanen[2], Gordon Wilcock[3], david smith[3], Donald Warden[3], Colin Masters[4], Qiao-Xin Li[4], Steven Collins[4], Christopher Fowler[4], Linda White[5], Christopher Winrow[1], Mary Savage[1], et al.

[1]*Merck & Co, Inc., PA, United States*
[2]*LAP&P consultants, Netherlands*
[3]*Oxford University, Oxford, United Kingdom*
[4]*The University of Melbourne, Australia*
[5]*Norwegian University of Science and Technology (NTNU), Norway*

Alzheimer's disease (AD) is the most common neurodegenerative dementia. Merck's β-secretase therapy against AD is currently undergoing Phase 3 clinical trials and shows dramatic reductions in Aβ monomer levels. With the recent emergence of Aβ oligomers (AβO) as the most toxic Aβ species in AD, our work has focused on deciphering the different utility of AβO in the diagnosis, prognosis and treatment of AD by: (1) establishing a sensitive, robust and automated assay for their scarce (pg/mL) detection in human CSF, and (2) demonstrating AβO's use as a diagnostic and/or a marker in evaluating drug/oligomer pharmacodynamics in preclinical/clinical models of APP processing.

To achieve the former, we used the Singulex' Erenna technology to develop an AβO-specific CSF assay that discriminated AD from control subjects in three commercial cohorts (J.Neurosci. 2014, 34(8):2884-97). Furthermore, using the assay and working collaboratively with our academic partners (University of Melbourne, Oxford University and NTNU), we have explored the correlation of CSF oligomers with PET classification and cognitive scores in three cross-sectional/longitudinal AD and Control cohorts (AIBL, OPTIMA, TrønderBrain).

Finally, in our effort to identify AβO as a pharmacodynamic biomarker in response to secretase inhibition, we used a cisterna magna-ported rhesus monkey preclinical model in a four-way crossover design. Treatment with secretase inhibitors (BACE, GS or vehicle) resulted in a significant (~80%) reduction in oligomers in rhesus CSF in a time-/dose-dependent fashion, enabling a revised model of rhesus CNS APP processing that includes a role for AβO.

Together, these findings highlight the potential utility of AβO as diagnostic, prognostic and, importantly, as a novel marker of pharmacodynamic response to secretase inhibitor therapy in AD. Future work is hoped to measure oligomer levels in CSF samples from subjects of BACEi clinical trials.

Measurement of neuronal function using an early frame amyloid PET multivariate classifier

Dawn Matthews[1], Ana Lukic[1], Randolph Andrews[1], Miles Wernick[1, 2], Stephen Strother[1, 3], Mark Schmidt[4], et al.

[1]*ADM Diagnostics, LLC, IL, United States*
[2]*Medical Imaging Research Center, Illinois Institute of Technology, IL, United States*
[3]*Rotman Research Institute, Baycrest Hospital, ON, Canada*
[4]*Janssen Research & Development, Janssen Pharmaceutica, Beerse, Belgium*

Background: Measurement of amyloid burden provides important confirmation of AD pathology for clinical trials and diagnosis. However, many amyloid+ early stage subjects do not worsen clinically during the timeframe of a clinical trial, suggesting that a measure of neurodegeneration predictive of decline can provide a useful adjunct. Previous studies have shown correspondence between perfusion measured by the early amyloid frames following tracer injection and FDG PET comparing ROIs affected in AD. Multivariate machine learning approaches, by taking into account relationships between affected regions and maximizing signal/noise, may offer a more sensitive means for detection of disease related changes as we have demonstrated with FDG.

Methods: Using summed dynamic florbetapir image frames acquired during the first six minutes post- injection for 104 ADNI subjects, we applied machine learning with iterative resampling to develop and test image classifiers aimed at measuring AD Progression. Training classes consisted of 10 NL amyloid-negative(-), 19 subjective memory complaints (SMC)-, 11 NL/SMC+, 9 MCI+, and 14 AD+ based upon clinical diagnosis and late timeframe amyloid status. Independent testing was applied through Leave-One-Out analysis and to 41 additional scans. Early frame amyloid (EFA) classification was compared to that of an independently developed FDG PET AD Progression classifier by scoring the FDG scans of the same subjects at the same time point. Score distributions and correlation with clinical endpoints were compared to FDG.

Results: The EFA classifier produced a primary pattern similar to that of the FDG classifier (Figure 1) whose expression correlated highly with the FDG pattern (R-squared 0.71 (Figure 2), and that within amyloid+ subjects (N=34) correlated with MMSE, CDR-sb, and ADAS-cog13 (R-squared 0.35, 0.37, 0.52).

Conclusions: These results show the ability to obtain a functional measure using EFA with the potential to achieve the predictive utility approaching FDG through the use of multivariate classifier approaches.

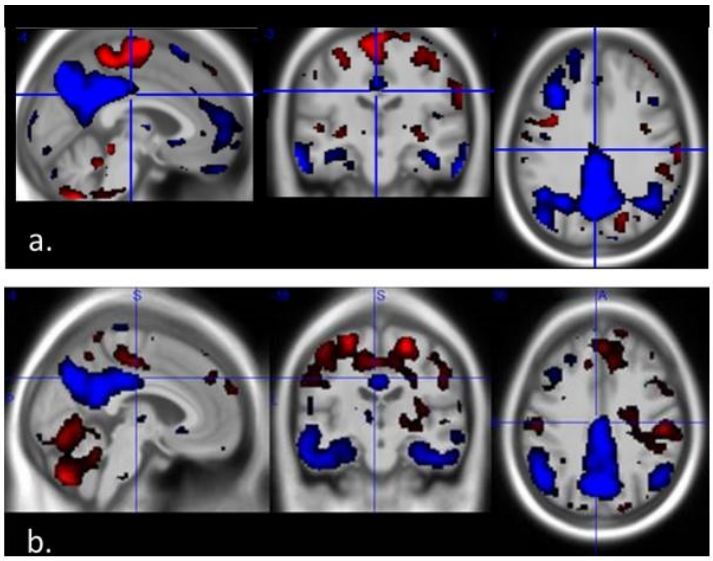

Figure 1. (a) FDG PET AD Progression classifier eigenimage and (b) Early frame amyloid AD Progression classifier eigenimage. Blue = hypometabolism (FDG) or hypoperfusion (EFA) and Red = preservation of metabolism (FDG) or perfusion (EFA), relative to whole brain.

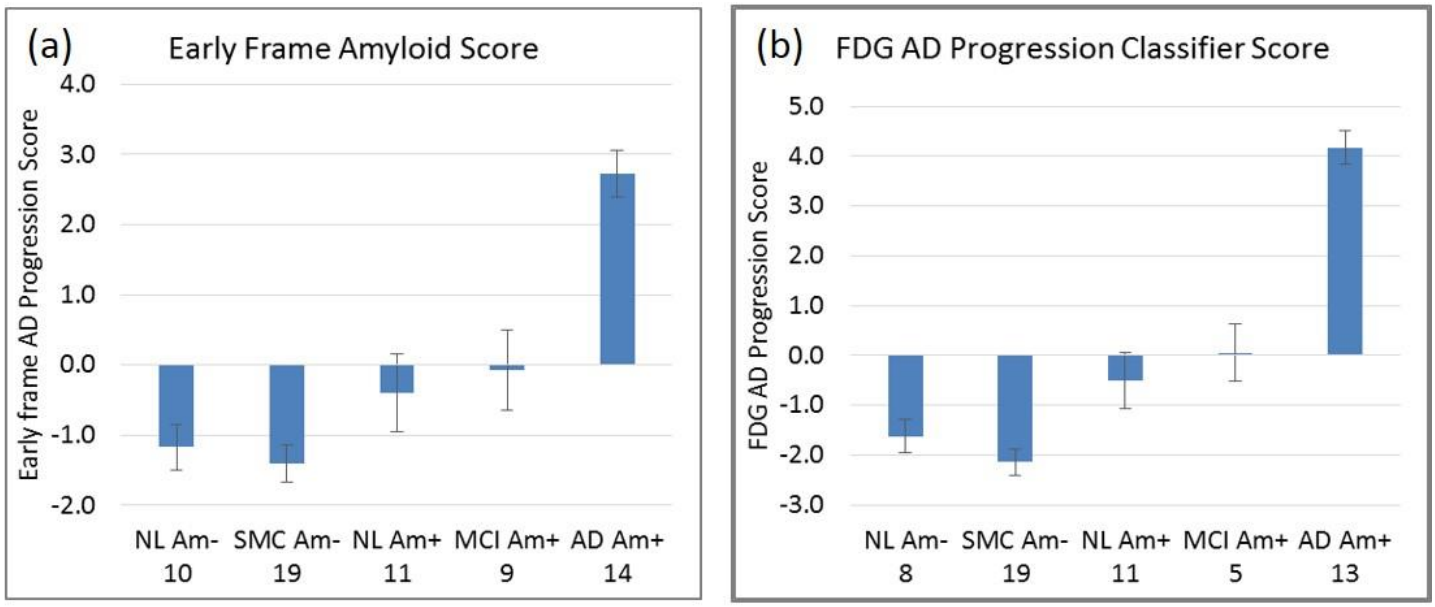

Figure 2. Classifier scores from (a) the early frame amyloid scans measured using the EFA functional classifier (Leave One Out independent test results) and (b) the FDG PET scans from the same subjects where available, using an independently developed FDG AD Progression classifier. Classifiers were blind to diagnosis and late frame amyloid status. Results are shown grouped according to these attributes. (Column height = group mean, bars = SEM; number = number per group. NL = cognitively normal, SMC = normal with subjective memory complaint; CV1 = classifier score)

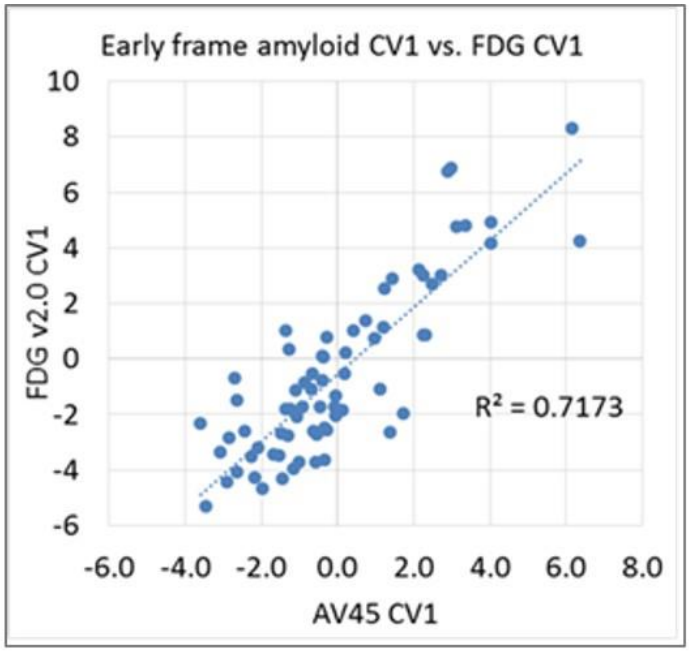

Figure 3. Correlation between EFA functional classifier and FDG PET AD Progression classifier scores (CV = Canonical Variate).

Preliminary analysis of the association between retinal nerve fiber layer thickness and cerebral amyloid deposition

Shannon Risacher[1, 2], Darrell WuDunn[1], John West[1, 2], Brenna McDonald[1, 2], Martin Farlow[1, 2], Sujuan Gao[1, 2], Liana Apostolova[1, 2], Fredrick Unverzagt[1, 2], Andrew Saykin[1, 2]

[1]*Indiana University School of Medicine, Indianapolis, IN, United States*
[2]*Indiana Alzheimer Disease Center, Indianapolis, IN, United States*

Introduction: Retinal degeneration and impaired retinal function have been observed in mild cognitive impairment (MCI) and Alzheimer's disease patients (AD) [1,2], and studies have suggested that amyloid deposition occurs on the retina concurrent with the brain [3]. We have previously reported on the relationship of contrast sensitivity, measured using frequency doubling technology (FDT), and cerebral amyloid deposition [4]. In this report, we complete a preliminary evaluation of the relationship of retinal nerve fiber layer thickness (RNFL), measured using optical coherence tomography (OCT), with cerebral amyloid deposition.

Methods: Nine cognitively normal participants from the Indiana Memory and Aging Study (IMAS) underwent OCT and amyloid PET imaging with [^{18}F]florbetapir. After standard preprocessing, [^{18}F]florbetapir SUVR images were created using mean whole cerebellum binding as a reference region. Mean regional SUVR from cortical, precuneus, and cingulate regions of interest (ROIs) generated using FreeSurfer version 5.1 were extracted. The relationship of RNFL thickness and [^{18}F]florbetapir SUVR was evaluated using a linear model, covaried for age. Partial correlation coefficients (r_p) are reported.

Results: Mean RNFL thicknesses in the superior and nasal retinal quadrants were significantly associated with mean cingulate ($p<0.05$; Fig 1A & 1B) and mean precuneus ($p<0.05$, Fig 1C & 1D) [^{18}F]florbetapir SUVR, and showed a trend for association with mean cortical [^{18}F]florbetapir SUVR ($p<0.1$; Fig 1E & 1F).

Conclusions: Significant associations between retinal neurodegeneration and cortical amyloid were observed. Given the previous reports of retinal amyloid deposition, the observed retinal changes may be in part due to retinal amyloid deposition.

[1] Kesler (2011). *Clinical Neurology and Neurosurgery*

[2] Risacher (2013). *Neurobiology of Aging*

[3] Frost (2014). *AAIC*

[4] Risacher (2012). *HAI*

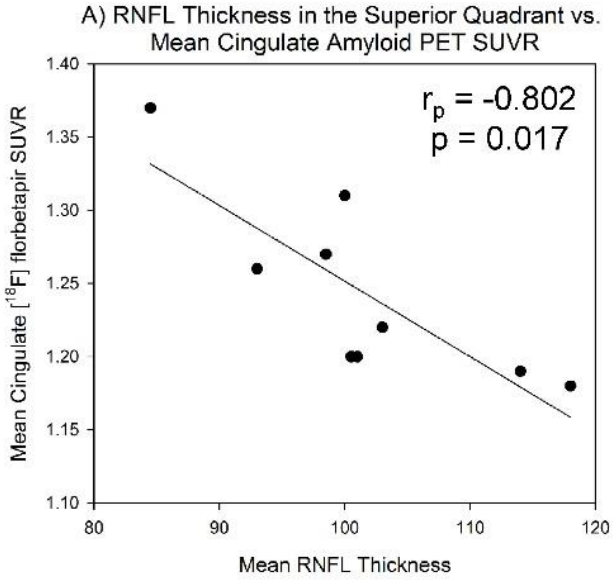
A) RNFL Thickness in the Superior Quadrant vs.
Mean Cingulate Amyloid PET SUVR
r_p = -0.802
p = 0.017
Mean Cingulate [^{18}F] florbetapir SUVR
Mean RNFL Thickness

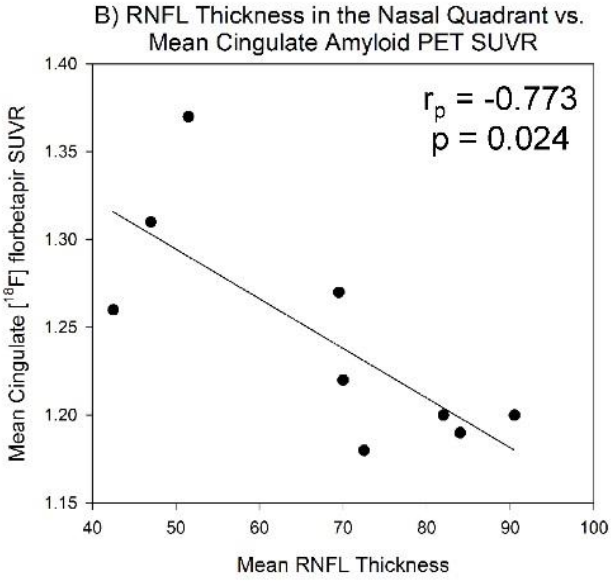
B) RNFL Thickness in the Nasal Quadrant vs.
Mean Cingulate Amyloid PET SUVR
r_p = -0.773
p = 0.024
Mean Cingulate [^{18}F] florbetapir SUVR
Mean RNFL Thickness

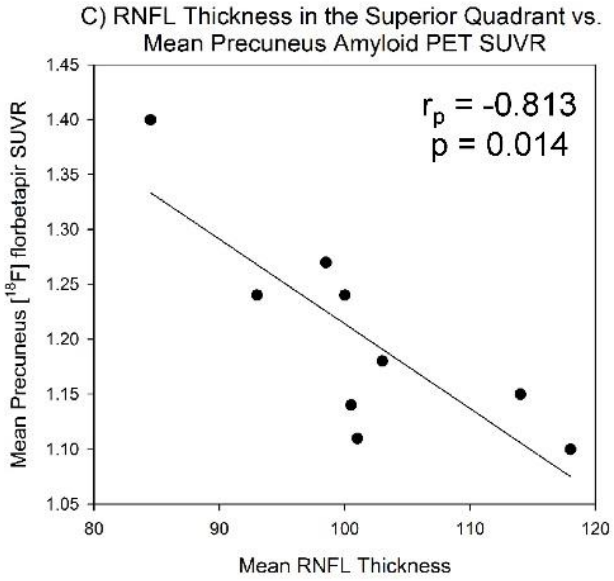
C) RNFL Thickness in the Superior Quadrant vs.
Mean Precuneus Amyloid PET SUVR
r_p = -0.813
p = 0.014
Mean Precuneus [^{18}F] florbetapir SUVR
Mean RNFL Thickness

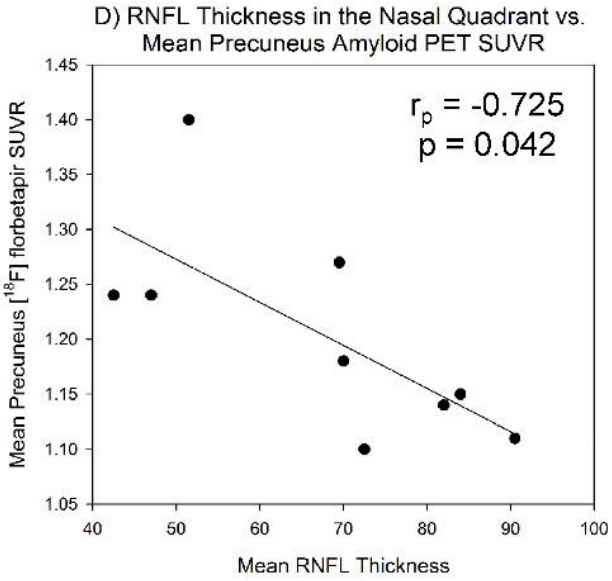
D) RNFL Thickness in the Nasal Quadrant vs.
Mean Precuneus Amyloid PET SUVR
r_p = -0.725
p = 0.042
Mean Precuneus [^{18}F] florbetapir SUVR
Mean RNFL Thickness

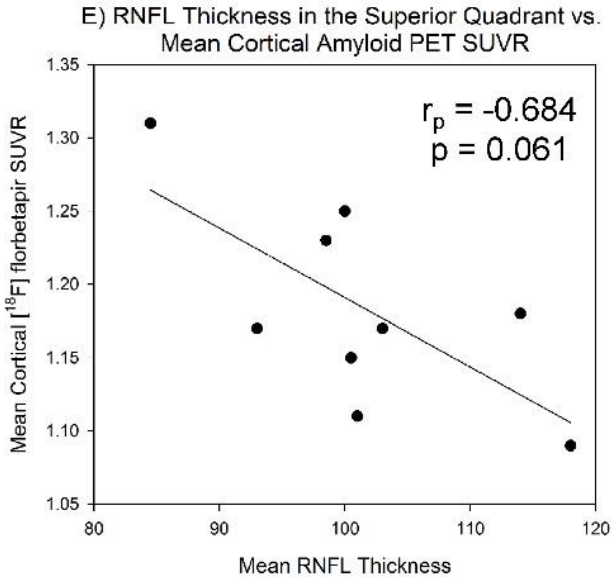
E) RNFL Thickness in the Superior Quadrant vs.
Mean Cortical Amyloid PET SUVR
r_p = -0.684
p = 0.061
Mean Cortical [^{18}F] florbetapir SUVR
Mean RNFL Thickness

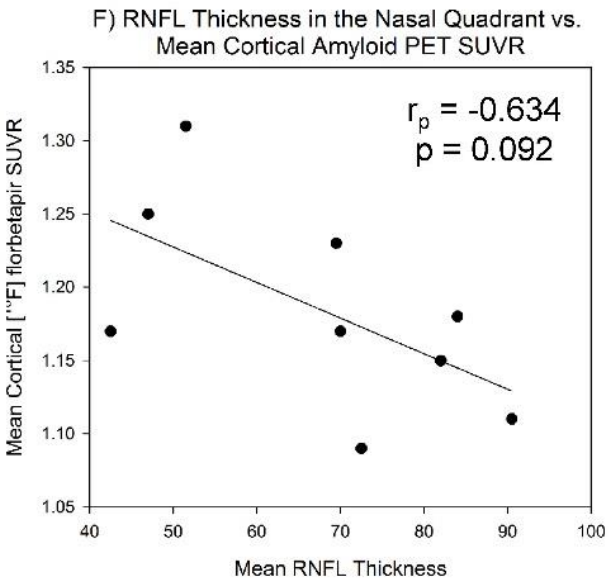
F) RNFL Thickness in the Nasal Quadrant vs.
Mean Cortical Amyloid PET SUVR
r_p = -0.634
p = 0.092
Mean Cortical [^{18}F] florbetapir SUVR
Mean RNFL Thickness

Initial evaluation of [^{18}F]AV-1451 tau PET from The Alzheimer's Disease Neuroimaging Initiative: Relation to amyloid PET, MRI, and memory

Shannon Risacher[1, 2], Kacie Deters[1, 2], John West[1, 2], William Jagust[3], Clifford Jack[4], Michael Weiner[5], Andrew Saykin[1, 2]

[1]*Indiana University School of Medicine, Indianapolis, IN, United States*
[2]*Indiana Alzheimer Disease Center, Indianapolis, IN, United States*
[3]*University of California, Berkeley, CA, United States*
[4]*Mayo Clinic, Rochester, MN, United States*
[5]*University of California, San Francisco, CA, United States*

Introduction: Amyloid-beta plaques, neurofibrillary tau tangles, neurodegeneration, and cognitive impairment are the hallmarks of AD. The PET tracer [^{18}F]AV-1451 was developed to bind to tau tangles *in vivo*. The goal of this study was an initial assessment of the relationship of [^{18}F]AV-1451 to other markers of AD pathology (amyloid PET, neurodegeneration, and cognition) in the ADNI cohort.

Methods: Nine participants underwent [^{18}F]AV-1451 scans, as well as longitudinal amyloid PET with [^{18}F]florbetapir, MRI, and neuropsychological testing, with the most recent visit coinciding with [^{18}F]AV-1451 scanning. [^{18}F]AV-1451 SUVR was extracted from hippocampal and cortical regions. Cross-sectional and two-year change in cortical [^{18}F]florbetapir SUVR, hippocampal grey matter density (GMD), and memory were determined. Mean [^{18}F]AV-1451 SUVR was compared between diagnostic groups. Relationships between cross-sectional and longitudinal amyloid, neurodegenerative, and cognitive measures and [^{18}F]AV-1451 SUVR were assessed. Due to the small sample size, only those with age-adjusted partial correlation coefficients (r_p)>0.5 are reported.

Results: Increased [^{18}F]AV-1451 SUVR was observed in MCI and AD relative to those with normal cognition but significant memory concerns (SMC; Fig 1). Strong associations between [^{18}F]AV-1451 SUVR and memory performance (Fig 2A), amyloid deposition (Fig 2B&C), and longitudinal change in hippocampal GMD (Fig 2D&E) were observed. Notably, consistent binding of [^{18}F]AV-1451 in the medial temporal lobe was observed across subjects at various intensities but cortical binding was highly variable across subjects (*data not shown*).

Conclusions: These preliminary findings are consistent with the strong association between amyloid and tau, as well as tau and atrophy rate. Memory was modestly related to tau deposition. Variation in cortical binding topography suggests the potential to identify phenotypic subtypes defined by tau distribution that will be examined in future studies as the sample size increases.

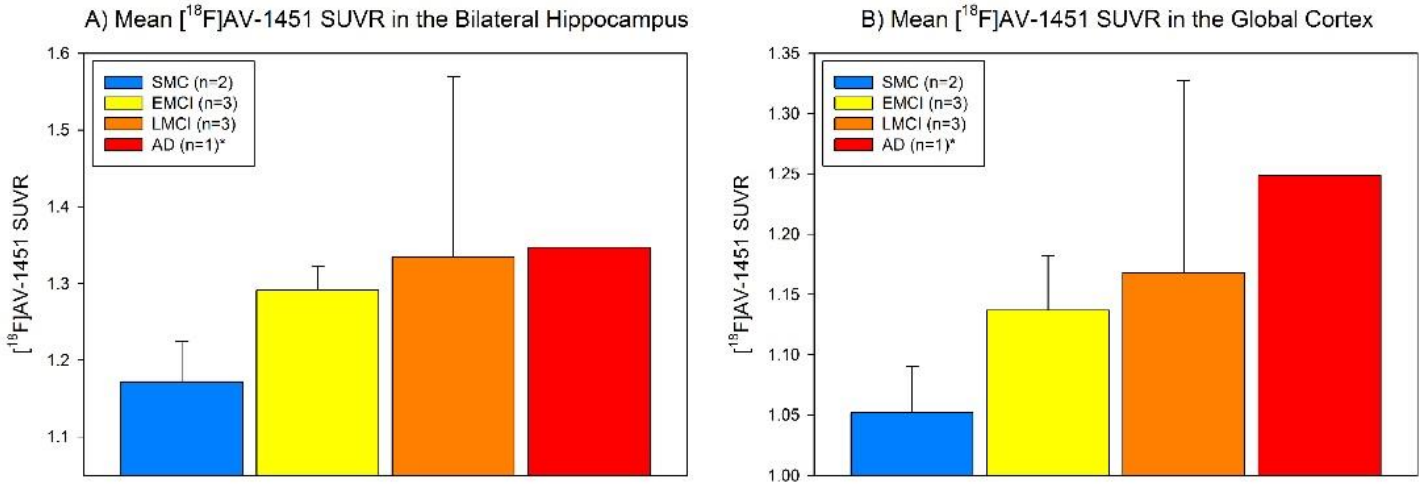

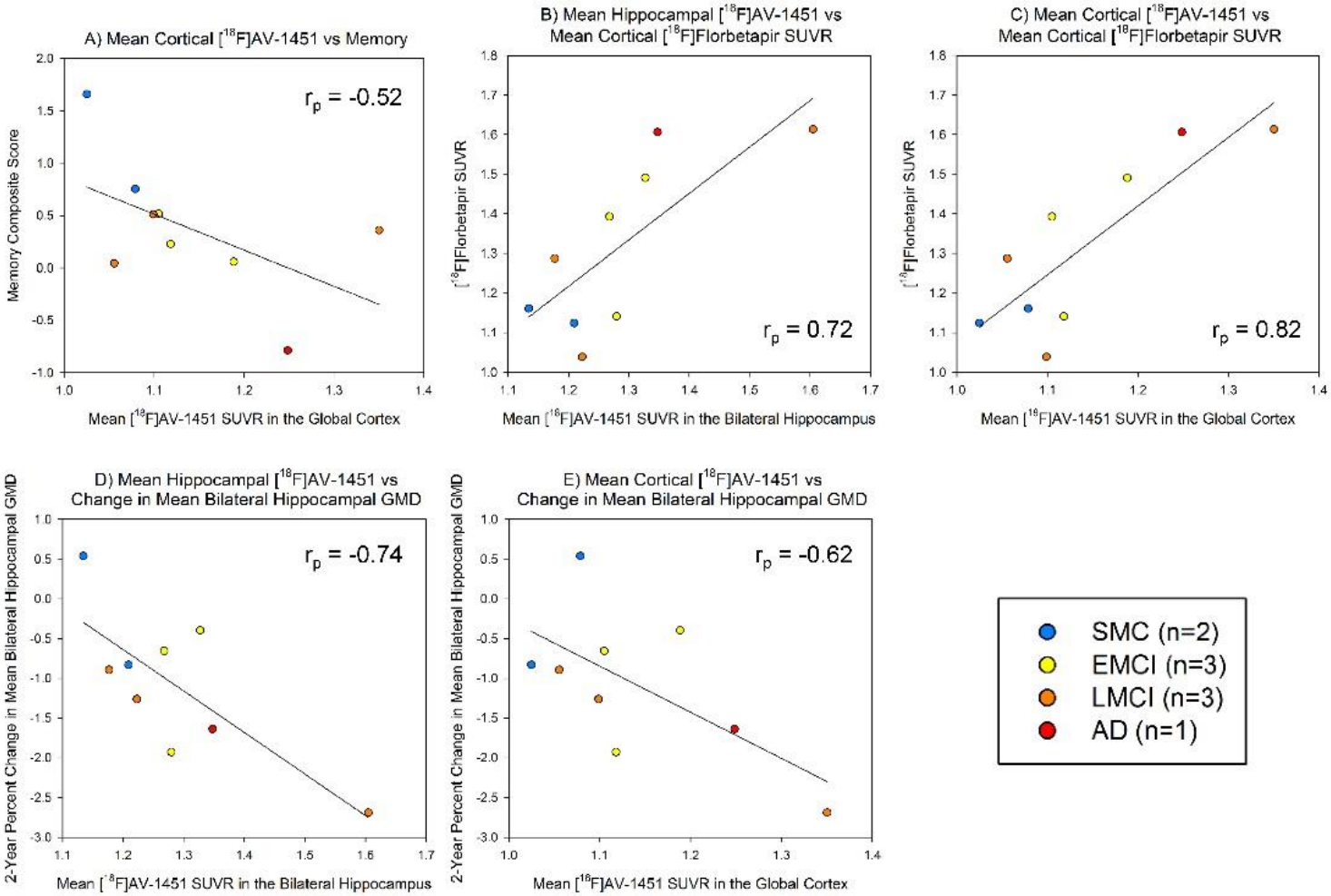
A) Mean Cortical [18F]AV-1451 vs Memory
Memory Composite Score
Mean [18F]AV-1451 SUVR in the Global Cortex
rp = -0.52
B) Mean Hippocampal [18F]AV-1451 vs Mean Cortical [18F]Florbetapir SUVR
[18F]Florbetapir SUVR
Mean [18F]AV-1451 SUVR in the Bilateral Hippocampus
rp = 0.72
C) Mean Cortical [18F]AV-1451 vs Mean Cortical [18F]Florbetapir SUVR
[18F]Florbetapir SUVR
Mean [18F]AV-1451 SUVR in the Global Cortex
rp = 0.82
D) Mean Hippocampal [18F]AV-1451 vs Change in Mean Bilateral Hippocampal GMD
2-Year Percent Change in Mean Bilateral Hippocampal GMD
Mean [18F]AV-1451 SUVR in the Bilateral Hippocampus
rp = -0.74
E) Mean Cortical [18F]AV-1451 vs Change in Mean Bilateral Hippocampal GMD
2-Year Percent Change in Mean Bilateral Hippocampal GMD
Mean [18F]AV-1451 SUVR in the Global Cortex
rp = -0.62
SMC (n=2)
EMCI (n=3)
LMCI (n=3)
AD (n=1)

Tracer kinetics of [^{18}F]Florbetapir in healthy controls and Alzheimer's disease

Sander C.J. Verfaillie[1], Sandeep Golla[2], Sofie M. Adriaanse[2], Marissa Zwan[1], Robert Schuit[2], Tessa Timmers[1, 2], Colin Groot[2], Patrick Schober[3], Lothar Schwarte[3], Philip Scheltens[1], Wiesje M. van der Flier[1, 4], Albert D. Windhorst[2], Adriaan A. Lammertsma[2], Bart N.M. van Berckel[2], Ronald Boellaard[2]

[1]Alzheimer Center and Department of Neurology, VU University Medical Center, Amsterdam, Netherlands
[2]Department of Radiology & Nuclear Medicine, VU University Medical Center, Amsterdam, Netherlands
[3]Department of Anaesthesiology, VU University Medical Center, Amsterdam, Netherlands
[4]Department of Epidemiology & Biostatistics, VU University Medical Center, Amsterdam, Netherlands

Background: Alzheimer's disease (AD) is a progressive neurodegenerative disorder characterized by accumulation of amyloid beta (Aβ). Aβ can be visualized using [^{18}F]florbetapir positron emission tomography (PET). The aim of this preliminary analysis was to identify the optimal model for describing tracer kinetics in AD patients and healthy controls.

Methods: Four probable AD patients (50% male, age: 65±6 years, MMSE: 21±3) and 3 healthy controls (66.6% male, age 65±5 years, MMSE: 30±0) were included. 90 minutes dynamic PET scans (Philips Ingenuity TF) were acquired immediately following bolus injection of [^{18}F]florbetapir (305±29 MBq). Continuous arterial sampling was performed until 65 min p.i., and seven additional manual samples were taken for metabolite analyses. After co-registration with a T1-weighted MRI scan, tissue time-activity curves were extracted from the dynamic PET scan using PVELAB[1] with the Hammers template. Several plasma input compartmental models were evaluated and the Akaike Information Criteria (AIC) was used to select the preferred model.

Results: Plasma metabolism was fast with a parent fraction of about 60% after just 5 minutes. [^{18}F]florbetapir kinetics were best described by a reversible two tissue compartment model with fitted blood volume fraction (2T4k_VB), irrespective of subject status and size of region of interest. Whole brain grey matter distribution volume (VT) was 4.51±0.87 and 5.05±0.62 for controls and AD patients, respectively. VT values of a few specific regions are shown in Figure 1.

Conclusion: This preliminary study indicates that 2T4k_VB appears to be the best model for describing *in vivo* kinetics of [^{18}F]florbetapir, both in healthy controls and in AD patients. Nevertheless, further studies are needed to substantiate these findings.

(1) Svarer C, Madsen K, Hasselbalch SG, Pinborg LH, Haugbol S, Frokjaer VG, et al. MR-based automatic delineation of volumes of interest in human brain PET images using probability maps. Neuroimage 2005 Feb 15;24(4):969-979.

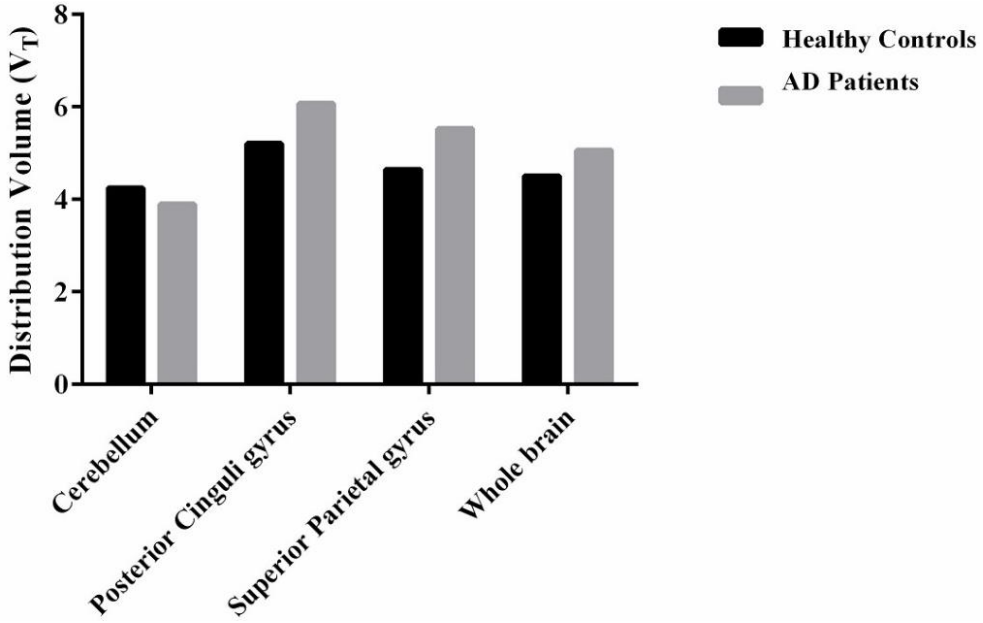

Principal component analysis-based scoring of PiB scans in the Mayo Clinic Study of Aging

David Jones, Val Lowe, Scott Przybelski, Matt Senjem, Brad Boeve, David Knopman, Ronald Petersen, Clifford Jack

Mayo Clinic, Rochester, MN, United States

Background: There are biological and non-biological sources of variability in C-11 PiB scans. Variability in white matter binding may confound methods of calculating standard uptake value ratio (SUVR) whether via explicit use of white matter ROIs or via partial volume averaging. Therefore we explored principal axes of variability using principal component analysis (PCA) in an effort to understa nd and isolate sources of variability encountered in PiB scanning of a large community dwelling sample of cognitively normal subjects.

Methods: We study 1,343 PiB scans of cognitively normal subjects in the Mayo Clinic Study of Aging. All scans were spatially normalized to a standard space, intensity normalized to cerebellar gray matter, and smoothed. In order to investigate subject related variability that is not necessarily dependent on regional variability, we performed PCA on the symmetric (1,343x1,343) distance matrix of the dataset.

Results: The first three principal components (PCs) explained 84.5% of the variance (PC1 = 50.5%, PC2 = 27%, PC3 = 7%) in the relationships between the subjects captured in the distance matrix. PC1 strongly associated with known patterns of Alzheimer's disease-related PiB binding (Fig 1A). PC2 was strongly associated with age and white matter (Fig 1B). PC3 was associated with age, cognition, and cerebral spinal fluid related imaging changes (Fig 1C). In generalized additive models, PC1 and PC2 could explain 88% of the deviance (P<0.001) in standard AD signature SUVR values (Fig 2). In an independent sample of CN (n=28) and AD (n=103) subjects, PC1 achieved 100% agreement with visual reads of PiB positivity.

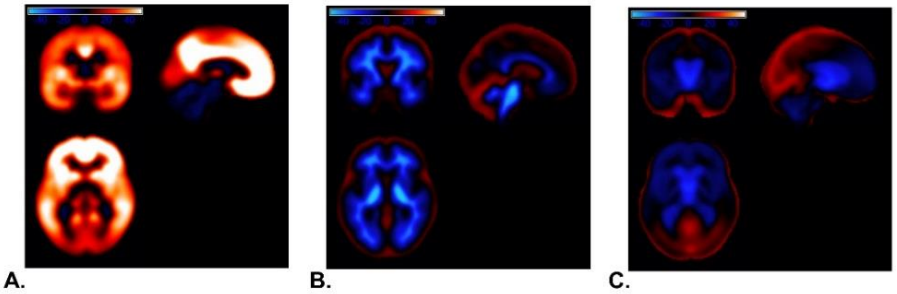

Figure 1: Voxel-wise association between PC1-3 (A-C respectively) and PiB images. The t-statistic for a one-sample t-test raging from (-50 to 50) is encoded in the color bars.

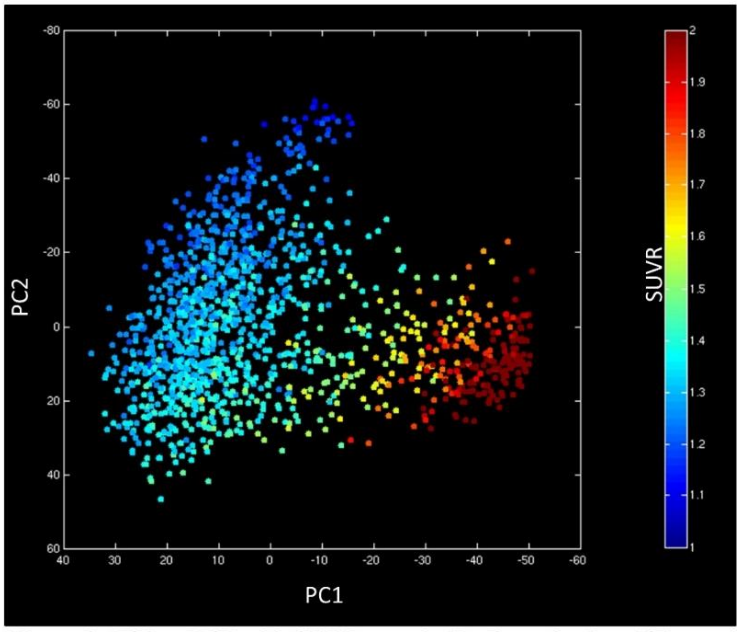

Figure 2: PC1 vs PC2 with SUVR encoded in the color bar. This plot demonstrates that there is additional subject-related variance that is captured by PC2 that is orthogonal to PC1, however SUVR alone is unable to separate these sources of variance.

Conclusions: Scoring PiB scans using PC1 is theoretically free from contamination by factors contributing to PC2 and PC3 and is able to achieve 100% agreement with visual reads of PiB positivity. Therefore, PC1 may be an attractive method of dichotomizing PiB scans in large population-based studies.

Patterns of longitudinal cerebral amyloid and blood flow changes

Murat Bilgel[1, 2], Lori Beason-Held[1], Dean Wong[3], Bruno Jedynak[4], Jerry Prince[2, 3, 5], Susan Resnick[1]

[1]*Laboratory of Behavioral Neuroscience, National Institute on Aging, Baltimore, MD, United States*
[2]*Department of Biomedical Engineering, Johns Hopkins University School of Medicine, Baltimore, MD, United States*
[3]*Department of Radiology, Johns Hopkins University School of Medicine, Baltimore, MD, United States*
[4]*Department of Mathematics and Statistics, Portland State University, Portland, OR, United States*
[5]*Department of Electrical and Computer Engineering, Johns Hopkins University School of Engineering, Baltimore, MD, United States*

Background: Cerebral metabolism/activity and amyloid accumulation have a complex relationship that has not been well-characterized longitudinally.

Method: We extracted longitudinal patterns from cerebral amyloid and regional cerebral blood flow (rCBF) data as measured by concurrent ^{11}C-PiB and ^{15}O-water PET imaging using 128 participants with up to 7 PET scans from Baltimore Longitudinal Study of Aging. 46 had elevated PiB levels at last visit. We used a novel method that temporally aligns individuals with similar PiB and rCBF images. This alignment in time allowed us to extract longitudinal trajectories that describe co-occurring changes in PiB and rCBF images. In analogy to modes obtained from principal component analysis (PCA), we extracted two orthogonal longitudinal trajectories, and computed a progression score for each PiB+rCBF pair that reflects their location along each of the two trajectories.

Results:

Figure. Estimated longitudinal patterns of PiB DVR and rCBF.

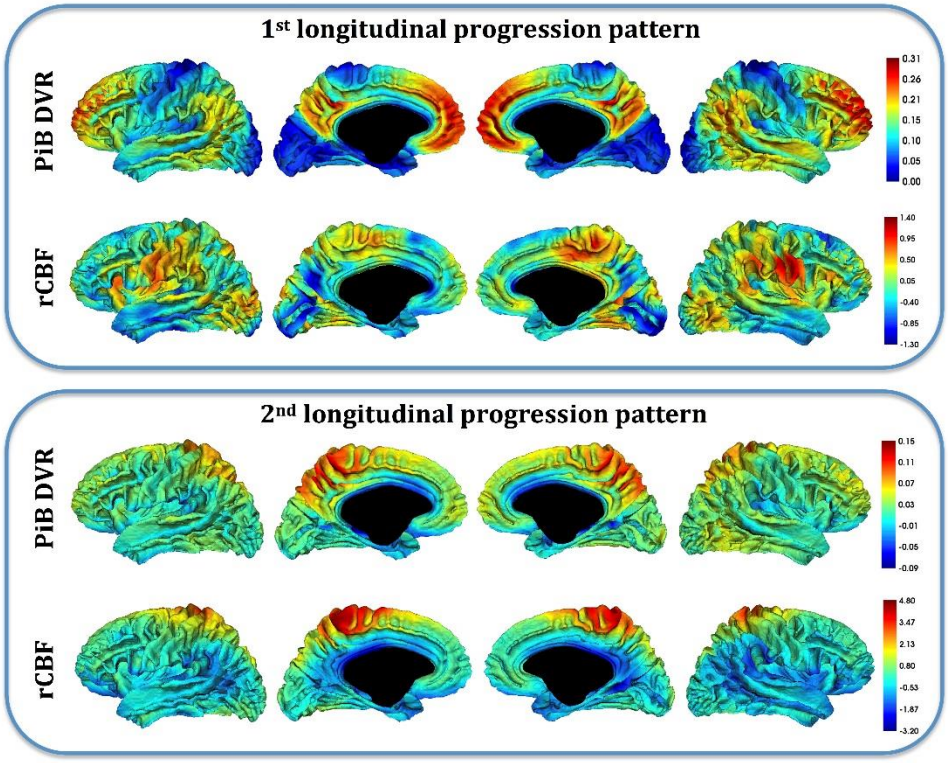

First pattern revealed PiB signal increases in precuneus, frontal and lateral parietal regions. rCBF decreased in precuneus, temporal, posterior and medial occipital regions, and increased in inferior-lateral and medial aspects sensorimotor strip.

Second pattern revealed PiB signal increases in medial sensorimotor strip and precuneus. rCBF decreased in insula, orbitofrontal, inferior temporal and lateral temporoparietal regions, and was preserved in medial sensorimotor strip.

Elevated PiB status was associated with higher progression scores in the first pattern (p<0.0001), adjusting for age and sex. Progression scores in the second pattern were associated with elevated PiB status after additionally adjusting for first pattern scores (p=0.01 at baseline and p=0.0003 at last visit).

Conclusions: The first pattern may reflect earlier changes in rCBF that co-occur with earlier amyloid accumulation, whereas the second pattern may reflect changes that occur in later stages. The presented method allows for exploration of heterogeneity in longitudinal progression and can be applied to jointly analyzing multiple types of images.

In vivo assessment of markers of Aβ & tau pathology in Vietnam War veterans with chronic post-traumatic stress disorder

Tia Cummins[1], Alby Elias[2], Mal Hopwood[2], Jeffrey Rosenfeld[5, 6], Vincent Dore[3, 4], Fiona Lamb[4], Rob Williams[1], Laura Margison[4], Olivier Salvado[3], Colin Masters[1], Victor Villemagne[1, 4], Christopher Rowe[1, 4]

[1]*The Florey Institute of Neuroscience & Mental Health, University of Melbourne, Australia*
[2]*Department of Psychiatry, University of Melbourne, Australia*
[3]*CSIRO Biomedical Informatics, the Australian eHealth Research Center, Brisbane, Australia*
[4]*Molecular Imaging & Therapy, Austin Health, Melbourne, Australia*
[5]*Department of Surgery, Central Clinical School, Monash University, Melbourne, Australia*
[6]*Department of Neurosurgery, Alfred Hospital, Melbourne, Australia*

Background: Epidemiological studies indicate a nearly twofold increase in risk of dementia associated with Post Traumatic Stress Disorder (PTSD) in military cohorts, however mechanisms contributing to this relationship are poorly understood. The aim of this study was to investigate if Vietnam war veterans without mild cognitive impairment or dementia, but with chronic combat related PTSD show evidence of Alzheimer's disease (AD) pathological markers, as assessed by amyloid and tau imaging with PET.

Methods: Sixty-seven male participants -30 veterans with chronic PTSD (aged 67.9±2.6 years) and 37 controls (aged 74.3±8.3 years)- underwent both tau and amyloid PET imaging scans with 18F-AV1451 and 18F-florbetaben or 18F-flutemetamol, respectively. While 18F-AV1451 SUVR was calculated using the cerebellar cortex as reference region, the whole cerebellum and the pons were used as reference regions for 18F-florbetaben and 18F-flutemetamol, respectively.

Results: Despite the PTSD cohort being significantly younger than the controls, there was a significant difference in 18F-AV1451 retention between the PTSD and control groups in the temporoparietal (1.21±0.12 vs. 1.13±0.13, p=0.017) and frontotemporal (1.14±0.12 vs. 1.06±0.13, p=0.018) regions. A similar, albeit not significant, trend was observed in the mesial temporal cortex (1.19±0.12 vs. 1.12±0.17, p=0.058). There was no significant difference in Aβ burden between the groups

Conclusions: Our preliminary findings suggest that chronic PTSD might be associated with higher neocortical tau deposition later in life. More studies to confirm these results are warranted.

APOE4 genotype potentiates the effect of amyloid on tau deposition in clinically normal older individuals

John Bark, Bernard Hanseeuw, Aaron Schultz, Elizabeth Mormino, Jasmeer Chhatwal, Kelly Judge, Reisa Sperling, Keith Johnson

Massachusetts General Hospital, Harvard Medical School, Boston, MA, United States

Background: Beta-amyloid (Aβ) and entorhinal tau deposits represent pathologic hallmarks of Alzheimer's disease (AD) that accumulate long before evident clinical symptoms, according to autopsy studies. A genetic risk factor for AD, APOE has been linked with earlier presence and greater accumulation of Aβ. In this cross-sectional study, we investigated the relationships among APOE, Aβ, and entorhinal tau deposition.

Methods: A subset of Harvard Aging Brain Study participants (n=120, female=56.6%, ages=65-90) underwent APOE genotyping, tau-PET (F18-T807 [AV1451]), amyloid-PET (C11-PiB), and volumetric MRI, with all imaging occuring within one year. Participants were dichotimzed by E4 status: Thirty-five (29.2%) participants were ε4 allele carriers. A SUVR was calculated using a FreeSurfer-defined entorhinal cortex region of interest for T807, while a DVR averaging cortical Aβ burden was calculated for PiB. Cerebellar gray was used for scaling all PET variables. We used linear models to evaluate the respective impact of E4 status and Aβ on tau and the E4*Aβ interaction effect. All analyses were age-adjusted.

Results: In separate models, Aβ (T=5.2, p<.0001) and E4 (T=3.2, p=.002) were significantly correlated with entorhinal tau deposition. Combined, only Aβ significantly correlated with tau (T=4.1, p<.0001), while E4 (T=1.3, p=.210) did not. The interaction between Aβ and E4 significantly correlated with tau deposition (T=2.4, p=.021), such that the relationship between Aβ and tau was stronger in E4 carriers (T=3.9, p=.0004) than in E4 non-carriers (T=2.1, p=.042). Similar results were found when using inferior temporal rather than entorhinal tau (data not shown).

Conclusion: These results suggest that the APOE4 genotype potentiates the effect of Aβ on tau deposition, in agreement with recent autopsy research (Farfel et al., 2015). Furthermore, earlier presence of Aβ among E4 carriers could explain higher tau levels. More participants and longitudinal imaging data will further elucidate the effect of APOE on Aβ and tau pathology.

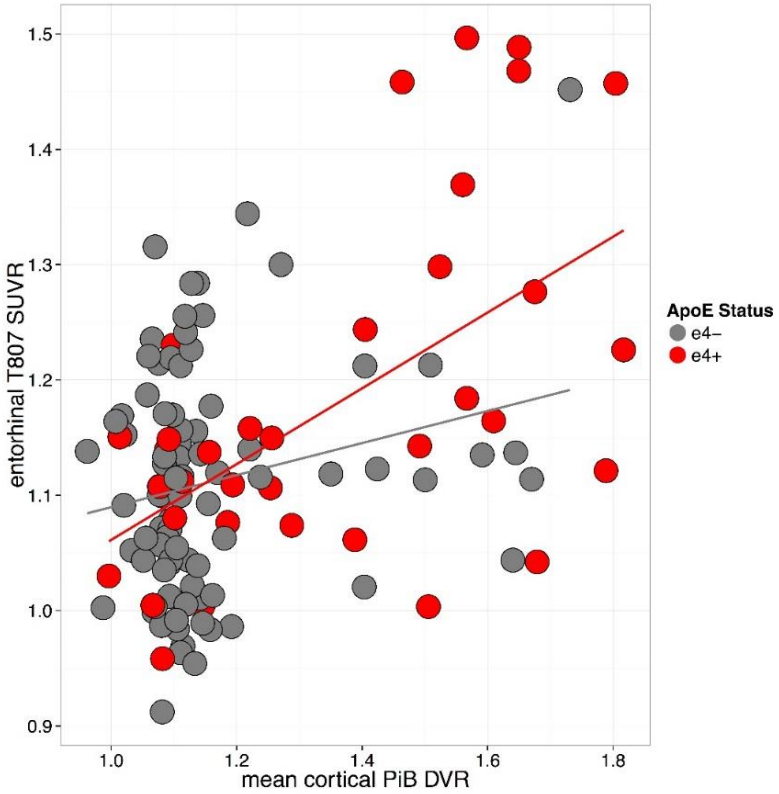

An update on imaging typical and atypical AD and FTLD spectrum tauopathies with [18F] AV1451 PET and PiB PET

Brad Dickerson, Sara Makaretz, Chenjie Xia, Scott McGinnis, Christina Caso, Keith Johnson

Massachusetts General Hospital/Harvard Medical School, Charlestown, MA, United States

Objective: To image tau pathology in vivo using PET in patients with clinically typical and atypical AD and Frontotemporal Lobar Degeneration (FTLD).

Background: A critical unmet need for AD and FTLD research, especially therapeutic trials, is the development of biomarkers to detect and quantify pathological tau in vivo in the broad spectrum of tauopathies.

Methods: We used [18F] AV1451 to scan a series of patients with AD and FTLD, including typical and atypical AD and vFTD, PPA, CBS, and PSP. We analyzed SUVR (cerebellum reference) data to localize and quantify [18F] AV1451 signal. We also co-registered analyzed [18F] AV1451 images to MRI images for visualization and calculation of % atrophy relative to controls.

Results: [18F] AV1451 signal was elevated in brain regions hypothesized to be involved in neurological dysfunction based on clinical symptoms and in which other evidence of neurodegeneration was present based on atrophy or hypometabolism.

Conclusions: [18F]AV1451 is very promising as a tau PET ligand for imaging tau pathology in vivo in patients with typical and atypical forms of AD. In vivo results suggest the potential for its use for certain applications in FTLD, but there is evidence of signal uptake in patients who likely do not have tau pathology. Furthermore, recent data from autoradiography studies raise questions.

Evidence that striatal amyloidosis is a marker of progression across the spectrum of Alzheimer's disease

Bernard Hanseeuw[1], John Bark[1], Jasmeer Chhatwal[1, 2], Heidi Jacobs[1], Gad Marshall[1, 2], Elizabeth Mormino[1], Kathryn Papp[1, 2], Rebecca Amariglio[1, 2], Dorene Rentz[1, 2], Jorge Sepulcre[1], Patrizia Vannini[1, 2], Aaron Schultz[1], Reisa Sperling[1, 2], Keith Johnson[1, 2]

[1]*Departments of Neurology, Psychiatry, Radiology, and the Athinoula A. Martinos Center for Biomedical Imaging, Massachusetts General Hospital, Harvard Medical School, Boston, MA, United States*
[2]*Center for Alzheimer Research and Treatment, Department of Neurology, Brigham and Women's Hospital, Harvard Medical School, Boston, MA, United States*

Background: Autopsy studies indicate that amyloidosis starts in neocortex and extends into striatum. Because amyloid (Aβ) is a risk factor for memory decline, we investigated in-vivo the longitudinal association between cortical and striatal Aβ and disease progression in cognitively normal (CN) older adults and symptomatic AD.

Methods: One hundred thirty-seven CN elderly (Harvard Aging Brain Study; ages=65-87; CDR=0) had longitudinal PiB-PET imaging. Ninety-nine had tau-PET (T807/AV1451) at follow-up. Participants underwent annual cognitive testing over four years: Memory composite z-scores were derived from the 6-trial Selective Reminding Test (SRT) and the Free and Cued SRT (FCSRT). We also analyzed baseline PiB-PET, logical memory, and clinical impairment in fifty-two patients with MCI or mild AD dementia (ages=50-85; CDR≥0.5). Striatal (caudate and putamen) and neocortical PiB DVR aggregates were compared, using cerebellar gray as reference. We used mixed-effect models with random intercepts, covarying age.

Results: R^2 between baseline striatal- and cortical-PiB DVR was 0.76.

CN: Memory decline was associated with baseline (striatal: T=-5.2/p=3*e-7, cortical: T=-4.3/p=2*e-5) and longitudinal (striatal: T=-3.1/p=.002, cortical: T=-2.8/p=.005) PiB. Controlling for baseline cortical-PiB, longitudinal striatal-PiB still related to memory decline (T=-1.9/p=.054).

Longitudinal striatal- and cortical-PiB related to entorhinal and inferior temporal T807 SUVr (all p<2*e-4). Controlling for baseline cortical-PiB, longitudinal striatal-PiB still related to entorhinal (T=2.0/p=.047) and inferior temporal (T=1.9/p=.056) T807.

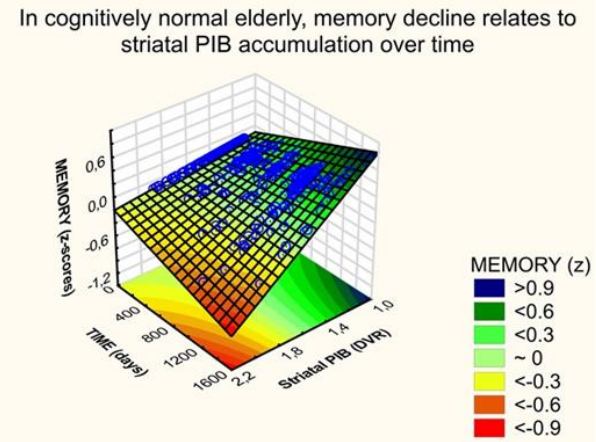

MCI/AD: Cross-sectional striatal- (T=-3.3/p=.002) and cortical-PiB (T=-2.1/p=.038) related to logical memory (delayed recall). Controlling for cortical-PiB, striatal PiB still related to memory (T=-2.7/p=.010). Striatal (T=2.8/p=.005) and cortical (T=2.5/p=.012) PiB both predicted longitudinal CDR sum-of-boxes. Modeled as simultaneous predictors, baseline striatal-PiB tended to predict increasing CDR-SB over time (T=1.7/p=.087) whereas cortical-PiB did not (T=-0.3/p=.747).

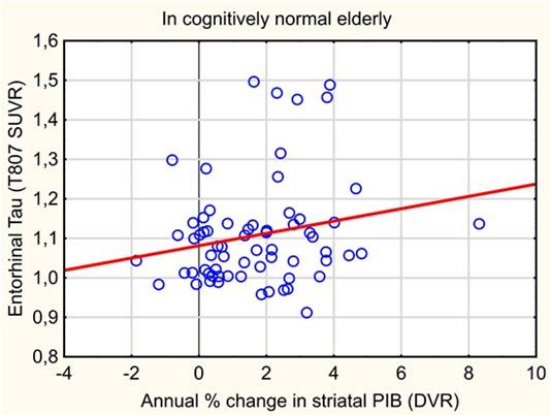

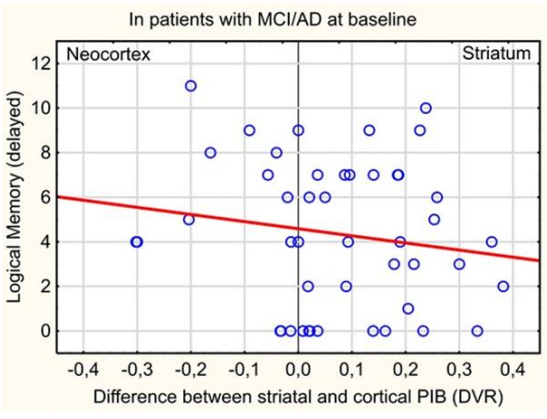

Conclusion: This data provides evidence that striatal Aβ accumulation relates to disease progression across the AD spectrum, and that the association is stronger than that of cortical Aβ, suggesting a temporal relationship more proximal to clinical decline.

Patterns of tau accumulation: Preliminary analyses of change in serial ^{18}F-T807-PET

Danielle M Cosio[1], Aaron P Schultz[1, 2], J Alex Becker[1], Chris Lee[1], Nick Andrea[1], Kelly Judge[1], Keith A Johnson[1, 2]

[1]*Department of Radiology, Massachusetts General Hospital, Harvard Medical School, Boston, MA, United States*
[2]*Athinoula A. Martinos Center for Biomedical Imaging, Department of Neurology, Massachusetts General Hospital, Harvard Medical School, Charlestown, MA, United States*

Background: Autopsy evidence suggests that tau deposition progresses according to a specific anatomic pattern (Braak and Braak, 1991). It is now possible to image tau accumulation in vivo with serial 18F-T807 (AV1451)-PET

Methods: We acquired 18F-T807-PET in 21 participants (age=72±8 yr; 13 clinically normal (CN), 8 with mild cognitive impairment or Alzheimer's disease) at two time points (lag=15.5±4.6 months). SUVR (80-100 min; cerebellar gray reference) were calculated from 32 right-left cortical and 3 subcortical FreeSurfer-defined regions (ROIs). Change in SUVR per year (cSUVR) was calculated in each ROI; ROIs were filtered by baseline SUVR>1.1, rank ordered by change in each subject, and tabulated across subjects. Asymmetry quotients were also calculated.

Results: Average number of accumulating (cSUVR>0) ROIs across all subjects was 31.2±9 of 67 possible, and the grand mean cSUVR was 0.09 in these accumulating ROIs. The greatest increases (seen in >60% of subjects) were observed in left middle temporal, bilateral pars triangularis, and left inferior temporal ROIs (Table 1). Hemispheric bias in accumulation and deposition were not significant. Number of accumulating ROIs did not differ between CN and impaired groups, but mean cSUVR in accumulating ROIs was greater in impaired subjects than CN (t=2.3, p=0.04). Mean values of the top 20 ROIs ranked by cSUVR were bimodal for the impaired group, either greater than 0.12 or less than 0.04. Values for CN ranged from 0.01 to 0.11 for CN. Middle and inferior temporal ROIs ranked highly (in >60% of subjects) within group-wise rankings for both diagnostic groups.

Conclusions: Initial results of serial T807-PET imaging suggest higher rates of tau accumulation for impaired populations, but also provide evidence of change in a similar anatomy among clinically normal subjects and corroborate neuropathological studies suggesting early neocortical spread occurring in inferior and middle temporal cortices.

Table 1: Top 20 increasing ROIs, individually defined – Full Sample

Overall Rank	ROI	Frequency in Top 20s	Percent of Subjects	Average Rank	Mean cSUVR
1	Inferior temporal (L)	14	66.70%	12	0.07
2	Pars triangularis (L)	14	66.7%	11	0.06
3	Fusiform (L)	14	66.7%	12	0.05
4	Middle temporal (L)	13	61.9%	8	0.10
5	Pars triangularis (R)	13	61.9%	10	0.08
6	Middle temporal (R)	12	57.1%	9	0.17
7	Inferior temporal (R)	12	57.1%	10	0.11
8	Superior temporal (L)	12	57.1%	10	0.08
9	Pars opercularis (L)	12	57.1%	11	0.04
10	Pars opercularis (R)	12	57.1%	14	0.04
11	Rostral anterior cingulate (L)	11	52.4%	11	0.04
12	Temporal pole (L)	10	47.6%	9	0.09
13	Amygdala (R)	10	47.6%	10	0.09
14	Cuneus (R)	10	47.6%	8	0.08
15	Banks STS (L)	9	42.9%	6	0.15
16	Isthmus cingulate (R)	9	42.9%	7	0.11
17	Precuneus (R)	8	38.1%	10	0.11
18	Temporal pole (R)	8	38.1%	12	0.09
19	Parahippocampal (L)	8	38.1%	12	0.08
20	Pericalcarine (L)	8	38.1%	9	0.06
21	Rostral anterior cingulate (R)	8	38.1%	12	0.03
22	Insula (L)	8	38.1%	14	0.02
23	Amygdala (L)	8	38.1%	11	0.01
24	Superior temporal (R)	7	33.3%	7	0.18
25	Inferior parietal (R)	7	33.3%	12	0.12
26	Superior frontal (R)	7	33.3%	12	0.07
27	Caudal anterior cingulate (R)	7	33.3%	13	0.06
28	Caudal middle frontal (L)	7	33.3%	10	0.06
29	Fusiform (R)	7	33.3%	13	0.04
30	Supramarginal (L)	7	33.3%	13	0.03
31	Entorhinal (L)	7	33.3%	9	0.1
32	Banks STS (R)	6	28.6%	11	0.18
33	Lateral occipital (R)	6	28.6%	6	0.15
34	Caudal middle frontal (R)	6	28.6%	14	0.11
35	Transverse temporal (L)	6	28.6%	7	0.09
36	Precuneus (L)	6	28.6%	14	0.09
37	Cuneus (L)	6	28.6%	9	0.08
38	Parahippocampal (R)	6	28.6%	14	0.05
39	Superior frontal (L)	6	28.6%	14	0.02
40	Ventral DC (L)	6	28.6%	16	0.02
41	Posterior cingulate (R)	5	23.8%	9	0.11
42	Pericalcarine (R)	5	23.8%	11	0.05
43	Isthmus cingulate (L)	4	19.0%	5	0.26
44	Inferior parietal (L)	4	19.0%	10	0.16
45	Ventral DC (R)	4	19.0%	12	0.10
46	Lateral occipital (L)	4	19.0%	6	0.09

Impact of 18F T807 (AV1451) binding in the choroid plexus on measurements in nearby structures

Christopher Lee[1], Danielle Cosio[1], Kelly Judge[1], Nicolas Andrea[1], Reisa Anne Sperling[2, 3], Keith Alan Johnson[1, 2]

[1]*Department of Radiology, Massachusetts General Hospital, Harvard Medical School, Boston, MA, United States*
[2]*Athinoula A. Martinos Center for Biomedical Imaging, Department of Neurology, Massachusetts General Hospital, Harvard Medical School, Charlestown, MA, United States*
[3]*Center for Alzheimer Research and Treatment, Brigham and Women's Hospital, Harvard Medical School, Boston, MA, United States*

Background: High levels of T807 binding are occasionally seen in the choroid plexus (CP), which extends along the floor of the lateral ventricle, inferiorly into the temporal horn. Since the CP closely overlies the hippocampus, it is highly likely that signal spill-in complicates measurement of hippocampal T807 binding.

Objective: We sought to investigate the impact of CP T807 on nearby regions by evaluating MR-PET co-registered data in cognitively normal and impaired groups, exploring age-dependence as a possible contributor.

Methods: We evaluated T807-PET (80-100min) in 79 low amyloid older normals (ON-low), 51 high amyloid older normals (ON-high), and 17 younger normals (YN). T807 SUVR (cerebellar reference) was calculated using MPRAGE and GTM partial volume correction in Freesurfer regions: Choroid plexus (CP), Hippocampus (H), Entorhinal cortex (ER), Inferior temporal gyrus (IT), Inferior parietal lobule (IP), Frontal pole (FP), Superior frontal gyrus (SF), Caudal middle frontal gyrus (CMF), and Rostral middle frontal gyrus (RMF). Pearson correlations were calculated between ROIs, and between ROIs and age, across all subjects and within groups. SUVR in ROIs was compared with age and with respect to amyloid burden assessed with PiB.

Results: Age was related to CP T807 in the older age range (r,p=0.20, 0.02), but not the younger (p=0.13), and did not differ according to cortical amyloid level. Adjusting for age, CP was associated with H ($p<2x10^{-16}$), and was not associated with ER, IT, IP, FP, SF, CMF or RMF.

Conclusions: CP T807 binding was age-related among older but not younger subjects, and did not depend on amyloid load. CP was related to H T807 in older but not younger subjects, and did not depend on amyloid load. These findings refine our understanding of high T807 signal in CP as an occurrence among older adults.

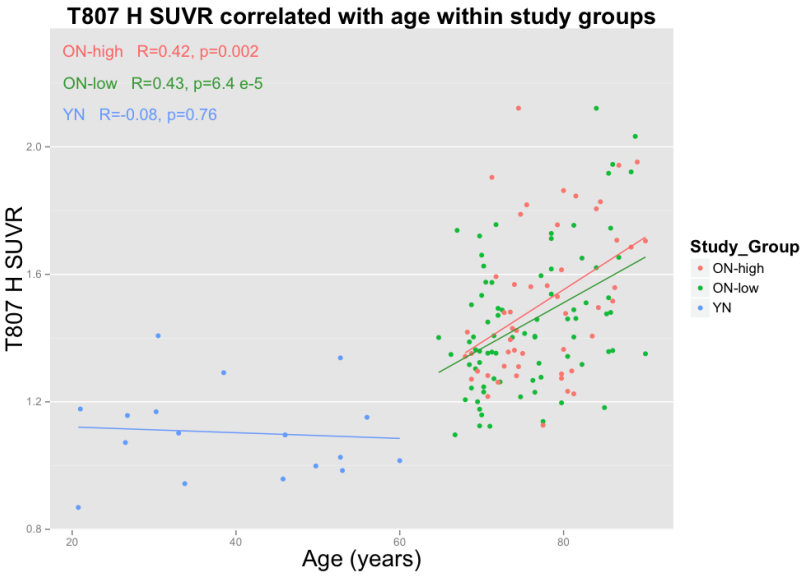

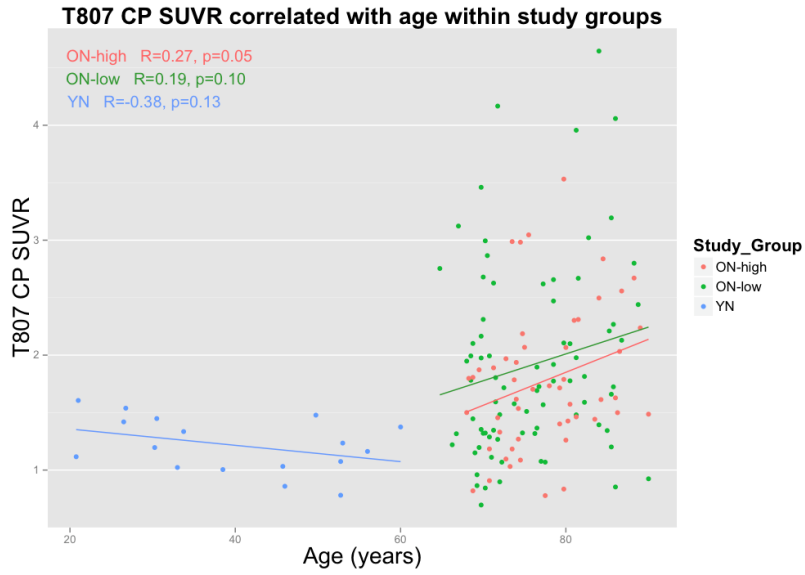

Figures 1 and 2. *Association between age and CP and H T807 SUVR*

Multimodal evaluation of the relationships between amyloid, tau and neurodegeneration in Alzheimer's disease

Leonardo Iaccarino[1, 2, 3], Gautam Tammewar[1], Daniel Schonhaut[1], Samuel N Lockhart[4], Rik Ossenkoppele[1, 4], James P. O'Neil[5], Mustafa Janabi[5], Suzanne L. Baker[4, 5], Nagehan Ayakta[1, 4], Andreas Lazaris[1, 4, 5], Maria Luisa Gorno-Tempini[1], Bruce Miller[1], William Jagust[1, 4, 5], Gil Rabinovici[1, 4, 5]

[1]*Memory and Aging Center, Sandler Neurosciences Center, University of California, San Francisco, CA, United States*
[2]*Vita-Salute San Raffaele University, Milan, Italy*
[3]*In vivo human molecular and structural neuroimaging unit, Division of Neuroscience, San Raffaele Scientific Institute, Milan, Italy*
[4]*Helen Wills Neuroscience Institute, University of California, Berkeley, CA, United States*
[5]*Life Sciences Division, Lawrence Berkeley National Laboratory, Berkeley, CA, United States*

Aim: To study the interplay between tau- and amyloid-PET biomarkers and gray matter volumes in AD.

Participants/Methods: We included twenty-one patients (age range 48-76, mean 61.2 yrs) with clinical probable AD (including a variety of AD phenotypes) and positive amyloid PET. All patients had a 3T T1-weighted MRI, ^{11}C-PiB and ^{18}F-AV1451 PET. ^{11}C-PiB 90-minutes DVR images and ^{18}F-AV1451 80-100 minutes SUVR images were created with cerebellar gray matter reference. MRIs were segmented into gray matter masks and warped to the MNI template using DARTEL in SPM12. ^{11}C-PiB and ^{18}F-AV1451 images were co-registered to the MRI and subsequently warped. Correlations between PET biomarkers were estimated with Biological Parametric Mapping (BPM) voxel-wise robust regression modeling, covarying for age and gender. Subsequently, further BPM analyses were run to estimate correlations between each PET biomarker and neurodegeneration, adding total intracranial volume (TIV) as a further nuisance covariate.

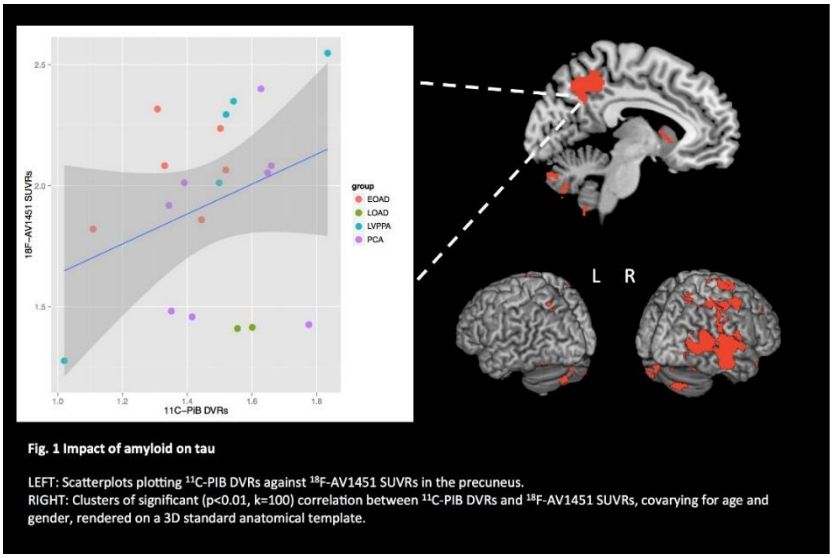

Fig. 1 Impact of amyloid on tau

LEFT: Scatterplots plotting ^{11}C-PIB DVRs against ^{18}F-AV1451 SUVRs in the precuneus.
RIGHT: Clusters of significant (p<0.01, k=100) correlation between ^{11}C-PIB DVRs and ^{18}F-AV1451 SUVRs, covarying for age and gender, rendered on a 3D standard anatomical template.

Results: BPM analysis showed a significant correlation (p<0.01, k=100) between ^{18}F-AV1451 and ^{11}C PiB-PET in medial/lateral parietal, middle and posterior cingulate, lateral temporal and dorsolateral prefrontal regions (Figure 1).

^{18}F-AV1451 binding showed significant (p<0.001, k=100) negative correlations with gray matter volume in occipital and retrolimbic (posterior cingulate) regions (Figure 2), while no significant correlations were found between ^{11}C-PIB and gray matter volumes at this threshold. Relationships between imaging markers were not driven by the inclusion of specific AD variants in the sample (Figures 1, 2).

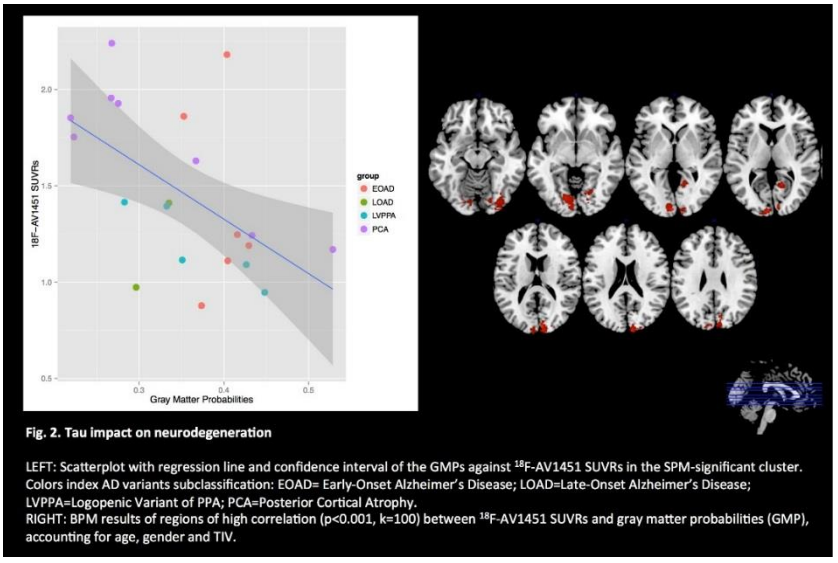

Fig. 2. Tau impact on neurodegeneration

LEFT: Scatterplot with regression line and confidence interval of the GMPs against ^{18}F-AV1451 SUVRs in the SPM-significant cluster. Colors index AD variants subclassification: EOAD= Early-Onset Alzheimer's Disease; LOAD=Late-Onset Alzheimer's Disease; LVPPA=Logopenic Variant of PPA; PCA=Posterior Cortical Atrophy.
RIGHT: BPM results of regions of high correlation (p<0.001, k=100) between ^{18}F-AV1451 SUVRs and gray matter probabilities (GMP), accounting for age, gender and TIV.

Discussion/Conclusion: Amyloid and tau accumulation were correlated in regions known to be affected in AD. In our sample, however, only tau burden was significantly related to neurodegeneration. These findings are consistent with a disease model in which the relationship between amyloid and neurodegeneration is mediated by the spread of tau.

In vivo cortical distribution of tau and amyloid deposits in cognitively normal elderly

Jorge Sepulcre[1, 2], Michel Grothe[3], Mert Sabuncu[2], Aaron Schultz[2], Bernard Hanseeuw[2], Reisa Sperling[2, 4, 5], Keith Johnson[1, 4, 5]

[1]*Division of Nuclear Medicine and Molecular Imaging, Department of Radiology, Massachusetts General Hospital and Harvard Medical School, Boston, MA, United States*
[2]*Athinoula A. Martinos Center for Biomedical Imaging, Charlestown, MA, United States*
[3]*German Center for Neurodegenerative Diseases (DZNE), Rostock, Germany*
[4]*Centre for Alzheimer Research and Treatment, Department of Neurology, Brigham and Women's Hospital and Harvard Medical School, Boston, MA, United States*
[5]*Department of Neurology, Massachusetts General Hospital and Harvard Medical School, Boston, MA, United States*

Background: Abnormal accumulation of amyloid-b (Ab) and Tau proteins in the human brain are two pathologic hallmarks of the Alzheimer's disease. As pathological processes begin decades before the onset of the clinical manifestations, the study of cortical distribution at early stages may be critical to understand the underpinnings of the disease. In this study, we aim to identify the in vivo brain spatial distributions of Tau and Ab deposits in a sample of cognitively normal participants in the Harvard Aging Brain Study. The overall goal of our work was to determine potential patterns of propagation and to provide cortical masks for individual staging in future works.

Methods: Eighty-eight subjects (age: 76.2 (6.2), M/F: 39/49) underwent PiB and 18F-T807 (AV1451) imaging acquisitions. Using cerebellar grey reference, PiB PET data was expressed as DVR and 18F-T807 as SUVR. We used a voxel-level hierarchical clustering approach to obtain the main clustering partitions corresponding to cortical distribution maps of PiB and 18F-T807. Then, we studied the nested hierarchical relationships between areas of distinctive pathological deposits.

Results: We found that Tau and Ab maps both display optimal cortical partitions at k=4 (Figure 1).

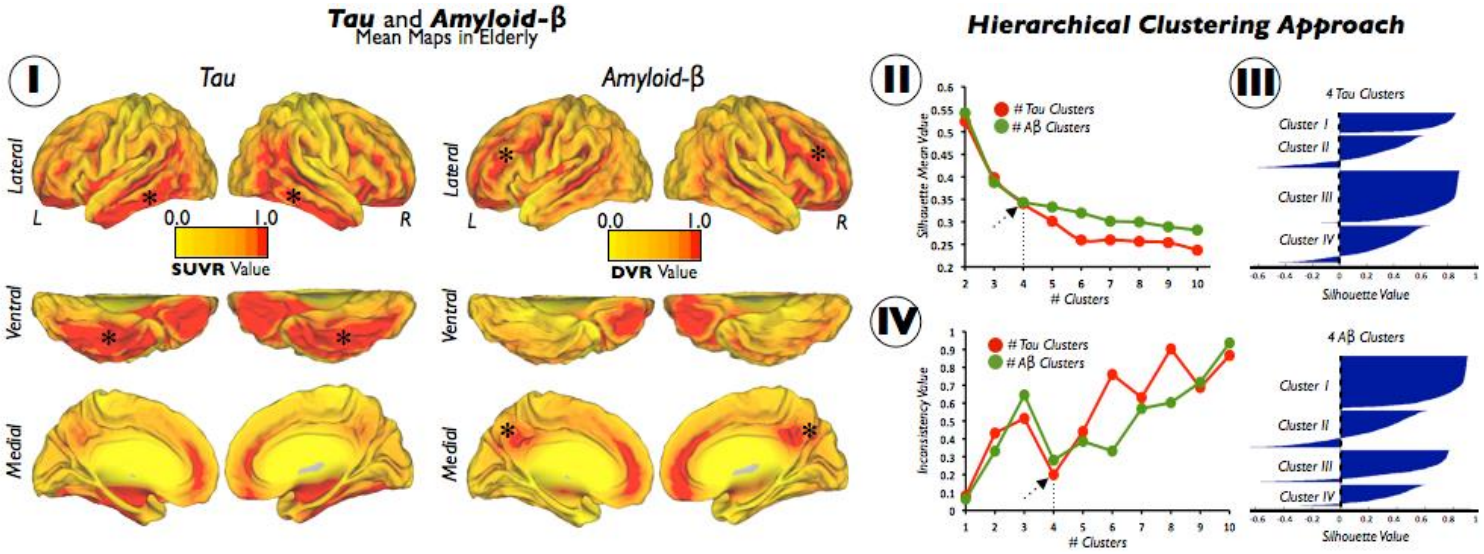

Figure 1

Tau deposits are grouped in the temporal lobe (Figure 2-I, red), distributed heteromodal areas (Figure 2-I, green), medial and visual regions (Figure 2-I, blue), and primary somatomotor cortex (Figure 2-I, yellow); while Aβ deposits are clustered in the heteromodal areas (Figure 2-II, red and green) and, rather patchy, distributed regions involving primary cortices, medial structures and temporal areas (Figure 2-II, blue and yellow). Moreover, we found that Tau deposits in the temporal lobe and distributed heteromodal areas are tightly nested.

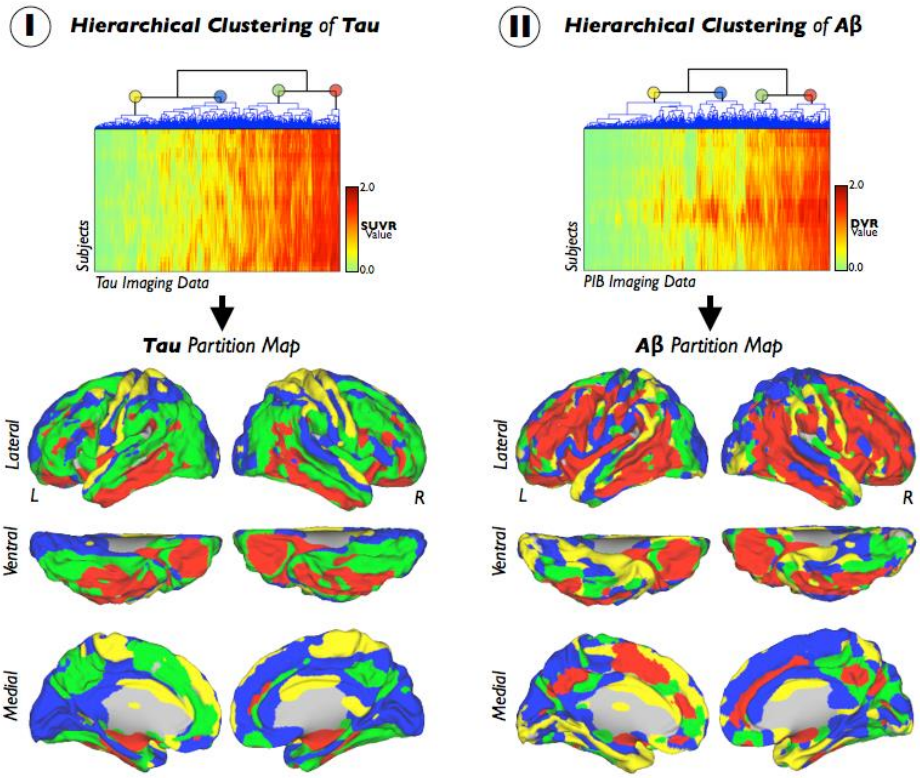

Figure 2

Conclusions: Our results show that Tau and Ab deposits in the elderly brain display very distinct cortical distributions, as well as deep overlaps between principal clusters of both pathologies in heteromodal regions.

Deficiency in anatomical DTI connectivity is associated with [^{18}F] THK-5351 accumulation in Alzheimer's disease

Etsuko Imabayashi, Jaroslav Rokicki, Koichi Kato, Harumasa Takano, Hiroshi Matsuda

Integrative Brain Imaging Center, National Center of Neurology and Psychiatry, Tokyo, Japan

Objective: To evaluate influence of [^{18}F] THK-5351 deposition on connectivity of medial temporal areas.

Methods: Participants were 6 PIB-positive Alzheimer's disease (AD) patients and 5 PIB-negative cognitively normal healthy controls (HC). We performed [^{18}F] THK-5351 PET, [^{11}C] PIB PET, structural MRI and DTI scan for each participant.

We first coregistered all the image modalities. Then we extracted the amygdala and the hippocampus VOI from structural MRI. Within these regions we identified high [^{18}F] THK-5351 accumulation areas using standardized uptake value ratio (SUVR≧2.5) in PET. SUVR was calculated for each PET image using the whole cerebellum as reference region. Finally we analyzed volumes of high [^{18}F] THK-5351 accumulation areas and moreover used them as seeds for fiber tracking.

Results: Only volume of [^{18}F] THK-5351 accumulation area in the amygdala was significantly ($p < 0.05$) larger for AD patients as compared with HC. Notably, no significant differences were detected if the volume of the whole hippocampus or amygdala VOI were used. Furthermore, fibers tracked from high [^{18}F] THK-5351 accumulation areas of the amygdala region were on average shorter than those tracked from areas with low (SUVR<2.5) accumulation of [^{18}F] THK-5351 for AD subjects only. In HC results were opposite, longer fibers were tracked from areas with high SUVR≧2.5.

Conclusions: These results suggest that [^{18}F] THK-5351 accumulation in AD patients is more prominent within the amygdala region as compared to the hippocampus. Moreover, pathological, not related to aging [^{18}F] THK-5351 accumulation could be related to neuronal loss and influence fiber length.

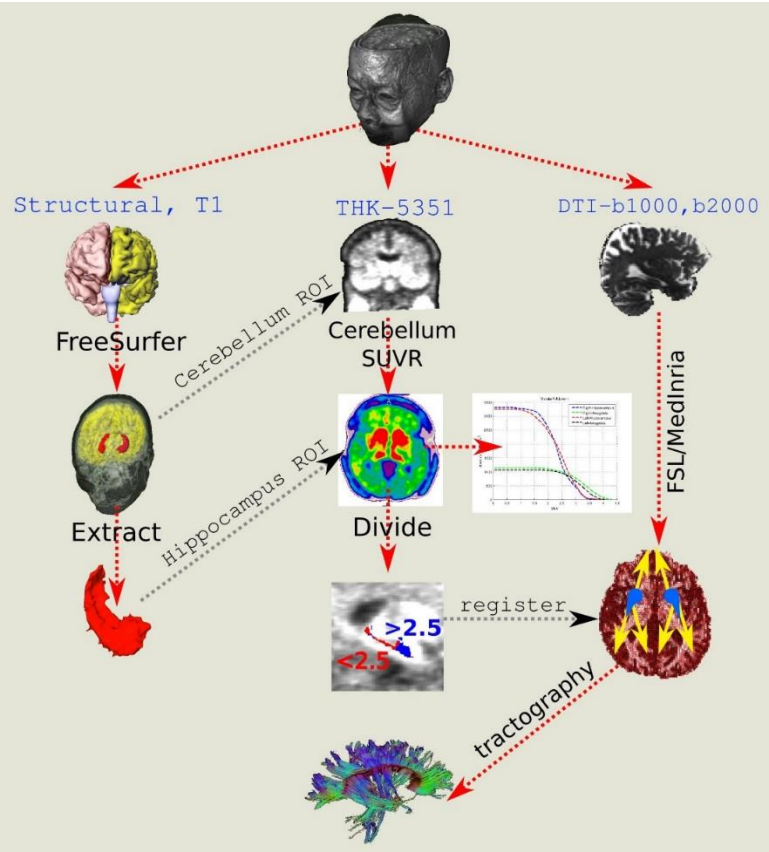

Characteristic patterns of brain perfusion deficit and amyloid deposition in AD, MCI and HC using dual-phase 18F-Florbetapir (AV-45/Amyvid) PET imaging

Ing-Tsung Hsiao[1], Kun-Ju Lin[2]

[1]*Chang Gung University, Kweishan, Taoyuan City, Taiwan*
[2]*Chang Gung Memorial Hospital, Taiwan*

Our goal was to investigate the characteristic patterns of brain perfusion and β-amyloid distribution in patients with Alzheimer's disease (AD), mild cognitive impairment (MCI), and cognitively healthy controls (HC) using dual-phase 18F-Florbetapir (AV-45/Amyvid) PET imaging. We also examined the potential associations between the imaging markers and the severity of cognitive decline as measured by the Mini-Mental State Examination (MMSE).

Methods: A total of 75 subjects (20 AD, 43 MCI, and 12 HC) underwent both dual-phase 18F-AV-45 PET scanning (perfusion pAV-45 imaging: 1-6 min post-injection; amyloid 18F-AV-45 imaging: 50-60min post-injection) and MRI imaging. Both regional and voxelwise analysis of pAV-45 and 18F-AV-45 images were performed to investigate the perfusion deficits and the beta-amyloid deposition in the three study groups. The associations of MMSE scores with global perfusion deficits and amyloid deposition were investigated with linear and segmental linear correlation analyses.

Results: HC generally had normal perfusion pAV-45 findings, whereas both MCI and AD patients showed evident perfusion deficits in the hippocampus, temporal, parietal, and middle frontal cortices. The motor-sensory cortex was relatively preserved. MMSE scores in the entire study cohort were significantly correlated with the degree of perfusion impairment measured from pAV-45 imaging ($r = 0.5259$, $P < 0.0001$). AD group displayed significantly higher 18F-AV-45 uptake than the two other study groups. However, MMSE scores correlated with 18F-AV-45 uptake only in HC and MCI patients with high MMSE. The amyloid deposition started from the precuneus, the frontal and temporal regions in the early MCI stage, ultimately reaching the maximum burden in the most advanced MCI stages.

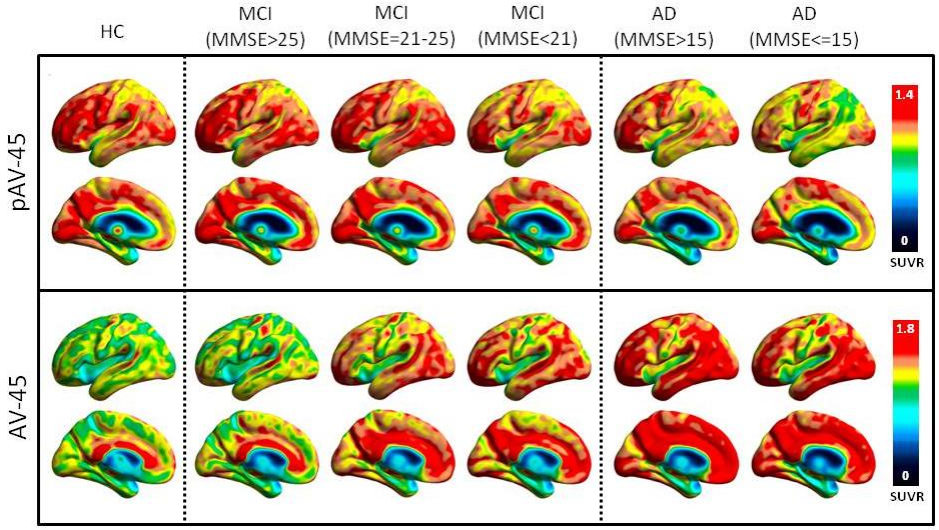

Conclusions: Our results indicate that brain perfusion deficits and beta-amyloid deposition in AD follow different trajectories that can be successfully traced using dual-phase 18F-AV-45 PET imaging.

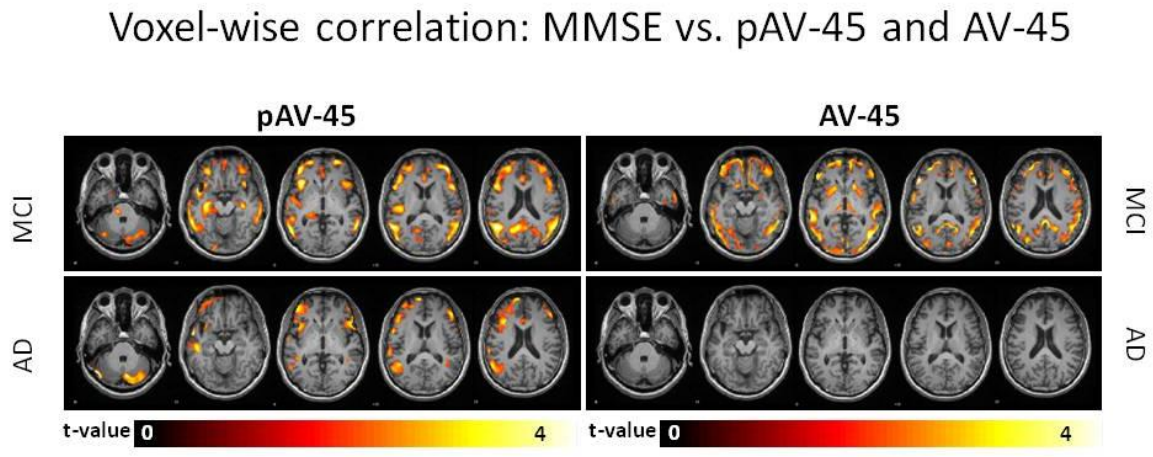

Effect of brain amyloidosis on the incidence and prevalence of neuropsychiatric behaviors in the elderly

Naira Goukasian[1], Triet Do[1], Jonathan Grotts[1], David Elashoff[1], Shannon Risacher[2], Andrew Saykin[2], Liana Apostolova[1, 2]

[1]*University of California, Los Angeles, CA, United States*
[2]*Indiana University School of Medicine, Indianapolis, IN, United States*

Background: The incidence and prevalence of neuropsychiatric behaviors in the elderly with and without cognitive decline may be influenced by amyloid pathology.

Methods: 275 cognitively normal (NC), 100 subjective cognitive complaint (SMC), 559 mild cognitive impairment (MCI) and 143 Alzheimer's dementia (AD) ADNI subjects received [18F]-Florbetapir PET scans. Yearly neuropsychiatric inventory (NPI) data was collected from the study partners at each visit. NPI symptoms were coded as present or absent. Fisher-exact or Wilcoxon rank test were used to NPI rates as appropriate. Survival analyses were used to determine hazard ratios for developing the most common NPI behaviors by amyloid status.

Results: Amyloid positive NC were older. Amyloid positive NC and SMC were more likely to be APOE4 positive, have higher CDR-SB and ADAScog, a lower FAQ and mean total NPI score (Table). Rate of de novo NPI symptoms in NC and SMC over time did not differ by amyloid status.

Amyloid positive MCI were older, more likely to be APOE4 positive, had higher CDR-SB, ADAScog, FAQ, mean total NPI and greater frequency of anxiety at baseline (Table). In MCI amyloid pathology was significant risk factor for developing apathy (hazard ratio [HR]=1.52, 95% CI 1.17-1.99, p=0.002), anxiety (HR 1.52, 95% CI 1.18-2.01, p=0.001) and agitation (HR=1.38, 95% CI 1.1-1.8, p=0.014) and reached trend level significance for irritability (HR=1.24, 95% CI 0.99-1.6, p=0.065)(Figure).

Amyloid positive AD were younger, more likely to be APOE4 positive, had higher CDR-SB, ADAScog and FAQ, lower mean total NPI and frequency of apathy at baseline. Rate of de novo NPI symptoms in AD over time did not differ by amyloid status.

Conclusions: Amyloid positive MCI subjects have higher prevalence and incidence of neuropsychiatric behaviors. Shorter follow-up for the AD and SMC groups might have contributed to the lack of difference in NPI symptom incidence over time.

TABLE / Variable	NC (N=275)			SMC (N=100)			MCI (N=559)			AD (N=143)		
	Amyloid-	Amyloid+	p	Amyloid-	Amyloid+	p	Amyloid-	Amyloid+	p	Amyloid-	Amyloid+	p
Age, yr	72.7	75.8	**<0.001**	69.9	75.3	**0.032**	70.6	73.6	NS	77.2	74.2	**0.033**
Gender, M/F %	52/48	41/59	NS	47/53	25/75	0.069	56/44	58/42	NS	80/20	53/47	**0.015**
CDR-SB, mean	0.027	0.041	**<0.001**	0.056	0.125	**<0.001**	1	1.5	**<0.001**	4.32	4.54	**<0.001**
ADAS13, mean	8.7	9.3	**<0.001**	8	10	**0.002**	12	17	**<0.001**	27	31	**<0.001**
FAQ, mean	0.17	0.14	**<0.001**	0.64	0.54	**0.009**	1.88	3.47	**<0.001**	12.3	13.2	**<0.001**
NPI total, mean	0.99	0.69	**0.001**	1.75	1.11	**0.032**	3.45	4.62	**<0.001**	9.96	7.28	**<0.001**
Anxiety BL, %	5	2.7	NS	8	7	NS	12	19	**0.019**	12	28	NS
Apathy BL, %	3	0	NS	6	4	NS	15	16	NS	64	37	**0.024**
Agitation BL, %	4.5	1.4	NS	4	11	NS	14	19	NS	36	29	NS
Irritability BL, %	9.9	5.5	NS	13	14	NS	26	26	NS	16	33	NS
Depression BL, %	8.4	1.4	**0.05**	13	11	NS	24	27	NS	28	38	NS
Disinhibition BL, %	2.5	0	NS	1	0	NS	9	10	NS	24	17	NS
Hallucinations BL, %	0.5	0	NS	0	0	NS	0.4	1	NS	0	5	NS
Delusions BL, %	0	0	NS	0	0	NS	0	2.4	**0.015**	4	8	NS
Elation BL, %	0	0	NS	0	0	NS	3	2	NS	0	2	NS
Aberrant Motor BL, %	1	0	NS	1	0	NS	3	5	NS	8	16	NS
Sleep BL, %	10.9	9.6	NS	24	7	0.087	20	20	NS	16	16	NS
Appetite BL, %	1.5	0	NS	4	4	N S	9	7	NS	36	21	NS

FIGURE

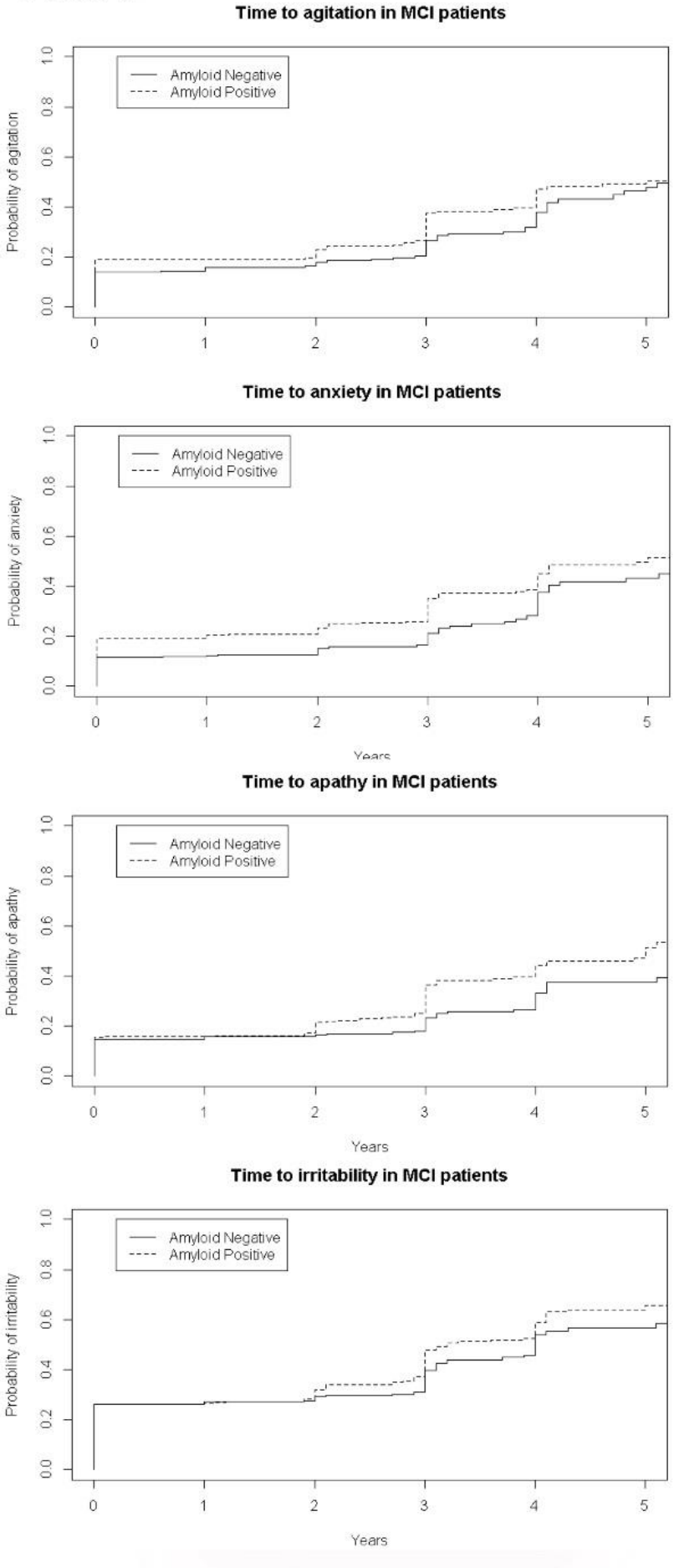
Time to agitation in MCI patients
Amyloid Negative
Amyloid Positive
Probability of agitation
0.0
0.2
0.4
0.6
0.8
1.0
0
1
2
3
4
5
Time to anxiety in MCI patients
Amyloid Negative
Amyloid Positive
Probability of anxiety
Years
Time to apathy in MCI patients
Amyloid Negative
Amyloid Positive
Probability of apathy
Years
Time to irritability in MCI patients
Amyloid Negative
Amyloid Positive
Probability of irritability
Years

Neuronally-derived exosomal proteins can predict brain amyloidosis ascertained with [^{18}F] Flutemetamol

Liana Apostolova[1, 2], Naira Goukasian[1], Karen Gylys[1], Greg Cole[1], Edmond Teng[1], Dale Bredesen[1, 4], Edward Goetzl[3]

[1]*University of California, Los Angeles, CA, United States*
[2]*Indiana University School of Medicine, Indianapolis, IN, United States*
[3]*National Institute on Aging, Bethesda, MD, United States*
[4]*Buck Institute for Research on Aging, Novato, CA, United States*

Background: Neuronally derived exosomes (NDE) are endosomal vesicles shed by neurons that can be readily extracted from plasma. Exosomal Aβ1-42, P-S396-tau and P-T181-tau levels have been show have high accuracy for discriminating mild cognitive impairment (MCI) of the Alzheimer's type and Alzheimer's dementia (AD) diagnosed with the Dubois Criteria from frontotemporal dementia and cognitively normal control subjects (NC)[1,2].

Objective: We examined levels of NDE-derived Aβ, P-S396-tau, P-T181-tau and neurogranin levels as predictors of brain amyloidosis in a cohort of NC, MCI and AD subjects.

Methods: 37 NC, 19 clinically-diagnosed MCI and 16 AD research participants from the ImaGene study had amyloid PET imaging with F18–Flutemetamol and provided plasma samples for NDE isolation, protein extraction and ELISA quantification. As plasma samples can vary with respect to the NDE content, all protein analyte levels were normalized using individual plasma CD81 NDE marker levels. F18–Flutemetamol scans were normalized to cerebellar gray matter. The mean Standard Uptake Value Ratio was dichotomized as positive and negative using the previously validated cut-off of 1.273. We developed two classifier models based on machine learning[3] aiming to predict amyloid PET status in the pooled cohort. The first classifier was provided with age, gender and the normalized levels of all four exosomal proteins. The second additionally included APOE4 genotype. Multiple comparison corrections were conducted by cross-validation with the leave-one-out approach.

TABLE

	NC (N=36)	MCI (N=18)	DEM (N=15)	P-VALUE
AGE (mean ± SD)	74.5 ± 8.2	70.9 ± 8.4	75.9 ± 7.6	0.160
GENDER (M:F)	11:14	10:9	7:9	0.444
APOE4 (carrier:noncarrier)	12:25	9:10	11:5	0.048
MMSE (mean ± SD)	28.5 ± 1.3	27.6 ± 2.1	20.5 ± 8.3	<0.001
SUVR (mean ± SD)	1.1 ± 0.3	1.2 ± 0.4	1.5 ± 0.4	0.009
SUVR≥1.27	38.5%	19.2%	42.3%	0.006
Aβ1-42 (mean pg/ml ± SD)	8.9 ± 4.1	10.9 ± 8.2	11.6 ± 7.5	0.265
P-T181-tau (mean pg/ml ± SD)	143 ± 56	149 ± 73	171 ± 125	0.299
P-S396-tau (mean pg/ml ± SD)	20.6 ± 11.1	24.2 ± 16.0	23.3 ± 15.2	0.594
NRGN (mean pg/ml ± SD)	206 ± 93	291 ± 194	178 ± 149	0.038

Results: The first classifier model achieved an accuracy of 81.1% (Figure). The only two features selected were P-T181-tau and Aβ1-42. The second classifier achieved an accuracy of 80.7% (Figure) and selected APOE4 genotype, P-T181-tau, gender, age, Aβ1-42 and neurogranin as predictors.

Conclusions: NDE proteins show promise for the prediction of amyloid pathology and the potential to increase diagnostic certainty by identifying underlying AD pathology in both clinical care and clinical trials.

FIGURE

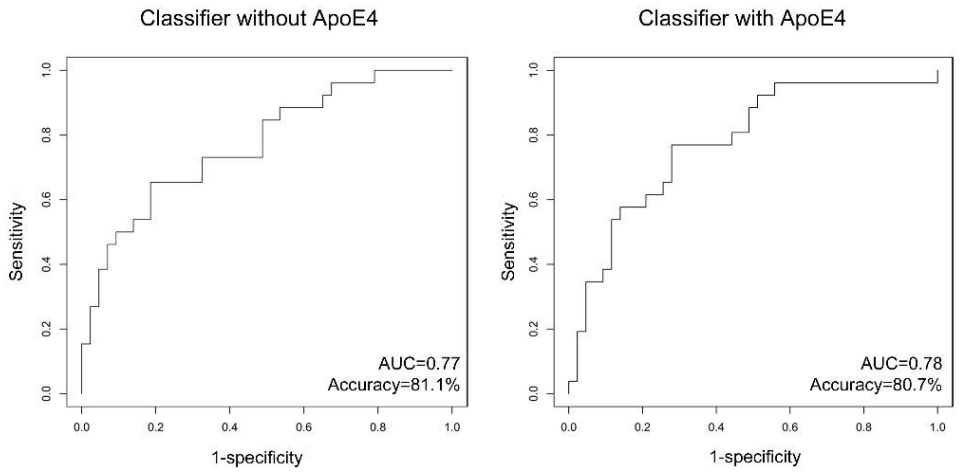

Florbetapir PET to diagnose cerebral amyloid angiopathy

M. Edip Gurol, J. Alex Becker, Panagiotis Fotiadis, Keith Johnson, Steven Greenberg

Massachusetts General Hospital, Boston, MA, United States

Introduction: Previous studies showed that Pittsburgh Compound B (PiB) labels vascular amyloid characteristic of cerebral amyloid angiopathy (CAA) on PET scans; PiB is not approved for clinical use, however.

Hypothesis: We hypothesized that Florbetapir, an FDA-approved PET tracer, can detect amyloid in CAA and help distinguish CAA-related intracerebral hemorrhage (ICH) from hypertensive ICH (HTN-ICH).

Methods: We prospectively enrolled non-demented survivors of primary ICH related to probable CAA (per Boston Criteria, n=10) and HTN-ICH (n=9). All patients underwent Florbetapir-PET, multimodal MRI, and additional PiB-PET for the CAA patients. Amyloid burden was assessed quantitatively using parametric maps and also visually, classified as positive or negative. Spatial correlations between Florbetapir and PiB retention were used to test vascular amyloid binding in CAA. We have tested the diagnostic value of Florbetapir by comparing global and occipital mean Florbetapir retention (standard uptake value ratio, SUVR) as well as Florbetapir positive/negative status between CAA and HTN-ICH groups.

Results: The CAA and HTN-ICH groups had similar age (66.9 vs 67.1), sex and white matter hyperintensity volumes (31ml vs 30ml, all $p>0.8$). Florbetapir uptake and PiB retention strongly correlated in CAA patients both globally within cerebral cortex ($r=0.96$, $p<0.001$) and regionally in occipital, frontal, temporal, parietal cortices (all $r>0.8$, all $p<0.01$). Mean global cortical Florbetapir uptake was significantly higher in CAA than HTN-ICH (SUVR: 1.41+0.16 vs 1.16+0.08, $p=0.001$) as was mean occipital SUVR (1.44+0.12 vs 1.17+0.08, $p<0.001$), remaining independent after correcting for global SUVR ($p=0.02$). Visual rating for Florbetapir positive/negative demonstrated perfect interrater agreement ($k=1$) between two trained neurologists blinded to all other information and was positive for all 10 CAA patients vs 1 of 9 HTN-ICH patients (sensitivity 100%, specificity 89%).

Conclusions: Florbetapir, like PiB, appears to label vascular amyloid in patients with CAA-related ICH. Data using the approved Florbetapir binary visual reading method suggest sufficient sensitivity and specificity for diagnostic use in appropriate clinical settings.

Correction for acquisition time discrepancies in SUVr analyses of ^{18}F-AV1451 tau images

Sudeepti Southekal, Michael D Devous Sr., Michael Navitsky, Ian Kennedy, Abhinay D Joshi, Mark A Mintun

Avid Radiopharmaceuticals, Inc., Philadelphia, PA, United States

Background: It has been suggested that ^{18}F-AV1451 standardized uptake value ratios 80-100 minutes post-injection ($SUVr^{80-100}$) can serve as a practical alternative to full kinetic modeling (Shcherbinin 2014). It is also known (Chien 2013, Shcherbinin 2014) that ^{18}F-AV1451 uptake does not reach equilibrium, with tissues showing rising SUVr values over time. Variations in acquisition start times over multiple follow up visits could therefore confound the interpretation of longitudinal $SUVr^{80-100}$ change. We developed a correction for differences in scan start time to account for uptake-dependent variations in ^{18}F-AV1451 $SUVr^{80-100}$ values.

Methods: Subjects were imaged as four 5-min frames, approximately 80 min after injection of ~10 mCi of ^{18}F-AV1451. Each frame was motion corrected, coregistered to the subject's T1-weighted MRI and spatially normalized to MNI space. Acquisition time correction factors were calculated for each image voxel as the slope of the linear regression line through the four time points, multiplied by the time offset. Performance was evaluated in a test-retest dataset (n=21 pairs of scans), using a data-driven neocortical volume-of-interest and a cerebellar reference region.

Results: Figure 1 shows the test vs. retest scatter plot with and without correction. In subject #2 with an elevated SUVr of 2.06 who was scanned 84 minutes after injection, time correction lowered the SUVr to 2.03. Subject #1 with a more normal SUVr of 1.12 and an ~8 min correction showed a negligible change (-0.003 SUVr units). SUVr %change ± SD was +0.03±4.18 before and +0.05±4.12 after correction.

Conclusion: Time correction achieved changes consistent with expectations based on kinetic behavior, in scans with substantial time offsets. There was minimal impact on the %SD in the test-retest dataset. We conclude that time correction may be useful, particularly in multi-center longitudinal trials with the potential of within-subject variability in scan start times.

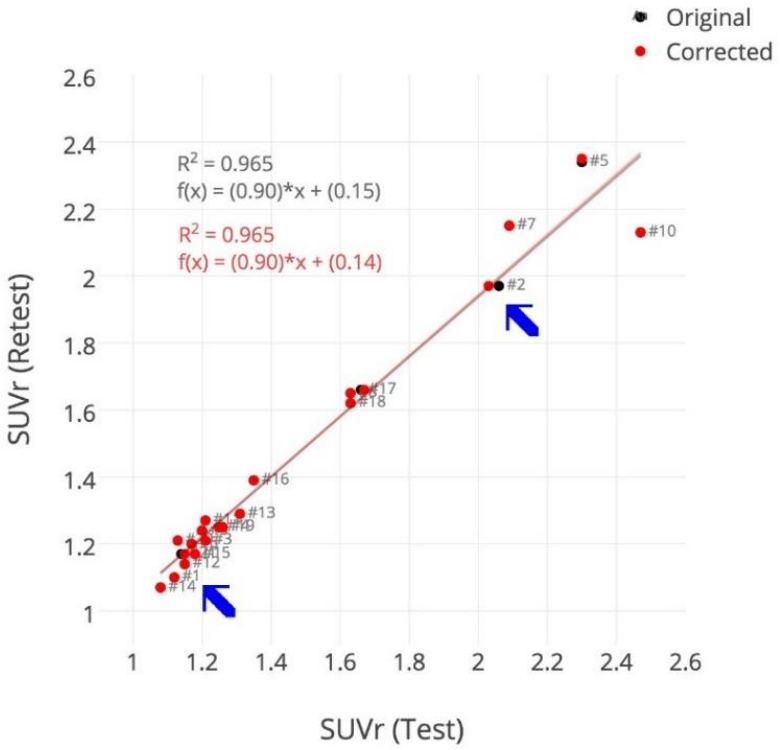

(Top) Scatter plot and (bottom) table showing test-retest data with and without correction for acquisition time discrepancies. Subject #2 (original SUVr 2.06) whose baseline scan began 84 minutes post-injection had a lower SUVr (2.03) after correction. Subject #1 (original SUVr 1.12) whose baseline scan began 88 minutes post-injection showed a negligible change. Correction had minimal impact on test-retest %SD.

#	Visit 1			Visit 2			Test-Retest Difference (Visit 2 – Visit 1)		
	Time (min)	SUVr Original	SUVr Corrected	Time (min)	SUVr Original	SUVr Corrected	ΔTime (min)	ΔSUVr Original	ΔSUVr Corrected
1	**88.07**	**1.12**	**1.12**	**80.07**	**1.10**	**1.10**	**-8.00**	**-0.02**	**-0.02**
2	**84.00**	**2.06**	**2.03**	**80.05**	**1.97**	**1.97**	**-3.95**	**-0.09**	**-0.06**
3	81.10	1.21	1.21	80.15	1.21	1.21	-0.95	0.00	0.00
4	79.78	1.26	1.26	79.05	1.25	1.25	-0.73	-0.01	-0.01
5	79.80	2.30	2.30	79.25	2.34	2.35	-0.55	0.04	0.05
6	80.17	1.17	1.17	80.10	1.20	1.20	-0.07	0.03	0.03
7	80.12	2.09	2.09	80.07	2.15	2.15	-0.05	0.06	0.06
8	80.05	1.63	1.63	80.07	1.65	1.65	0.02	0.03	0.03
9	79.63	1.20	1.20	79.68	1.24	1.24	0.05	0.04	0.04
10	80.67	2.47	2.47	80.85	2.13	2.13	0.18	-0.34	-0.34
11	80.05	1.21	1.21	80.23	1.27	1.27	0.18	0.06	0.05
12	79.75	1.15	1.15	80.05	1.14	1.14	0.30	-0.01	-0.01
13	79.23	1.31	1.31	79.65	1.29	1.29	0.42	-0.02	-0.03
14	79.28	1.08	1.08	79.73	1.07	1.07	0.45	-0.01	-0.01
15	79.60	1.18	1.18	80.05	1.17	1.17	0.45	-0.01	-0.01
16	79.43	1.35	1.35	79.95	1.39	1.39	0.52	0.04	0.03
17	79.35	1.66	1.67	80.00	1.66	1.66	0.65	0.00	-0.01
18	79.28	1.63	1.63	79.95	1.62	1.62	0.67	-0.01	-0.01
19	79.20	1.25	1.25	79.95	1.25	1.25	0.75	0.00	0.00
20	79.97	1.13	1.13	81.43	1.21	1.21	1.47	0.08	0.08
21	**77.00**	**1.14**	**1.15**	**80.07**	**1.17**	**1.17**	**3.07**	**0.03**	**0.02**

Genetic polymorphism of cytochrome P450 family member is associated with brain amyloid load

Andrea Benedet[1], Aurélie Labbe[2], Sulantha Mathotaarachchi[1], Monica Shin[1], Tharick Pascoal[1], Min-Su Kang[1], Serge Gauthier[3], Judes Poirier[2], Pedro Rosa-Neto[1, 2, 3]

[1]*Translational Neuroimaging Laboratory, McGill University Research Centre for Studies in Aging, Canada*
[2]*Douglas Hospital Research Centre, McGill University, Canada*
[3]*McGill University Research Centre for Studies in Aging, Canada*

Background: The cytochromes P450 (CYP) are extensively known by their role at metabolizing several endogenous and exogenous substrates. They are produced in many human tissues including the brain, and have functions such as modulating blood-flow regulation, and participating in neuroinflammatory processes. The aim of our study is to verify whether genetic polymorphisms of CYP are associated with [18F]florbetapir PET uptake.

Methods: [18F]florbetapir PET imaging was employed to assess brain Aβ levels in 256 subjects from the ADNI (186 CN, 70 AD). The genotyped data was obtained with IlluminaHumanOmni2.5 beadchip. The linear association between global [18F]florbetapir SUVR and SNPs from four genes of cytochrome P450 (CYP3A4, CYP2C9, CYP2C19 and CYP1A1) was evaluated (30 tests), adjusting for age, gender, diagnosis and ApoE-e4 carriage. The associations found significant were tested in the voxel-wise level using RMINC tool. Results were corrected for multiple comparisons using Bonferroni and Random-Field Theory. To corroborate findings, the significant association was also tested using CSF Aβ as phenotype.

Results: The analysis unveiled one significant association between brain amyloid load and a SNP from CYP2C19 (rs4388808; P=0.001), in which carriers of the minor allele (MA) have lower global SUVR. No difference in age, diagnosis and ApoE-e4 status was found between groups. The voxel-wise analysis showed a significant effect of the SNP in the frontal and posterior cingulate cortices. The MA of the SNP was also associated with higher CSF Aβ (P=0.002), as expected.

Discussion: The rs4388808, here associated with amyloid load, is an intronic variant of the CYP2C19 gene that has demonstrated an impact in its mRNA expression levels. Despite previous reports relating CYP2C19 with steroidal metabolism in the brain, its other functions are not fully elucidated. In general, CYP are associated with the permeability of the brain-blood barrier and with the production of cholesterol, both associated with amyloid clearance.

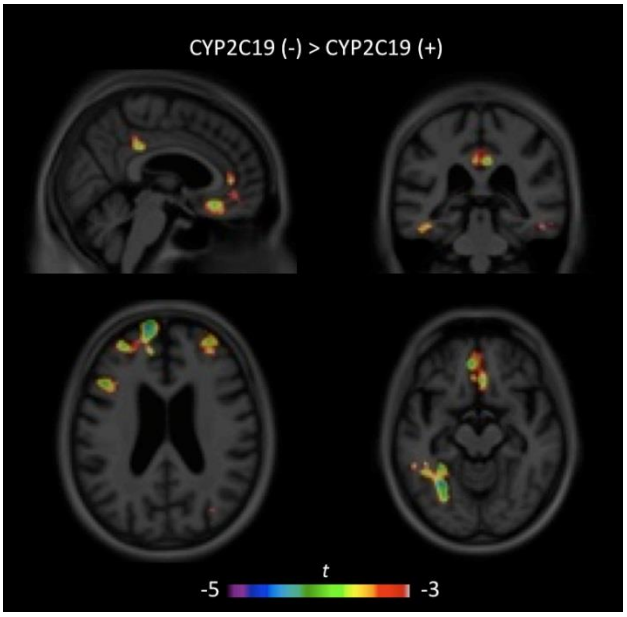

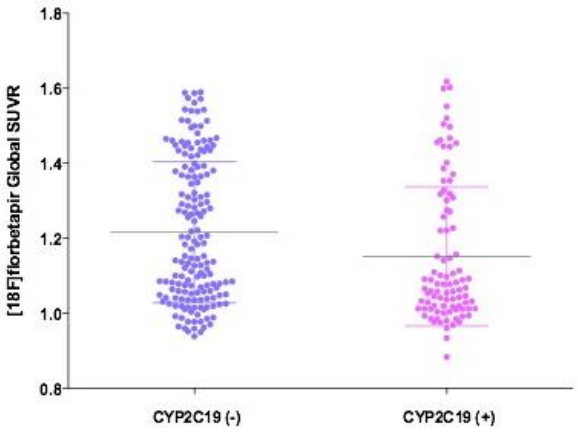

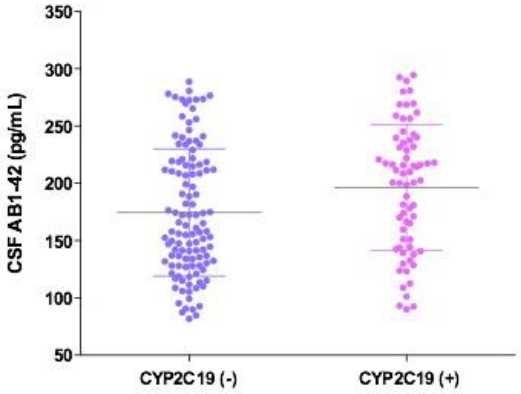

Measuring longitudinal amyloid change using florbetapir PET

Abhinay Joshi[1], Ian Kennedy[1], Michael Navitsky[1], Michael J. Pontecorvo[1], Mark A. Mintun[1], Michael D Devous Sr.[1], Alzheimer's Diesease NeuroImaging Initiative ADNI[2]

[1]*Avid Radiopharmaceuticals, Inc., PA, United States*
[2]*Alzheimer's Disease Neuroimaging Initiative, CA, United States*

Background: Recent studies (Landau et.al. 2015 and Chen et.al. 2015) suggest white matter (WM) reference regions reduce variability in longitudinal (2 scans over ~2 year follow-up) cortical SUVR measurements using florbetapir F 18, which may improve assessment of disease progression. To explore the effectiveness of such techniques over longer time intervals, we used ADNI data acquired at approximately 2 and 4 years after baseline. We also compared measurements of amyloid accumulation in Aβ+ subjects using either atlas-based WM or subject-specific, MRI-derived WM reference regions.

Methods: Participants (66: 18 CN, 16 EMCI and 32 LMCI) underwent a baseline (V1) florbetapir scan followed by two imaging sessions (V2 and V3) at 23±2 and 47±3 months post baseline. Mean cortical SUVr (mcSUVr >1.10= Aβ+ relative to cerebellum) values were calculated as previously described (Clark et.al.2012). Two alternative reference regions were explored; 1) atlas-based WM (centrum semiovale, mcSUVrwm), and 2) subject-specific, MRI-derived WM (mcSUVrwmss). Changes in SUVr (V2-V1; V3-V1) were examined.

Results: Mean SUVR increase from V1 to V2 or V3 in Aβ+ subjects was higher using either atlas-based or subject-specific regions than using cerebellum, and variability (SD of change) was lower (V2-V1: ΔmcSUVr = 1.6±5.9%, ΔmcSUVrwm= 2.7±3.7%, ΔmcSUVrwmss= 4.4±4.4%) and (V3-V1: ΔmcSUVr= 3.7±8.1%, ΔmcSUVrwm= 5.5±4.4%, ΔmcSUVrwmss= 9.7±7.2%). The signal to noise ratio (SNR) (Δmean/ΔSTD) for detecting increased SUVr at V2 was greatest using subject-specific WM (0.24 mcSUVr to 0.71 mcSUVrwm to 0.99 mcSUVrwmss). Similar results were obtained at V3: 0.43 to 1.22 to 1.34.

Conclusion: Analysis of this small sample showed that use of either WM reference regions is associated with increased apparent SNR compared to cerebellum in the measurement of increasing amyloid binding. As expected, the longer time interval at V3 (compared to V2) was associated with further increased SNR ratio using all three reference regions.

Thursday, January 14, 2016 - 10:25am - 11:25

Podium Presentations
SESSION 4: Non-AD tauopathies

Chairs: ***Agneta Nordberg, Karolinska Institutet***
Gil Rabinovici, University of California, San Francisco

10:25-11:25	**SESSION 4:** **NON-AD TAUOPATHIES**	**CHAIRS:** **Agneta Nordberg** Karolinska Institutet **Gil Rabinovici** University of California, San Francisco
10:25-10:40	18F-AV-1451 binding corresponds to disease severity and laterality in non-AD tauopathy syndromes with distinct tau filament strains	**Richard Tsai** University of California, San Francisco
10:40-10:55	Elevated [18F]AV-1451 binding matches the distribution of Tau pathology in Progressive Supranuclear Palsy	**Daniel Schonhaut** University of California, San Francisco
10:55-11:10	Binding characteristics of Tau PET tracer [18F]AV-1451	**Giorgio Attardo** Avid Radiopharmaceuticals, Inc.
11:10-11:25	In vivo [F-18]-AV-1451 (T807) PET imaging in the first two autopsy-confirmed non-Alzheimer tauopathy cases studied at MGH	**Marta Marquie** MassGeneral Institute for Neurodegenerative Disease
11:25-12:05pm	Discussion	

18F-AV-1451 binding corresponds to disease severity and laterality in non-AD tauopathy syndromes with distinct tau filament strains

Richard Tsai[1], Alexandre Bejanin[1], Daniel Schonhaut[1], Rik Ossenkoppele[1, 2], James O'Neil[3], Mustafa Janabi[3], Suzanne Baker[2, 3], Andreas Lazaris[1, 2, 3], Nagehan Ayakta[1, 2], Gautam Tammewar[1, 2], Marilu Gorno-Tempini[1], Bruce Miller[1], Adam Boxer[1], William Jagust[1, 2, 3], Gil Rabinovici[1, 2, 3]

[1]*Memory and Aging Center, Sandler Neurosciences Center, University of California, San Francisco, CA, United States*
[2]*Helen Wills Neuroscience Institute, University of California, Berkeley, CA, United States*
[3]*Life Sciences Division, Lawrence Berkeley National Laboratory, CA, United States*

Objective: To assess 18F-AV-1451 PET images in clinically heterogeneous non-AD tauopathy syndromes.

Methods: Clinical syndromes including MAPT mutation carriers (n=4, mean age 59, MMSE 21), nonfluent variant primary progressive aphasia (nfvPPA, n=3, mean age 62, MMSE 27) and corticobasal syndrome (CBS, n=5, mean age 61, MMSE 26) underwent 18F-AV-1451, PIB PET and MRI brain. 18F -AV-1451 images were summed, and standardized uptake value ratios were calculated for the 80-100 minute interval using mean activity in the cerebellar gray matter (excluding dentate nucleus) as the reference region.

Results: Symptomatic MAPT cases one (V337M mutation, CDR 2) and two (P301L, CDR 2) showed frontal and temporal uptake (Figure 1). Case two, who was PIB-positive, also showed more posterior binding in parietal and occipital cortex. Cases three and four (CDR 0.5 and 0), showing no evident cortical atrophy, demonstrated mild punctate frontal and posterior cingulate cortex uptake respectively. All three nfvPPA cases demonstrated frontal operculum uptake, two showed left greater than right while the other (left handed patient) had a less asymmetric pattern (Figure 2). CBS cases one through four demonstrated varying degrees of 18F-AV-1451 uptake in the dentate, putamen, globus pallidus and white matter, and in general showed lateralization consistent with symptoms (Figure 3). CBS case five, suspected to have underlying Alzheimer's disease (AD) as the causative pathology based on early cognitive symptoms predating motor symptoms and positive PIB-PET, showed much higher 18F-AV-1451 uptake extending into the peri-rolandic cortex, an area spared in typical AD.

Discussion: We found elevated 18F-AV-1451 binding matching the expected distribution of tau pathology in non-AD tauopathy syndromes. 18F-AV-1451 binds to different tau filaments in MAPT carriers, with signal intensity correlating to clinical severity. Signal overlap with off-target binding may make early detection a challenge, especially in CBS. The 18F-AV-1451 tracer warrants further exploration in non-AD tauopathies.

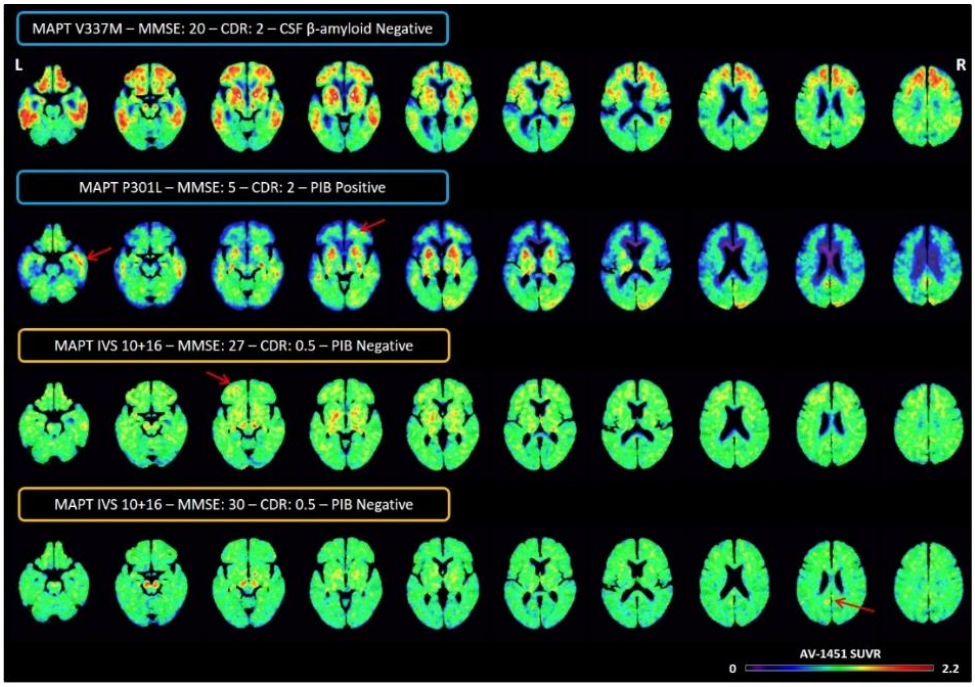

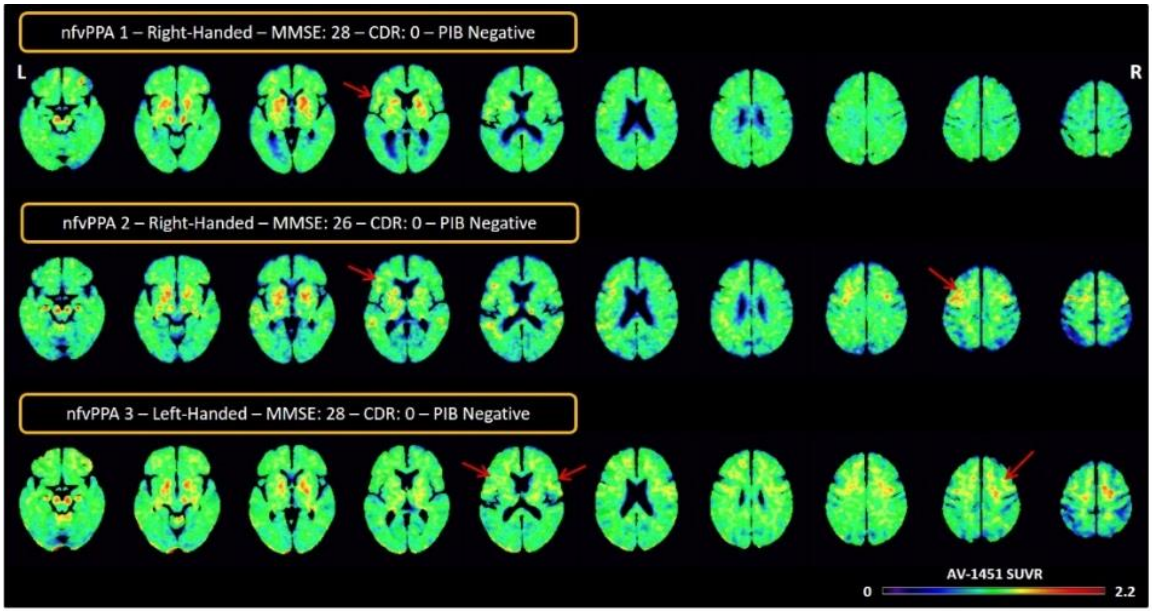
nfvPPA 1 – Right-Handed – MMSE: 28 – CDR: 0 – PIB Negative
L
R
nfvPPA 2 – Right-Handed – MMSE: 26 – CDR: 0 – PIB Negative
nfvPPA 3 – Left-Handed – MMSE: 28 – CDR: 0 – PIB Negative
AV-1451 SUVR
0
2.2

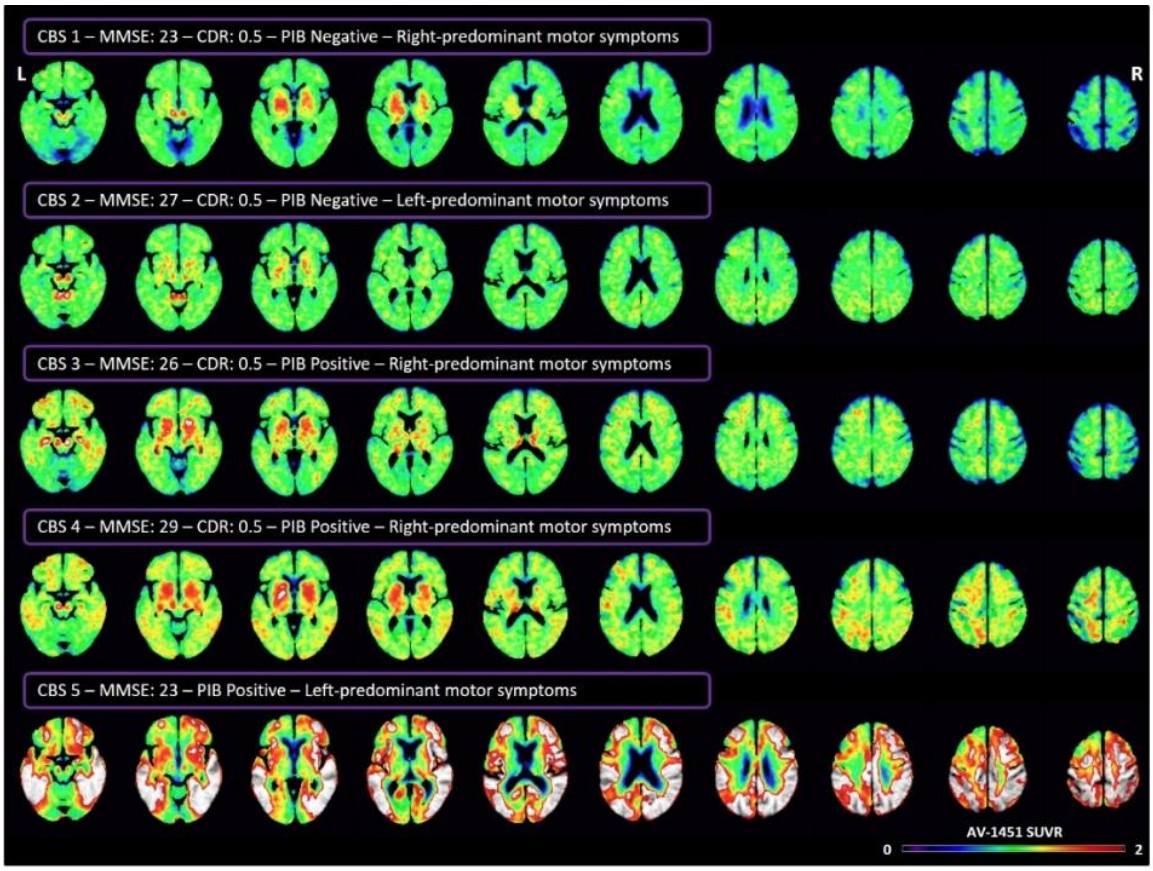
CBS 1 – MMSE: 23 – CDR: 0.5 – PIB Negative – Right-predominant motor symptoms
L
R
CBS 2 – MMSE: 27 – CDR: 0.5 – PIB Negative – Left-predominant motor symptoms
CBS 3 – MMSE: 26 – CDR: 0.5 – PIB Positive – Right-predominant motor symptoms
CBS 4 – MMSE: 29 – CDR: 0.5 – PIB Positive – Right-predominant motor symptoms
CBS 5 – MMSE: 23 – PIB Positive – Left-predominant motor symptoms
AV-1451 SUVR
0
2

Elevated [^{18}F]AV-1451 binding matches the distribution of tau pathology in progressive supranuclear palsy

Daniel Schonhaut[1], Adam Boxer[1], Brad Dickerson[2], Irene Litvan[3], Murray Grossman[4], Abhinay Joshi[5], Andrew Siderowf[5], Michael Devous[5], Erik Roberson[6], Bruce Miller[1], Keith Johnson[2], Rik Ossenkoppele[1], William Jagust[1, 2], Gil Rabinovici[1]

[1]*Department of Neurology, University of California, San Francisco, CA, United States*
[2]*Department of Neurology, Massachusetts General Hospital, MA, United States*
[3]*Department of Neurology, University of California, San Diego, CA, United States*
[4]*Department of Neurology, University of Pennsylvania, PA, United States*
[5]*Avid Radiopharmaceuticals, Inc., PA, United States*
[6]*University of Alabama Birmingham, AL, United States*
[7]*University of California, Berkeley, CA, United States*

Background: There have been conflicting reports from post-mortem assays regarding binding of [^{18}F]AV-1451 (formerly T807) to tau-positive lesions in non-AD tauopathies. Here we describe *in vivo* findings from a multi-site study of AV-1451 in progressive supranuclear palsy (PSP), a primary 4-repeat tauopathy.

Methods: [^{18}F]AV-1451-PET was performed in 17 mild-to-moderate PSP patients and 31 cognitively normal, PIB-negative controls (NC) recruited from four centers (Table 1). 80-100min SUVR images were created, normalizing by cerebellar gray matter (excluding dentate nucleus). We assessed voxelwise differences between AV-1451 SUVR in patients and controls using SPM12, adjusting for age. Additionally, we assessed mean SUVR in eight regions-of-interest (ROIs): caudate, pallidum, putamen, thalamus, subthalamic nucleus (STN), substantia nigra, dentate nucleus of the cerebellum (DN) and pons. Finally, we performed voxelwise regressions between disease severity (PSP Rating Scale (PSPRS)) and AV-1451 in patients, adjusting for site.

Results: Individual patients showed high tracer retention in midbrain and putamen, although most NC also had uptake in these regions. Uptake more distinct to PSP was seen in pallidum in all patients, and DN and frontal gray/white matter in a subset of patients (Figure 1). Voxelwise contrasts showed elevated AV-1451 in bilateral pallidum, putamen, thalamus, STN, dorsal midbrain, DN, and frontal white matter in PSP versus NC (Figure 2; $p<0.05$, uncorrected), with bilateral pallidum surviving FWE correction ($p<0.05$), matching tau pathology distribution in post-mortem studies of PSP. ROI analyses were consistent with voxelwise results (Figure 2). Increasing PSPRS correlated with left pallidum AV-1451 on voxelwise regression ($p<0.05$, uncorrected).

Conclusions: AV-1451 retention was elevated in PSP compared to controls in regions that closely match the pathological distribution of tau at autopsy. Pallidum had clearest separation between patients and controls, and left pallidum retention increased with disease severity. These findings suggest AV-1451-PET may be a useful *in vivo* biomarker of tau burden in PSP.

Table 1: Subject Demographics

	N	Site	Age	Sex (m/f)	MMSE	PSPRS
PSP	17	8 UCSF 5 AVID (UPenn/UCSD) 4 MGH	68.8 ± 5.6	12/5	25.8 ± 2.6	31.1 ± 15.4
NC	31	22 UCSF 9 MGH	75.9 ± 6.7	14/17	28.9 ± 1.1	

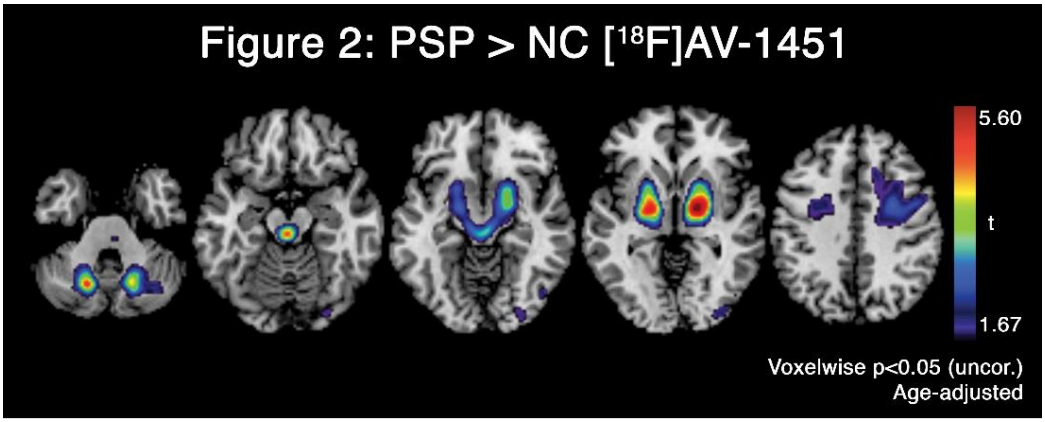
Figure 2: PSP > NC [18F]AV-1451
5.60
t
1.67
Voxelwise p<0.05 (uncor.)
Age-adjusted

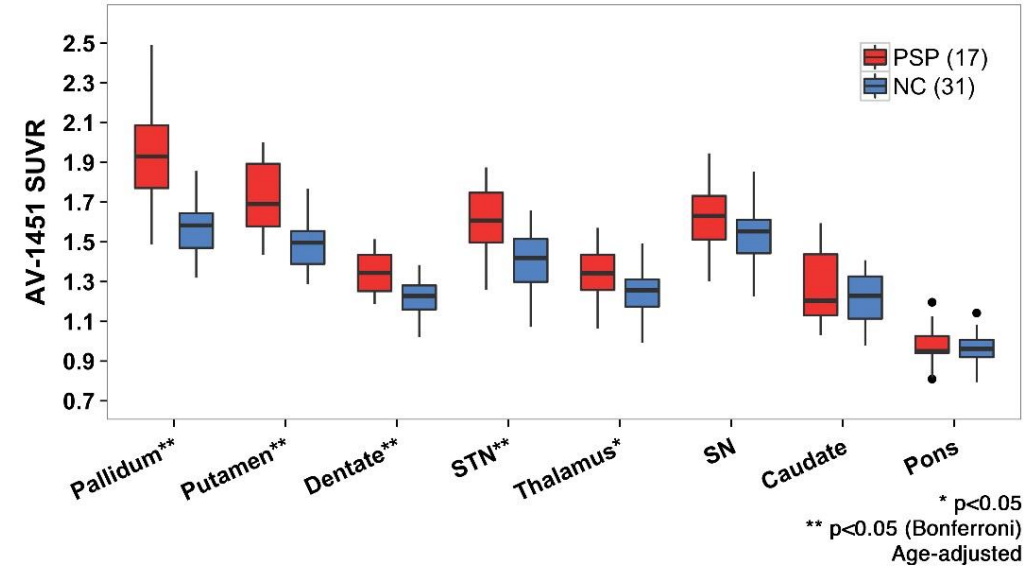
AV-1451 SUVR
2.5
2.3
2.1
1.9
1.7
1.5
1.3
1.1
0.9
0.7
PSP (17)
NC (31)
Pallidum**
Putamen**
Dentate**
STN**
Thalamus*
SN
Caudate
Pons
* p<0.05
** p<0.05 (Bonferroni)
Age-adjusted

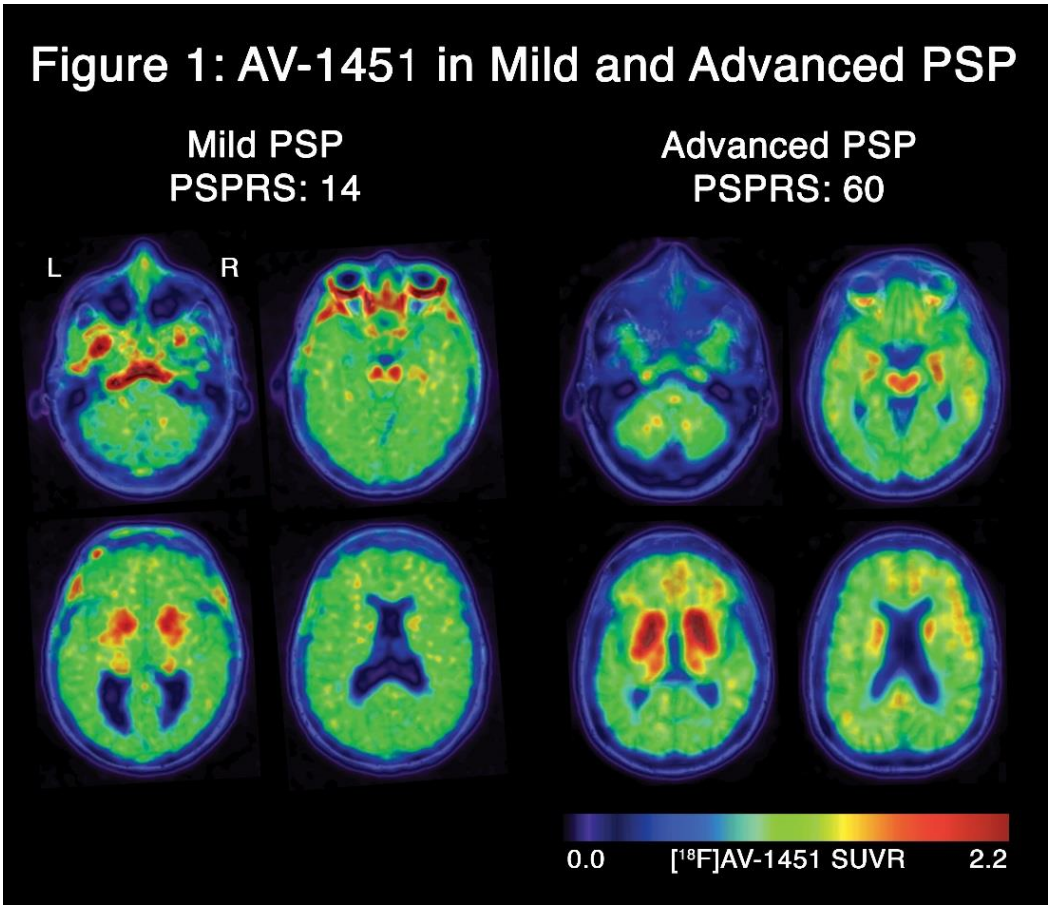
Figure 1: AV-1451 in Mild and Advanced PSP
Mild PSP
PSPRS: 14
Advanced PSP
PSPRS: 60
L
R
0.0
[18F]AV-1451 SUVR
2.2

Binding characteristics of tau PET tracer [18F]AV-1451

Giorgio Attardo, Yin-Guo Lin, Felipe Gomez, Kelly Conway, Qianwa Liang, Lois Lazor, Jason Goodman, Carey Horchler, Mark Mintun

Avid Radiopharmaceuticals, Inc., Philadelphia, PA, United States

Background: [18F]AV-1451 is known to bind AD brain derived aggregated tau with a KD of 0.6 nM. Recently, Marquie et al concluded 1) [18F]AV-1451 doesn't bind tau in PSP or PiD; and 2) reported off-target binding to neuromelanin-containing tissue. Objective: Further understand the specific binding characteristics of [18F]AV-1451 in AD and non-AD tauopathies compared to AT-8 tau antibody binding, and off-target binding in normal controls.

Methods: Binding studies of [18F]AV-1451were conducted with AD and normal brain homogenates, and by autoradiography (ARG) on multiple cases of AD, PSP, PiD, and normal controls. ARG signal matching to AT-8 was done on the same tissue with a NanoZoomer 2.0HT.

Results: Tau Binding: [18F]AV-1451 ARG signal in aggregated tau-rich AD brain sections was intense and matched the location of the AT-8 positivity. In non-AD tauopathies, ARG was positive with a lower signal intensity and frequency than AD (5 of 8 PiD and 5 of 17 PSP) and partially corresponded with AT-8 signal distribution. Off-Target Binding: KD values ranging from 4 nM to 30 nM were obtained from normal cortical tissue homogenates devoid of pathological tau. This specific binding was confirmed by ARG. [18F]AV-1451 had a KD of 2.0 nM in MAO-A compared to 0.6 nM for PHF-tau. Kinetic binding studies showed that koff for MAO-A was approximately 9-fold higher than for PHF-tau.

Conclusion: [18F]AV-1451 ARG signal matched AT-8 IHC in AD but not as well in PSP and PiD, possibly due to differences in composition of tau aggregates. Some off-target binding comprises MAO-A binding, although the much higher koff for MAO-A may explain the lack of MAO-A signal distribution on human in vivo [18F]AV-1451 PET imaging.

In vivo [F-18]-AV-1451 (T807) PET imaging in the first two autopsy-confirmed non-Alzheimer tauopathy cases studied at MGH

Marta Marquie[1, 2], Marc D. Normandin[2], Charles R. Vanderburg[1, 2, 3], Avery C. Meltzer[1, 2], Michael Siao[1, 2], Elizabeth A. Bien[1, 2, 3], Lisa G. Rycyna[1, 2, 3], Isabel M. Costantino[1, 2], Sara Makaretz[2], William E. Klunk[4], Chester A. Mathis[4], Milos D. Ikonomovic[4], Manik L. Debnath[4], John H. Growdon[2], Bradford C. Dickerson[2], Teresa Gomez-Isla[1, 2], et al.

[1]*MassGeneral Institute for Neurodegenerative Disease, MA, United States*
[2]*Massachusetts General Hospital, MA, United States*
[3]*Harvard NeuroDiscovery Center, MA, United States*
[4]*University of Pittsburgh School of Medicine, PA, United States*

Introduction: AV-1451 is a PET tracer tailored to allow *in vivo* detection of paired helical filament-(PHF)-tau-containing lesions. There is great need to better understand the regional and substrate specific binding patterns of this tracer not only in AD brains but also in non-AD tauopathies.

Objective: To carefully examine the correlation of *in vivo* and postmortem AV-1451 binding patterns in the first two cases of autopsy-confirmed non-AD tauopathy studied at MGH.

Methods: Detailed neuropathologic examination, phosphor-screen and nuclear emulsion autoradiography, [H-3]-AV-1451 binding assays and SDD-AGE tau measurements on postmortem samples containing multiple brain regions from two subjects with a clinical diagnosis of bvFTD (MAPT P301L mutation carrier) and PSP, respectively, who had [F-18]-AV-1451 PET imaging within 8 months of death.

Results: In both subjects, we observed elevated [F-18]-AV-1451 signal on *in vivo* PET imaging predominantly in striatum, midbrain and inferior temporal region, and some weaker scattered signal in grey/white matter junction. At autopsy, the P301L mutation carrier showed multiple tau grains in several brain regions both in cortex and white matter, and predominant basal ganglia involvement with glial tauopathy. A neuropathological diagnosis of PSP was confirmed in the second subject. In both cases, autoradiography failed to show any detectable [F-18]-AV-1451 binding in any of the regions examined with the exception of entorhinal cortex (reflecting incidental age-related neurofibrillary tangle pathology) and neuromelanin-containing neurons in the substantia nigra (reflecting off-target binding). Correlation analyses of regional patterns of *in vivo* uptake, in vitro binding assays and detailed biochemical quantification of soluble and insoluble tau pools at postmortem are currently ongoing.

Conclusion: Our results suggest that AV-1451 does not bind to non-PHF tau lesions primarily made of straight tau filaments with an affinity that could explain the *in vivo* signal in these two non-AD tauopathy cases. This emphasizes the need for further clinico-pathological correlation studies.

Thursday, January 14, 2016 - 1:30 - 2:30pm

Podium Presentations

SESSION 5: Anatomic Correlations

Chairs: ***Clifford Jack, Jr., Mayo Clinic, Rochester***
Susan Resnick, National Institutes of Health, National Institute on Aging

1:30-2:30	**SESSION 5:** **ANATOMIC CORRELATIONS**	**CHAIRS:** **Clifford Jack, Jr.** Mayo Clinic, Rochester **Susan Resnick,** National Institutes of Health, National Institute on Aging
1:30-1:45	PET tau imaging with AV-1451 in FTD with suspected underlying tauopathies and non-tauopathies relative to Alzheimer's and controls	**David Jones** Mayo Clinic, Rochester
1:45-2:00	Specific hippocampal subfield volumes mediate tau-related memory performance in amyloid positive individuals	**Heidi Jacobs** Massachusetts General Hospital/Harvard Medical School
2:00-2:15	Association between T807 and retrospective cortical thinning in cognitively normal elderly	**Molly LaPoint** Massachusetts General Hospital/Harvard Medical School
2:15-2:30	Identifying cortical areas of change in longitudinal 18F-T807 PET	**J. Alex Becker** Massachusetts General Hospital/Harvard Medical School, Boston
2:30-3:10	Discussion	

PET tau imaging with AV-1451 in FTD with suspected underlying tauopathies and non-tauopathies relative to Alzheimer's and controls

David Jones, Val Lowe, Heather Wiste, Matthew Senjem, David Knopman, Ronald Petersen, Clifford Jack, Brad Boeve

Mayo Clinic, Rochester, MN, United States

Background: Tau-PET imaging with AV-1451 is a promising research tool for investigating tau pathology in Alzheimer's disease (AD). However, the utility of AV-1451 binding in frontotemporal dementia (FTD) is uncertain. FTD syndromes are pathologically associated with underlying FTLD-tau pathology in roughly half of the FTD cases and with non-tau pathology in the remainder. We therefore investigated AV-1451 binding in subjects with clinical FTD suspected of having underlying tauopathies (MAPT mutation carriers, n=3) and non-tauopathies (PGRN mutation carrier [n=1] and sematic variant of primary progressive aphasia [svPPA, n=1]).

Methods: Tau PET with AV-1451 imaging was performed subjects with FTD (n=5), AD (n=21), and cognitively normal (n=120). Three FTD subjects had PiB-PET scans (svPPA, PGRN, one MAPT case, and all were negative). Uptake of AV-1451 was assessed by visual read and by regional analysis with intensity standardization to cerebellar grey matter (SUVR).

Results: On visual inspection there appears to be AV-1451 binding in all FTD cases irrespective of suspected FTLD-tau status. However, the magnitude of this binding is far below what is seen in AD, and largely falls within the range seen in controls except for the svPPA case (Fig1).

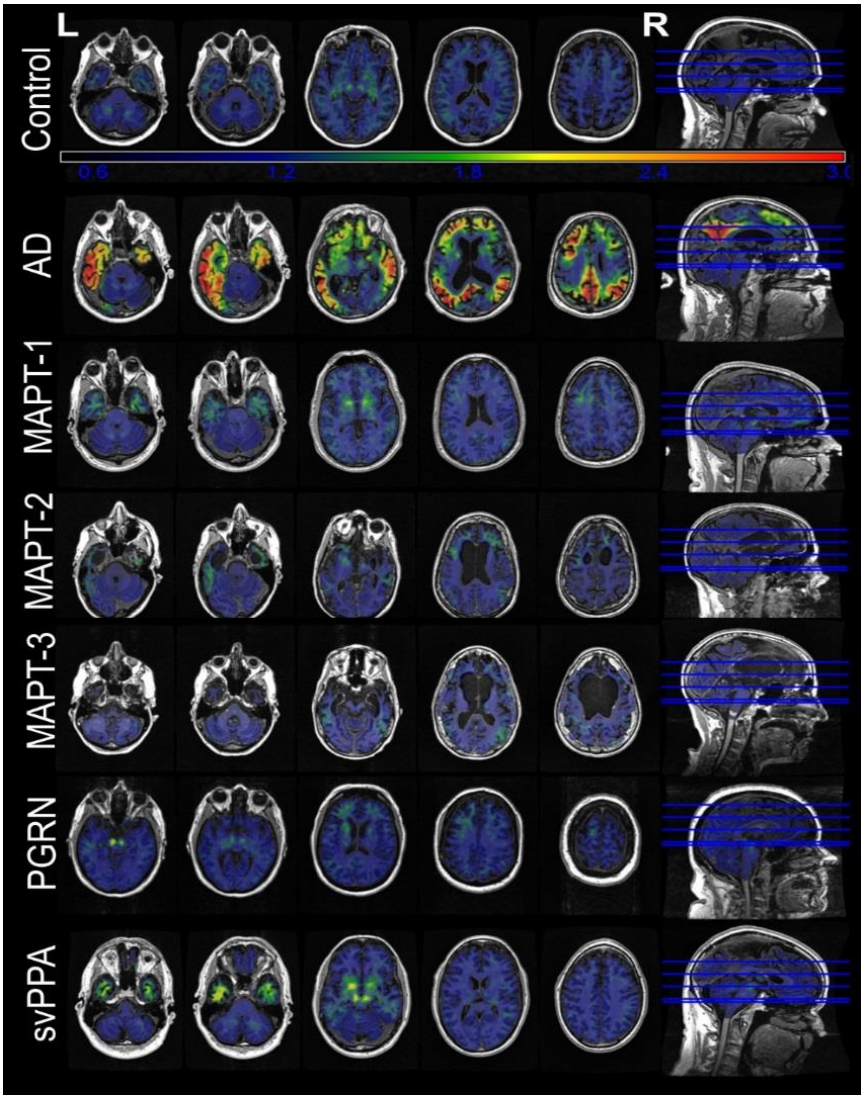

Figure 1

The SUVR quantification shows that the AV-1451 binding in the FTD cases is largely in the range of binding in CNs except for the svPPA case which is in the AD range isolated to the temporal poles (Fig2). Low level binding may appear visually distinct when scaled to the control range (Fig3 inset), but the intensity for these regions is marginally above the control range in one MAPT case and within the control range for the rest (Fig3).

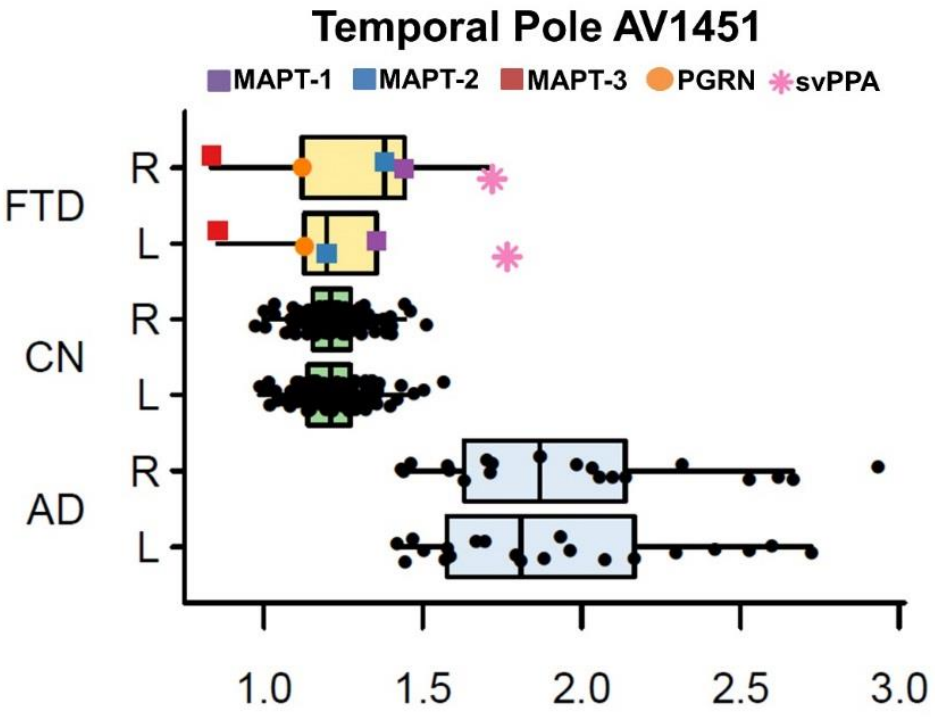

Figure 2

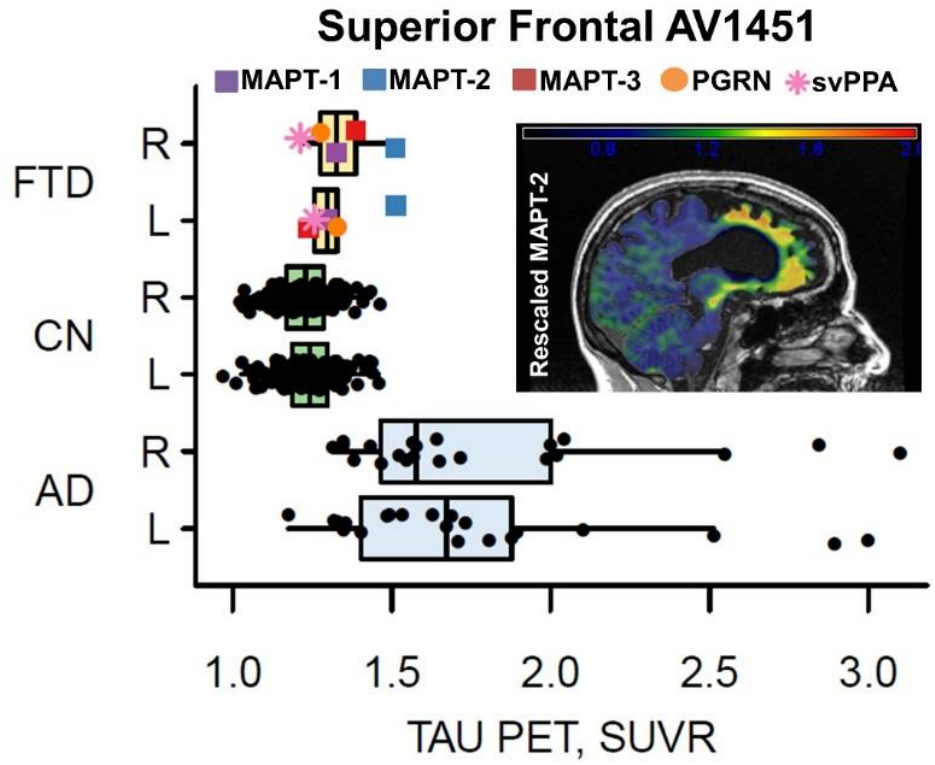

Figure 3

Conclusions: Autopsy confirmation is required, but it appears that AV-1451 binding levels are unable to distinguish underlying FTLD pathology and that the magnitude of binding in these cases is largely within the control range.

Specific hippocampal subfield volumes mediate tau-related memory performance in amyloid positive individuals

Heidi Jacobs[1, 2, 3], Aaron Schultz[2, 3, 4], Jean Augustinack[2], Rebecca Amariglio[4, 5], Bernard Hanseeuw[3, 4, 5], Kathryn Papp[4, 5], Dorene Rentz[4, 5], Reisa Sperling[3, 4, 5], Keith Johnson[1, 2, 3, 4, 5]

[1]*Department of Radiology, Massachusetts General Hospital, Harvard Medical School, Boston, MA, United States*
[2]*Division of Nuclear Medicine and Molecular Imaging, Massachusetts General Hospital, Boston, MA,United States*
[3]*Athinoula A. Martinos Center for Biomedical Imaging, Massachusetts General Hospital, Boston, MA,United States*
[4]*Center for Alzheimer Research and Treatment, Department of Neurology, Brigham and Women's Hospital, Boston, MA, United States*
[5]*Department of Neurology, Massachusetts General Hospital, Harvard Medical School, Boston, MA, United States*

Introduction: Detection at autopsy of the impact of tau and amyloid pathology has been associated with cognitive impairment, and the degree of impairment is more closely linked to tau than amyloid pathology. The relationship between tau pathology and memory in normal aging is multifactorial, but recent advances enable direct assessment of component parts of this relationship. We examined the cross-sectional association between tau deposition and memory, specifically evaluating the impact of amyloid deposition and tissue volume in six specific hippocampal subfields (HCsf: CA1, CA3, CA4, dentate gyrus, subiculum and presubiculum).

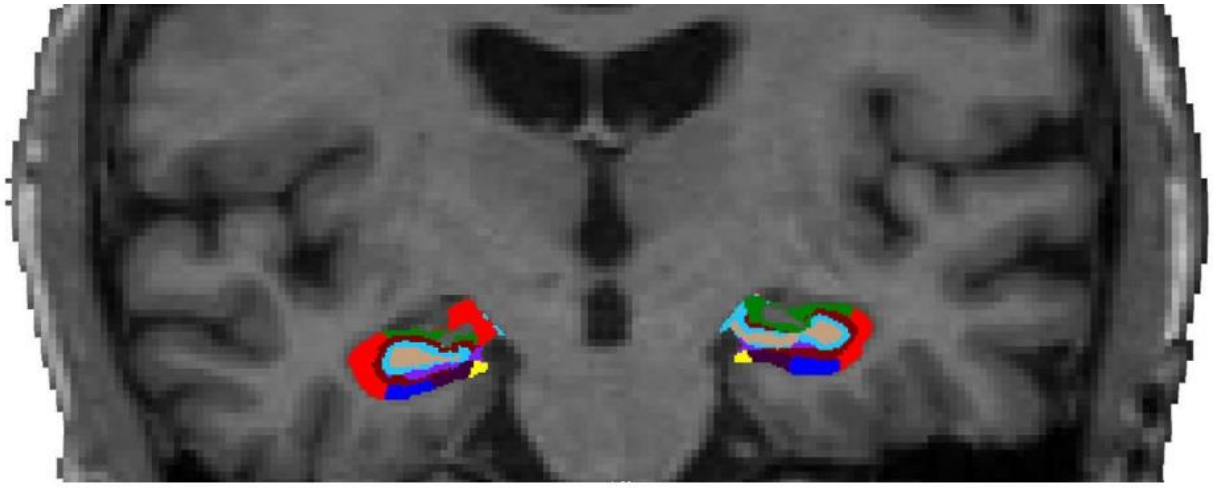

yellow = parasubiculum; dark purple = presubiculum; dark blue = subiculum;
red = CA1; green = CA3; grey = CA4; light blue = dentate gyrus

Methods: We included one-hundred-sixteen older individuals (76.24 years ± 6.25, CDR=0). HCsf volumes (FreeSurfer6) were corrected for intracranial volume. Neocortical amyloid deposition was quantified using an aggregate PiB-DVR and dichotomized at DVR=1.19. T807 binding in entorhinal (EC) cortex was expressed in SUVR. Cerebellar gray was used as reference. Memory was investigated using delayed recall scores of the selective reminding test. Mediation and moderation analyses were performed to investigate the influence of HCsf volumes and amyloid deposition on the association between T807 binding and memory. All analyses were age-corrected.

Results: Amyloid deposition was not associated with any HCsf volume. Only the subiculum and presubiculum volumes were negatively associated with EC-T807 binding. These two HCsf volumes and EC-T807 binding correlated with memory. Mediation analyses revealed that the association between EC-T807 binding and memory was partially mediated (bias-bootstrapped 95%CI) by both HCsf volumes. The indirect effect via the subiculum was moderated by amyloid status (p =0.04).

A Direct effect

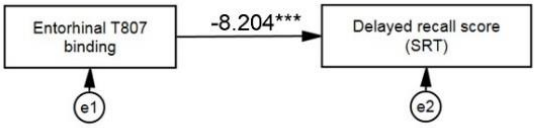

B Partial mediation by hippocampal subfield volumes

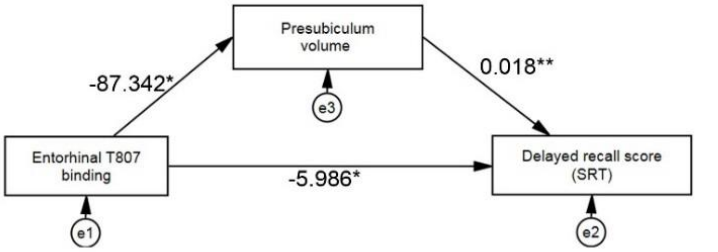

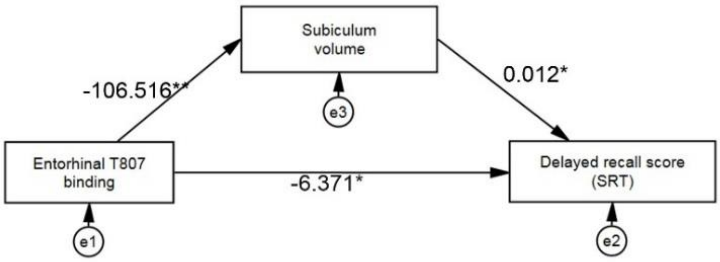

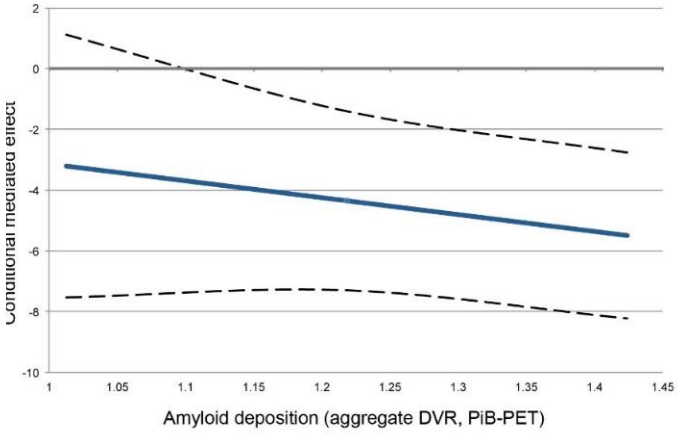

At higher levels of amyloid, the mediation of the subiculum on the relation between entorhinal T807 binding and memory is more negative, compared to lower levels of amyloid deposition

C Moderation of the indirect effect by amyloid deposition

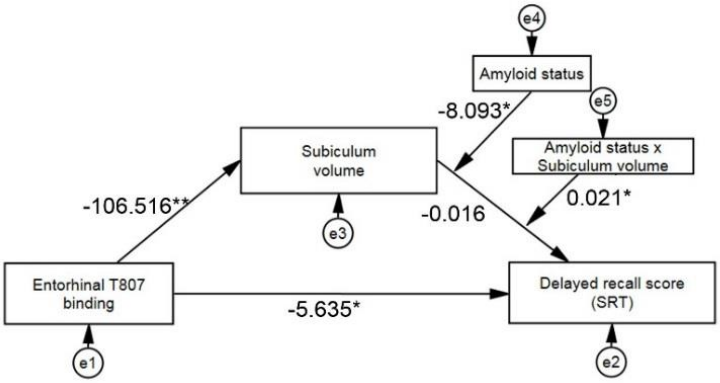

Discussion: Specifically the subiculum is associated with memory. Postmortem work showed that the (pre)subiculum is the earliest HCsf vulnerable to tau. This in-vivo study, while correlational, now suggests a progression to volume changes, putatively secondary to tau, in the proximate subiculum. The moderation by amyloid, suggests that tau is necessary, but not sufficient for memory decline.

Association between T807 and retrospective cortical thinning in cognitively normal elderly

Molly LaPoint[1], Jasmeer Chhatwal[1], Jorge Sepulcre[2], Danielle M. Cosio[2], Keith A. Johnson[2], Reisa A. Sperling[3], Aaron P. Schultz[1]

[1]*Department of Neurology, Massachusetts General Hospital/Harvard Medical School and the Athinoula A. Martinos Center for Biomedical Imaging, Boston, MA, United States*
[2]*Department of Radiology, Massachusetts General Hospital/Harvard Medical School and the Athinoula A. Martinos Center for Biomedical Imaging, Boston, MA, United States*
[3]*Center for Alzheimer Research and Treatment, Department of Neurology, Brigham and Women's Hospital, Harvard Medical School and the Athinoula A. Martinos Center for Biomedical Imaging, Boston, MA, United States*

Background: Tau pathology has been strongly associated with neuronal death and brain atrophy in autopsy studies. However, the temporal evolution of tau pathology and cortical atrophy remains to be elucidated in living humans. Here we examine the relationship between T807 (AV1451)-PET as a marker of tau pathology and retrospective cortical thinning over the prior three years.

Methods: We examined 100 cognitively normal elderly subjects (age=74±6.3 years) from the Harvard Aging Brain Study with 2-3 MRs (mean visits = 2.3±0.5) over approximately 3 years (mean years of follow-up =2.8±0.7), retrospective to cross-sectional T807. Tau measurements were GTM partial volume corrected SUVRs with a cerebellar grey reference region. Thirty-four FreeSurfer-defined ROIs were used for both cortical thickness and T807. We examined region-to-region relationships between T807 signal and cortical thickness in the same ROI, as well as inferior temporal T807 signal to all cortical thickness ROIs. All linear mixed effects models included baseline age and sex as covariates.

Results: For region-to-region comparisons, significant associations between T807 and cortical thinning were observed in the right superior temporal gyrus (t(219)=-2.60,p=0.01), right middle temporal gyrus (t(219)=-3.11,p=0.002), and right temporal pole (t(219)=-3.69,p=0.0003). For inferior temporal tau, significant relationships were observed between T807 signal and thinning in the right middle temporal gyrus (t(219)=-2.41,p=0.02), right fusiform (t(219)=-3.32,p=0.001), and bilateral parahippocampal gyri (left t(219)=-3.62,p=0.0004; right t(219)=-2.22,p=0.03).

Conclusion: We observed significant negative relationships between both local and inferior temporal T807 signal and longitudinal change in cortical thickness in lateral and medial temporal regions. The T807 scan is largely proximal to the last MR visit for each subject, so the observed cortical thinning is retrospective. Further study is ongoing to determine how tau is related to prospective changes in cortical thickness.

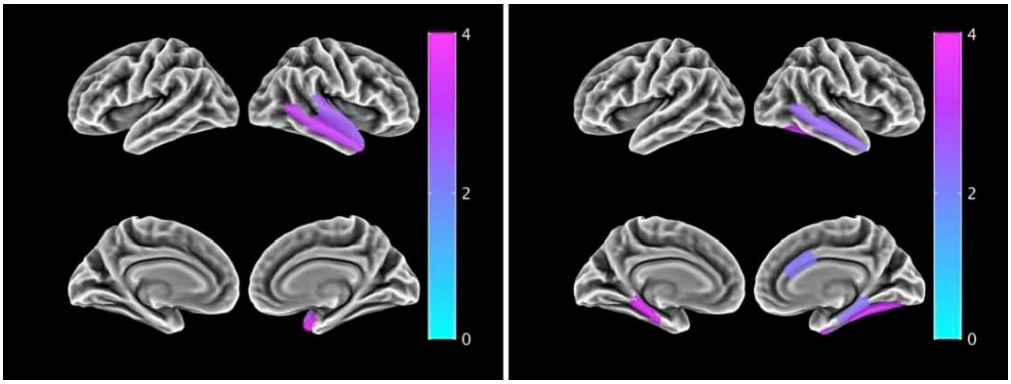

Figure 1: *ROIs displaying a negative relationship (p<0.05) between cortical thinning and local T807 (left) and inferior temporal T807 (right).*

Identifying cortical areas of change in longitudinal 18F-T807 PET

J. Alex Becker[1], Danielle Cosio[1], Kelly Judge[1], Christopher Lee[1], Reisa Sperling[2, 3], Keith Johnson[1, 3]

[1]Department of Radiology, Massachusetts General Hospital, Harvard Medical School, Boston, MA, United States
[2]Department of Neurology, Brigham and Women's Hospital, Harvard Medical School, Boston, MA, United States
[3]Athinoula A. Martinos Center for Biomedical Imaging, Boston, MA, United States

Introduction: Autopsy studies have shown that tau deposition in early Alzheimer's disease occurs predominantly in inferior and middle temporal cortex, and in subject-specific patterns which do not necessarily respect anatomical boundaries. The PET ligand 18F-T807 (AV1451) allows measurement of within-subject change in tau binding. We investigated longitudinal tau binding using a region-of-interest-free approach.

Methods: Two time-points of T807 PET (10mCi, 80-100min) were acquired in each of 26 subjects (baseline age 68±13yr, interval 1.26±0.45yr; 13 normal, 8 MCI or AD, 5 CTE). Time-points were registered to a subject-specific T807 template which was rigidly transformed to baseline MPRAGE. T807 data was sampled at the midpoint of the Freesurfer-calculated grey-matter-ribbon, surface-smoothed at 10mm FWHM, and expressed as SUVR (cerebellar cortex). Baseline T807 vertices with SUVR>=1.20 were clustered with nearest-neighbors defined by the cortical surface triangulation, average SUVR and cluster size (number of vertices) calculated across time-points from baseline clusters, and average SUVR rate of change calculated for each cluster. Both maximum rate (MaxRate) and average of top two rates (TTRate) were examined for each subject.

Results: Of 26 subjects, 21 (81%) and 5 (19%) had positive or negative MaxRate, respectively (positive: median 0.07yr^-1 (0.02,0.11) (1st,3rd quartiles), maximum 0.24 yr^-1; negative: median -0.02 (-0.07,-0.01)), while 8 (31%) had positive TTRates (median 0.05 yr^-1 (0.02,0.10), maximum 0.21). Among subjects with positive MaxRate median cluster size was 477 vertices (284,1693), maximum 21230.

Conclusions: Our initial findings with Tau-PET a group of normal and impaired subjects suggest that most experienced increases in tau binding over time in at least one cluster. Some negative rates are likely due to a combination of misregistration and mis-identification of reference region, refinements of which will be objects of future work.

Thursday, January 14, 2016 - 3:55 - 4:25pm

Keynote Lecture

New CSF and plasma biomarkers for neurodegenerative diseases

Henrik Zetterberg

University of Gothenburg

Identification of biomarkers is increasingly important in the diagnosis and therapeutic decision making in most areas of medicine and particularly so in neurological conditions due to difficulties of tissue sampling. Sensitive methods to measure markers are constantly sought and in clinical neuroscience cerebrospinal fluid (CSF) is one of the most promising biomarker matrices due to the relative enrichment of CNS-related proteins in CSF as compared to blood. Still, the most interesting biomarkers in CSF are at low concentrations and so are not easily measured. Many of these molecules may also be circulating in blood but at even lower concentrations than in CSF.

The presentation will review recent breakthroughs in ultrasensitive measurement techniques for the analysis of low abundant markers of CNS disease in CSF and blood.

Thursday, January 14, 2016 - 4:40 - 5:25pm

Podium Presentations

SESSION 6: Tau PET: Clinical and Cognitive Correlations

Chairs: ***William Jagust, University of California, Berkeley***
Reisa Sperling, Massachusetts General Hospital/Harvard Medical School

4:40-5:25	**SESSION 6:** **TAU PET: CLINICAL AND COGNITIVE CORRELATIONS**	**CHAIRS:** **William Jagust** University of California, Berkeley **Reisa Sperling** Massachusetts General Hospital/Harvard Medical School
4:40-4:55	Aβ+ clinically normal participants with elevated Tau show greatest decline in the preclinical AD cognitive composite	**Elizabeth Mormino** Massachusetts General Hospital/Harvard Medical School
4:55-5:10	Association between in vivo tau deposition and concomitant cognition mediated by metabolic dysfunction in AD	**Laure Saint-Aubert** Karolinska Institutet
5:10-5:25	Tau-PET imaging with AV-1451 in Alzheimer's disease	**Val Lowe** Mayo Clinic, Rochester
5:25-5:55	Discussion	

Aβ+ clinically normal participants with elevated tau show greatest decline in the preclinical Alzheimer's disease cognitive composite

Elizabeth Mormino[1], Kate Papp[2], Aaron Schultz[1], Bernard Hanseeuw[1], Catherine Munro[1], Sehily Jaimes[1], Tamy-Fee Meneide[1], Emily Kilpatrick[2], Sarah Aghjayan[2], Victoria Jonas[2], Dylan Kirn[2], Jonathan Jackson[2], Rebecca Amariglio[2], Dorene Rentz[1, 2], Reisa Sperling[1, 2], Keith Johnson[1, 3]

[1]*Department of Neurology, Massachusetts General Hospital, Harvard Medical School, MA, United States*
[2]*Center for Alzheimer Research and Treatment, Brigham and Women's Hospital, Harvard Medical School, MA, United States*
[3]*Department of Radiology, Massachusetts General Hospital, Harvard Medical School, MA, United States*

Objective: To determine the contribution of Aβ and Tau to longitudinal cognitive decline among clinically normal subjects (CNs).

Methods: Two hundred and seventy seven clinically normal participants from the Harvard Aging Brain Study have completed baseline PIB PET scanning and at least one follow up annual neuropsychological testing session (age=73.8±6.1, mean follow up=3.08±0.97 years). A subset of 129 additionally underwent Tau PET imaging with T807/AV-1451 (age=73.5±6.1, mean follow up=3.53±0.73). Linear mixed models examined the association between PET biomarkers (Aβ status and inferior temporal Tau) with longitudinal decline on the Preclinical Alzheimer's disease Cognitive Composite (PACC). The PACC is the primary cognitive endpoint in the A4 trial and is derived from the Logical Memory delayed recall, Free and Cued Selective Reminding Test total cued recall score, the MMSE total score, and the Digit Symbol total score. Age, sex, and education were covaried.

Findings: In the full sample, Aβ+ CNs showed significantly more decline in PACC compared to Aβ- CNs (beta=-0.087, p-value=0.0004). When both Aβ status and inferior temporal Tau were modeled as simultaneous predictors in the subset of 129 CN, Aβ status was no longer significant (beta=-0.006, p=0.82) whereas higher inferior temporal Tau was associated with greater decline (beta=-0.47, p=0.0007). The interaction between Aβ and inferior temporal Tau was also significant (beta=-0.82, p=0.0031), such that the association between inferior temporal Tau and decline in PACC was only present among Aβ+ CN.

Interpretation: Greater risk of short-term decline in Aβ+ CN that also have elevated Tau is consistent with the current conceptualization of preclinical AD. These high risk individuals may be ideal candidates for secondary prevention trials using cognitive endpoints. However, whether efficacy of anti-amyloid treatment will be optimal in Aβ+ CN with either elevated or low Tau is currently unknown.

Association between *in vivo* tau deposition and concomitant cognition mediated by metabolic dysfunction in Alzheimer's disease

Laure Saint-Aubert[1], Konstantinos Chiotis[1], Rita Almeida[2], Anders Wall[3], Ove Almkvist[1, 4, 5], Agneta Nordberg[1, 4]

[1]*Department NVS, Center for Alzheimer Research, Translational Alzheimer Neurobiology, Karolinska Institutet, Stockholm, Sweden*
[2]*Department of Neuroscience, Karolinska Institutet, Stockholm, Sweden*
[3]*PET Centre, Uppsala University Hospital, Uppsala, Sweden*
[4]*Department of Geriatric Medicine, Karolinska University Hospital Huddinge, Stockholm, Sweden*
[5]*Department of Psychology, Stockholm University, Stockholm, Sweden*

Introduction: Close association between neurofibrillary tangles and cognitive performance has been reported from autopsy studies in Alzheimer's disease (AD). The recent development of tau-specific tracers for imaging now allows *in vivo* quantification of the regional distribution of tau deposition, and offers the opportunity to monitor the progression of tau pathology along with cognitive decline. In this study, we investigated the relationship between cognitive performance and concomitant tau deposition as well as metabolism, in the brain of patients at prodromal or dementia-stage of AD.

Methods: Nineteen patients, nine with AD dementia and ten MCI PIB-positive, were included in this study. All patients underwent (*S*)-[18F]THK5117 (also known as [18F]THK5317), [18F]FDG and [11C]PiB PET scans, as well as episodic memory and global cognition assessment. The relationship between cognitive performance and the different PET tracers' regional uptake was assessed using linear regression models. The hypothesis of a mediation role of [18F]FDG regional uptake on the association between (*S*)-[18F]THK5117 retention and cognition was tested using causal mediation analysis.

Results: Cognitive performance was positively associated with [18F]FDG uptake in several regions of the brain. Significant negative associations were also found between episodic memory performance as well as global cognition and (*S*)-[18F]THK5117 regional retention, mainly in temporal regions. This relationship between (*S*)-[18F]THK5117 retention and cognition appeared to be mediated by [18F]FDG regional uptake.

Conclusions: These findings support the idea that *in vivo* imaging using (*S*)-[18F]THK5117 tau tracer can monitor cognitive decline in AD. The present study illustrates the close association between cerebral tau deposition and concomitant cognitive decline in AD, and suggests a mediating role of local metabolic dysfunction on this association.

Tau-PET imaging with AV-1451 in Alzheimer's disease

Val Lowe, Heather Wiste, Mukesh Pandey, Matthew Senjem, Bradley Boeve, Keith Josephs, Ping Fang, Melissa Murray, Kejal Kantarci, David Jones, Christopher Schwarz, David Knopman, Ronald Petersen, Clifford Jack

Mayo Clinic, Rochester, MN, United States

Background: Braak staging provides a framework for AD-related sequencing of Tau deposition. With the advent of Tau-PET, evaluating regional patterns of Tau deposition in patients and comparison to the Braak staging framework is now possible. We performed Tau-PET imaging with AV-1451 to determine uptake patterns in participants within the AD-pathway.

Methods: Tau-PET with AV-1451 was performed on 137 clinically normal (CN) and 28 cognitively impaired AD-pathway participants (6 amnestic MCI, 22 AD, all PiB+). Uptake of AV-1451 was assessed as cortical to cerebellar grey matter ratios (SUVr) in cortical regions of interest (ROIs). Regional Tau-PET diagnostic separability between groups (area under the ROC curve [AUROC]), ROI clustering, and Spearman correlations of Tau-PET with age and MMSE were assessed. For each ROI, Tau-PET SUVr values were normalized to a common scale using the range among CN participants <60y. Within a subject, these scaled values were used to rank-order each ROI from least to most abnormal.

Results: Diagnostic separability in typical AD regions was high (AUROC 0.9 to 1.0).). (Figure 1) Moderate (-0.3 to -0..4) negative correlations with MMSE were seen in typical AD ROIs in the entire group. Age correlations were seen in CN and impaired participants. ROI clustering demonstrated associated subsets of ROIs in CN and impaired participants. Elevated Tau was seen in CN participants in medial temporal regions in PiB positive and PiB negative participants. Within-subject ROI abnormality ranking demonstrated angular, occipital, posterior cingulate, and precuneus in addition to medial temporal ROIs as the most abnormal 10 ROIs in the impaired group (Figure 2).

Figure 1. Diagnostic separability of Tau PET SUVr in all regions. CN (blue) and amyloid positive impaired (orange) subject group SUVr box plots are shown for each region. All regions except nonspecific regions (midbrain, pallidum and putamen) show excellent separability.

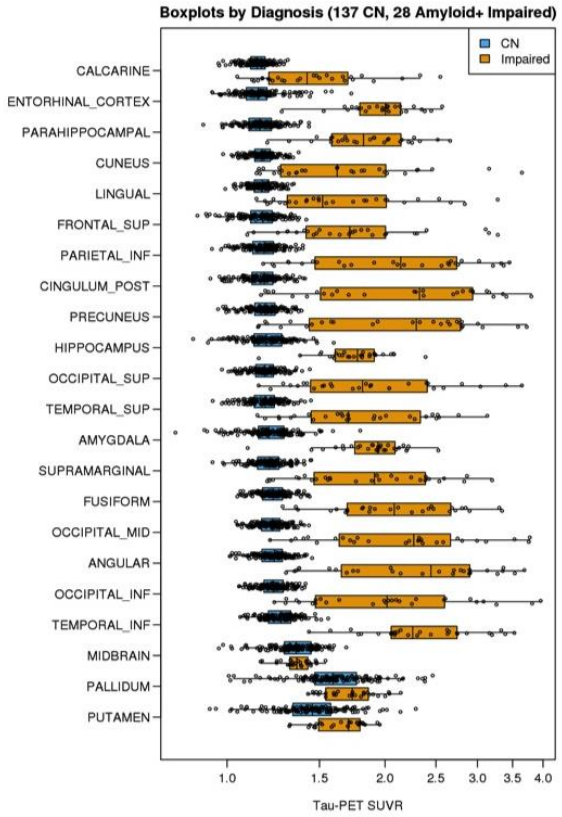

Figure 2. Distribution of within-subject Tau PET regional SUVr rankings shown in impaired participants. Tau-PET values in each ROI were normalized to a common scale using the range of SUVr values among 43 CN subjects aged <60. The figure shows the distribution of within-subject ranks for each ROI among impaired subjects from lowest/least abnormal rank (midbrain) to highest/most abnormal rank (inferior temporal region). Notably, non-medial temporal lobe regions are represented in the most abnormal regions of Tau-PET signal.

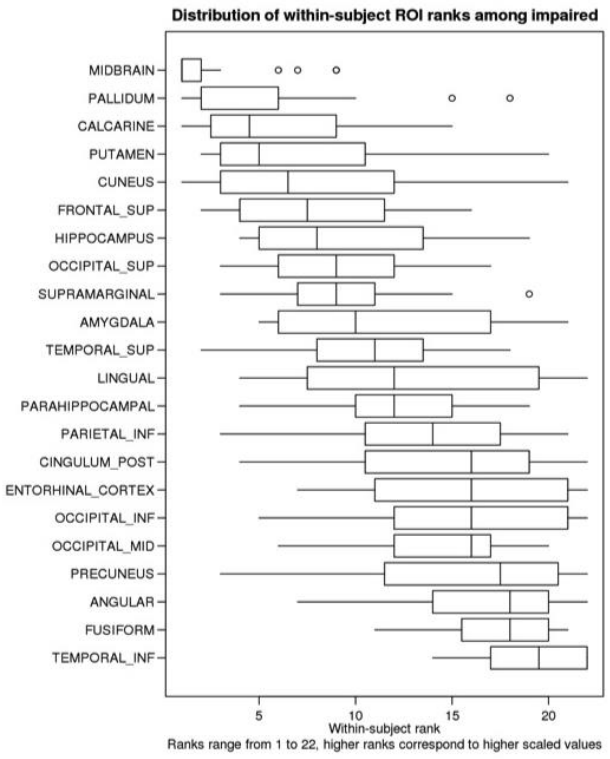

Conclusions: Tau-PET with AV-1451 generally supports the Braak staging sequence of Tau deposition in the AD dementia pathway. Medial temporal lobe AV-1451 uptake in the CN group may suggest subclinical, early AD-pathology Tau vs. primary age related tauopathy.

Friday, January 15, 2016 - 8:00 - 8:45am

Podium Presentations

SESSION 7: Tau PET: Connectivity and PS1

Chairs: ***Tammie Benzinger, Washington University in St. Louis***
Trey Hedden, Massachusetts General Hospital

8:00-8:45	**SESSION 7:** **TAU PET: CONNECTIVITY AND PS1**	**CHAIRS:** **Tammie Benzinger** Washington University in St. Louis **Trey Hedden** Massachusetts General Hospital
8:00-8:15	Tau covariance patterns in AD patients resemble intrinsic connectivity networks in young adults	**Rik Ossenkoppele** University of California, San Francisco
8:15-8:30	Amyloid, Tau, and functional connectivity MRI	**Aaron Schultz** Massachusetts General Hospital/Harvard Medical School
8:30-8:45	Patterns of Tau deposition using [18F]-AV-1451 in autosomal dominant Alzheimer's disease: Results from the DIAN	**Tammie Benzinger** Washington University in St. Louis
8:45-9:15	Discussion	

Tau covariance patterns in AD patients resemble intrinsic connectivity networks in young adults

Rik Ossenkoppele[1, 2, 3], Daniel Schonhaut[1, 2], Jesse Brown[1], James O'Neill[4], Mustafa Janabi[4], Suzanne Baker[3], Michael Schöll[2], Joel Kramer[1], Maria-Luisa Gorno-Tempini[1], Bruce Miller[1], Bill Seeley[1], Bill Jagust[3], Gil Rabinovici[1]

[1]*University of California, San Francisco, CA, United States*
[2]*University of California, Berkeley, CA, United States*
[3]*VU University Medical Center, Amsterdam, Netherlands*
[4]*Lawrence Berkeley National Laboratory, CA, United States*

Introduction: According to the network model of neurodegeneration, the spread of pathology is not a random sequence of events but rather occurs selectively along functionally connected brain regions. Here we test the hypothesis that the distribution of filamentous tau (as measured with [18F]AV1451 PET) follows the functional architecture observed in the healthy brain.

Methods: We performed [18F]AV1451 covariance analyses in 27 AD patients (Table-1) and seed-based functional connectivity in 1000 young healthy adults (18-35 years, www.neurosynth.org), based on 4 atrophy peak voxels identified in a previous paper on distinct clinical variants of AD. These peak voxels were located in right middle occipital gyrus [rMOG] for posterior cortical atrophy, left superior temporal gyrus [lSTG] for logopenic variant PPA, right middle frontal gyrus [rMFG] for early-onset AD, and left posterior cingulate gyrus [lPPC]) as the common denominator. For [18F]AV1451, we generated SUVR images for the interval between 80-100 minutes post-injection, and used the mean SUVR values from 4mm spheres drawn around the peak voxels as independent variables in whole-brain voxelwise covariance analyses of [18F]AV1451 uptake ($p<0.05$ FWE corrected, no covariates). For resting-state fMRI data, we used the peak voxels as seeds to extract intrinsic connectivity maps. We then performed visual inspection of the covariance and functional connectivity maps to assess their overlap, and goodness-of-fit analyses for [18F]AV1451 covariance maps against 8 predefined functional network templates.

Results: There was a striking overlap between [18F]AV1451 covariance and intrinsic connectivity maps (Figure-1). Goodness-of-fit showed strongest overlap between rMOG and the higher visual network, lSTG and the language network, rMFG and the executive control network, and lPCC with the posterior default mode network (Table-2).

Conclusion: The spatial pattern of tau observed in AD patients does resemble the functional organization of the healthy brain, supporting the notion that tau pathology spreads through circumscribed brain networks.

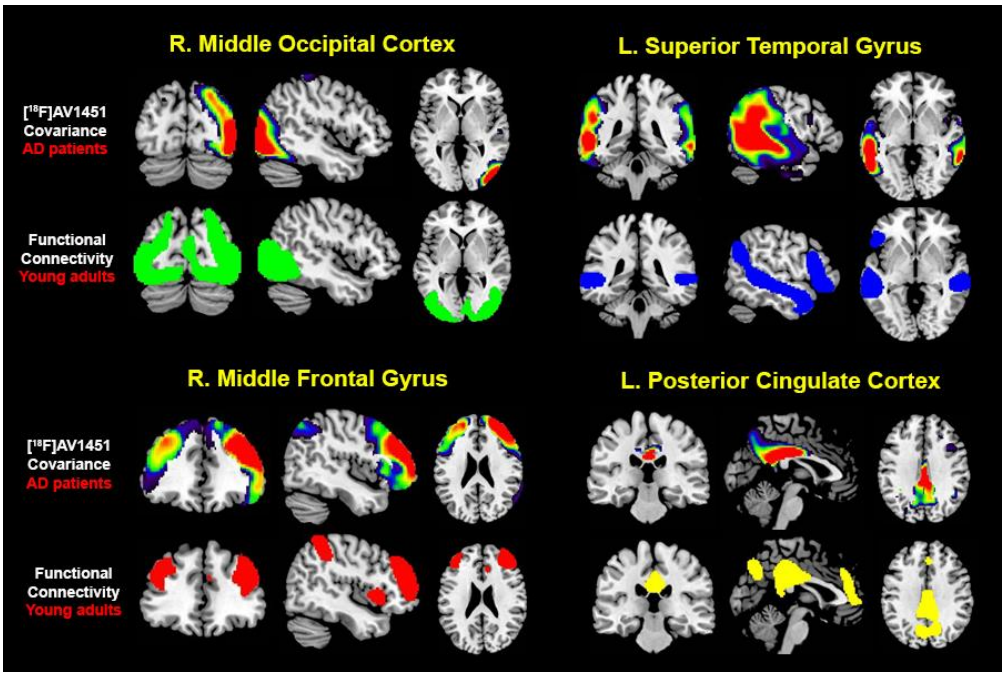

Table 1. Patient characteristics

	AD patients
N	27
Variant	Logopenic variant PPA (n=8) Posterior cortical atrophy (n=7) Early-onset AD (n=6) Late-onset AD (n=5) Corticobasal syndrome (n=1)
Age	64±8
Sex (m/f)	14/13
Education	17±3
MMSE	21±6
[^{11}C]PIB status	26 positive, 1 unknown (lvPPA)

Table 2. Goodness-of-fit between [^{18}F]AV1451 covariance maps and template networks

SEED* / **NETWORK****	**R. Middle occipital gyrus** *(x=39, y=-88, z=10)*	**L. Superior temporal gyrus** *(x=-56, y=-40, z=1)*	**R. Middle frontal gyrus** *(x=40, y=42, z=30)*	**L. Posterior cingulate** *(x=-2, y=-33, z=28)*
Higher-visual	4.61	-1.83	-2.57	-0.89
Language	-0.32	4.49	0.16	0.77
R. Executive-control	-0.52	0.55	4.31	1.05
Posterior DMN	-0.08	1.26	0.45	3.28
Ventral DMN	0.50	-0.05	0.61	1.56
L. Executive-control	-1.41	2.24	1.52	0.37
Salience	-0.49	2.73	0.78	0.46
Sensorimotor	0.20	-1.30	-1.15	-0.35

* Derived from Miglaccio et al. (2009) Neurology: "Clinical syndromes associated with posterior atrophy: Early age at onset AD spectrum."

** Derived from Shirer et al. (2012) Cerebral Cortex: "Decoding subject-driven cognitive states with whole-brain connectivity patterns"

Amyloid, tau, and functional connectivity MRI

Aaron Schultz[1], Jasmmer Chhatwal[1], Trey Hedden[2], Jorge Sepulcre[2], Elizabeth Mormino[1], Willem Huijbers[4], Bernard Hanseeuw[1], Molly LaPoint[1], Danielle Cosio[2], Emily Shaw[2], Reisa Sperling[3], Keith Johnson[2]

[1]Department of Neurology, Massachusetts General Hospital/Harvard Medical School and the Athinoula A. Martinos Center for Biomedical Imaging, Boston, MA, United States
[2]Department of Radiology, Massachusetts General Hospital/Harvard Medical School and the Athinoula A. Martinos Center for Biomedical Imaging, Boston, MA, United States
[3]Center for Alzheimer Research and Treatment, Department of Neurology, Brigham and Women's Hospital, Harvard Medical School, and the Athinoula A. Martinos Center for Biomedical Imaging, Boston, MA, United States
[4]German Centre for Neurodegenerative Diseases (DZNE), Department of Population Health Sciences, Bonn, Germany

Background: Previous studies have demonstrated relationships between functional connectivity MRI (fcMRI) and amyloid burden. While effects in the context of clinically impaired individuals have been widely replicated, the amyloid effect within cognitively normal elderly has been weak and inconsistent. We examine the relationship between functional connectivity and both PiB-PET and T807-PET to assess whether tau imaging can help elucidate the relationship between AD molecular markers and fcMRI in a preclinical cohort.

Methods: We examined 116 participants from the Harvard Aging Brain Study (HABS) who completed PiB-PET, T807(AV1451)-PET, and MRI with resting state fcMRI within one year. Amyloid was assessed as DVRs (40-60min), and then binarized into low (N=82) and high (N=34) amyloid groups. Tau measurements were made with T807-PET SUVRs (80-100min) within FreeSurfer defined entorhinal and inferior temporal regions using a cerebellar grey reference. fcMRI analyses focused on four canonical cortical networks including DMN, VAN/SAL, DAN, and Left/Right FPCN. Age, sex, and fcMRI QA metrics were included as covariates.

Results: Examination of the T807 and FC relationship by amyloid group revealed a significant relationship in the high amyloid group between inferior temporal T807 and functional connectivity in the VAN ($t(27)=-4.68, p<0.001$) and DMN ($t(27)=-2.31, p=0.028$), with trend level effects in the DAN ($t(27)=-1.80, p=0.082$) and right FPCN ($t(27)=-1.97, p=0.059$) such that increased T807 signal was associated with decreased connectivity. No relationship with inferior temporal T807 was observed in the low amyloid group, and no significant relationship with entorhinal T807 was observed in either group.

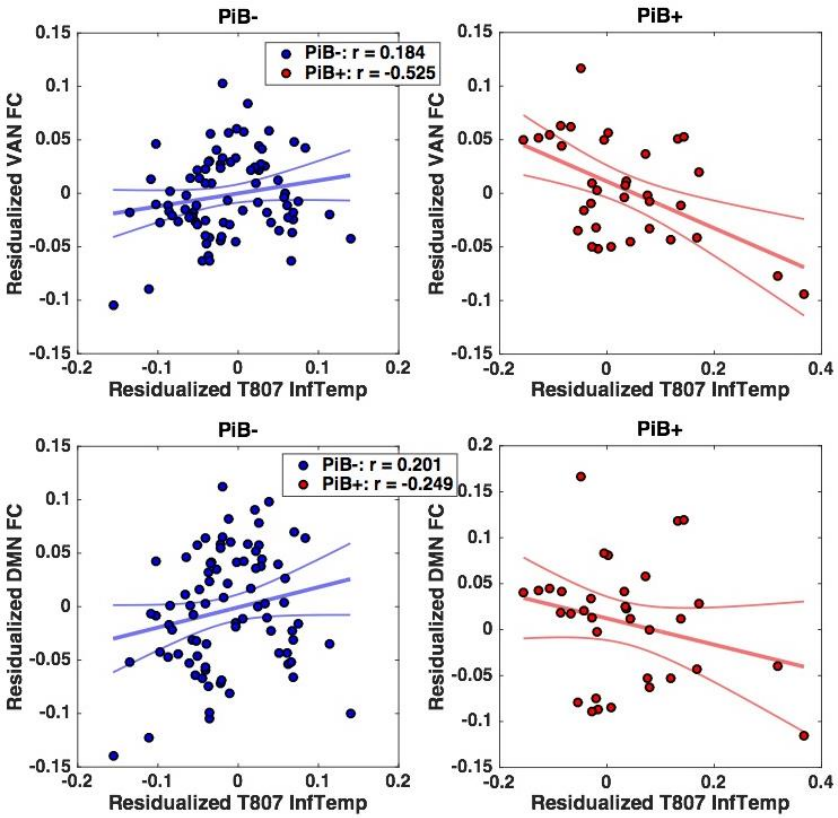

Conclusion: We observed significant negative relationships between inferior temporal T807 and functional connectivity within high amyloid individuals, suggesting that functional connectivity decreases as a function of increasing tau pathology. Additional follow-up with longitudinal fcMRI data as well as additional high amyloid individuals with a broader range of elevated T807 signal is needed, as is replication in other cohorts.

Patterns of tau deposition using [18F]-AV-1451 in autosomal dominant Alzheimer's disease: Results from the DIAN

Tammie Benzinger[1, 2, 4, 6], Karl Friedrichsen[1, 6], Yi Su[1, 6], Brian Gordon[1, 2, 6], Jon Christensen[1, 6], Russ Hornbeck[1, 6], Shruti Mishra[1, 6], Patricia Aldea[6], Lisa Cash[1, 2, 6], Beau Ances[2, 3, 6], Jon McConathy[1, 3, 6], Robert Koeppe[7], Nigel Cairns[2, 3, 5, 6], John Morris[2, 3, 6], Randall Bateman[3, 6]

[1]*Department of Radiology, Washington University School of Medicine, MO, United States*
[2]*Knight Alzheimer's Disease Research Center, MO, United States*
[3]*Department of Neurology, Washington University School of Medicine, MO, United States*
[4]*Department of Neurological Surgery, Washington University School of Medicine, MO, United States*
[5]*Department of Neuropathology, Washington University School of Medicine, MO, United States*
[6]*Washington University in Saint Louis, MO, United States*
[7]*Department of Radiology, University of Michigan, MI, United States*

Background: 18F-AV-1451 is a PET tracer used for the evaluation of neurofibrillary tangle pathology in vivo. The objective of the current work is to examine the patterns of AV1451 uptake in autosomal dominant Alzheimer's disease (ADAD), compared to late-onset Alzheimer's disease (LOAD).

Methods: Participants in the Dominantly Inherited Alzheimer Network (DIAN) undergoing imaging visits at Washington University during 2015 were asked to participate in AV1451 tau PET imaging, in addition to MRI and 11C-PiB amyloid and 18F-FDG PET. Comparisons are made between the uptake patterns of AV1451, PiB, and FDG in these participants. Additionally, the patterns of AV1451 uptake in DIAN participants are compared to a cohort of 63 participants in a study of LOAD. Standardized uptake value ratios (SUVRs) were obtained from the 80-100 minute post-injection window, using whole cerebellum as the reference region.

Results: Patterns of tau deposition within the temporal lobe are similar for cognitively impaired participants from DIAN compared to sporadic AD. However, DIAN participants with only mild impairment (Clinical Dementia Rating (CDR) = 0.5) have apparently increased uptake in the precuneus, parietal lobe, and frontal lobe compared to sporadic AD (Figure 1). Glucose hypometabolism in symptomatic DIAN participants is confined to regions with elevated AV1451 uptake (Figure 2). Enrollment is ongoing; additional data is required for full statistical modeling.

Conclusions: AV1451 uptake in DIAN participants is similar to patterns in sporadic AD, but with apparent greater spread for a given dementia severity. In DIAN participants, regions of FDG hypometabolism are co-localized with regions of elevated AV1451 uptake.

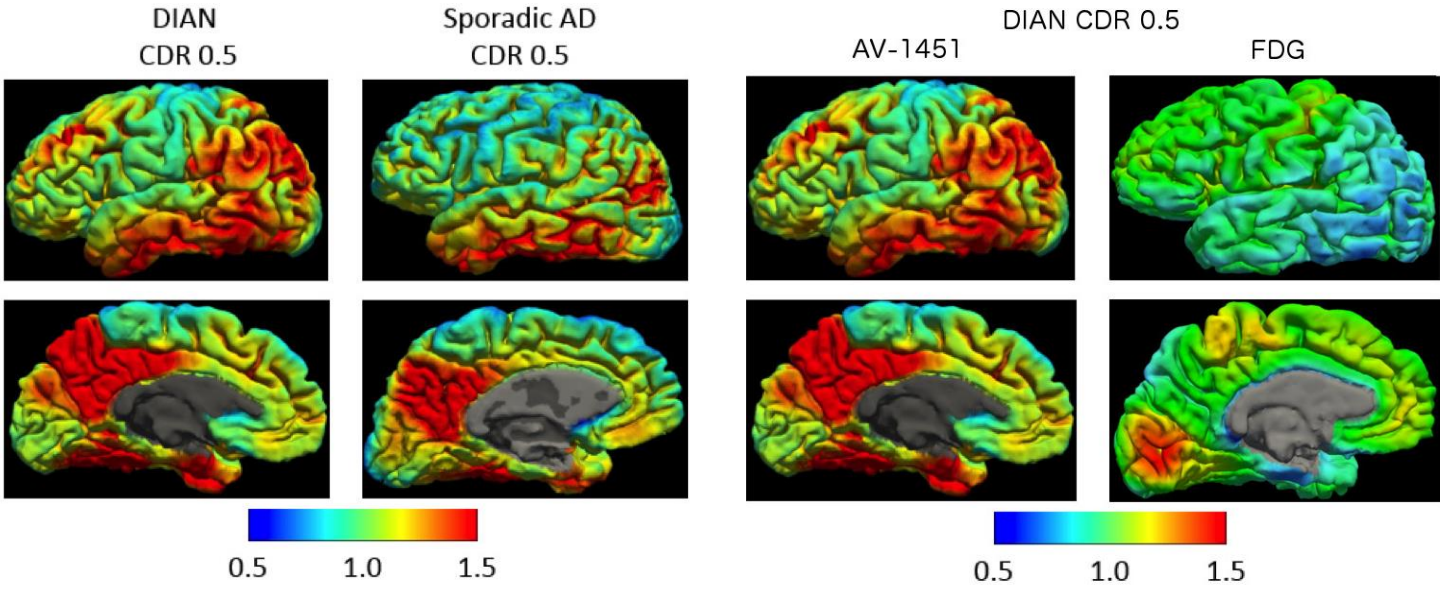

Poster Session (odd-numbered)

Laforce, Robert – PO1

Clinical utility of amyloid PET in the differential diagnosis of atypical dementias and its impact on caregivers

Mohamed Reda Bensaidane[1, 2], Rémi W. Rémi W.[1, 5], Marie-Pierre Fortin[1, 5], Michèle Houde[1, 5], Pedro Rosa-Neto[3], Stéphane Poulin[1, 5], Louis Verret[1, 5], Jean-Paul Soucy[4], Jean-Mathieu Beauregard[2, 5], Robert Jr Laforce[1, 2, 5]

[1]*Clinique Interdisciplinaire de Mémoire du Centre Hospitalier Universitaire, QC, Canada*
[2]*Université Laval, QC, Canada*
[3]*McGill Centre for Studies in Aging, QC, Canada*
[4]*McGill University, QC, Canada*
[5]*CHU de Québec-Université Laval, QC, Canada*

Background: Recent studies have supported a role for amyloid PET in distinguishing Alzheimer's disease (AD) pathology from other protein accumulations leading to dementia. We investigated the clinical utility of amyloid PET in the differential diagnosis of atypical cases and its impact on caregivers.

Methods: Using amyloid tracer NAV4694, we prospectively scanned 28 patients (mean age 59.3 yo, sd 5.8; mean MMSE 21.4, sd 6.0) with an atypical syndrome as determined by dementia experts. All patients had a full workup (i.e., history, examination, blood tests, neuropsychology, MRI and FDG-PET), yet no certain diagnosis. Amyloid PET was then conducted and determined positive or negative based on qualitative and quantitative reads by two independent nucleists. Physicians rated whether amyloid PET was associated with a diagnostic change and altered management. They also reported their degree of confidence in diagnosis pre and post-amyloid PET. Caregivers were met 1-3 months after revelation of the diagnosis and completed a 21-item Likert scale questionnaire along with a 1-hour interview designed to assess the impact of the amyloid scan.

Results: Our cohort was 50% amyloid positive and 50% negative. Interrater reliability was 100%. Amyloid PET was associated with a diagnostic change in 9/28 cases (32.1% that is 17.8% changed from AD to non-AD, and 14.3% from non-AD to AD). There was a significant increase (44%) in diagnostic confidence following the scan. Altered management occurred in 71.4% (20/28) of cases. Caregiver impact was favorable in all domains assessed including anxiety, depression, quality of life and prognosis.

Conclusions: This study suggests an additive role for amyloid PET in atypical cases with an unclear diagnosis beyond the detailed workup of a tertiary memory clinic. Amyloid PET increased diagnostic confidence and generated significant alterations in management. The overall process was positive on caregivers notably by encouraging quality time spent with their loved ones.

Increased sensitivity of AV45-PET for the detection of early stage amyloidosis after correction of white matter spill-in effects

Michel Grothe[1], Jorge Sepulcre[2, 3], Gabriel González-Escamilla[4], Christian Sorg[5], Stefan Teipel[1, 6]

[1]*German Center for Neurodegenerative Diseases (DZNE), Rostock, Germany*
[2]*Division of Nuclear Medicine and Molecular Imaging, Department of Radiology, Massachusetts General Hospital and Harvard Medical School, Boston, MA, United States*
[3]*Athinioula A. Martinos Center for Biomedical Imaging, Charlestown, MA, United States*
[4]*Department of Physiology, Anatomy and Cellular Biology, Pablo de Olavide University, Seville, Spain*
[5]*Department of Neuroradiology and Psychiatry, and TUM-Neuroimaging Center, Technical University Münich, Germany*
[6]*Department of Psychosomatic Medicine, University of Rostock, Germany*

Amyloid-sensitive PET is an increasingly used biomarker for the detection of cerebral amyloid pathology, but its sensitivity may critically depend on the way the PET scans are analyzed. Here we explored the effect of different image processing strategies on the concordance of amyloid-PET findings with cerebrospinal fluid (CSF) Aβ42 levels; an alternative biomarker of cerebral amyloidosis.

We investigated the effects of 2- and 3-compartment models of partial volume correction (PVC-2/-3) and choice of reference region on the correlation between cortical AV45-PET uptake ratios (AV45-SUVR) and CSF-Aβ42 using data from 603 subjects enrolled in ADNI-2. Furthermore, in a subset of 152 cognitively normal subjects the ability to detect regional AV45-SUVR increases in groups with decreased CSF-Aβ42 levels was compared between the different processing approaches.

When using a whole cerebellar reference region, PVC-3, which also controls for spill-in effects of white matter (WM) signal, resulted in a significantly increased correlation of AV45-SUVRs with CSF-Aβ42 levels. This effect was most pronounced for the lower range of AV45-SUVRs (Figure-1), and was not observed for the simpler PVC-2 model. Using PVC-3, cognitively normal subjects within the 3rd quintile of CSF-Aβ42 values (mean = 202 pg/ml) showed significantly increased AV45-SUVR values in fronto-temporo-parietal association areas compared to subjects within the highest CSF-Aβ42 quintile (≥ 241 pg/ml), and amyloid signal further extended across the cortex in subjects within the lowest CSF-Aβ42 quintiles (Figure-2). In uncorrected data, significant AV45-SUVR increases were only detected in subjects within the two lowest CSF-Aβ42 quintiles. Use of a WM reference region had similar effects as PVC-3 and these effects were non-additive.

Preprocessing techniques that account for the contamination of gray matter signal by unspecific WM binding can uncover biologically meaningful signal in AV45-PET scans that would typically be regarded as “amyloid-negative”, and thus increase their sensitivity for detecting early stage amyloidosis.

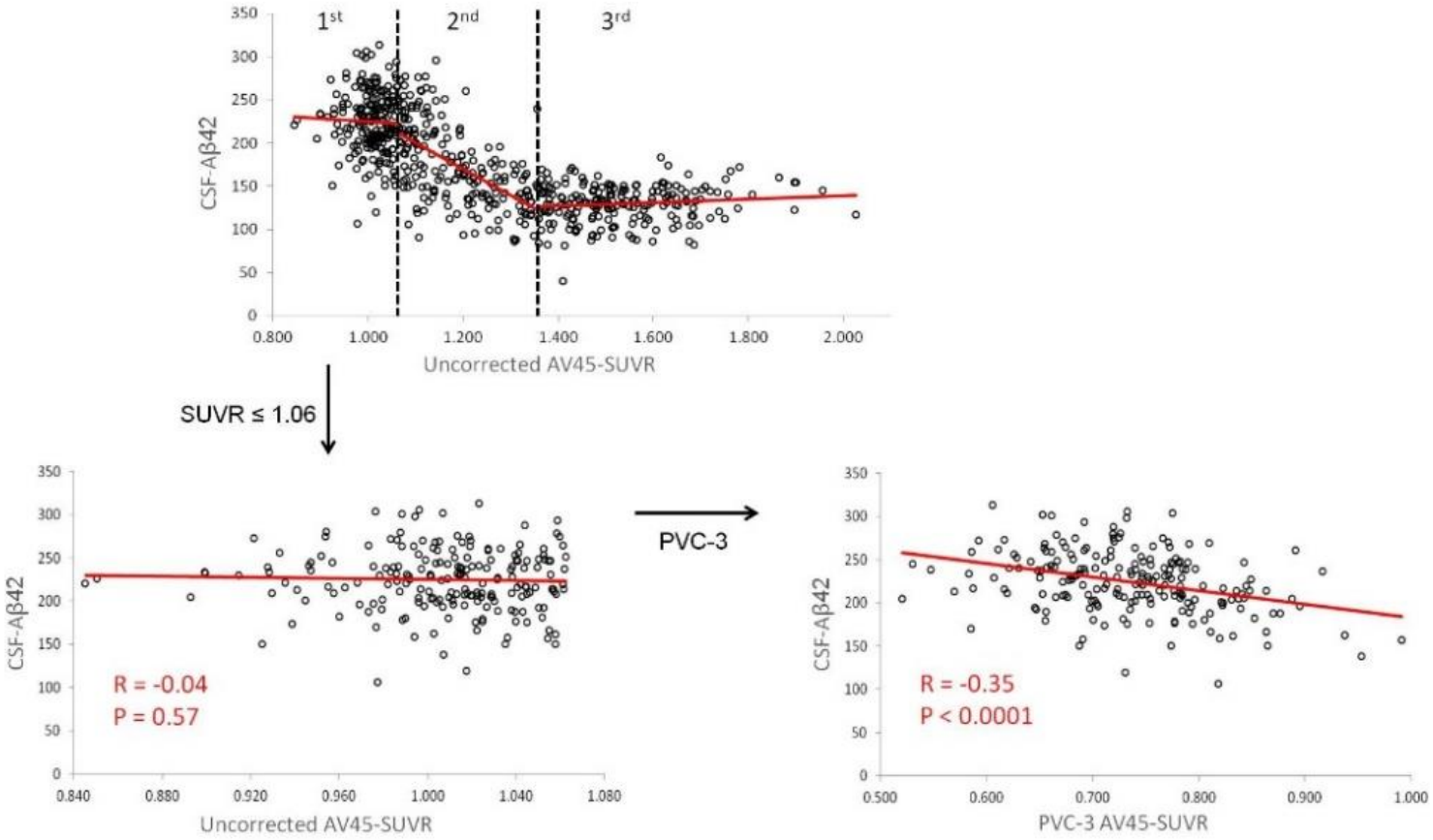

Figure 1. The effect of PVC-3 on the relation between cortical AV45-SUVRs and CSF-Aβ42 at the low range of AV45-SUVR values

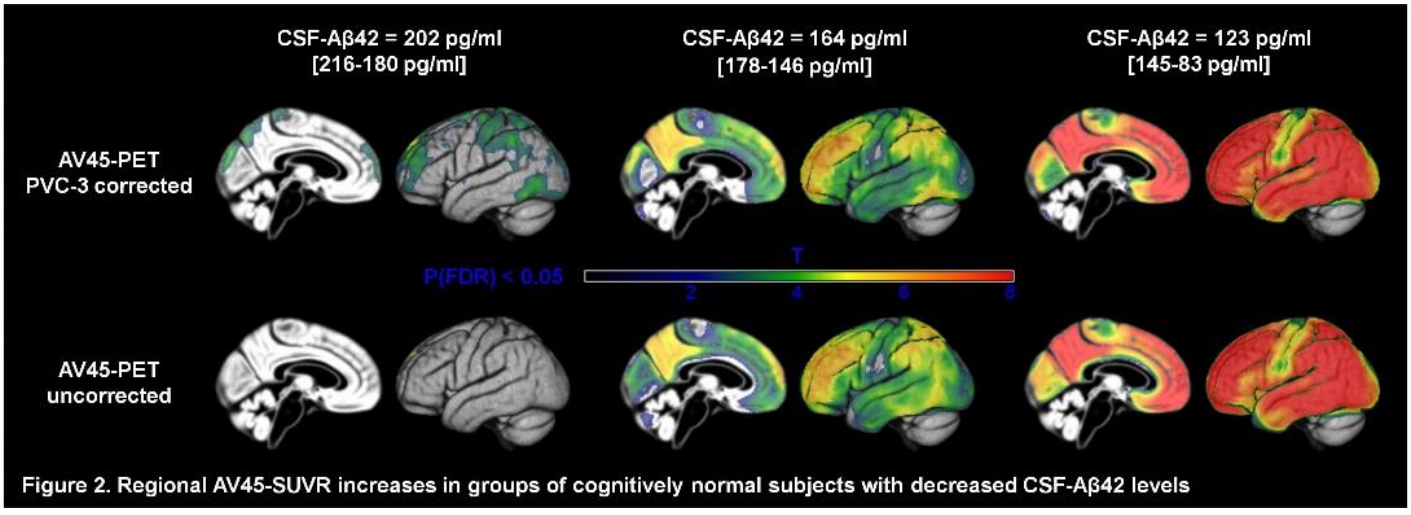

Figure 2. Regional AV45-SUVR increases in groups of cognitively normal subjects with decreased CSF-Aβ42 levels

The incremental diagnostic value of 18F-Florbetapir imaging in naturalistic patients with cognitive impairment: final results from the INDIA-FBP study

Marina Boccardi[1], Daniele Altomare[1], Clarissa Ferrari[2], Cristina Festari[1], Luigi Antelmi[3], Anna Tarallo[1], Patrizio Pasqualetti[4], Cristina Muscio[1, 5], Ugo Guerra[6], Barbara Paghera[7], Alessandro Padovani[8], Giovanni Frisoni[1, 3, 9]

[1]*Laboratory of Alzheimer's Neuroimaging and Epidemiology, IRCCS Centro San Giovanni di Dio Fatebenefratelli, Brescia, Italy*
[2]*Unit of Statistics, IRCCS Centro San Giovanni di Dio Fatebenefratelli, Brescia, Italy*
[3]*LANVIE - Laboratory of Neuroimaging of Aging, University Hospitals of Geneva, Switzerland*
[4]*Fatebenefratelli Hospital of Isola Tiberina, Roma, Italy*
[5]*European Foundation Biomedical Research (FERB), Center of Excellence Alzheimer, Ospedale Briolini, Gazzaniga, Bergamo, Italy*
[6]*Nuclear Medicine, Poliambulanza Foundation, Istituto Ospedaliero, Brescia, Italy*
[7]*Nuclear Medicine, University of Brescia and Spedali Civili of Brescia, Italy*
[8]*Centre for Neurodegenerative Disorders, Neurology Unit, University of Brescia and Spedali Civili of Brescia, Italy*
[9]*Memory Clinic, University Hospitals and University of Geneva, Switzerland*

Background: Little evidence is available on the incremental value of amyloid imaging in the diagnostic procedure. This study evaluated the incremental diagnostic value of 18F-Florbetapir PET (FBP-PET) on top of routine assessment of cognitive impairment in the current north-Italian clinical context.

Methods: The study included 228 consecutive patients from 18 Italian memory clinics. A diagnostic probability of Alzheimer Disease (AD) between 15% and 85% was required. Physicians formulated a clinical diagnosis, rated their diagnostic confidence (50-100%), and prescribed a therapeutic plan 1) after routine clinical work-up, and 2) after FBP-PET results.

Results: 35% AD patients tested negative (Aβ–); 43% of frontotemporal (FTD) and 48% subcortical-diseases tested positive (Aβ+). Diagnosis changed into Non-AD in 79% of AD patients testing Aβ–, and into AD in 81% of FTD and in 27% of subcortical-disease testing Aβ+. Diagnostic confidence increased after FBP-PET for patients with: confirmed diagnoses of AD (+11%, $p<0.001$), confirmed diagnosis of Non-AD (+9%, $p<0.001$), and revised diagnoses (AD into Non-AD: +13%, $p<0.001$; Non-AD into AD: +14%, $p=0.003$). Change in prescribed cognition-specific medications (AChEI and memantine) after FBP-PET was significant ($p<0.001$). The 90% of new prescriptions occurred in Aβ+ and 86% of the removals in patients Aβ–.

Conclusions: Our data support the incremental diagnostic value of both positive and negative FBP-PET scans on relevant clinical outcomes. After replication, these data will allow evidence-based recommendations for amyloid imaging prescription.

Roadmap to the biomarker-based diagnosis of Alzheimer's disease

Giovanni B. Frisoni[1, 2], Marina Boccardi[1], Clifford R. Jack Jr[3], Bengt Winblad[4], For the Biomarker Roadmap Initiative[2]

[1]*IRCCS S Giovanni di Dio-Fatebenefratelli, Brescia, Italy*
[2]*University Hospitals and University of Geneva, Switzerland*
[3]*Mayo Clinic, Rochester, MN, United States*
[4]*European Alzheimer's Disease Consortium; Department of Neurobiology, Care Sciences and Society, Karolinska Institute, Stockholm, Sweden*

Background: The diagnosis of Alzheimer's disease (AD) is shifting from a clinical to a clinical-pathological paradigm. Biomarkers of Alzheimer's pathology (hippocampal atrophy on MR, cortical hypo-metabolism on FDG-PET, decreased Abeta42 and increased tau and phospho-tau in CSF, and increased amyloid ligands uptake on PET) are at different stages of development. The lack of coordinated development at the European and global level is delaying authorization by regulatory agencies, reimbursement by payers, implementation in the clinic, and ultimately the development of effective treatments.

Objective: Outlining the actions required to accelerate this course.

Methods: A group of international AD biomarker and international canc er biomarker experts adapted a 5-phase framework for biomarker development used in oncology to AD biomarkers. The 5 sequential phases include: 1) preclinical exploratory studies, 2) clinical assay development for clinical disease, 3) prospective longitudinal repository studies, 4) prospective diagnostic studies, and 5) disease control studies. Primary and secondary aims are defined for each phase (Table). Current maturity of biomarkers according to this framework was assessed from available literature on: neuropsychology; amyloid-PET; CSF Abeta42, tau and phospho-tau; FDG- PET; hippocampal atrophy.

Phases for the development of biomarkers as adapted from the oncology framework (Pepe et al., J Natl Cancer Inst 2001) to the case of the pre-dementia diagnosis of Alzheimer's disease.

PHASES	AIMS	description
Phase 1		
Preclinical Exploratory Studies	Primary Aims	To identify leads for potentially useful biomarkers and prioritize identified leads.
Phase 2		
Clinical Assay Development for Clinical Disease	Primary Aim	to estimate the true and false positive rate or ROC curve and assess its ability to distinguish subjects with and without the disease.
	Secondary Aim 1	To optimize procedures for performing the assay and to assess the reproducibility of the assay within and between laboratories.
	Secondary Aim 2	To determine the relationship between biomarker tissue measurements made on tissue (phase 1) and the biomarker measurements made on the noninvasive clinical specimen (phase 2).
	Secondary Aim 3	To assess factors (e.g. sex, age, etc.), associated with biomarker status or level in control subjects. If such factors affect the biomarker, thresholds for test positivity may need to be defined separately for target subpopulations.
	Secondary Aim 4	To assess factors associated with biomarker status or level in diseased subjects—in particular, disease characteristics.
Phase 3		
Prospective Longitudinal Repository Studies	Primary Aim 1	To evaluate the capacity of the biomarker to detect the earliest disease stages.
	Primary Aim 2	To define criteria for a biomarker positive test in preparation for phase 4.
	Secondary Aim 1	To explore the impact of covariates on the discriminatory abilities of the biomarker before clinical diagnosis.
	Secondary Aim 2	To compare markers with a view to selecting those that are most promising.
	Secondary Aim 3	To develop algorithms for positivity based on combinations of markers.
	Secondary Aim 4	To determine a biomarker testing interval for phase 4 if repeated testing is of interest.
Phase 4		
Prospective Diagnostic Studies	Primary Aim	to determine the operating characteristics of the biomarker-based test in a relevant population by determining the detection rate and the false referral rate. Studies at this stage involve testing people and lead to diagnosis and treatment.
	Secondary Aim 1	To describe the characteristics of disease detected by the biomarker test—in particular, with regard to the potential benefit incurred by early detection.
	Secondary Aim 2	To assess the practical feasibility of implementing the diagnostic program and compliance of test-positive subjects with work-up and treatment recommendations.
	Secondary Aim 3	To make preliminary assessments of the effects of biomarker testing on costs and mortality associated with the disease.
	Secondary Aim 4	To monitor disease occurring clinically but not detected by the biomarker testing protocol.
Phase 5		
Disease Control Studies	Primary Aim	to estimate the reductions in disease-associated mortality, morbidity, and disability afforded by biomarker testing.
	Secondary Aim 1	To obtain information about the costs of biomarker testing and treatment and the cost per life saved or per quality-adjusted life year.
	Secondary Aim 2	To evaluate compliance with testing and work-up in a diverse range of settings.
	Secondary Aim 3	To compare different biomarker testing protocols and/or to compare different approaches to treating test positive subjects in regard to effects on mortality and costs.

Results: For all biomarkers, available validation studies fulfil Phase 1. The aims of phases 2 and 3 are addressed inconsistently by current literature. Only preliminary evidence is available for some Phase 4 aims for amyloid-PET, CSF biomarkers, hippocampal atrophy, and FDG PET, while phase 5 aims have never been addressed. Compared to other biomarkers, Amyloid imaging is at a relatively advanced stage of validation, however it also suffers from inconsistent proceeding in validation studies (Figure below).

Conclusions: This evidence highlights research priorities and identifies a roadmap of actions, aimed to accelerate AD biomarker implementation in the clinic. The intended users of the roadmap are funding agencies of healthcare research, scientists and scientific societies, and policy makers.

Current state of development and validation of biomarkers for the early and differential diagnosis of Alzheimer's disease. PA: primary aim. SA: secondary aim.Green: fully achieved; yellow: partly achieved; orange: preliminary evidence; red: not achieved; white: not applicable.

Biomarker	Phase I Preclin. Explorat. Studies	Phase II Clinical Assay Development for Clinical Disease					Phase III Prorospective Longitudinal Repository Studies						Phase IV Prospective Case Finding Studies					Phase V Disease Control Studies			
	PA 1	PA	SA 1	SA 2	SA 3	SA 4	PA 1	PA 2	SA 1	SA 2	SA 3	SA 4	PA	SA 1	SA 2	SA 3	SA 4	PA	SA 1	SA 2	SA 3
Neuropsychology																					
CSF																					
Amyloid PET																					
FDG PET																					
Hippocampal volume on MR																					

Reference tissue normalization in longitudinal 18F-Florbetapir positron emission tomography of late mild cognitive impairment

Sepi Shokouhi[1], John Mckay[1], Suzanne Baker[2], Hakmook Kang[3], Aaron Brill[1], Harry Gwirtsman[4], William Riddle[1], Daniel Claassen[5], Baxter Rogers[1]

[1]*Vanderbilt University Department of Radiology & Radiological Sciences, TN, United States*
[2]*Center of Functional Imaging at Lawrence Berkeley National Lab, CA, United States*
[3]*Vanderbilt University Department of Biostatistics, TN, United States*
[4]*Vanderbilt University Department of Psychiatry, TN, United States*
[5]*Vanderbilt University Department of Neurology, TN, United States*

Introduction: Semi-quantitative methods, such as the standardized uptake value ratio (SUVR), require the normalization of the radiotracer activity to a reference tissue to monitor changes in the accumulation of Aβ plaques measured with positron emission tomography (PET). The objective of our study is to evaluate the effect of reference tissue normalization in a test-retest 18F-florbetapir SUVR study using cerebellar gray matter, white matter (two different segmentation masks), brainstem and corpus callosum as reference regions.

Methods: We calculated the correlation between 18F-florbetapir PET and concurrent cerebrospinal CSF Aβ1-42 levels in a late mild cognitive impairment cohort with longitudinal PET and CSF data over the course of two years. In addition to conventional SUVR analysis using mean/median values of normalized brain radiotracer activity, we investigated a new image analysis technique—the weighted two-point correlation function (wS2)—to capture potentially more subtle changes in Aβ-PET data.

Results: Compared to the SUVRs normalized to cerebellar gray matter, all cerebral-to-white matter normalization schemes resulted in a higher inverse correlation between PET and CSF Aβ1-42, while the brainstem normalization gave the best results (high and most stable correlation). Compared to the SUVR mean/median values, the wS2 values were associated with the lowest coefficient of variation and highest inverse correlation to CSF Aβ1-42 levels across all time points and reference regions, including the cerebellar gray matter.

Conclusion: The selection of reference tissue for normalization and the choice of image analysis method can affect changes in cortical 18F-florbetapir uptake in longitudinal studies.

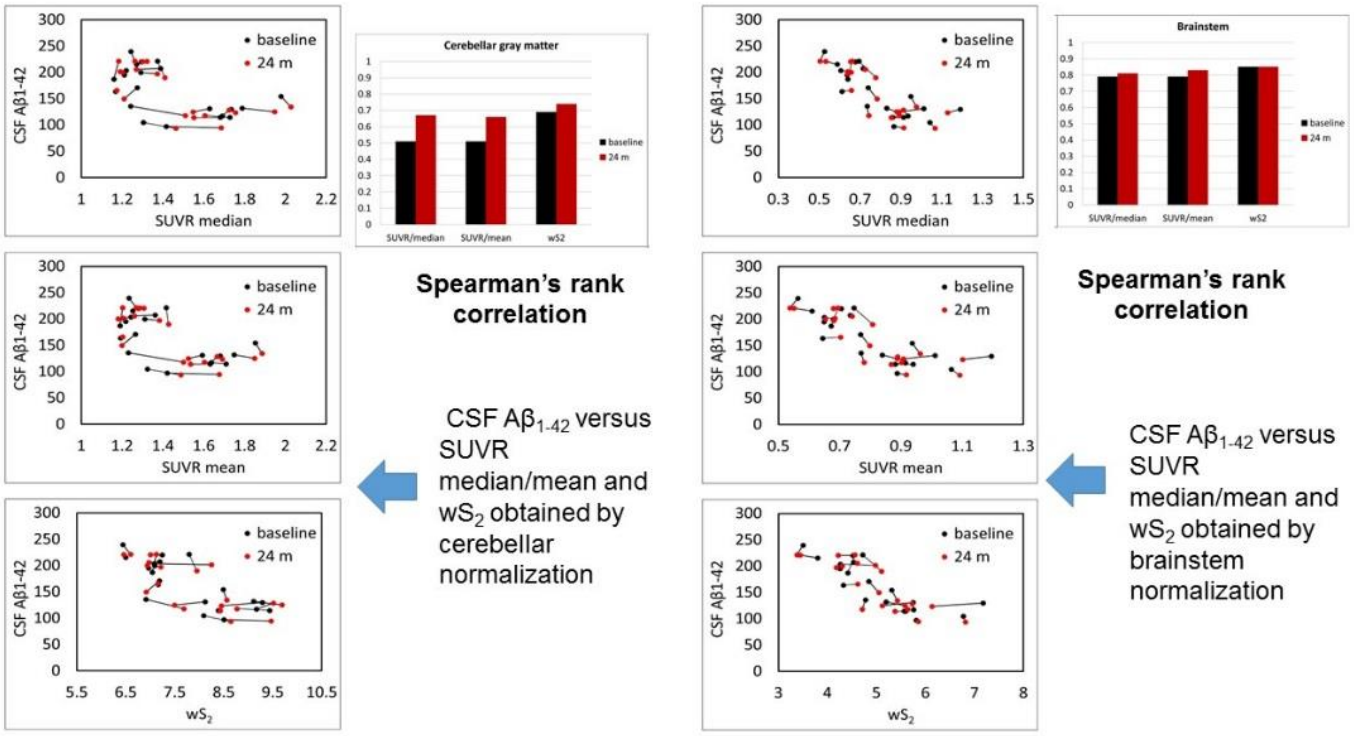

Glucose metabolism and metabolic connectivity patterns in ADNI subjects are continuously modulated by β-amyloid

Felix Carbonell[1], Donald G. McLaren[1], Alex P. Zijdenbos[1], Barry J. Bedell[1, 2]

[1]*Biospective Inc., QC, Canada*
[2]*Research Institute of the McGill University Health Centre, QC, Canada*

Background: Regional glucose hypometabolism is characteristic of Alzheimer's disease (AD). However, during the pre-clinical stage of AD, this hypometabolism has been primarily associated with APOE ε4 status, rather than fibrillar β-amyloid load. In contrast, we have previously observed that patterns of metabolic connectivity are more related to β-amyloid than APOE ε4 status. A major limitation of such analysis has been the dichotomous classification of subjects as amyloid-positive or amyloid-negative based on visual reads or pre-defined SUVR thresholds of amyloid PET data. The dichotomous treatment of a continuous variable, such as β-amyloid, potentially obscures the actual relationships between the variables of interest, and reduces the power to detect significant effects on glucose metabolism and metabolic connectivity patterns.

Methods: In the present work, we have utilized multiple linear regression to assess the impact of continuously increasing β-amyloid burden (from florbetapir PET data) on glucose metabolism and metabolic connectivity (from FDG PET data) in a population of 454 ADNI subjects across the AD spectrum.

Results: We observed that increasing fibrillar β-amyloid burden was associated with significant reductions in glucose metabolism in regions of the default mode network. We also found that β-amyloid burden significantly decreases the slope of the relationship between several seeds-of-interest and whole brain metabolism (Figure).

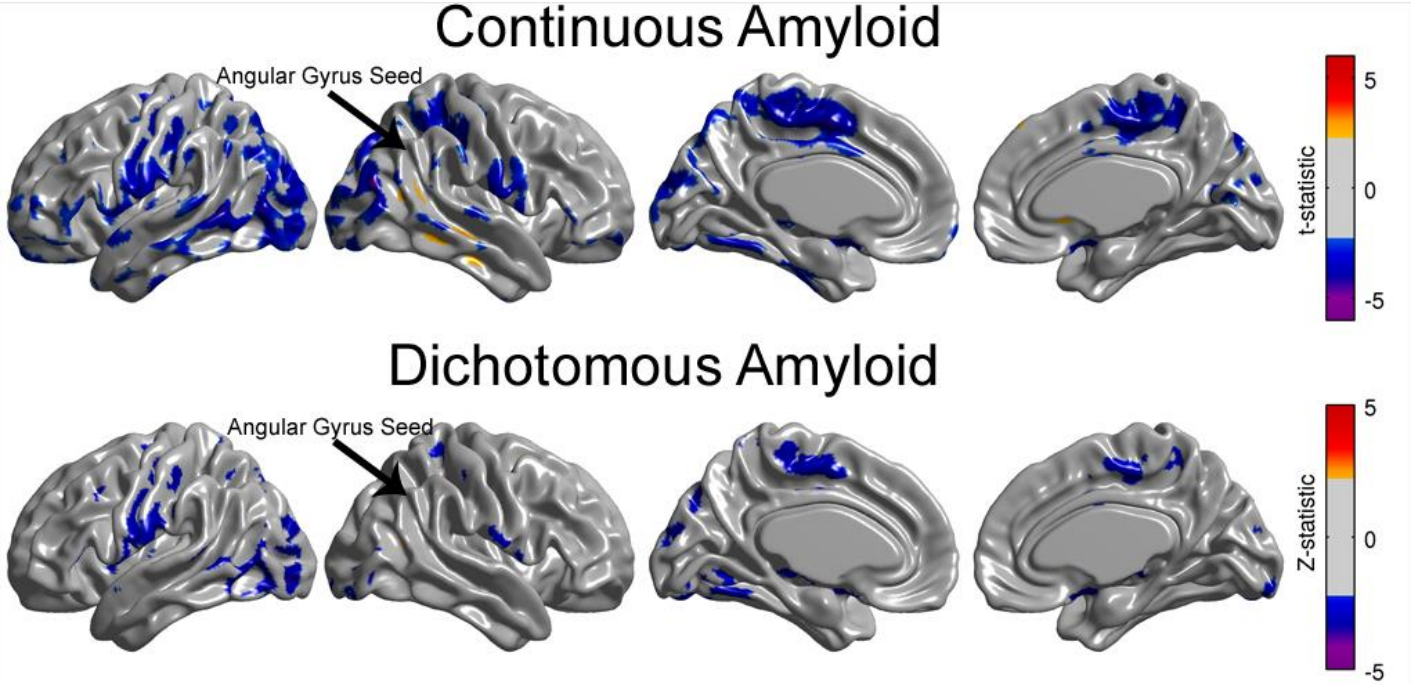

A key finding of this study was our ability to identify a physiologically-relevant florbetapir PET SUVR cutoff value that is associated with subsequent decline in metabolic connectivity. Increased metabolic correlations below this cutoff value can potentially be explained by globally synchronized decreases in metabolism at early stages of β-amyloid deposition, which are followed by regionally heterogeneous metabolic decrease at higher β-amyloid levels.

Conclusions: We conclude that sophisticated statistical modeling of β-amyloid burden as a continuously varying effect provides novel insight into the evolution of neural dysfunction, which is not possible with the conventional dichotomization approach.

Influence of [18F]Flutemetamol amyloid deposition on memory in cognitively normal elderly twins

Elles Konijnenberg[1], Anouk Den Braber[1, 2], Leoni Goossens[1], Sofie Adriaanse[3], Mara Ten Kate[1], Linda Wesselman[1], Maqsood Yaqub[3], Dorret Boomsma[2], Philip Scheltens[1], Bart Van Berckel[3], Pieter Jelle Visser[1, 4]

[1]*Alzheimer Center, Department of Neurology, VU University Medical Center, Neuroscience Campus, Amsterdam, Netherlands*
[2]*Department of Biological Psychology, VU University, Amsterdam, Netherlands*
[3]*Department of Radiology & Nuclear Medicine, VU University Medical Center, Neuroscience Campus, Amsterdam, Netherlands*
[4]*Department of Psychiatry and Neuropsychology, School for Mental Health and Neuroscience, Alzheimer Center Limburg, Maastricht University, Maastricht, Netherlands*

Background: Amyloid pathology precedes clinical dementia by decades. There is conflicting evidence on whether amyloid load as assessed by PET is related to subtle memory dysfunction in cognitively healthy elderly. This may relate to the type of memory test used. The aim of the study is to assess the correlation between amyloid load and memory performance on different types of memory tests in cognitively healthy elderly subjects.

Methods: We present preliminary data on the first 78 subjects (monozygotic twins) that were enrolled in the EMIF-AD PreclinAD study. Inclusion criteria were age ≥60 years and delayed recall score >-1.5 SD of demographic adjusted normative data on the CERAD word list. Dynamic [18F]flutemetamol (FMM) scans were performed with combined data from two scans (30 minutes starting directly after FMM injection and 90-110 minutes post injection). With cerebellar grey matter as reference region non-displaceable binding potential (BPND) in the posterior cingulate cortex was calculated using RPM1. Memory performance was measured by delayed recall on Rey Auditory Verbal Learning Task (RAVLT) and Rey figure, total errors on CANTAB Paired Associate Learning Task (PAL) and total score from Face Name Associative Memory task-Names (FNAME-N). The correlation between BPND and cognition was analyzed using GEE models with correction for twin status.

Results: Subjects had a median age of 64.4 years and were more often female (63%), had on average 16 years of education and a MMSE score of 29. Increased BPND correlated with poorer memory on the Rey figure (B=-10.2,p=0.02) and PAL (B=37.5,p<0.01) but not the RAVLT (B=-3.4,p=0.09) and FNAME-N (B=-15.0,p=0.09). After correction for age, education and gender only PAL (B=6.2,p=0.10) and Rey figure (B=-6.2,p=0.08) remained borderline significant.

Conclusion: Higher FMM BPND in cognitively healthy elderly subjects is associated with lower scores on paired associated learning and visual memory. Effects were partly mediated by demographic characteristics; these interactions with amyloid on memory function will be further studied in the whole cohort.

Implications of tau deposition as measured using [18F]-AV-1451 on staging of preclinical sporadic Alzheimer's disease

Shruti Mishra[1], Yi Su[1], Karl Friedrichsen[1], Brian Gordon[1, 2], Jon Christensen[1], Patricia Aldea[1], Nigel J Cairns[2, 3, 5], Anne M Fagan[2, 3], Jonathan McConathy[1], John C Morris[2, 3], Beau M Ances[3], Tammie LS Benzinger[1, 2, 4]

[1]*Department of Radiology, Washington University in St. Louis, MO, United States*
[2]*Knight Alzheimer's Disease Research Center, Washington University in St. Louis, MO, United States*
[3]*Department of Neurology, Washington University in St. Louis, MO, United States*
[4]*Department of Neurological Surgery, Washington University in St. Louis, MO, United States*
[5]*Department of Pathology & Immunology, Washington University in St. Louis, MO, United States*

Background: 18F-AV-1451 is a Positron Emission Tomography (PET) tracer used as a biomarker of tauopathy *in vivo*. The objective of the current work is to evaluate spatial patterns of AV1451 accumulation that are sensitive to preclinical and clinical Alzheimer's disease.

Methods: Sixty-three participants, 51 cognitively normal (CN) (mean age 73y, SD 6y) with a Clinical Dementia Rating (CDR) of 0 and 12 individuals with CDR > 0 (mean age 77y, SD 8y), were imaged using 18F-AV1451. Regions of interest (ROIs) were generated using Freesurfer. Standardized uptake value ratios (SUVRs) normalized to the whole cerebellum and partial volume corrected were calculated for each ROI and entered into a k-means clustering analysis. Clusters obtained from this analysis were compared with ROI groupings as predicted by Braak neurofibrillary tangle staging. Of the 51 CN individuals, 50 also underwent PET beta-amyloid imaging with either [18F]-Florbetapir (AV45) or [11C]-PIB in the previous 24 months, and were categorized as beta-amyloid positive or negative.

Results: Analyses showed that the ideal number of clusters was two. Mean SUVR across all ROI groupings for total cohort of CN and cognitively abnormal participants had a significant correlation with CDR sum of boxes, with cluster 1 and Braak 5/6 groupings demonstrating the greatest correlations. Mean SUVR within ROIs from cluster 1, Braak stage 1/2, and Braak stage 5/6 discriminated between beta-amyloid PET positive and negative individuals within CN cohort. ROIs predicted to be affected late in the disease (Braak stage 5/6) were grouped in cluster 1.

Conclusions: AV-1451 accumulation in ROIs affected early in Alzheimer's disease can differentiate among preclinical stages as defined by National Institute of Aging and Alzheimer's Association's criteria for PET beta-amyloid biomarkers. ROIs affected early may be more widespread than those predicted by Braak tangle staging.

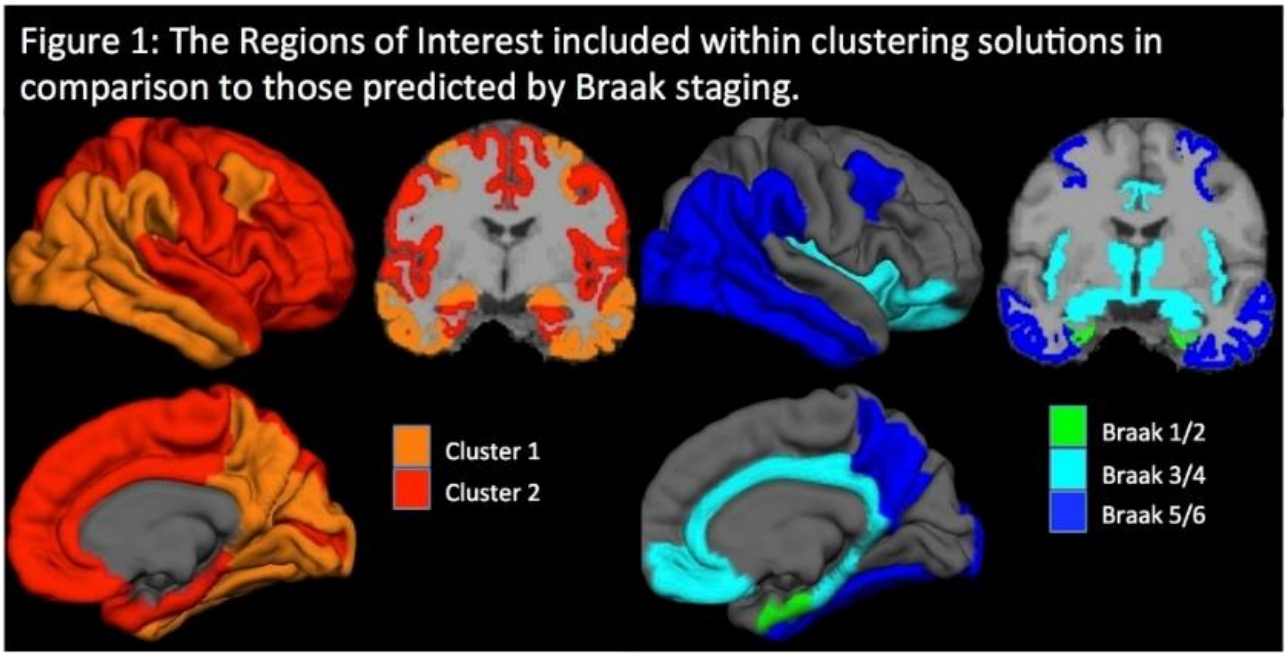

Figure 2: Mean SUVR within ROIs of each cluster in all CDRs vs. Sum of Boxes from Most Recent Clinical Assessment

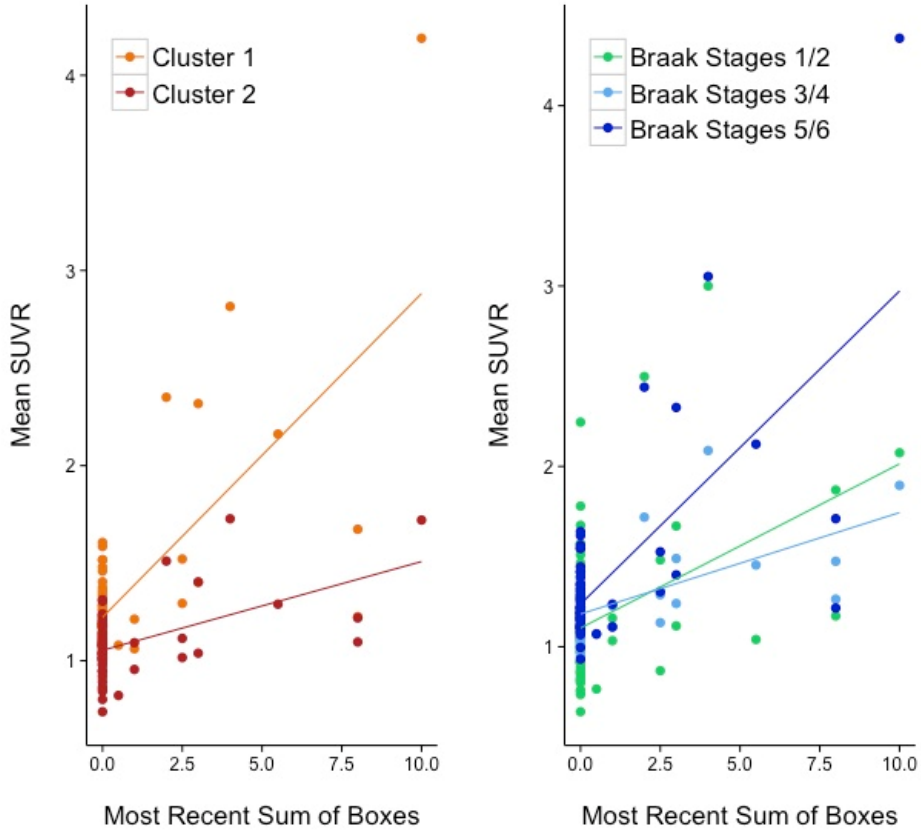

Figure 3: Mean SUVR within each cluster of ROIs in CDR=0 Amyloid PET Pos and Neg cohorts

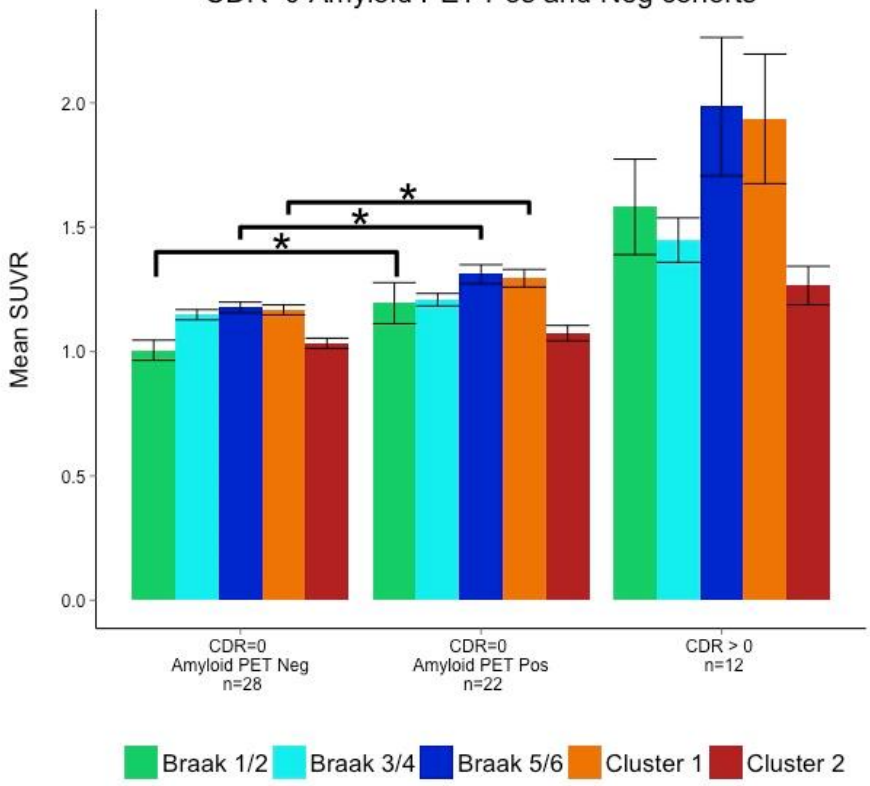

Tau PET is associated with increased hippocampal fMRI activity during successful memory encoding

Willem Huijbers[1, 2], Aaron Schultz[1, 3], Kathryn Papp[4], Molly LaPoint[1], Danielle Cosio[3], Jasmeer Chhatwal[1, 3], Keith Johnson[1, 3], Reisa Sperling[1, 3, 4]

[1]*Athinoula A. Martinos Center for Biomedical Imaging, Department of Neurology, Massachusetts General Hospital, Harvard Medical School, Charlestown, MA, United States*
[2]*German Centre for Neurodegenerative Diseases (DZNE), Department of Population Health Sciences, Bonn, Germany*
[3]*Department of Radiology, Massachusetts General Hospital, Harvard Medical School, Boston, MA, United States*
[4]*Center for Alzheimer Research and Treatment, Department of Neurology, Brigham and Women's Hospital, Harvard Medical School, Boston, MA, United States*

Rationale: Alzheimer's disease (AD) is associated with functional alterations in brain regions that support memory encoding. In prodromal AD, amyloid accumulation is linked to increased task-related functional magnetic resonance imaging (fMRI) activity in the hippocampus and precuneus. In clinically normal older adults, the relationship between amyloid accumulation and task-related hippocampal activity has remained elusive. Some fMRI studies found increased hippocampal activity, while several others have not. One possibility is that preclinical changes in fMRI activity are mediated by early neocortical tau accumulation in temporal lobe regions.

Methods: We examined 108 clinically normal older adults enrolled in the Harvard Aging Brain Study (aged 63-90, M=74.8, female=73). We measured fMRI activity during successful encoding of novel faces, and amyloid accumulation with PiB-PET imaging. In a subset of 40 participants (aged 66-90, M=76.1, female=25), we also measured tau accumulation using T807 (AV1451). Amyloid was quantified using a FreeSurfer defined set of neocortical regions and tau was measured in inferior temporal regions.

Results: In the subset with T807 imaging, we found that greater tau accumulation was related to increased hippocampal fMRI activity (R =0.41, p=0.009), while the relationship with precuneus fMRI activity was not significant (R=0.26, p=0.104). In the full sample, we found trend level relationships between amyloid accumulation and increased fMRI activity in the precuneus (R=0.16, p=0.090) and decreased activity in the hippocampus (R=-0.17, p=0.089). While amyloid and tau accumulation are related (R=0.39, p=0.014), we did not observe interactions between amyloid, tau and fMRI activity. In a linear model with both amyloid and tau included, only the relationship between tau and hippocampal activity was significant (β=0.69, p=0.005).

Conclusion: Increased hippocampal fMRI activity in clinically normal older individuals during successful memory encoding is more closely related to tau than amyloid accumulation. Together, these findings provide novel insight into the preclinical trajectory of aberrant hippocampal activity.

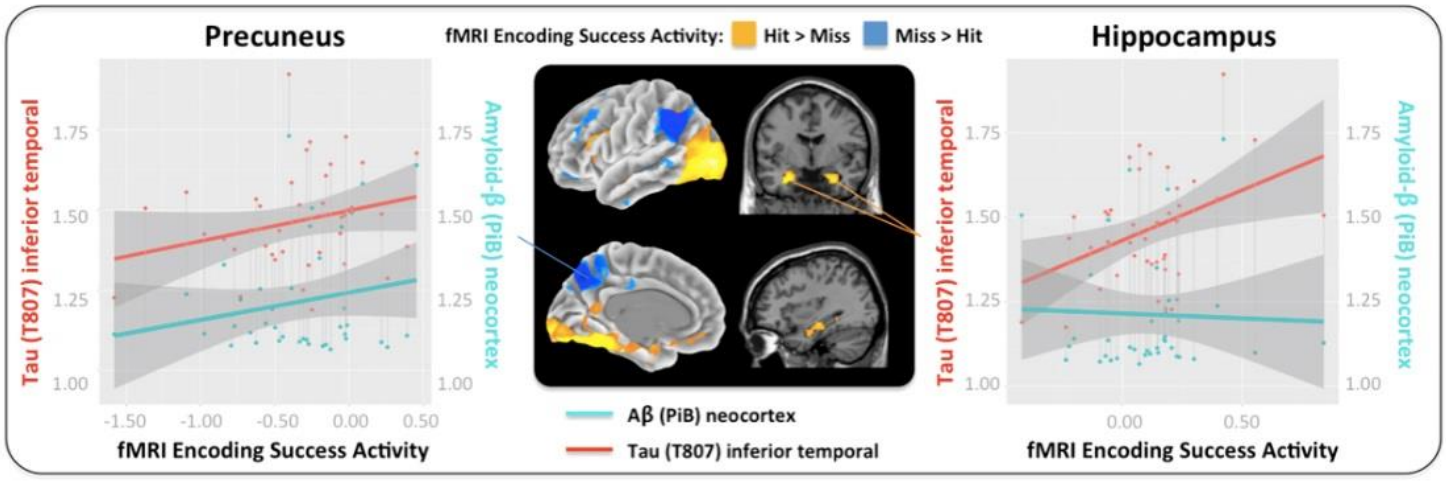

Perfusion markers derived from dynamic F18 Florbetapir PET scans correlate with measures of global cognition and function

Sergey Shcherbinin[1], Jennifer Eads[1], Adam Schwarz[1], John Sims[1], Alzheimer's Disease Neuroimaging Initiative[2]

[1]*Eli Lilly & Co, IN, United States*
[2]*Data used in preparation of this abstract were obtained from the Alzheimer's Disease Neuroimaging Initiative (ADNI) database (adni.loni.usc.edu)*

Objectives: Recent findings suggest utility of the early frames of F18 Florbetapir (AV-45) PET as a proxy for FDG PET to measure neuronal dysfunction. We examined the relationship between Florbetapir-derived perfusion markers and baseline assessments of global cognition and function.

Methods: We analyzed dynamic AV-45 [0-20 min] and FDG [30-60 min] images for 103 subjects (20 HC, 39 SMC, 17 EMCI, 15 LMCI, 12 AD) from the ADNI database. We generated static SUVR images (AV-45 $SUVR_{0\text{-}5min}$, AV-45 $SUVR_{1\text{-}6min}$, and FDG $SUVR_{30\text{-}60min}$) by integrating the corresponding dynamic acquisitions using cerebellar grey matter as a reference region. A tracer delivery map (AV-45 R_1) was created from AV-45 [0-20 min] dynamic images using SRTM2 model (PMOD v3.5) and the same reference region.

Results: The AV-45 R_1 strongly correlated with AV-45 $SUVR_{0\text{-}5min}$ (r=0.95-0.99) and AV-45 $SUVR_{1\text{-}6min}$ (r=0.93-0.98) across 80 AAL atlas-based regions. FDG $SUVR_{30\text{-}60min}$ correlated with AV-45 $SUVR_{0\text{-}5min}$, AV-45 $SUVR_{1\text{-}6min}$ and AV-45 R_1 with similar coefficients r=0.58-0.94 across 80 regions. The strongest correlations with MMSE, ADAS-cog and FAQ for all aforementioned maps were observed in temporal and parietal regions. The AV-45 $SUVR_{0\text{-}5min}$ values calculated in four composite regions (temporal left/right and parietal left/right) across 39 amyloid-positive subjects showed Pearson correlations with ADAS-cog (-r=0.44-0.71, significant in four regions), FAQ (-r=0.45-0.64, significant in four regions) and MMSE (r=0.29-0.55, non-significant in parietal left). These results closely followed those observed for FDG $SUVR_{30\text{-}60min}$ with correlations coefficients -r=0.62-0.80 (ADAS-cog), -r=0.47-0.64 (FAQ) and r=0.58-0.70 (MMSE).

Conclusions: Regional perfusion estimates derived from early frames of AV-45 dynamic scans showed similarly high correlation with FDG uptake values. In amyloid positive subjects, AV-45 $SUVR_{0\text{-}5min}$ uptake in the temporal and parietal regions showed significant correlation with ADAS-cog and FAQ scores.

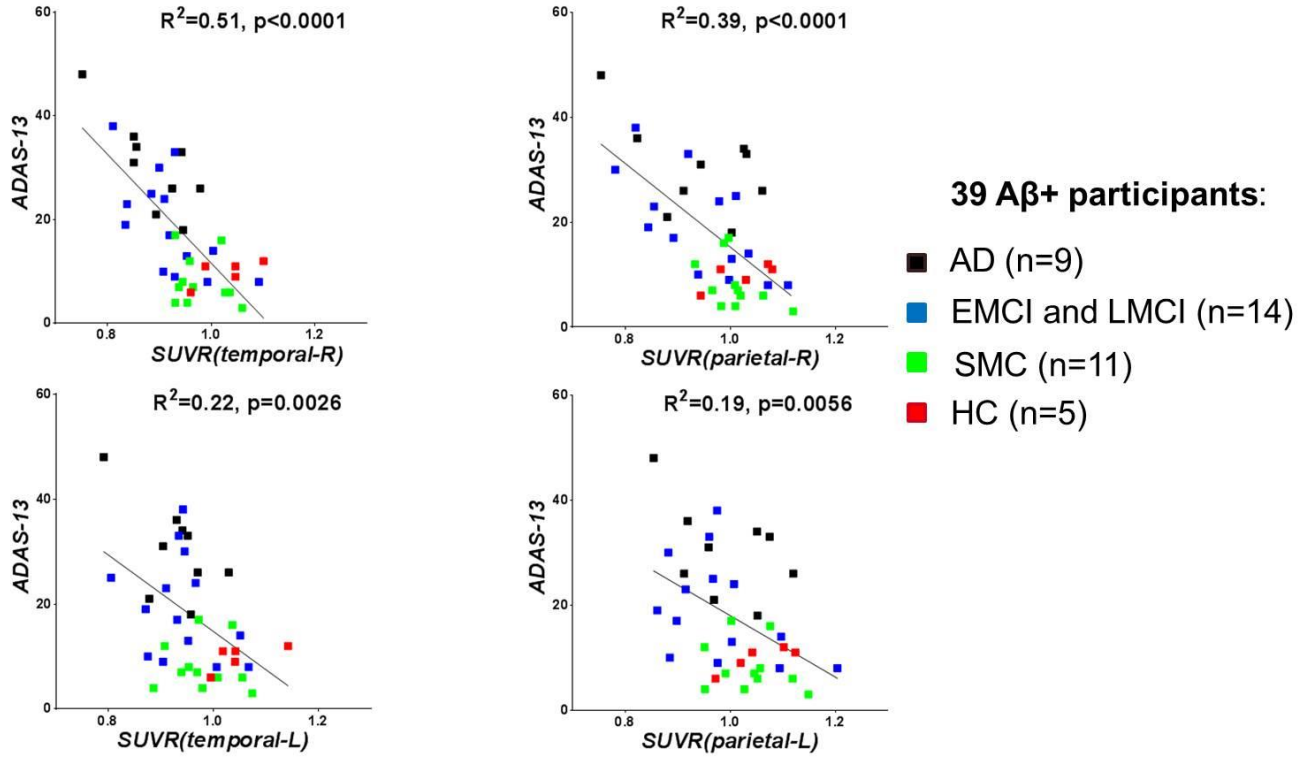

Amyloid deposition combined with CSF markers of neuroinflammation predict neurite loss in cognitively asymptomatic individuals

Andrew Merluzzi[1], Douglas Dean[2], Annie Racine[1], Cynthia Carlsson[1, 6], Bradley Christian[5], Sterling Johnson[1, 6, 7], Ozioma Okonkwo[1, 7], Jennifer Oh[1], Nagesh Adluru[2], Gaurav Suryawanshi[2], Henrik Zetterberg[3], Kaj Blennow[3], Sanjay Asthana[1, 6, 7], Hui Zhang[4], Andrew Alexander[5], Barbara Bendlin[1, 7]

[1]*Wisconsin Alzheimer's Disease Research Center, University of Wisconsin School of Medicine and Public Health, WI, United States*
[2]*Waisman Laboratory for Brain Imaging and Behavior, University of Wisconsin-Madison, WI, United States*
[3]*University of Gothenburg, Mölndal, Academy at the University of Gothenburg, Sweden*
[4]*University College London, United Kingdom*
[5]*Department of Medical Physics, University of Wisconsin School of Medicine and Public Health, WI, United States*
[6]*Geriatric Research Education and Clinical Center, Wm. S. Middleton Veterans Hospital, WI, United States*
[7]*Wisconsin Alzheimer's Institute, WI, United States*

Background: Inflammation is a well-established feature of Alzheimer's disease (AD) and may contribute to neural injury. However, the role of neuroinflammation in preclinical AD is largely unknown. We hypothesized that elevated neuroinflammation in concert with amyloid deposition would be associated with altered microstructure in brain regions associated with early AD.

Methods: Cognitively healthy participants (n=53, age=62.3 ± 6.2 years) underwent lumbar puncture and brain imaging. Cerebrospinal fluid was assayed for YKL-40 and MCP-1, markers of microglial activation. Amyloid burden was determined with PiB-PET using average DVRs from eight bilateral regions of interest (Figure 1), while Hybrid Diffusion Imaging modeled with Neurite Orientation Dispersion and Density Imaging was used to produce maps of neurite density (NDI), orientation dispersion (ODI), and volume fraction of isotropic diffusion (Viso). Linear regression was used to test for main effects of amyloid and inflammation, as well as the amyloid X inflammation interaction using voxel-wise analysis in SPM12. Significance was inferred at $p<0.001$ uncorrected with cluster extent > 25 voxels (controlling for age, sex, APOEε4 and parental history of AD).

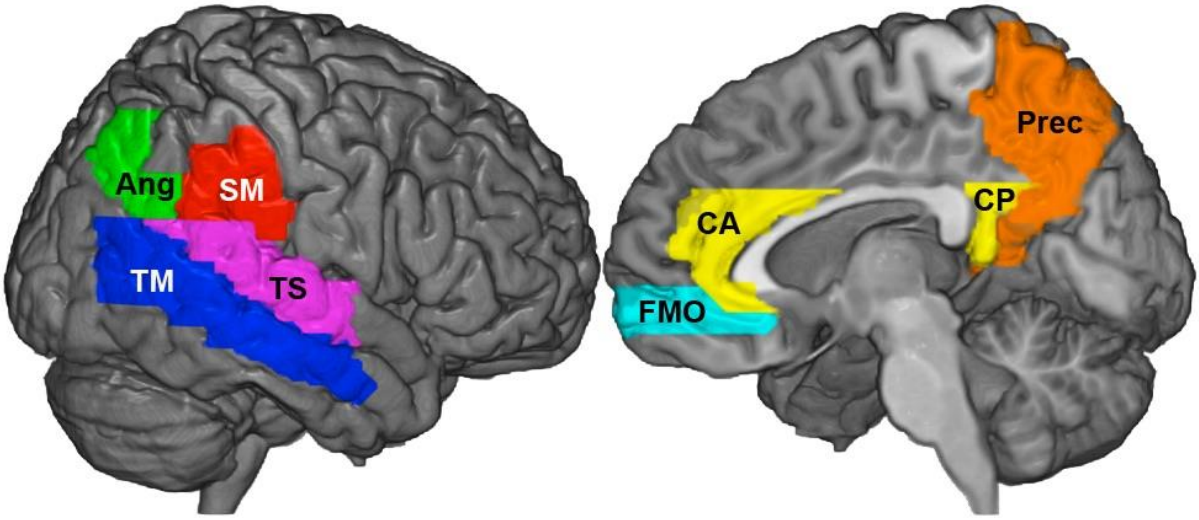

Results: Significant interactions were observed between neuroinflammation and amyloid. Elevated amyloid and higher YKL-40 were associated with lower NDI in left hippocampus (Figure 2, Panel A), precuneus, and insula; higher Viso in bilateral cingulate cortex (Figure 2, Panel B); and higher ODI in posterior bilateral white matter. Similarly, elevated amyloid and higher MCP-1 were associated with decreased NDI (Figure 3, Panel A), ODI (Figure 3, Panel B), and Viso in the left temporal pole.

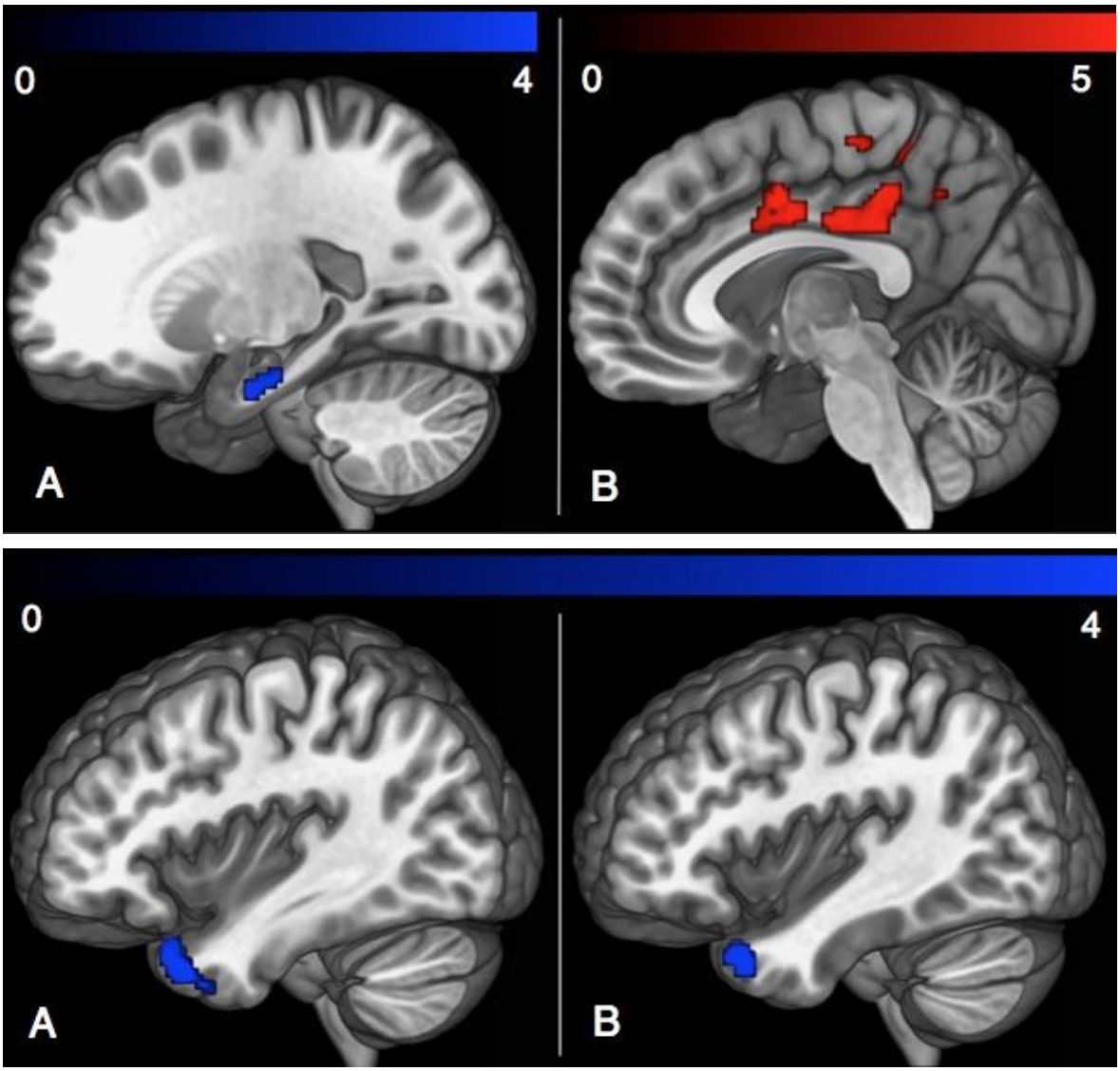

Conclusions: While amyloid or neuroinflammation alone were not predictive of neural damage, their interaction was associated with altered microstructure in AD-sensitive brain regions. These findings suggest that markers of microglial activation may show utility for identifying individuals at risk for neural injury due to preclinical AD, including amyloid deposition in the asymptomatic stage.

Subjective memory complaints are related to decreased hippocampal metabolism in clinically normal older adults with high amyloid burden

Patrizia Vannini[2, 3], Bernard Hanseeuw[1, 2], Catherine Munro[1], Rebecca Amariglio[3], Aaron Schultz[1, 2], Gad Marshall[1, 3], Dorene Rentz[1, 2, 3], Alvaro Pascual-Leone[5], Keith Johnson[1, 2, 3, 4], Reisa Sperling[1, 2, 3]

[1]Department of Neurology, Massachusetts General Hospital, Harvard Medical School, Boston, MA, United States
[2]2Athinoula A. Martinos Center for Biomedical Imaging and the Department of Psychiatry, Massachusetts General Hospital, Harvard Medical School, Charlestown, MA, United States
[3]Center for Alzheimer Research and Treatment, Department of Neurology, Brigham and Women's Hospital, Harvard Medical School, Boston, MA, United States
[4]Department of Radiology, Division of Molecular Imaging and Nuclear Medicine, Massachusetts General Hospital, Harvard Medical School, Charlestown, MA, United States
[5]Berenson-Allen Center for Noninvasive Brain Stimulation, Beth Israel Deaconess Medical Center, Harvard Medical School, Boston, MA, United States

Background: Subjective memory complaints (SMC) are common in the elderly and may represent preclinical signs of incipient Alzheimer's disease (AD). The concurrent relationship between SMCs and AD biomarkers is a research topic of major interest and a promising approach for very early identification of subjects with AD. Here, we used resting state FDG-PET to map the metabolic correlates of SMC in a group of cognitively normal elderly subjects with and without amyloid burden.

Methods: 251 older individuals (mean age 73.3 years; CDR=0) participated in the Harvard Aging Brain Study (Dagley et al. 2015). Subjective memory concerns were measured using the Memory Functioning Questionnaire (Gilewski et al., 1990), where a lower score reflects increased complaints. Whole-brain FDG-PET images were analyzed as standard uptake volume ratios, using cerebellum (gray matter only) as reference. Voxel-wise correlations between FDG-PET, SMC, and amyloid were conducted controlling for objective memory performance (Logical memory, Wechsler Memory scale (Wechsler, 1981)) and age. A statistical threshold of $p<0.005$ correcting for multiple comparisons using a cluster extent of $k\geq324$ voxels (FDR-correction) was applied. Subjects were classified into low and high amyloid burden groups using a Gaussian mixture model approach.

Results: Whole brain analysis revealed a significant interaction between SMC and amyloid burden only in bilateral medial temporal lobe (MTL), including hippocampus, enthorinal cortex and parahippocampus (Fig. 1A). In these regions, individuals with high amounts of amyloid and increased complaints demonstrated decreased FDG metabolism (Fig. 1B).

Conclusion: These results provide further evidence that increased memory concerns in older adults are related to FDG hypometabolism, specifically in the MTL, and biomarker evidence of Aβ accumulation. The findings may offer insight into the behavioral and pathological changes that occur in aging and early AD. SMC may be an early indicator of AD-related functional metabolic disruption that increases risk of progression to AD dementia.

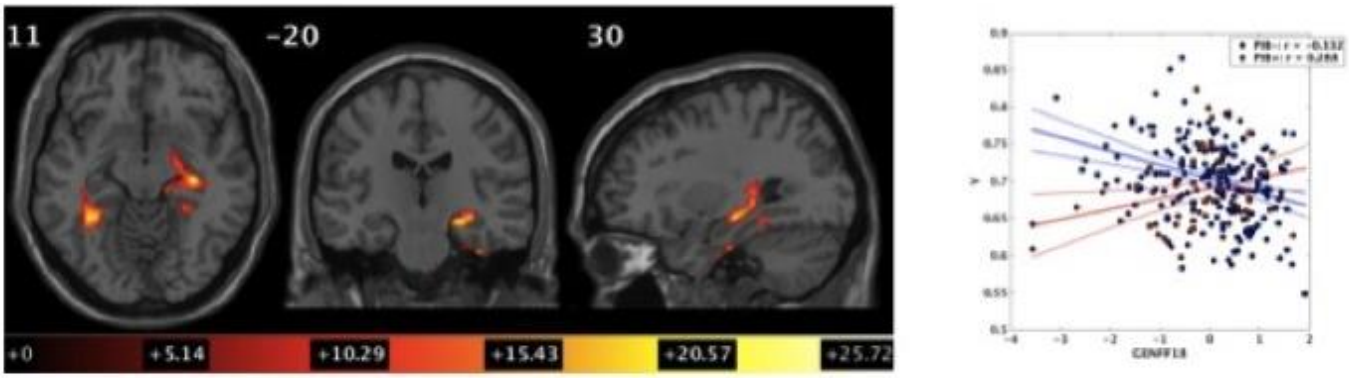

Fig 1. (A) Map demonstrating FDG-PET metabolism where an interaction between subjective memory complaints and amyloid is found. (B) FDG metabolism in an ROI in the right hippocampus plotted against subjective memory complaints scores in the low and high Aβ group. The relationship between FDG metabolism and subjective memory varies with Aβ burden, such that in the high Aβ group (red line), increased subjective memory complaints (lower subjective memory composite score) was related to decreased FDG metabolism.

Relationships between cognitive assessments and ^{18}F AV-1451 uptake patterns correlate with cognitive change over 9 months

Michael Devous, Sr, Abhinay Joshi, Ming Lu, Ian Kennedy, Michael Navitsky, Michael Pontecorvo, Mark Mintun

Avid Radiopharmaceuticals, Inc., Philadelphia, PA, United States

Background: Literature suggests the extent of neuropathologic tau correlates with cognitive impairment. We explored relationships between 18F-AV-1451 uptake and cognitive function, and whether baseline relationships predict cognitive change.

Methods: We analyzed ^{18}F-AV-1451 PET scans from 86 amyloid-positive healthy controls (n=5), MCI (n=47) or AD (n=34). Scans were acquired 80-100 min post-injection of 370 MBq ^{18}F-AV-1451. Voxel-wise SUVr was calculated relative to a cerebellar reference region. Cognitive assessments at baseline and ~9 months later included MMSE, ADAS-cog, Wechsler Logical Memory Immediate and Delayed Recall, Digit Span, Digit Symbol Substitution Test (DSST), Trails, Boston Naming, Clock Drawing, and Line Orientation. Pearson correlation analyses comparing voxel-wise SUVr values to cognitive scores produced voxel-wise correlation images. Clusters in correlation images were converted to VOIs by thresholding correlation images at r>0.4. We examined whether these VOIs predicted decline in the respective cognitive scores by 1) comparing 9 month cognitive change for subjects in the upper versus lower SUVR tertile and 2) by evaluating the correlation between baseline SUVR and change in cognition across all subjects.

Results: Correlation patterns differed across cognitive domains (Fig 1) and appeared to follow known spatial distributions of relevant functional neuroanatomy (e.g., impairment of working memory domains associated with increased left temporal lobe tau). Baseline SUVr in the test-specific VOIs predicted global cognitive decline as assessed by MMSE (Upper vs lower tertile p = 0.0016; across subjects r = -0.52) and ADAS (p = 0.07, r = 0.37) (Table 1). Some trends were also evident in domain specific tests such as the DSST (p = 0.06, r = -0.27).

Conclusions: Voxel-wise SUVr values correlated with cognitive scores; higher SUVR in this distribution was associated with greater cognitive decline over 9 months for some domains. PET imaging of neuropathologic tau may reflect underlying neurodegeneration in AD.

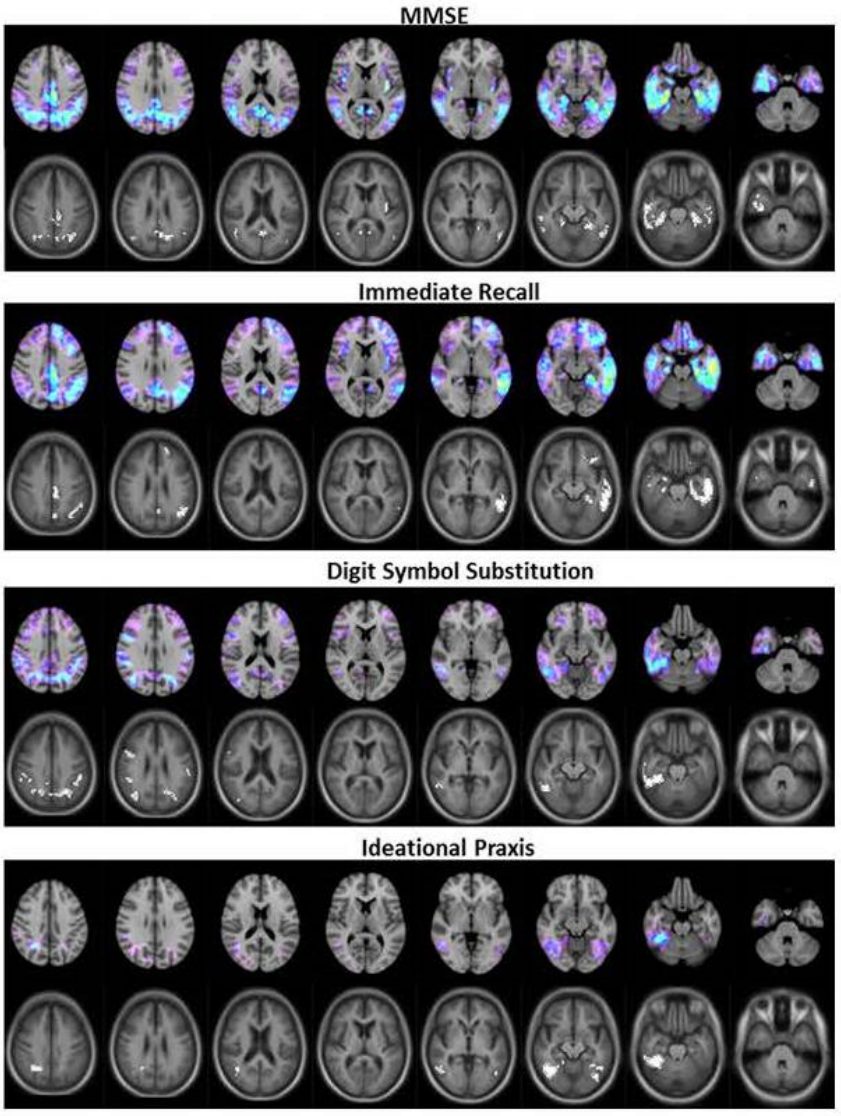

Figure 1. Representative correlation maps showing the relationship between baseline tau and baseline cognition as well as the associated VOI extracted by thresholding on R>0.4

Table 1

Groups split using upper 1/3 and lower 1/3 SUVr (Aβ+ Subjects Only)

	ADAS	Constructional Praxis	Ideational Praxis	Immediate Recall	MMSE	Word Recall
SUVr (max. lower 1/3, min. upper 1/3)	1.26, 1.75	1.18, 1.60	1.23, 1.73	1.28, 1.73	1.22, 1.79	1.24, 1.77
N (subjects) lower 1/3	23	23	23	23	21	23
N (subjects) upper 1/3	23	23	23	23	21	23
p : 9 month change in cognitive score	0.070	1.00	0.099	0.066	**0.0016**	0.45
R (across-all subject)	0.37	0.06	0.30	-0.10	**-0.52**	0.16

	Clock Draw	Delayed Recall	Digit Span	DSST	Orientation	Remembering Test Instructions	Word Recognition
SUVr (max. lower 1/3, min. upper 1/3)	1.29, 1.85	1.36, 1.63	1.30, 1.89	1.17, 1.58	1.21, 1.66	1.22, 1.39	1.33, 1.59
N (subjects) lower 1/3	23	23	23	23	23	23	23
N (subjects) upper 1/3	23	23	23	23	23	23	23
p : 9 month change in cognitive score	0.44	0.06	0.68	0.06	0.14	**0.04**	0.92
R (across-all subject)	-0.10	-0.18	-0.15	-0.27	0.30	0.35	-0.07

Diagnostic value of cerebrospinal fluid Aβ ratios in amyloid PET defined preclinical Alzheimer's disease

Katarzyna Adamczuk[1, 2], Jolien Schaeverbeke[1, 2], Hugo Vanderstichele[3], Johan Lilja[4], Natalie Nelissen[5], Koen Van Laere[6, 2], Patrick Dupont[1, 2], Kelly Hilven[7], Koen Poesen[8], Rik Vandenberghe[1, 2, 9]

[1]*Laboratory for Cognitive Neurology, KU Leuven, Belgium*
[2]*Alzheimer Research Centre KU Leuven, Leuven Institute of Neuroscience and Disease, Belgium*
[3]*ADx NeuroSciences, Ghent, Belgium*
[4]*GE Healthcare, Uppsala, Sweden*
[5]*Department of Psychiatry, Oxford University, United Kingdom*
[6]*Nuclear Medicine and Molecular Imaging Department, KU Leuven and University Hospitals Leuven, Belgium*
[7]*Laboratory for Neuroimmunology, KU Leuven, Belgium*
[8]*Laboratory Medicine, University Hospitals Leuven, Belgium*
[9]*Neurology Department, University Hospitals Leuven, Belgium*

Introduction: In this study of preclinical Alzheimer's disease (AD) we assessed the added diagnostic value of using cerebrospinal fluid (CSF) Aβ ratios rather than Aβ42 in isolation for detecting individuals who are positive on amyloid positron emission tomography (PET).

Methods: Thirty-eight community-recruited cognitively intact older adults (mean age 73, range 65-80 years) underwent ^{18}F-flutemetamol PET and CSF measurement of Aβ1-42, Aβ1-40, Aβ1-38, and total tau (ttau). ^{18}F-flutemetamol retention was quantified using standardized uptake value ratios in a composite cortical region ($SUVR_{comp}$) with reference to cerebellar grey matter. Based on a prior autopsy validation study, the $SUVR_{comp}$ cut-off was 1.57. Sensitivities, specificities and cut-offs were defined based on receiver operating characteristic analysis with CSF analytes as variables of interest and ^{18}F-flutemetamol positivity as the classifier. We also determined sensitivities and CSF cut-off values at fixed specificities of 90% and 95%.

Results: Seven out of 38 subjects (18%) were positive on amyloid PET. Aβ42/ttau, Aβ42/Aβ40, Aβ42/Aβ38, and Aβ42 had the highest accuracy to identify amyloid-positive subjects (area under the curve (AUC) $\geq$ 0.908). Aβ40 and Aβ38 had significantly lower discriminative power (AUC = 0.571). When specificity was fixed at 90% and 95%, Aβ42/ttau had the highest sensitivity among the different CSF markers (85.71% and 71.43%, respectively). Sensitivity of Aβ42 alone was significantly lower under these conditions (57.14% and 42.86%, respectively). Four CSF analytes, Aβ42/ttau, Aβ42/Aβ40, Aβ42/Aβ38, and Aβ42, showed a significant exponential or hyperbolic correlation with the ^{18}F-flutemetamol $SUVR_{comp}$ values ($r^2 \geq 0.41$, $P > 10\text{-}4$).

Conclusion: For the CSF-based definition of preclinical AD, if a high specificity is required, our data support the use of Aβ42/ttau rather than using Aβ42 in isolation.

Tau distribution in probable CAA

Hee Jin Kim[1, 2], Hanna Cho[3], Young Kyoung Jang[1, 2], Yeo Jin Kim[1, 2], Juyoun Lee[1, 2], Jin San Lee[1, 2], Duk L. Na[1, 2], Chul Hyoung Lyoo[3], Sang Won Seo[1, 2]

[1]Departments of Neurology, Samsung Medical Center, Sungkyunkwan University School of Medicine, Seoul, South Korea
[2]Neuroscience Center, Samsung Medical Center, Seoul, South Korea
[3]Department of Neurology, Gangnam Severance Hospital, Yonsei University College of Medicine, Seoul, South Korea

Background: Cerebrovascular deposition of beta-amyloid (cerebral amyloid angiopathy, CAA) is associated with cerebral hemorrhages such as lobar hemorrhage, cerebral microbleeds, and cortical superficial siderosis. CAA is known to have close relationship with Alzheimer's disease, which have parenchymal amyloid and hyperphosphorylated tau as the disease hallmark. Along with rapid development in molecular imaging, [18F] T807, one of the tau tracers, provided valuable information on distribution of tau in Alzheimer's disease patients. In this study, we investigated the distribution of tau in clinically probable CAA patients.

Methods: Three patients who were clinically diagnosed as probable CAA underwent [18F] T807-PET to measure paired helical filament tau burden and two of the three patients underwent [11C] Pittsburgh Compound B (PiB)-PET to measure amyloid burden.

Results: Our cases had asymmetrical distribution of cerebral microbleeds or cortical superficial siderosis: the first case had left hemisphere dominant distribution of cerebral microbleeds and the second and third cases had posterior dominant distribution of cerebral microbleeds. The region that had cerebral microbleeds or cortical superficial siderosis largely overlapped with regions that showed increased [18F] T807 retention as well as increased [11C] PiB retention. In particular, there was asymmetric high [18F] T807 uptake in the posterior region, to the side where vascular amyloid burden was high.

Conclusions: Our finding provides us preliminary in vivo evidence that vascular amyloid is associated with local production of abnormal hyperphosphorylated tau.

Evaluating partial volume effect correction methods in amyloid PET images. A tool based on realistic Monte Carlo simulations

Gemma Salvadó[1, 2], Berta Marti-Fuster[2, 3], Aida Niñerola-Baizán[1, 2], Carles Falcon[1, 4], Francisco Lomeña[5, 6], José Luis Molinuevo[4, 7], Domènec Ros[1, 2], Javier Pavía[1, 5], Juan Domingo Gispert[1, 4]

[1]*Centro de Investigación Biomédica en Red de Bioingeniería, Biomateriales y Nanomedicina, Barcelona, Spain*
[2]*Unitat de Biofísica i Bioenginyeria, Departament de Ciències Fisiològiques I, Facultat de Medicina, Universitat de Barcelona, Barcelona, Spain*
[3]*Athinoula A. Martinos Center for Biomedical Imaging, Department of Radiology, Massachusetts General Hospital, Charlestown, MA, United States*
[4]*Barcelonaβeta Brain Research Center, Pasqual Maragall Foundation, Barcelona, Spain*
[5]*Servei de Medicina Nuclear, Hospital Clínic, Barcelona, Spain*
[6]*Centro de Investigación Biomédica en Red de Salud Mental (CIBERSAM), Barcelona, Spain*
[7]*Alzheimer's Disease and Other Cognitive Disorders Unit, Hospital Clínic, Institut d'Investigacions Biomèdiques August Pi i Sunyer (IDIBAPS), Barcelona, Spain*

Background: Quantification of amyloid PET images allows us to study pathological alterations in Alzheimer's disease. However, the accuracy of amyloid load measurements is affected by the degrading partial volume effect (PVE). Several methods for PVE correction (PVC) have been proposed in the literature but their performance evaluation is usually hampered by the lack of gold standard reference values.

Objective: To develop a tool for assessing the reliability of PVC methods for amyloid PET studies.

Methods: The tool is based on SimSET, a Monte Carlo (MC) code that allows the simulation of PET studies in a framework where the ground truth is known. In order to simulate realistic amyloid PET studies, activity maps (AMs) were created using a previously validated iterative simulation/reconstruction process which compares simulated images with a real study. Normal and pathological Florbetaben scans were used to create AMs with different uptake ratios with the aid of the WFU PickAtlas. PET images were corrected with the Müller-Gärtner (PVC-MG) method and SUVr was employed to quantify uptake of the corrected and uncorrected images. Uptake was measured in the whole, frontal, parietal and temporal grey matter (GM) ROIs and the whole cerebellum was used as reference region. Then, the recovery coefficient (RC) between calculated and reference SUVr was obtained.

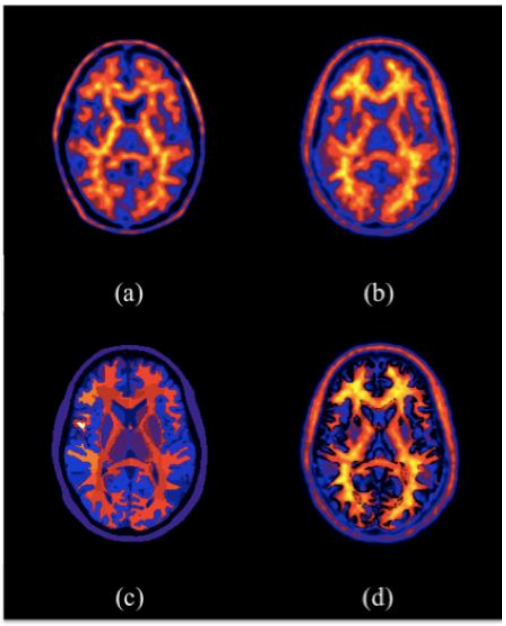

Figure 1: Axial Slice of amyloid real PET (a), simulated PET (b), simulation activity map (c) and PVC-MG corrected PET (d)

Results: Figure 1 shows all images used/obtained in the simulation and correction processes. Figure 2 shows the RC values obtained. Corrected images present RC values closer to one (the optimal value) than the uncorrected images.

Conclusions: A tool for the evaluation of PVC methods in a realistic framework was developed. Our findings show a good performance of the PVC-MG correction method despite the fact that its performance is degraded as the difference in intensity between GM and white matter is reduced.

Figure 2: RC values for uncorrected and PVC-MG corrected images in the four ROIs (whole, frontal, parietal and temporal GM) selected and for the four subjects (one control and three pathologicals).

	Whole GM		Frontal GM		Parietal GM		Temporal GM	
	Uncorrected PET	PVC-MG corrected PET	Uncorrected PET	PVC-MG corrected PET	Uncorrected PET	PVC-MG corrected PET	Uncorrected PET	PVC-MG corrected PET
Control	2,11	0,99	2,37	0,91	2,17	0,86	2,40	1,11
Pathological 1	1,68	0,88	1,71	0,76	1,75	0,75	1,67	0,97
Pathological 2	1,45	0,82	1,42	0,71	1,46	0,71	1,42	0,91
Pathological 3	1,31	0,79	1,25	0,68	1,30	0,68	1,28	0,87

Head-to-head comparison of SUVR methods in amyloid cross-sectional and longitudinal studies

Gregory Klein[1], Mehul Sampat[1], Davis Staewen[1], Caroline Lemon[1], Joyce Suhy[1], Eric Reiman[2], Kewei Chen[2]

[1]*BioClinica, Inc., Newark, CA, United States*
[2]*Banner Alzheimer's Institute, Banner Health, Phoenix, AZ, United States*

Objectives: Recently, standard uptake value ratio (SUVR) analyses using cerebral white matter reference regions have shown improved power to track florbetapir PET measured longitudinal amyloid-β (Aβ) change [Chen2015, Landau2015]. We present a head-to-head comparison between SPM and Freesurfer based [KC1] methods using white matter and other reference regions, and the Alzheimers Disease Neuroimaging Initiative (ADNI) florbetapir dataset.

Methods: Baseline and 24-m followup data from 399 ADNI subjects (157 Normal, 204 MCI, 32 AD) who also had corresponding MRI scans were included. Apolipoprotein E (APOE) ε4 homozygotes (HM), heterozygotes (HT) and non-carrier status was used to stratify the analysis. Mean-cortical SUVRs were computed using SPM and Freesurfer methods described previously [Chen2015, Landau2015]. The SPM method used a corpus callosum (CC) and centrum semiovale (CS) white matter reference region; the Freesurfer method used reference regions including eroded subcortical white matter, CC, whole cerebellum or [KC2] cerebellar cortex. Longitudinal Cohen's d effect sizes were computed for AD, MCI and Normal groups, as well as for "likely decliners" defined as baseline Aβ+ Normals, APOEHT+HM Normals, Aβ+ MCIs, APOEHT+HM MCIs. Cross-sectional effect size was also compared.

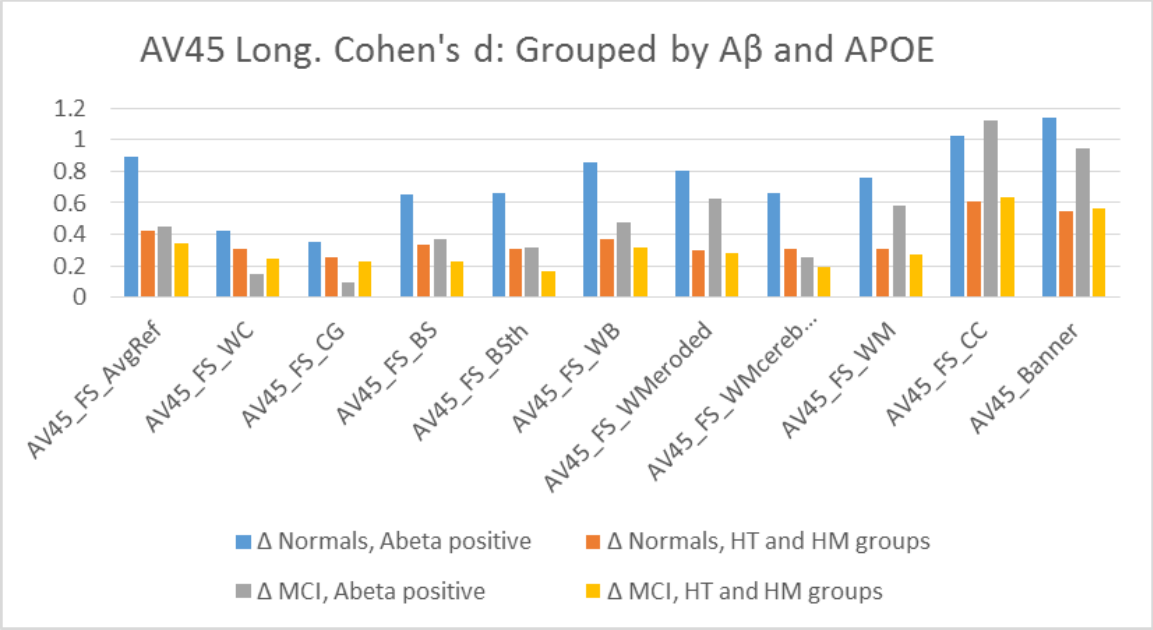

Figure 1. Comparison of longitudinal effect size for the Freesurfer (AV45_FS_*) method using various potential reference regions and the SPM technique (AV45_Banner). Overall, the Freesurfer method using the corpus callosum and the SPM method showed the highest longitudinal effect size

Results: Longitudinal effect size was largest across most comparison groups using the SPM (CC and CS reference) and Freesurfer (CC reference) methods. Effect sizes of the SPM and Freesurfer methods were comparable, but only when using the Freesurfer CC reference region. Longitudinal effect sizes of the Freesurfer method for all other reference regions were considerably lower. Freesurfer showed a slightly higher cross-sectional effect size for most reference regions compared to the SPM method, but overall the cross-sectional effect size was very high for all techniques.

Conclusions: SPM and Freesurfer SUVR methodologies can produce similar longitudinal effect size, but only when the Freesurfer method includes a corpus callosum reference region.

[Chen2015] J Nucl Med 2015; 56:560–566.

[Landau2015] J Nucl Med 2015; 56:567–574

A hybrid amyloid read paradigm for reducing discordance between qualitative and visual reading results

Gregory Klein[1], James Goodman[4], Laigao Chen[4], Claire Leurent[4], Derk Purcell[1, 2, 3], jerome Barakos[1, 2], Joyce Suhy[1]

[1]*BioClinica, Newark, CA, United States*
[2]*California Pacific Medical Center, San Francisco, CA, United States*
[3]*University of California San Francisco, CA, United States*
[4]*Pfizer Inc, Cambridge, MA, United States*

Objectives: PET amyloid assessments can be assessed visually or quantitatively, each having their own challenges. Qualitative reads by experienced readers can be performed via tracer vendor qualitative reading guidelines. However, features such as high non-specific binding, image noise and extensive cortical thinning could result in readings inconsistent with quantitative results, especially near quantitative cutpoint values. We present results of a hybrid visual/quantitative reading method designed to increase concordance of visual and quantitative methods. consensus read using the SUVR.

Methods: Two experienced amyloid readers trained via the Lilly Amyvid reading criteria assessed Amyvid PET data from 139 elderly subjects. A composite standard uptake value ratio (SUVR) score was also obtained for each subject using a whole cerebellar reference region and the Freesurfer method described previously [Landau2014]. Final amyloid status for each subject was determined via a hybrid visual/quantitative SUVR decision tree. Briefly, for each subject, reader #1 obtained a visual read without SUVR information. If the SUVR was within 0.1 SUVR units of a 1.1 cutpoint, or if the SUVR was in disagreement with the visual read, then a second reader was used to obtain a final consensus read using the SUVR.

Results: In the hybrid visual/SUVR decision tree, 39% of all cases went to consensus read. Discordance between SUVR and the first visual read was 8.6%. After SUVR-assisted consensus, discordance between quantitative and visual assessment was 4.3%.

Conclusion: Though a gold standard of amyloid burden was not available, results indicate that a hybrid qualitative visual / quantitative method can be used to obtain greater concordance between quantitative and visual results. However, clinical studies using only visual or only SUVR information for eligibility decisions must understand the implications of potential differences between the visual and quantitative methodologies. [Landau2015] J Nucl Med 2015; 56:567–574.

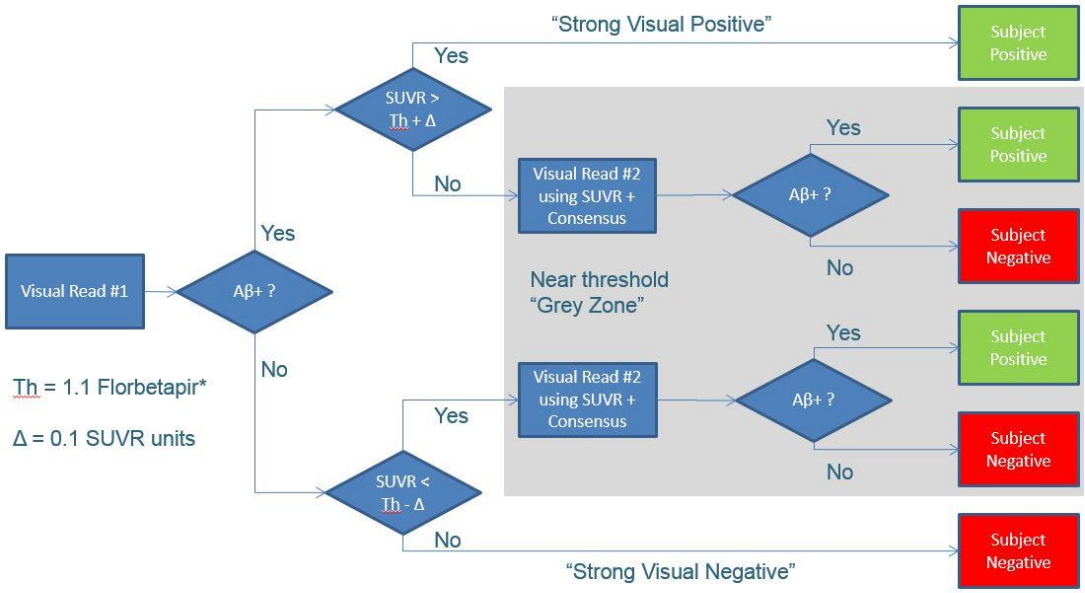

*Determined via Freesurfer analysis. Landau. Eur J Nucl Med Mol Imaging, 2014 Jul;41(7):1398-407

Figure 1. Hybrid Visual/SUVR Amyloid PET Decision Tree. A second reader is brought in for a consensus read if either the SUVR is close to the SUVR cutpoint, or if there is a disgreement etween visual and SUVR assessment.

Functional impact of cerebral iron and Amyloid-β plaque burden in cognitively normal Super-agers, as estimated by simultaneous quantitative susceptibility mapping-MRI and 18F-Flutametamol-PET

Jiri Van Bergen[1], Xu Li[2], Frances Quevenco[1], Sandra Leh[1], Rafael Meyer[1], Anton Gietl[1], Valerie Treyer[1], Alfred Buck[1], Roger Nitsch[1], Peter Van Zijl[2], Christoph Hock[1], Paul Unschuld[1]

[1]*University of Zurich, Switzerland*
[2]*Kennedy Krieger Institute and Johns Hopkins School of Medicine, MD, United States*

Background: The aging brain is characterized by distinct pathological alterations that include extracellular accumulation of Amyloid-β (Aβ), increased iron load and altered functional properties. This study aimed to investigate cerebral Aβ and iron, as well as associated functional brain network activity in a context of cognitively normal aging.

Methods: 25 cognitively normal elderly participants ("super-agers", mean age= 87.6 (SD 2.97) years), were administered 18F-Flutemetamol-PET for estimating Aß-plaque burden, Quantitative-Susceptibility-Mapping (QSM) MRI for cerebral iron load, and functional-MRI (fMRI) at rest for assessing functional connectivity with the posterior cingulate cortex, using a 3T SIGNA General Electrics Healthcare combined PET-MR instrument. Standardized uptake value ratios (SUVR) for 18F-Flutametamol (85-105 minutes post injection) were calculated by time-of-flight reconstruction (voxel size=1.2x1.2x2.78mm3) and used for splitting the study sample in two groups: "Aβ-positive" (n=6) and "Aβ-negative" (n=19). QSM images were reconstructed from a 3D multi-echo GRE sequence (TR/TE/ΔTE=40/3/4ms, voxel size=1x1x1mm3, flip angle=15°) using the echoes with echo time between 15 and 27ms. fMRI resting-state scans were performed using a gradient-echo EPI sequence (TR: 2.55s).

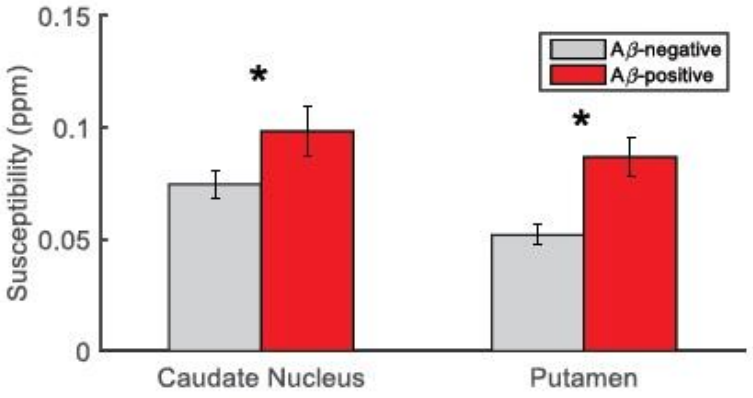

Figure 1: Differences in mean susceptibility as a measure of regional iron (average of left and right) for Aβ-positive and Aβ-negative groups. * indicates significant difference with p-FDR-corrected < 0.05.

Results: Local iron load as judged from differences in QSM significantly differed between groups (p-FDR-corrected < 0.05, **Figure 1**) for the caudate nucleus and putamen (both sides).

By applying the CONN-toolbox, connectivity patterns associated with high cortical Aβ (10361 voxels) and high cortical iron (20112 voxels) could be identified (extent threshold FDR-corrected for p<0.05, **Figure 2**), which showed a high degree of spatial overlap (7568 voxels) and also temporal synchronicity (adjusted-R2=0.59).

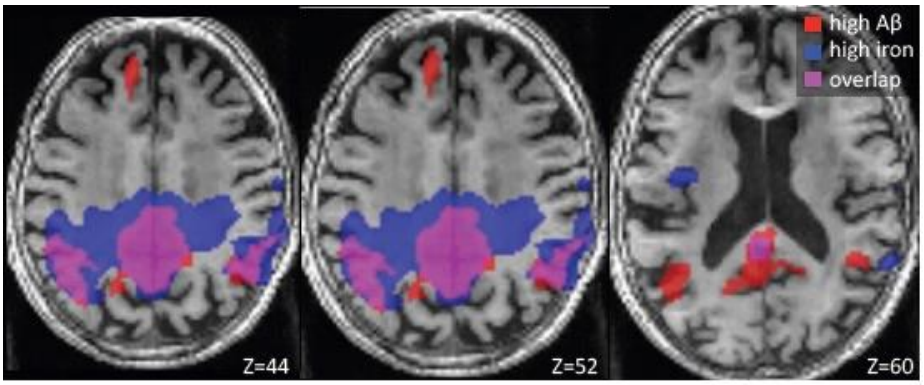

Figure 2: Functional connectivity patterns associated with high cortical Aß (as inferred from 18F Flutemetamol PET), high cortical iron (blue, as inferred from QSM-MRI) and voxels included in both (purple, overlap).

Discussion: The co-occurence of cortical Aβ-plaque load with iron accumulation in basal ganglia gray-matter nuclei indicates the presence of common age-related brain change in cognitively normal super-agers. Additional research is needed to characterize potential compensatory mechanisms that allow for normal cognitive performance, including a potential role of functional network connectivity for conveying resilience against pathologies accumulating in the aging brain.

Progress in the development of a PET tracer for aggregated alpha-synuclein

Dale Mitchell[1], Kevin Nash[1], David Hardick[1], Paul Kotzbauer[2], Zhude Tu[2], Jinbin Xu[2], Robert Mach[3], Jamie Eberling[4], Edilio Borroni[5], Luca Gobbi[5], Michael Honer[5], Joël Mercier[6], N. Scott Mason[7], William Klunk[7], Chester Mathis[7]

[1]*BioFocus, Canterbury, United Kingdom*
[2]*Washington University, MO, United States*
[3]*University of Pennsylvania, PA, United States*
[4]*Michael J. Fox Foundation, NY, United States*
[5]*Hoffman-La Roche Ltd., Basel, Switzerland*
[6]*UCB, Braine-L'alleud, Belgium*
[7]*University of Pittsburgh, PA, United States*

The Michael J Fox Foundation (MJFF) is supporting a consortium to develop novel positron emission tomography (PET) radiotracers for imaging alpha-synuclein in the brain. These agents could be useful biomarkers for the presence and distribution of alpha-synuclein in synucleinopathies, including Parkinson's Disease and dementia with Lewy bodies. Such agents will be critical for the development of therapeutics aimed at lower alpha-synuclein levels in the brain.

Following a high throughput screen to identify novel compounds that bind alpha-synuclein fibrils, several series of hit compounds were subjected to hit confirmation and assessed for binding affinity and selectivity for alpha-synuclein over amyloid-beta and tau using brain tissue homogenates and autoradiography. Compounds were prioritized based on selectivity and calculated properties for good CNS penetration.

Several of the hit compounds have binding affinities of less than 10nM and show some selectivity over amyloid-beta and tau. Currently, medicinal chemistry programs are underway to optimize the lead compounds. One of the lead compounds, BF814174, has relatively high affinity for a-syn in PD brain (Kd in the range of 2-8 nM and Bmax in the range of 60-200 nM) and relatively low affinity for Abeta and tau in AD brain (Kd about 70 nM and Bmax about 3000 nM). BF814174 is moderately lipophilic with a measured logD of 3.4. [C-11]BF814174 demonstrated good brain uptake at early times (SUV = 2.1 at 2 min) post iv injection in wild-type mice and good brain clearance in these mice over 60 min post injection (SUV = 0.21 at 60 min). MicroPET studies of [C-11]BF814174 in nonhuman primates demonstrated brain penetration and good initial brain uptake. Analogues of BF814174 are being prepared to improve both properties and affinity and are being evaluated in a radioligand binding assay in PD tissue using tritiated BF814174.We hope to deliver a selective alpha-synuclein PET tracer for use by the research and drug development communities.

Fluid and crystallized discrepancy in healthy adults: The relationship with beta-amyloid and cortical thickness

Ian McDonough[1, 3], Gérard Bischof [2, 3], Kristen Kennedy[3], Karen Rodrigue[3], Michelle Farrell[3], Denise Park[3]

[1]*The University of Alabama, AL, United States*
[2]*University Hospital Cologne/Institute of Neuroscience & Medicine Research Centre, Germany*
[3]*Center for Vital Longevity, TX, United States*

Measures of basic cognitive processes (fluid abilities) are highly correlated with measures of knowledge (crystallized abilities) in healthy adults. Fluid abilities, however, decline more rapidly than crystallized abilities in early stages of Alzheimer's disease (AD). We hypothesized that cognitively-normal older adults who evidenced lower fluid ability compared to crystallized ability (a discrepancy) would show evidence of early AD neuropathology indexed via in vivo measures of cortical thickness and beta-amyloid (Aβ) deposition in regions vulnerable to AD. A sample of older adults (n = 112) aged 65 to 89 underwent a cognitive battery, structural MRI, and a subset (n = 75) also underwent PET imaging. Of this sample, 60 older adults evidenced an ability discrepancy where fluid ability was lower than crystallized ability. As predicted, the magnitude of the ability discrepancy was independently associated with thinner cortex, a higher burden of Aβ, and greater chronological age. Thus, a substantial ability discrepancy in old age appears to be a behavioral marker of neuropathology consistent with biomarkers that are suggestive of preclinical dementia.

Optimization of standard uptake value ratio quantification through investigation of different brain target and reference regions for the detection of change in amyloid beta PET in the ongoing Phase 1b PRIME study of aducanumab

Ping Chiao[1], Jeff Sevigny[1], John O'Gorman[1], Tianle Chen[1], Marilyn Grand'Maison[2], Alex P. Zijdenbos[2], Barry J. Bedell[2, 3]

[1]*Biogen, Cambridge, MA, United States*
[2]*Biospective Inc., Montréal, QC, Canada*
[3]*Research Institute of the McGill University Health Centre, Montréal, QC, Canada*

Background: Standardized uptake volume ratio ($SUVR = SUV_{target}/SUV_{reference}$) is commonly used to quantify tracer uptake in amyloid beta positron emission tomography (Aβ-PET). Selection of target and reference regions of interest (ROI) influences signal strength and noise, directly impacting the sensitivity of SUVR quantification of change in Aβ.[1-3]

Objective: To illustrate how the components of effect size (based on SUVR mean change from baseline and variability) are dependent on target and reference ROI selection using data from the ongoing Phase Ib PRIME study (NCT01677572) of aducanumab (BIIB037) in patients with prodromal/mild Alzheimer's disease.

Methodology: Florbetapir PET data were processed using a fully automated pipeline that included inter-frame motion correction, co-registration to 3D T1-weighted MRI, non-linear transformation to stereotaxic space and atlas-based labeling of target and reference ROI. SUVR was calculated at baseline (screening) and Weeks 26 and 54 for patients randomized to placebo and each of four aducanumab doses (1, 3, 6 and 10 mg/kg) using various reference ROIs. In addition to a composite cerebral cortical ROI[4], individual cortices were assessed as target ROI.

Results: Reference ROI selection affected the effect size of the active treatment arms of PRIME (Week 54 data in Figure 1). Of the reference ROIs used, pons generated largest effect sizes. Use of anterior cingulate cortex or striatum as target ROI resulted in greater effect sizes than composite cortex.

Figure 1. Effect size of Aβ-PET composite score at Week 54 by reference region

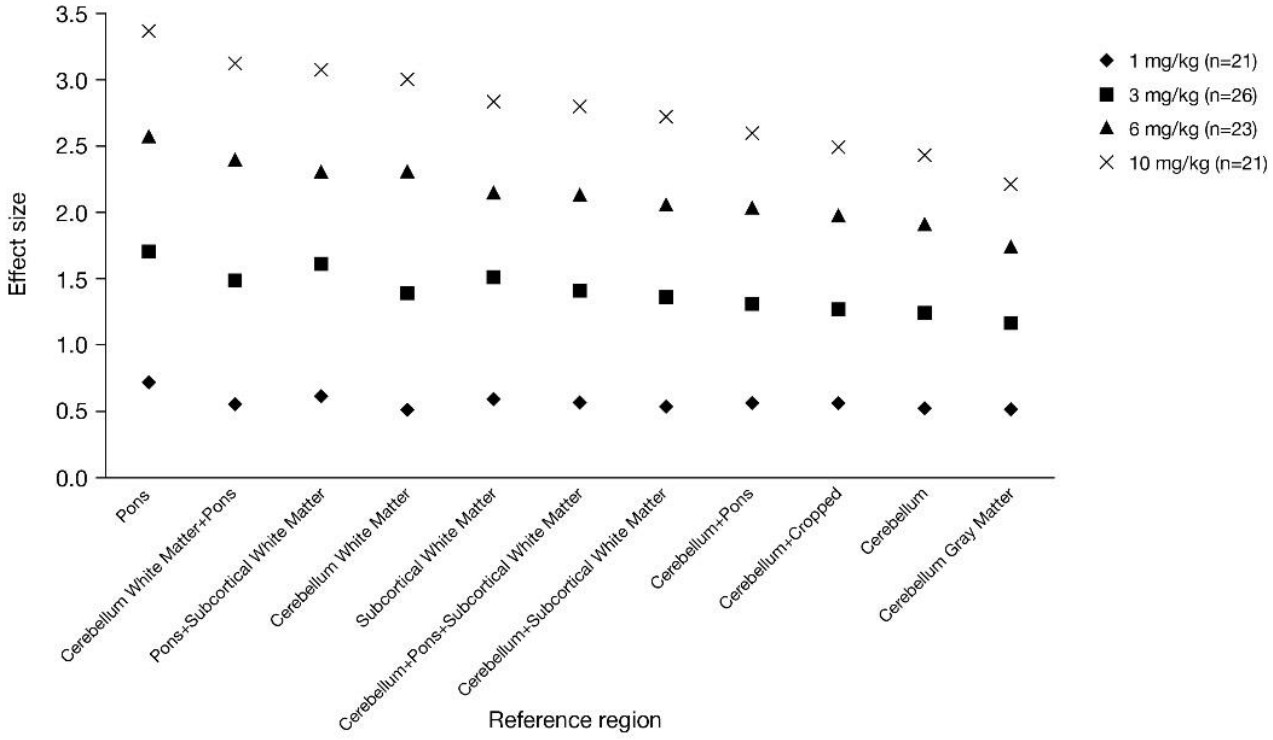

Effect sizes were calculated using the adjusted mean change and standard deviation calculated from an ANCOVA model for change from baseline, with factors of treatment, laboratory apolipoproteinE ε4 status and baseline SUVR.

Conclusions: Dose-dependent reductions in SUVR were consistently observed with aducanumab treatment regardless of reference/target ROIs used. Selection of these ROIs can be optimized to improve the sensitivity of SUVR quantification. This observation warrants further investigation in other data sets.

References

1. Chen et al. J Nucl Med 2015;560-566.
2. Fleisher et al. AIC 2015;IC-P-030.
3. Klunk et al. Alzheimers Dement 2015;11:1-15.
4. Ostrowitzki et al. Arch Neurol 2012;69:198-207.

Significant two-year increases of fibrillary and oligomeric amyloid beta loads in human brain only in mild cognitive impairment rather in healthy aging and Alzheimer's disease

Albert Gjedde[1, 2], Tharick Pascoal[2, 3], Sulantha Mathotaarachchi[2, 3], Sara Mohades[2, 3], Andrea Benedet[2, 3], Monica Shin[2, 3], Min Su Kang[2, 3], Serge Gauthier[2, 3], Pedro Rosa-Neto[2, 3]

[1]*Department of Neuroscience and Pharmacology, Panum Institute, University of Copenhagen, Denmark*
[2]*Department of Neurology and Neurosurgery, McGill University, QC, Canada*
[3]*Translational Neuroimaging Laboratory, Douglas Mental Health University Institute, Montreal, QC, Canada*

Fibrillary amyloid-beta (fAb) may arise from monomeric Ab (mAb) via oligomeric Ab (oAb). We claimed that fAb competes with mAb for access to mAb and oAb. Individuals with healthy aging (HA, n=162), mild cognitive impairment (MCI, n=349), or Alzheimer's disease (AD, n=58) had PET of [^{18}F]florbetapir in brain, and mAb in CSF, at baseline and two years. We fitted Standardized Uptake Value ratios (SUVR) from PET and mAb from CSF by relation between binding potential and capacity,

$$SUVR\text{-}1=(Bmax/Vd)/[\ (Cn + C1)[1+(Kn/Cn)]\ ] \quad (1)$$

where Bmax is maximum binding of fAb, Vd is distribution volume of unbound ligand(s), Cn is concentration of oAb, C1 is concentration of mAb, and Kn is affinity of oAb incorporation into fAb, using the relationships,

$$Cn+C1=\beta+\alpha\ C1 \quad \text{and} \quad Kn=R\ (1-\alpha)-\beta \quad (2)$$

where R optimized the fit at 2600 pg/ml. Calculations of mAb in CSF and oAb and fAb used parameters inserted into (2). Regression of (1) to SUVR-1 and C1 yielded estimates of α at 0.66±0.10 (SE), β at 100±27 pg/ml, and Bmax/Vd at 930±119 pg/ml.

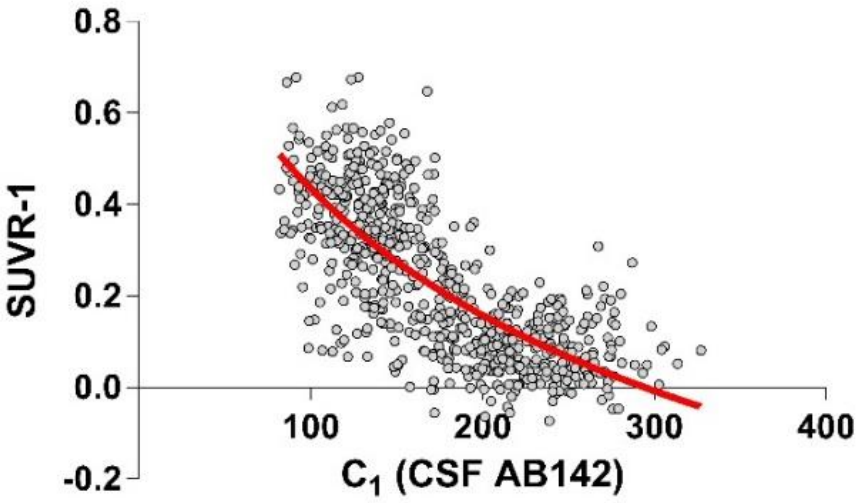

Best-fit values	
A	0.6598
B	100.3
Bmax	930.2
Std. Error	
A	0.09834
B	26.5
Bmax	118.6

Inserted into (2), parameters yielded oAb in HA at 40.5±1.7 pg/ml (SEM), MCI at 47.2±1.1 pg/ml, and AD at 61.6+2.3 pg/ml. In two years, the concentration of oAb increased significantly only in MCI (n=117), from 47±2 to 50±2 pg/ml at P<0.0005 in two-tailed paired t-testing. In two years, fAb increased significantly only in MCI (n=108), from 46±3 to 49±3 pg/ml at P<0.001.

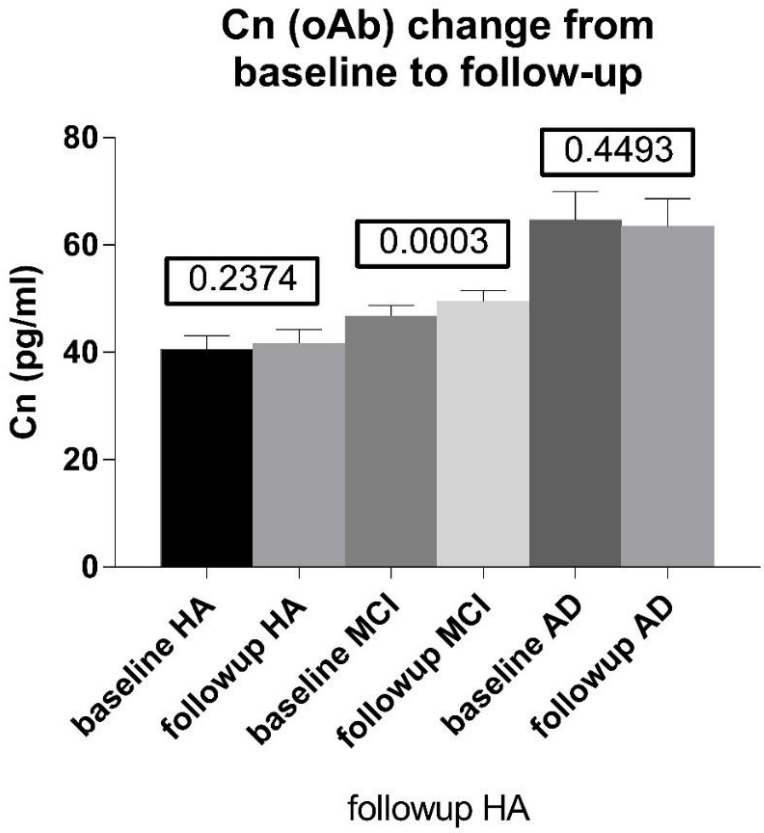

Of 108 subjects with MCI at complete follow-up, 13 converted to AD, with numerical decline of mAb, and increases of SUVR, oAb and fAb, but only change of SUVR was significant at P<0.05.

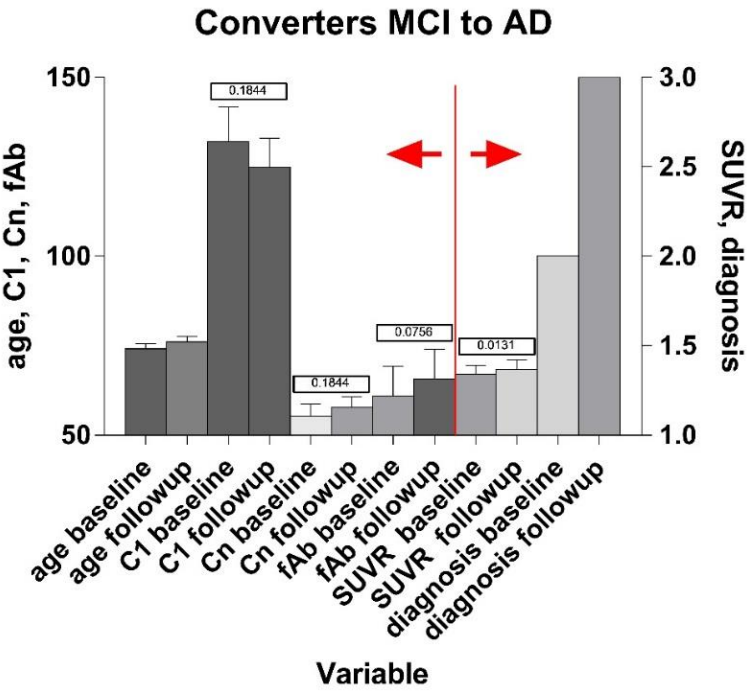

Significant change of oAb occurred only in MCI, consistent with oAb as requirement for formation of fAb, at expense of mAb formation and release to CSF.

Imaging protein aggregations and brain inflammation in subjects with mild cognitive impairment, using ^{11}C-PK11195, ^{11}C-PiB and ^{18}F-AV1451 PET

Peter Parbo[1, 2], Frederik Husum[1], Rainer Hinz[3], Hans Brændgaard[4], Hanne Gottrup[4], Joel Aanerud[2], David Brooks[1, 2]

[1]*Department. of Clinical Medicine, Aarhus University, Aarhus, Denmark*
[2]*Department of Nuclear Medicine and PET Centre, Aarhus University Hospital, Aarhus, Denmark*
[3]*Wolfson Molecular Imaging Centre, University of Manchester, United Kingdom*
[4]*Department of Neurology, Aarhus University Hospital, Aarhus, Denmark*

Introduction: To gain knowledge on the role of brain inflammation in the neurodegeneration of Alzheimer's disease, we investigated the relationship between microglial activation, and beta-amyloid (Aβ) and tau aggregations in a group of MCI subjects.

Methods: Six MCI subjects (aged 65-76) were imaged with ^{11}C-PiB, ^{18}F-AV1451 and ^{11}C-PK11195 PET. Another 24 MCI subjects just had PiB and PK11195 PET. The PiB and AV1451 images were quantitated as SUVR with cerebellum cortex as reference. PK11195 was quantitated using supervised cluster analysis and simplified reference tissue model. All subjects also had T1 weighted MRI and standard neuropsychological testing. Patients were compared with age matched healthy control data.

Results: As has been reported, we found cortical tau in only those MCI subjects who also had amyloid deposition. We saw discordance between levels of inflammation and protein aggregation: Two cases without amyloid or tau, showed raised levels of cortical inflammation. Conversely 1 subject with amyloid and tau aggregation was inflammation negative. In our 19 Aβ positive subjects there was no correlation between cortical amyloid and inflammation loads. The global cognitive scores of MMSE show negative correlations with both PiB and AV1451 ratio levels.

Conclusion: Patterns of Aβ deposition and tau aggregation appear to follow Braak staging. We did not find consistent correlations between the presence of inflammation and protein aggregation. This group of MCI subjects is being followed with repeat PET scans to further investigate the relationship between brain inflammation and protein aggregation.

Comparison of three FDG PET analysis techniques in the tracking of Alzheimer's disease and evaluation of disease-modifying treatments

Kewei Chen, Xiaoying Kuang, Ji Luo, Auttawut Roontiva, Wendy Lee, Pradeep Thiyyagura, Robert Bauer III, Vivek Devadas, Eric Reiman

Banner Alzheimer's Institute, Phoenix, AZ, United States

Background: We sought to compare the ability of three different FDG PET image-analysis techniques to track Alzheimer's disease (AD) and evaluate disease-modifying treatments, including: 1) our statistical region of interest (sROI) method, which tracks cerebral glucose metabolism changes in an empirically pre-specified ROI that was found to be preferentially affected by AD, 2) our cross-sectional HCI (C-HCI), which characterizes the extent to which the magnitude and spatial extent of cerebral hypometabolism in each FDG-PET image correspond to that in AD dementia patients, and 3) our new longitudinal HCI (L-HCI) method, which characterizes the extent to which the magnitude and spatial extent of longitudinal cerebral metabolism declines correspond to that in AD dementia patients.

Methods: Baseline and 24-mo PET scans from 399 ADNI subjects were included. The three methods were used to track the AD-related CMRgl decline in amyloid-positive (Aβ+) patients with the clinical diagnoses of probable AD dementia and mild cognitive impairment (MCI) due to AD and in Aβ+ and Aβ- unimpaired older adults all whose baseline Aβ+ was defined by florbetapir PET.

Results: The magnitude of AD-related CMRgl decline by each method was ranked as dementia due to AD > MCI due to AD > amyloid positive NC > amyloid negative NC ($p<0.05$). We estimate the respective need for the 70, 94, and 109 AD Aβ+ dementia patients per group and 154, 214, and 441 MCI Aβ+ patients per group using the L-HCI, sROI and C-HCI methods to detect a 25% AD-slowing treatment effect in a twelve-month, multi-center RCT with 80% power and two-tailed alpha=0.05.

Conclusion: The sROI and L-HCI are capable of characterizing the cerebral glucose metabolism decline over time for patients characterized as Aβ+ at baseline. Our findings provide additional support for the increased power associated with the uses of FDG and amyloid PET in anti-Aβ trials.

Maturity of increased cortical uptake of amyloid ligands on PET as a biomarker for Alzheimer's disease in the context of a structured 5-phase development framework

Konstantinos Chiotis[1], Laure Saint-Aubert[1], Marina Boccardi[2], Anton Gietl[3], Agnese Picco[4], Andrea Varrone[5], Valentina Garibotto[6], Karl Herholz[7], Flavio Nobili[4], Agneta Nordberg[1, 8]

[1]*Dept NVS, Center for Alzheimer Research, Translational Alzheimer Neurobiology, Karolinska Institutet, Stockholm, Sweden*
[2]*LENITEM (Laboratory of Epidemiology, Neuroimaging and Telemedicine), IRCCS S.Giovanni di Dio Fatebenefratelli, Brescia, Italy*
[3]*Division of Psychiatry Research and Psychogeriatric Medicine, University of Zurich, Switzerland*
[4]*Department of Neuroscience, Rehabilitation, Ophthalmology, Genetics, Maternal and Child Health, University of Genoa, Italy*
[5]*Department of Clinical Neuroscience, Centre for Psychiatry Research, Karolinska Institutet, Stockholm, Sweden*
[6]*Department of Neurology, Geneva University Hospitals, Geneva, Switzerland*
[7]*University of Manchester, Institute of Brain, Behaviour and Mental Health, Wolfson Molecular Imaging Centre, Manchester, United Kingdom*
[8]*Department of Geriatric Medicine, Karolinska University Hospital Huddinge, Stockholm, Sweden*

Introduction: The use of biomarkers has been proposed for diagnosing Alzheimer's disease (AD) in recent criteria, but some biomarkers have not been sufficiently investigated to justify their routine clinical use. An inter-societal task force aiming to develop a roadmap for the rational implementation of AD biomarkers in clinical routine evaluated the maturity of amyloid PET imaging based on a framework comprising 5 sequential phases.

Methods: We performed a literature review to assess the maturity of amyloid PET imaging as a biomarker for the Mild Cognitive Impairment (MCI) population. The review was performed, in line with the evaluation of other AD biomarkers in parallel reviews, in the light of the 5-phase framework for biomarker development: the identification of the rationale of amyloid PET based on pathology (Phase 1), the evaluation of its ability to discriminate patients from controls (Phase 2), the evaluation of its ability to detect AD at the earliest stages of the disease (Phase 3), the definition of operating characteristics in a relevant MCI population (Phase 4), and the estimation of disease-associated mortality, morbidity, and disability reduction (Phase 5).

Results: There is adequate evidence that the main aims of phases 1 (rationale for use) and 2 (discriminative ability) have been achieved. The aims of phase 3 (early detection ability) have been partly achieved, while phase 4 (performance in representative MCI patients) studies are currently on-going. Phase 5 studies (quantification of impact and costs) are still to come.

Conclusions: Since the emergence of amyloid PET imaging, there has been much investigation of its ability to specifically target AD pathology and to predict the conversion of MCI to AD dementia Future investigations will primarily be large, phase 4 studies that will assess the utility of amyloid PET imaging in routine clinical practice.

Tau PET imaging in neurodegenerative tauopathies – a multimodal paradigm

Konstantinos Chiotis[1], Laure Saint-Aubert[1], Antoine Leuzy[1], Elena Rodriguez-Vieitez[1], Irina Savitcheva[2], Vesna Jelic[3], Anders Wall[4], Gunnar Antoni[4], Agneta Nordberg[1, 3]

[1]*Dept NVS, Center for Alzheimer Research, Translational Alzheimer Neurobiology, Karolinska Institutet, Stockholm, Sweden*
[2]*Department of Radiology, Karolinska University Hospital Huddinge, Stockholm, Sweden*
[3]*Department of Geriatric Medicine, Karolinska University Hospital Huddinge, Stockholm, Sweden*
[4]*PET Centre, Uppsala University Hospital, Uppsala, Sweden*

Introduction: The wide spectrum of degenerative tauopathies includes Alzheimer's disease (AD), corticobasal degeneration, progressive supranuclear palsy and frontotemporal lobar degeneration. Aim of this study was to evaluate the presence and regional distribution of tau pathology in patients with degenerative tauopathies with the use of (S)-[^{18}F]THK5117 (also known as [^{18}F]THK5317) PET.

Methods: Non-AD patients were recruited, including two patients with a diagnosis of behavioral variant of frontotemporal lobar degeneration, one with semantic dementia, one with progressive supranuclear palsy, one with corticobasal degeneration, and two mild cognitive impairment patients negative for amyloid deposition ([^{11}C]PIB status). All patients underwent T1 MRI and multi-tracer PET imaging with (S)-[^{18}F]THK5117, [^{11}C]PIB and [^{18}F]FDG. (S)-THK5117 DVR, PIB SUVR and FDG SUVR images were created with respect to the cerebellar grey matter. In addition, (S)-THK5117 SUV images were used for the assessment of the patient with a diagnosis of progressive supranuclear palsy. Region- and voxel-wise comparisons were performed with respect to groups of young healthy volunteers (n=5, 20-30 years) and AD patients (n=20).

Results: All non-AD patients were found to have composite cortical PIB retention below the threshold for "positivity" (<1.40 SUVR). (S)-THK5117 retention in non-AD patients was higher than in the healthy volunteers, although the regional distribution was found to be different than the AD patients. Moreover, the regions of abnormally high (S)-THK5117 retention were found to agree with the expected distribution of tau pathology, from neuropathological studies, in these diseases. Areas of regional agreement between decreased FDG uptake and increased (S)-THK5117 retention were also observed.

Conclusion: (S)-THK5117, a tau-specific PET tracer, can image the expected regional load of tau pathology in patients clinically diagnosed with degenerative tauopathies. Moreover, the regional distribution of increased (S)-THK5117 retention in non-AD patients differs from that of AD patients, therefore, providing a tool for the differential diagnosis of different dementia syndromes.

Comparison of regional AV-1451 tau-PET binding across syndromic variants of Alzheimer's disease

Jennifer Whitwell, Keith Josephs, Nirubol Tosakulwong, Stephen Weigand, Ronald Petersen, Val Lowe, Clifford Jack

Mayo Clinic, Rochester, MN, United States

Background: Patients with Alzheimer's disease typically present with episodic memory loss (dementia of the Alzheimer's type (DAT)). However, 25% can have an atypical presentation dominated by language difficulties (logopenic aphasia (lvPPA)), or visuo-spatial/perceptual deficits (posterior cortical atrophy (PCA)). Tau-PET imaging using AV-1451 demonstrates striking uptake in DAT. It remains unclear whether elevated uptake occurs in atypical AD and whether regional patterns of uptake differ from DAT.

Aim: To investigate tau-PET imaging in atypical AD.

Methods: Tau-PET imaging using AV-1451 was performed in three patients with PCA and three with lvPPA; all six had a positive beta-amyloid PiB-PET scan. These six patients were compared to an age-matched group of 101 controls and 19 patients with DAT. Regional tau-PET uptake was assessed within medial and lateral temporal, parietal, frontal and occipital grey matter regions using the automated anatomical labelling atlas.

Results: Compared to controls, elevated tau uptake was observed in all PCA and lvPPA subjects. The PCA subjects all showed greatest uptake in occipital lobe and asymmetric patterns of uptake, with greatest involvement of the right hemisphere. Two PCA subjects showed additional widespread involvement of frontal, temporal and parietal lobes, with more focal and mild patterns observed in the third. The lvPPA subjects all showed left-sided patterns of uptake with the lateral temporal lobes showing striking uptake in two subjects. The third lvPPA subject showed widespread uptake throughout the cortex. Regional patterns of uptake in PCA and lvPPA overlapped with those observed in DAT, although there was a tendency for the left hippocampus to be involved to a greater degree in DAT.

Conclusions: AV-1451 PET imaging is sensitive in atypical AD and shows striking uptake in regional patterns that match the known atrophic signatures of these syndromes. There is some evidence for AV-1451 to detect subtle differences between atypical AD and DAT.

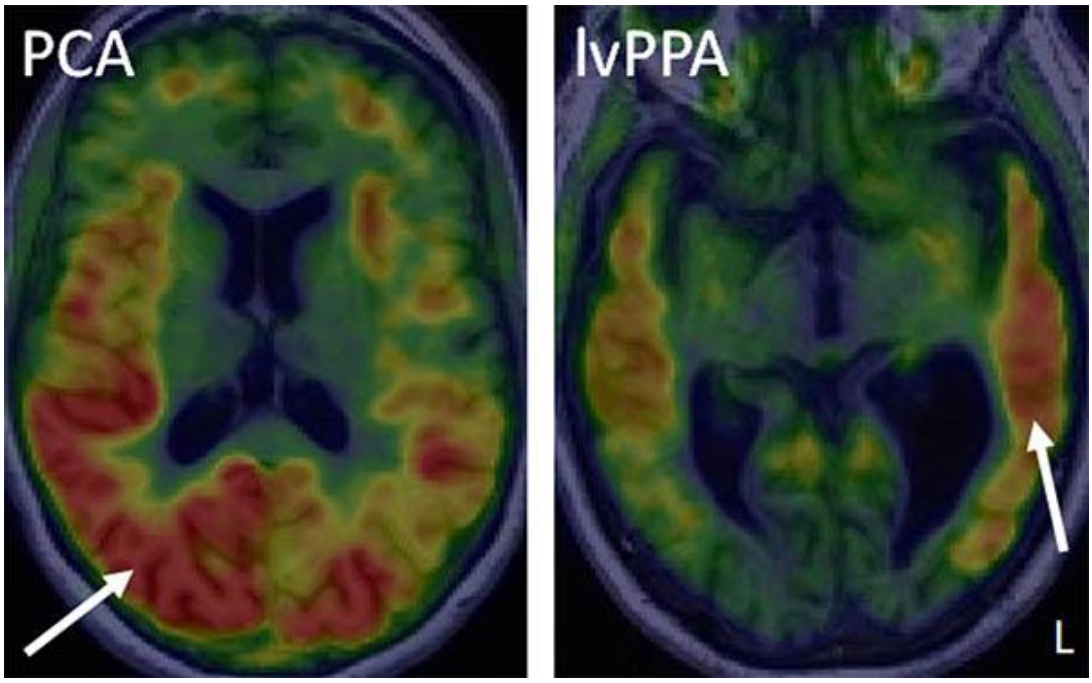

The association between brain amyloid and gait speed is influenced by cognition and APOE-ε4 genotype in older adults without dementia

Neelesh Nadkarni[1], Oscar Lopez[2], Subashan Perera[1], Julie Price[3], Chet Mathis[3], William Klunk[4], Snitz Beth[2], Steven Dekosky[6], Jeff Williamson[5]

[1]*Division of Geriatric Medicine and Gerontology, Department of Medicine, University of Pittsburgh, PA, United States*
[2]*Department of Neurology, University of Pittsburgh, PA, United States*
[3]*Department of Radiology, University of Pittsburgh, PA, United States*
[4]*Department of Psychiatry, University of Pittsburgh, PA, United States*
[5]*Section on Geriatrics and Gerontology, Department of Internal Medicine, Wake Forest University, Winston-Salem, NC, United States*
[6]*Department of Neurology, University of Florida, Gainesville, FL, United States*

Background: It is not known whether Aβ is associated with gait speed in older adults without dementia and whether cognition and APOE-ε4 influence this relationship.

Aim: To compare gait speed in dementia-free older adults with high Aβ [PiB(+)] and low Aβ [PiB(-)] and examine the influence of cognition and APOE-ε4 positive genotype on the association between global PiB retention and gait speed.

Methods: We analyzed data from the Pittsburgh site of the Gingko Evaluation of Memory study on participants who received a PiB-PET scan concurrent with gait assessments. Gait speed was averaged over two consecutive 15' traverses. We compared PiB(+) and PiB(-) groups on demographic, health and key brain characteristics using t-tests. We examined the magnitude of association between PiB retention and gait speed using linear regressions adjusting for demographics, weight, cardiovascular disease, hippocampal volumes and small-vessel disease burden. We included MMSE and APOE-ε4 status, separately and in combination, in the unadjusted and fully adjusted model. We also repeated the regressions excluding those with mild cognitive impairment.

Results: In this sample (n=183, 86 years, 42% female) PiB(+) and PiB(-) groups were similar on demographic, cardiovascular and general cognitive and physical function measures. PiB(+) group walked slower than the PiB(-) group (0.87 m/sec vs 0.95 m/sec, p=0.009). Higher PiB retention was significantly associated with slower gait speed (p=0.003) even after controlling for all above covariates. Further adjustment for MMSE (p=0.048) or APOE-ε4 status (p=0.1) or both (p=0.14) rendered this relationship non-significant. In the cognitively normal subgroup (n=145) the association between higher PiB retention and slower gait did not withstand covariate adjustments - MMSE and/or APOE-ε4 had lesser influence on this relationship.

Conclusion: Greater cortical Aβ is associated with slower gait; this relationship is influenced by cognition and APOE-ε4 status in elders without dementia and is less robust in cognitively normal elders.

A lifespan approach to understanding the relationship of amyloid beta deposition to obesity: Results from The Dallas Lifespan Brain Study

Allison Parker[1], Michelle Farrell[1], Melissa Rundle[1], Michael Devous[2], Denise Park[1]

[1]*Center for Vital Longevity, University of Texas, Dallas, TX, United States*
[2]*Avid Radiopharmaceuticals, Inc., Philadelphia, PA, United States*

Introduction: Based on increasing evidence that amyloid deposition is an anticedant of dementia due to Alzheimer's disease (AD), there is growing interest in identifying potentially modifiable risk factors that limit amyloid deposition. Past studies have demonstrated that markers of poor health, including a sedentary lifestyle (Head et al., 2012) and hypertension (Rodrigue et al., 2013), are associated with greater amyloid deposition. Obesity has also been linked with neurodegeneration and increased risk for AD (reviewed in Bischof & Park, 2009). In the present study, we examined the impact of age and obesity, as measured by Body Mass Index (BMI), on amyloid deposition in a lifespan sample of adults age 30-89, hypothesizing that with increased age, obese adults would show greater amyloid accumulations than non-obese adults.

Methods: Amyloid deposition was measured in 262 participants (age 30-89) using F-18 florbetapir PET imaging as part of the Dallas Lifespan Brain Study. Participants were classified as obese or not obese using a cut off BMI of 30.

Results: An ANCOVA on mean cortical SUVR, controlling for gender and education, yielded an Age main effect ($p < .001$) as well as an Age x Obesity interaction that was in the predicted direction, significant at $p = .06$ (Figure 1).

Conclusion: This finding suggests that amyloid deposition appears to accelerate with age in obese adults supporting the hypothesis that obesity is a risk factor for amyloid deposition. Longitudinal data will soon be available from this cohort, allowing us to relate obesity to accrual of amyloid. An important unaddressed question is whether a decrease in BMI will decrease the rate of amyloid accrual.

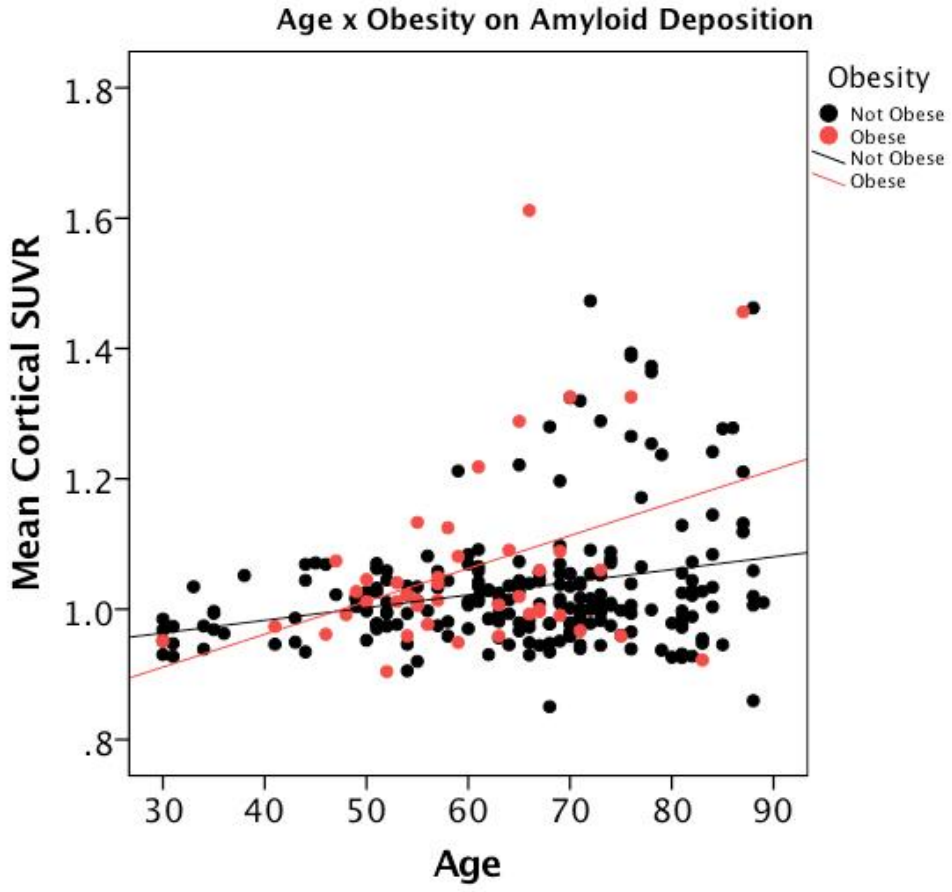

Baseline amyloid PET imaging characteristics in Verubecestat (MK-8931) prodromal trial

Cyrille Sur[1], Gregory Klein[2], Yuki Mukai[1], Yi Mo[1], Tiffini Voss[1], Ying Zhang[1], James Koss[1], Joyce Suhy[2], David Michelson[1], Michael Egan[1]

[1]*Merck Sharp & Dohme, PA/NJ, United States*
[2]*Bioclinica, CA, United States*

Subjects with amnestic mild cognitive impairment (aMCI) and evidence of increased amyloid in the brain are at high risk of conversion to AD. Verubecestat is a potent inhibitor of beta secretase (BACE) and its efficacy is being assessed in a phase III trial (NCT01953601). A positive amyloid PET scan is an eligibility criterion for this trial. Here, we report on the characteristics of amyloid PET imaging and its relationship with cognitive measures in the screened population.

More than 600 aMCI individuals underwent PET imaging using [18F]Flutemetamol in over 15 countries. All the PET scans were visually assessed according to [18F]Flutemetamol label and standard uptake value ratio (SUVR) were computed using the pons as a reference region. Subjects met inclusion criteria for MCI which included a MMSE $\geq$ 24 and a score of <1SD below the control mean on the Delayed Memory Index (DMI) from the Repeatable Battery for the Assessment of Neuropsychological Status (RBANS).

Using a centralized visual read, ~73% of screened aMCI were determined to be positive with a range of 67-79% across countries. The mean SUVR for all screened subjects was 0.72±0.16, and 0.81±0.09 and 0.52±0.06 for visually positive and negative subjects, respectively. Comparing the visual to a quantitative method and a SUVR cut-off value of 0.62, the concordance between visual and SUVR methodology was ~95%. Using univariate logistic regressions, MMSE ($p=0.005$) and RBANS DMI ($p<0.001$) were significant in predicting PET positivity by visual read, however only RBANS DMI remained significant ($p<0.001$) in a multivariate model.

In conclusion RBANS DMI was the best single predictor of amyloid PET positivity and over 70% of screened aMCI individuals were PET positive. High concordance was found between SUVR measurement and visual read of PET images further validating the visual read centralized approach to support enrollment in large prodromal AD trials.

Longitudinal accrual of amyloid is associated with degradation of white matter tracts connected to the hippocampus in cognitively-normal adults

Zhuang Song, Michelle Farrell, Xi Chen, Denise Park

Center for Vital Longevity, University of Texas at Dallas, TX, United States

Introduction: The hippocampus is particularly vulnerable to early AD pathologies and is also critically responsible for the prominent memory decline observed in AD. Cortical Aβ deposition may serve as a reasonable indicator of AD-related pathologies in the medial temporal lobe, which may result in synaptic loss of the hippocampus. We tested the hypothesis that increasing cortical Aβ deposition is associated with degradation of white matter tracts that connect to the hippocampus in preclinical AD.

Methods: Cognitively normal adults (aged 55-75, N=37) from the Dallas Lifespan Brain Study had florbetapir F 18 positron emission tomography (PET) that assessed cortical Aβ deposition at two time points spaced roughly 3.5 years apart. Standardized uptake value ratio (SUVr) was derived from the PET as the ratio of mean Aβ tracer uptake within eight predefined cortical gray matter regions to the reference uptake in centrum semiovale and whole cerebellum. In addition, diffusion tensor imaging (DTI) was used to assess white matter tract integrity. Based on the ICBM-DTI-81 white matter atlas, our ROI analysis of longitudinal DTI was focused on diffusivity changes in two white matter tracts that connect to the hippocampus: the fornix (crux and stria terminalis) and the parahippocampal cingulum,

Results: Longitudinal accrual of Aβ plaques was associated with increased radial diffusivity in the fornix ($p=0.04$), but not in the parahippocampal cingulum. The effect of increased Aβ deposition was not significant for axial diffusivity changes in either tract ($p>0.20$). Importantly, the increase of radial diffusivity in the fornix was marginally associated with episodic memory decline in the same period of time ($p=0.10$).

Conclusion: These findings suggest that increases of Aβ deposition may degrade the hippocampal function by limiting its connectivity to other memory-related brain regions through the fornix, which may lead to memory impairment as the disease progresses.

Laminar distribution pattern of ^{3}H-THK5117 and ^{3}H-Deprenyl in AD brain tissue in comparison to pathological immunostaining

Laetitia Lemoine[1], Laure Saint-Aubert[1], Fredrik Engman[1], Inger Nennesmo[2], Per-Göran Gillberg[1], Agneta Nordberg[1, 3]

[1]*Translational Alzheimer Neurobiology division, Department of Neurobiology, Care Sciences and Society, Karolinska Institutet, Stockholm, Sweden*
[2]*Department of Pathology, Karolinska University Hospital, Huddinge, Sweden*
[3]*Department of Geriatric Medicine, Karolinska University Hospital, Huddinge, Sweden*

Introduction: The relationship between different hallmarks in AD are still unclear. In this study, we aimed to understand the possible relationship between tau deposits and activated astrocytes by analysing their laminar distribution in post-mortem brain tissue from confirmed AD cases and controls.using both PET ligands and specific antibodies

Methods: Autoradiography with ^{3}H-THK5117 and ^{3}H-deprenyl (^{3}H-DED) were performed on large frozen brain section from 3 AD cases and 1 control. Using a new technique, regional selections through the cortical ribbon were manually defined on the resulting autoradiograms using ImageJ software and the average of binding intensity through the neuronal layer was calculated. Five regions of interest in temporal and frontal gyrus were selected. The boundaries of the different cortical layers for each AD case were determined using corresponding immunostaining images of tau deposit (AT8) and activated astrocytes (GFAP).

Results: Visual assessement of the autoradiogram showed similar laminar distributions between ^{3}H-THK5117 and ^{3}H-DED. Two bands could be observed in the temporal gyrus, one in the superficial and one in the deep layer, when only one superficial band could be observed in the frontal gyrus for all cases. Different pattern between the cases are also distinguishable with cases showing more astrocytosis or Tau deposits in different layers. More detailled analysis of the cortical layer and comparison with the semi-quantitative ranking using the corresponding immunostaining allow us to determine that layer 2 was the superfical and layer 5 was the deep layer affected.

Conclusion: Tau deposits (using ^{3}H-THK5117) and activated astrocytes (using ^{3}H-Deprenyl) showed similar binding patterns suggesting that they are spatially related in AD. The result obtained with the PET ligand and antibodies (AT8,GFAP) were complementary. Finally, the individual difference between the patient in activated astrocytes and tau deposits could explain their different phenotype.

An amyloid-PET connectome for Alzheimer's disease

Rohan Katipally[1], Stephen Correia[1, 2], Stephen Salloway[1, 3]

[1]*The Warren Alpert Medical School of Brown University, RI, United States*
[2]*Providence Veterans Affairs Medical Center, RI, United States*
[3]*Memory and Aging Program, Butler Hospital, RI, United States*

Purpose: Develop an amyloid-PET connectome pipeline. Compare connectome networks across subjects with normal cognition (NC), mild cognitive impairment (MCI), and Alzheimer's disease (AD).

Background: Connectome approaches, often using functional MRI and diffusion tensor MRI, have become an attractive technique to study how disrupted brain connectivity may underlie cognitive decline. Connectomes depict the brain as a network of regions (nodes) and connections (edges) between them. Edges are quantified metrics (e.g. correlations) between nodes based on brain structure, function, or in this cas e, biochemical markers. Connectomes generated directly from amyloid-PET data would represent networks of amyloid deposition, with edges reflecting correlations of amyloid deposition between pairs of regions. Thus, the pattern, rather than the magnitude, of deposition may be studied.

Methods: Florbetapir-PET data was obtained from the Alzheimer's Disease Neuroimaging Initiative 2 (NC=266, MCI=332, AD=144, total=742). Florbetapir standard uptake value ratios (SUVr) were calculated for 38 nodes parcellated by the Desikan-Killiany cortical atlas. Edge strength was the partial correlation of SUVr between each pair of nodes across all subjects in a group, producing a group-level connectome. Permutation testing was used for group-wise comparisons of networks at a single density and area under the curve analysis is planned.

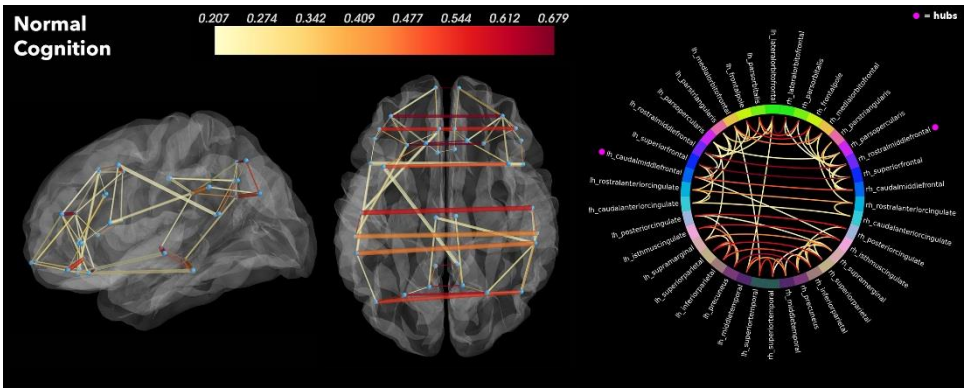

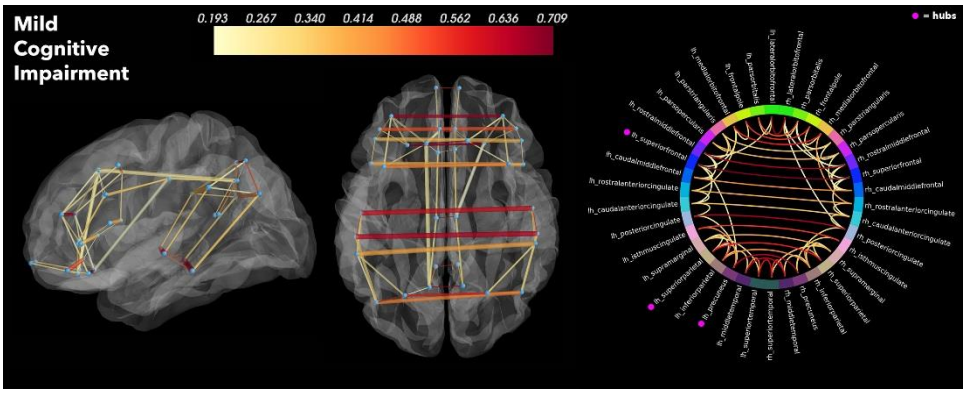

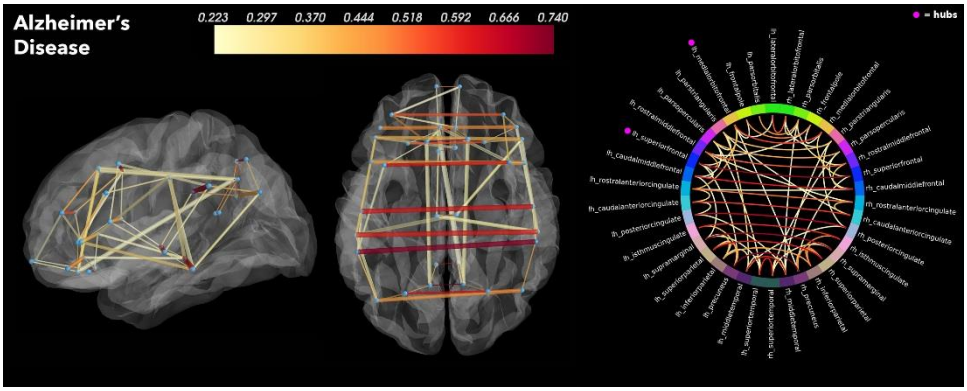

Results: All three groups exhibited hubs of amyloid deposition in frontal areas, whereas the MCI group uniquely had hubs in the superior parietal area and precuneus. Assortativity was greater in the MCI amyloid network than the NC network ($p<0.05$).

Conclusions: The finding of parietal hubs in MCI is consistent with current regional biomarkers for amyloid, such as the precuneus. Further analysis will provide more insight into changes in the amyloid deposition network across the progression of AD. This pipeline can be applied to other PET studies using ligands other than florbetapir, such as tau-PET, for further elucidation of the impact of disease on brain networks.

[18F]AV-1451 is a PET tracer capable of detecting varying levels of pathological tau in AD post-mortem cortical tissue sections

Yin-Guo Lin, Felipe Gomez, Qianwa Liang, Mark A. Mintun, Giorgio Attardo

Avid Radiopharmaceuticals, Inc., Philadelphia, PA, United States

Background: Previous evidence has shown that [18F]AV-1451 is a selective PET biomarker to detect pathological tau in Alzheimer's disease (AD). This study applies a direct correlation technique of autoradiography to immunohistochemistry to explore the ability of [18F]AV-1451 to identify small differences in tau accumulation in AD. the potential ability of [18F]AV-1451 to detect a small progression or regression in tau aggregation would have important implications in its clinical use.

Objective: To determine if the autoradiography (ARG) signal from [18F]AV-1451 matches closely with the distribution and signal intensity of the Tau-antibody AT8 in AD when immunofluorescence (IF) is performed on the same brain section used for ARG.

Methods: [18F]AV-1451 (20 µCi) was added to fresh frozen brain sections (10 µm) from 30 AD and 10 age-matched controls to obtain autoradiography (ARG) images. The same tissue sections were stained with the phospho-Tau antibody AT8 and labeled with a fluorescent dye. The IF preparations were imaged using a NanoZoomer 2.0HT (Hamamatsu), which allows for both a macroscopic and microscopic view of the immunofluorescence signal. Further analysis of section areas and signal intensity were performed using Photoshop and Image J software.

Results: There was a good correlation (r = 0.997) between the percentage of cortical grey matter with AT8 signal and that of the [18F]AV-1451 ARG signal in AD brain sections (Fig.1. Fig.2). In addition, the intensity of the ARG signal matched the distribution of pathological tau as shown by IF with cross-subject correlation of > 0.9.

Conclusion: [18F]AV-1451 ARG signal strongly correlates with the distribution of pathological tau when immunostaining with AT-8 tau antibody is performed on the same section as ARG. These results further support [18F]AV-1451 as a biomarker for pathological tau aggregation in AD.

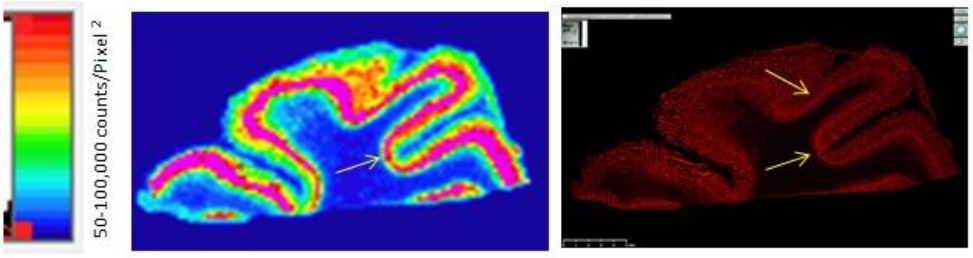

Fig. 1 Autoradiography of [18F]AV-1451 in frontal cortex of AD brain sections (left). The same section stained with the tau AT8 antibody using immunofluorescence (right). Yellow arrows indicate the layered distribution.

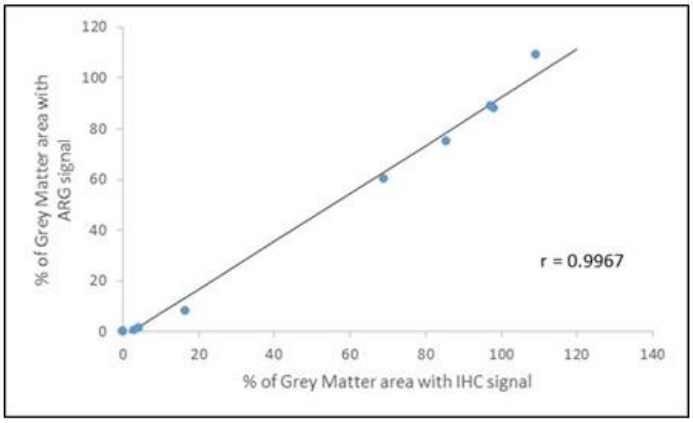

Fig. 2 Correlation between the percentage of cortical grey matter (GM) with AT8 signal and that of the [18F]AV-1451 ARG signal in AD brain sections.

Differential regional uptake of 18F-flutemetamol in healthy controls and patients with mild cognitive impairment correlates to cognitive assessment scores

Katherine Gray[1, 2], Richard Joules[1], Robin Wolz[1, 2], Derek Hill[1]

[1]*IXICO plc, London, United Kingdom*
[2]*Biomedical Image Analysis Group, Department of Computing, Imperial College London, United Kingdom*

The PET tracer 18F-flutemetamol, allows for in vivo imaging of amyloid in the brain. In this cross-sectional study we examine the association of localised flutemetamol retention in healthy controls (HC) and patients with mild cognitive impairment (MCI).

A subset of 38 HC and 15 MCI participants with both flutemetamol PET and structural MRI was acquired from the publically available AIBL dataset [Ellis,IntPsychogeriatrics,2009]. MRI were segmented into 142 anatomically defined regions using a whole brain extension to the LEAP automated segmentation technique [Wolz,NeuroImage,2010]. Each PET image was aligned with its corresponding MRI, and regional uptake values extracted. Preliminary comparisons between groups were performed, and regional uptake values correlated against global clinical dementia rating (CDR) and mini-mental state examination (MMSE) scores. Flutemetamol retention was increased in the cortex and putamen for MCI participants compared to the HC group, consistent with previously reported findings [Engler,Brain,2006 Klunk,AnnsNeurology,2004]. When performing group classifications, the right superior parietal lobule was identified as highly informative for discriminating MCI and HC groups allowing for a group discrimination accuracy of 75%.

Widespread statistically notable ($p<0.05$, passing Bonferroni test for multiple comparisons) correlations were observed between both CDR and MMSE scores and flutemetamol retention across the cortex. Strongest correlations were observed in orbital frontal and parietal regions, consistent with previously reported findings obtained using the PIB tracer [Grimmer,NeurobiologyOfAging,2009], we also report strong correlations in V1 (Figure 1).

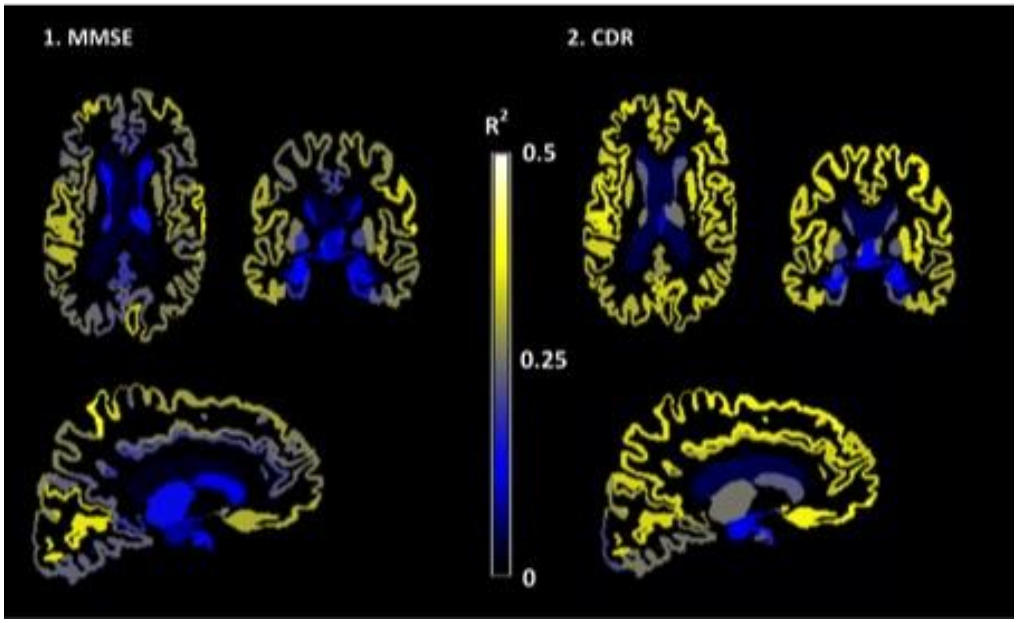

Figure 1: Squared correlation coefficients for the relationship between localized measures of flutemetamol retention and cognitive scores; specifically, 1) mini mental state examination score (MMSE) and 2) Cognitive decline rate score (CDR)

Regional flutemetamol retention is correlated with cognitive scores at baseline. Amyloid PET images are often analysed by dichotomising according to a pre-defined cut-point, and these preliminary results indicate that regional analysis can provide additional information. With the release of MMSE and CDR scores for an 18 month follow up we will investigate the relationship between changes in cognitive score and flutemetamol at baseline with the motivation of identifying biomarkers associated with disease progression rates.

Tau PET imaging with (S)-18F-TKH5117 in Alzheimer´s disease and other taupathies in a multi-tracer design

Konstantinos Chiotis[1], Laure Saint-Aubert[1], Irina Savitcheva[2], Vesna Jelic[3], Pia Andersen[3], My Jonasson[4, 5], Jonas Eriksson[6, 7], Mark Lubberink[4], Ove Almkvist[1, 3, 8], Anders Wall[4, 6], Gunnar Antoni[6, 7], Agneta Nordberg[1, 3]

[1]*Dept NVS, Center for Alzheimer Research, Translational Alzheimer Neurobiology, Karolinska Institutet, Stockholm, Sweden*
[2]*Dept Radiology, Karolinska University Hospital Huddinge, Stockholm, Sweden*
[3]*Dept Geriatric Medicine, Karolinska University Hospital Huddinge, Stockholm, Sweden*
[4]*Radiology, Dept Surgical Sciences, Uppsala University, Sweden*
[5]*Medical Physics, Uppsala University Hospital, Uppsala, Sweden*
[6]*PET Centre, Uppsala University Hospital, Uppsala, Sweden*
[7]*Pre-clinical PET Platform, Uppsala University, Sweden*
[8]*Dept Psychology, Stockholm University, Sweden*

Introduction: In order to explore different taupathies including Alzheimer disease (AD) and other non-AD dementia disorders we measured regional (S)-[18F]THK5117 retention in brain in relation to markers of neurodegeneration and amyloid plaque deposition.

Methods: Thirty-six subjects, thirteen patients with mild cognitive impairment (MCI), nine patients with AD, five patients with non-AD taupathies, and nine healthy controls underwent (S)-[18F]THK5117, [11C]PIB and [18F]FDG PET, magnetic resonance imaging (MRI) and cognitive testing.

Results: Test-retest variability for (S)-[18F]THK5117-PET measured in five patients was very low (1.2-3.8%). A significant higher isocortical (S)-[18F]THK5117 retention was observed in both MCI [11C]PIB positive (p=0.002) and dementia-stage (p=0.001) AD patients in comparison the healthy controls, with an excellent discrimination (area under the curve >98%). The regional retention of (S)-[18F]THK5117 retention at different stages of AD strongly resembled the classical staging of tau pathology. Patients with non-AD dementia showed no amyloid pathology and high (S)-[18F]THK5117 retention with a regional distribution different from that seen in AD patients. One year follow-up PET studies are now ongoing.

Conclusion: Tau PET imaging using (S)-[18F]THK5117-PET reflects tau pathology spreading, and when used in conjunction with other imaging biomarkers will be important tools to further understand the difference in underlying pathophysiological mechanisms of various taupathies.

Amyloid-β plaque burden is associated with quality of life in cognitively normal "super-agers"

Anton Gietl[1], Rafael Meyer[1], Andreas Buchmann[1], Antje Saake[1], Alfred Buck[2], Linjing Mu[2, 3], Roger Schibli[2, 3], Sandra Leh[1], Paul Unschuld[1], Roger Nitsch[1], Valerie Treyer[2], Christoph Hock[1]

[1]*Division of Psychiatry Research, University of Zurich, Switzerland*
[2]*Department of Nuclear Medicine, University Hospital Zurich, Switzerland*
[3]*Department of Chemistry and Applied Biosciences, Center for Radiopharmaceutical Sciences of ETH-PSI-USZ, Institute of Pharmaceutical Sciences, ETH Zurich, Switzerland*

Background: Quality of life (QOL) represents the subjective perception and evaluation of the individual's living conditions. The WHO-Quality-of-Life-Questionnaire (WHOQOL-Old) assesses QOL in the elderly in six domains (sensory abilities, autonomy, past present and future activity, social participation, death and dying, and intimacy). The current study examines QOL in a population of very old subjects with preserved functional abilities to test, whether QOL is associated with Amyloid-β-plaque-burden in this group of "super agers".

Methods: 36 subjects (26 male, 10 female/ mean age: 87.7± 3.1/ mean MMSE: 28.7± 1.4) underwent clinical and neuropsychological assessment followed by 18F-Flutemetamol-PET for estimating Aß-plaque-burden. Standardized-uptake-value-ratios (cerebellar grey matter reference, 85-105 minutes post injection) were determined and a cut-off was calculated to separate "Aβ-positive" (n=7) and "Aβ-negative" (n=29) subjects. WHOQOL-Old was completed by all participants.

Results: The groups did not differ in age, education, MMSE-score or neuropsychological performance. WHOQOL-Old Score was higher in "Aβ-negative" subjects (95.0 ± 9.3 vs. 84.1 ± 13.0; U=50.5 p=0.041) indicating higher QOL. Especially the domain scores "autonomy"-example item: "having the possibility to do things one likes to do" (16.8 ± 1.7 vs. 13.9 ± 3.1; U37.5 p=0.009) and intimacy (16.0 ± 3.2 vs. 13.0 ± 3.3; U48.5, p=0.033); example items: "opportunities to love or to be loved"; were higher in "Aβ-negative" subjects. When Amyloid-deposition was considered quantitatively, a weak negative correlation with WHOQOL-Score was observed.

Discussion: Our data suggest that QOL is associated with Amyloid-β-plaque-burden in very old subjects with preserved functional activities. This would imply that even in this population, where we could not detect group differences in cognition, Abeta-deposition is not benign. An alternative explanation would be that QOL reduces stress, thereby exerting a positive effect on amyloid-deposition. However this would presume that the QOL-construct contains stable elements exerting this effect over a significant part of the lifespan.

Differential effects of Aβ deposition and Apolipoprotein E genotype on default mode network functional connectivity

Susan Resnick[1], Yongxia Zhou[1], Murat Bilgel[1, 2], Bennett Landman[3], William Seeley[4], Dean Wong[5]

[1]*Laboratory of Behavioral Neuroscience, Intramural Research Program, National Institute on Aging, NIH, MD, United States*
[2]*Department of Biomedical Engineering, Johns Hopkins University, MD, United States*
[3]*Department of Electrical Engineering, Vanderbilt University, TN, United States*
[4]*Department of Neurology, University of California, San Francisco, CA, United States*
[5]*Department of Radiology, Johns Hopkins University, MD, United States*

Background: While the Apolipoprotein E (APOE) ε4 risk allele is associated with higher levels and earlier onset of amyloid-β (Aβ) deposition, emerging evidence indicates that Aβ and APOE genotype have different associations with brain structure and function. We used resting state functional magnetic resonance (rsfMR) imaging to investigate possible differential associations of Aβ and APOE genotype with functional connectivity (FC).

Methods: Participants were 92 (49 female) non-demented individuals in the PET-PiB substudy of the Baltimore Longitudinal Study of Aging who had rsfMR assessments. Based on 2-class Gaussian clustering of mean cortical DVR values, 20 (mean age=82.3) were classified as PiB+ and 72 (mean age=76.2) as PiB-. APOE genotypes were available for 78 individuals with PET-PiB and rsfMR, with 18 ε4+ (mean age=73.9) and 60 ε4- (mean age=77.8). Resting state echo planar images were acquired (voxel size=3x3x4mm3, matrix=80x80x37, TR/TE=2000/30msec, frames=180). FC analysis was conducted using a standard image processing pipeline, and default mode network (DMN) connectivity was assessed using a DMN Core region, combining seeds in the posterior cingulate and medial prefrontal cortex. Contrasts of DMN FC maps ($p<0.01$, cluster=10), adjusted for age, sex, education, and race, were performed stratifying by PiB status and APOE genotype separately.

Results: PiB+ compared with PiB- individuals showed several small clusters of higher DMN Core FC, including frontal DMN and thalamus and lower FC in precuneus and putamen. In contrast, APOE ε4+ compared with APOE ε4- showed higher DMN FC in the dorsal attention network, pronounced in supramarginal/visual association regions, and lower FC in orbital frontal and temporal cortex, including entorhinal cortex.

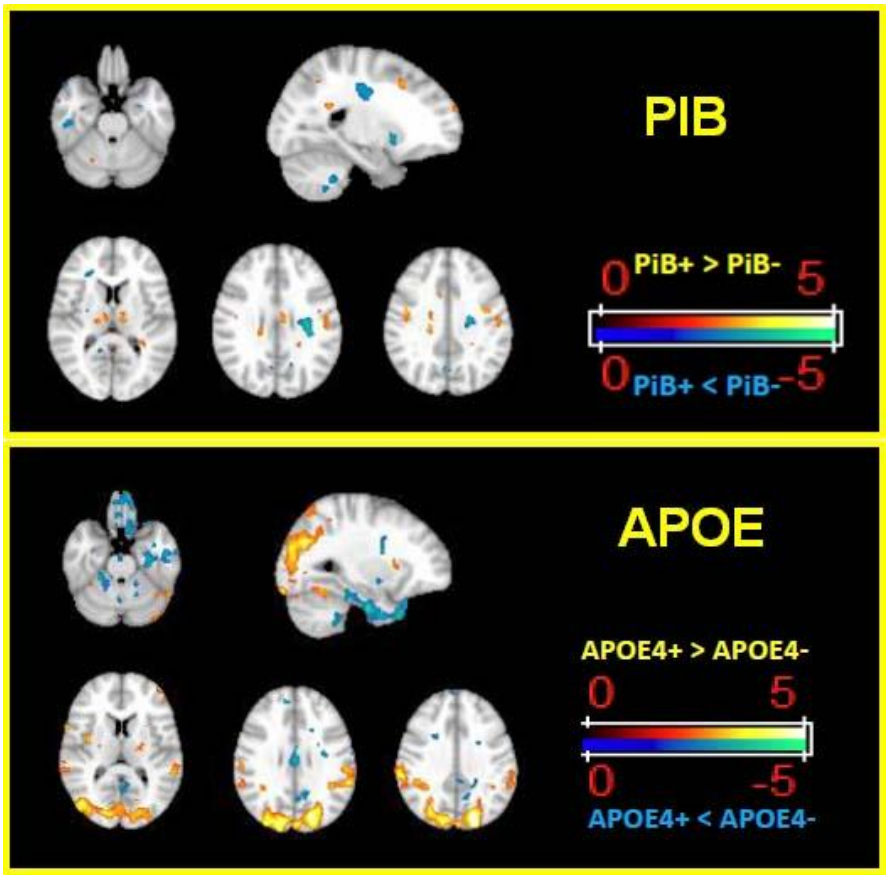

Conclusion: Our findings demonstrate differential associations of Aβ and APOE genotype with DMN network activity in individuals without cognitive impairment. Distinct effects of Aβ and APOE on brain function offer clues to the pathobiology of preclinical changes in AD.

Comparison of Early-Phase (S)-[18F]THK5117 and [11C]PIB PET as proxies of brain perfusion in Alzheimer's disease

Elena Rodriguez-Vieitez[1], Antoine Leuzy[1], Konstantinos Chiotis[1], Laure Saint-Aubert[1], Mark Lubberink[2], Anders Wall[2], Agneta Nordberg[1, 3]

[1]Translational Alzheimer Neurobiology, Center for Alzheimer Research, Dept. NVS, Karolinska Institutet, Stockholm, Sweden
[2]Section of Nuclear Medicine and PET, Department of Surgical Sciences, Uppsala University, Uppsala, Sweden
[3]Department of Geriatric Medicine, Karolinska University Hospital Huddinge, Stockholm, Sweden

Objectives: The investigation of early-phase PET uptake is of practical interest as it may add value to PET scans by providing a proxy for brain perfusion. Our aim was to assess the early-phase standardized uptake value ratio (SUVr) of the tau PET tracer (S)-[18F]THK5117 (also known as [18F]THK5317) and Simplified Reference Tissue Model R1 as proxies for brain perfusion, and to compare them with early-phase [11C]PIB and [18F]FDG.

Methods: Eleven prodromal AD (pAD) and nine AD dementia patients underwent PET imaging with (S)-[18F]THK5117, [11C]PIB and [18F]FDG. Early-phase (S)-[18F]THK5117 images were generated by time-weighted frame summation, using different initial time points (0, 1, and 2 min) and durations (1-10 min), and normalized to the cerebellar gray matter (GM). A 1-8 min [11C]PIB and 30-45 min [18F]FDG SUVr images were created with reference to the cerebellar GM. Intra- and inter-subject Pearson's r correlations were performed between both early-phase (S)-[18F]THK5117 SUVr and R1 with [18F]FDG SUVr, both regionally and voxelwise. The discriminative ability of the different PET measures for classification of pAD versus AD was estimated from receiver operating characteristic area under the curve (AUC) values.

Results: Positive correlations were found for (S)-[18F]THK5117 R1 and early-phase (S)-[18F]THK5117 perfusion indices versus [18F]FDG, most prominently in occipital, parietal and lateral temporal cortices. Head-to-head comparison between early-phase (S)-[18F]THK5117 and early-phase [11C]PIB showed no differences. The discriminative ability of all PET markers evaluated was highest in parietal, lateral temporal, and posterior cingulate cortices. On a regional basis, no significant differences were observed between the AUC values achieved by the different PET markers.

Conclusions: Our findings suggest that early-phase (S)-[18F]THK5117 and R1 provide information on brain perfusion, closely related to metabolism. As such, a single PET study with (S)-[18F]THK5117 may provide information about tau pathology and brain perfusion in AD, with potential clinical interest.

ER-V, AL equal contributors

Depressive symptoms and tau PET imaging across the Alzheimer's disease spectrum

Jennifer Gatchel[1], Nancy J. Donovan[3], Deborah Blacker[2], Aaron Schultz[2], John Alex Becker[2], Jasmeer Chhatwal[2], Kathryn Papp[3], Rebecca Amariglio[3], Dorene Rentz[3], Reisa Sperling[2, 3], Keith A. Johnson[2], Gad A. Marshall[2, 3]

[1]*McLean Hospital, MA, United States*
[2]*Massachusetts General Hospital, MA, United States*
[3]*Brigham and Women's Hospital, MA, United States*

Background: Depressive symptoms are common manifestations of prodromal Alzheimer's disease (AD) and AD dementia that are associated with functional impairment and disease progression. The *in vivo* association between tau (one of the main AD proteinopathies), depression, and cognitive decline is not well elucidated in cognitively normal (CN) elders and those with mild cognitive impairment (MCI) and AD dementia.

Objective: To investigate the cross-sectional association between depressive symptoms and cortical tau in CN, MCI and mild AD dementia. We hypothesized that increased tau in the entorhinal cortex (EC) and inferior temporal (IT) cortex would be associated with increased depression.

Methods: We measured depressive symptoms using the Geriatric Depression Scale (GDS), from which three factors (dysphoria, apathy-anhedonia and anxiety-concentration) were derived, and *in vivo* cortical tau using T807 (18F-AV-1451) positron emission tomography (PET) in 150 older adults: 123 CN and 27 symptomatic (17 MCI; 10 mild AD dementia). We employed generalized linear regression models to evaluate the relation of GDS score to EC or IT tau in separate backward elimination models. Predictors included age, gender, global cognition, and tau. In secondary analyses, similar models were built for each of the GDS factor scores, and also included cortical amyloid (PiB-PET) and its interaction with tau as predictors.

Results: Increased GDS score was significantly associated with increased EC tau (partial r=0.254, p=0.002); increased age (p=0.039) and male gender (p=0.003) were significant predictors in this model. Increased EC tau was significantly associated with increased dysphoria (partial r=0.201; p=0.022) and increased anxiety-concentration (partial r=0.191, p=0.030). The interaction between EC tau and amyloid was significantly associated with increased GDS score (partial r=0.243; p=0.003).

Conclusion: These results suggest an association between increased depressive symptoms and greater EC tau in individuals across the AD spectrum. Probing this association longitudinally across stages of pathogenesis may inform treatment approaches.

Tau and amyloid PET imaging in a Colombian kindred with autosomal-dominant Alzheimer's disease: A preliminary report

Yakeel Quiroz[1, 2, 3], Reisa Sperling[1, 3, 4], Ana Baena[2], Joseph Arboleda-Velasquez[5], Aaron Schultz[1, 3], Danielle Cosio[1, 3], Molly Lapoint[1, 3], Kelly Judge[1, 3], Sehily Jaimes[1, 4], Daniel Norton[1], Eric Reiman[6], Francisco Lopera[2], Keith Johnson[1, 3]

[1]*Massachusetts General Hospital, Harvard Medical School, Boston, MA, United States*
[2]*Grupo de Neurociencias, Universidad de Antioquia, Medellin, Antioquia, Colombia*
[3]*Athinoula A. Martinos Center for Biomedical Imaging, Charlestown, MA, United States*
[4]*Brigham and Women's Hospital, Harvard Medical School, Boston, MA, United States*
[5]*Schepens Eye Research Institute, Harvard Medical School, Boston, MA, United States*
[6]*Banner Alzheimer's Institute, Phoenix, AZ, United States*

Background: Examining rare families with autosomal dominant mutations that cause early-onset Alzheimer's disease (AD) provides a unique model for studying the trajectory of AD-related pathology, especially in the preclinical stages. We used PET imaging to characterize the relation between amyloid burden and tau accumulation in the brains of young, asymptomatic PSEN1 E280A mutation carriers and non-carriers from a Colombian kindred with autosomal dominant AD (ADAD). We hypothesized that amyloid-beta deposition precedes tau tangle formation both within and beyond the medial temporal lobe in ADAD.

Methods: Six cognitively-unimpaired carriers of the PSEN1 mutation (mean age 32 years) and six non-carriers (mean age 36 years) traveled to Boston for tau and amyloid imaging. [C11] PIB PET cerebral-to-cerebellar DVRs and [F18] T807-PET cerebral-to-cerebellar SUVRs were compared based on mutation status. Both PiB and T807 utilized structural ROIs as defined by Freesurfer. Groups were matched for age, sex, education level, and neuropsychological test performance.

Results: Compared with non-carriers, cognitively unimpaired mutation carriers had significantly higher mean cortical PIB DVRs (carriers: 1.16 +/-0.06, non-carriers: 1.05 +/-0.02, $p<0.001$). The group differences for T807 SUVRs were in the expected direction but were non-significant (inferior temporal lobe regions; carriers: 1.15 +/-0.12, non-carriers: 1.13 +/-0.06, $p= 0.74$; entorhinal cortex; carriers: 1.21 +/-0.40, non-carriers: 1.02 +/-0.06, $p= 0.28$). There was also a trending association between amyloid burden and T807 binding in entorhinal cortex ($r= 0.57$, $p=0.07$), which was in part driven by the oldest mutation carrier in this sample (age 38), who was still several years away from usual clinical onset at age 44.

Conclusion: Initial findings from this ongoing longitudinal study are consistent with the hypothesis that mutation carriers express amyloid deposition before tau deposition. Studying amyloid and tau concomitantly in ADAD is a promising method for clarifying the temporal relationship between the emergence of tau and amyloid pathology.

Regional differences in the progression of amyloid accumulation and cognitive consequences in healthy adults across the lifespan

Michelle Farrell, Sara B. Festini, Xi Chen, Denise C. Park

University of Texas at Dallas, TX, United States

Introduction: Autopsy (Braak and Braak, 1991) and amyloid PET imaging data (Villain et. al., 2012; Sepulcre et. al., 2013) have converged to suggest that the orbitofrontal cortex (OFC) is one of the earliest sites of amyloid accumulation, whereas posteromedial regions exhibit accumulation later and are potentially more closely linked to cognitive decline. In the present study, we measured longitudinal amyloid accumulation over 3.5 years in adults aged 30-89, and hypothesized orbitofrontal and posteromedial regional accumulation would differ as a function of age and initial amyloid positivity. Furthermore, we expected the rate of accumulation in posteromedial regions would be associated with AD-typical episodic memory deficits. Lastly, we examined whether orbitofrontal amyloid accumulation would have a detrimental impact on cognition, particularly on complex, high-demand reasoning tasks which may be more sensitive to neural insult.

Methods: Participants from the Dallas Lifespan Brain Study who completed MRI and florbetapir PET at baseline and 3.5-year follow-up (n=83) were included. ROIs were derived from manually-edited Freesurfer parcellations, normalized to cerebellum and subcortical white matter.

Results: Across the lifespan, there was a significantly higher proportion of amyloid accumulators in the lateral OFC (39.8%) than precuneus (19.3%), see Figure 1a/2a. Furthermore, this discrepancy in frequency of accumulators between lateral OFC and precuneus was also observed in middle-aged adults (28.1% vs. 9.4%) and baseline amyloid-negative individuals (33.7% vs. 11.8%). Finally, increasing precuneus accumulation predicted lower follow-up episodic memory performance (Figure 2b). Interestingly, increasing regional accumulation in both the lateral orbitofrontal and pars orbitalis was related to lower follow-up reasoning performance (Figure 1b).

Figure 1. Lateral Orbitofrontal Amyloid Accumulation. (a) Amyloid accumulators (red) were observed throughout the lifespan in the lateral OFC and (b) rate of accumulation predicted lower reasoning performance

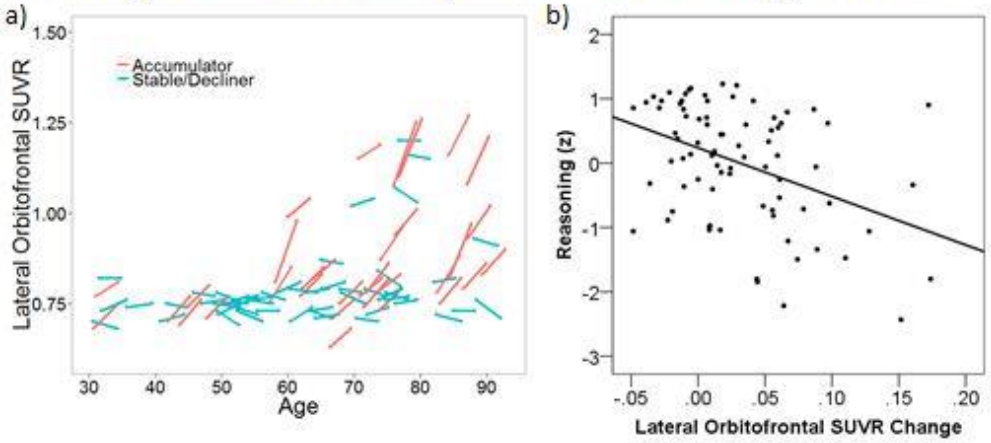

Figure 2. Precuneus Amyloid Accumulation. (a) Amyloid accumulators (red) were not observed in the precuneus until age 58 and (b) the rate of accumulation predicted lower episodic memory performance.

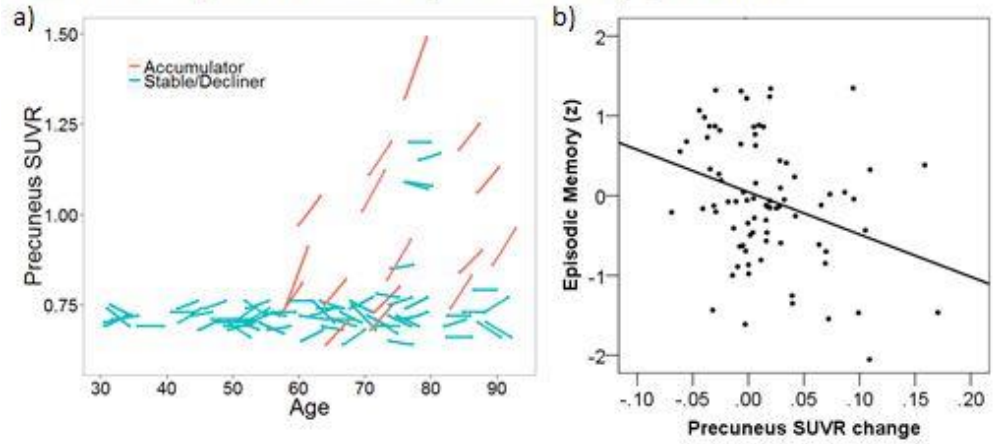

Conclusion: These findings provide evidence that precuneus amyloid accumulation may have greater neural toxicity and specificity for AD and episodic memory. Further research is needed to understand whether earlier accumulation in orbitofrontal regions may be related to functional or structural impairments that lead to poorer reasoning performance.

Regional kinetics of [^{18}F]AV-1451 uptake and Gadolinium concentration in young and older subjects

Belen Pascual[1], Elijah Rockers[1], Sahil Bajaj[1], Jeff Anderson[2], Zhong Xue[3], Christof Karmonik[2], Joseph Masdeu[1]

[1]Houston Methodist Neurological Institute, Houston Methodist Hospital, Weill Cornell Medicine, Cornell University, TX, United States
[2]MRI Core, Houston Methodist Research Institute, Weill Cornell Medicine, Cornell University, TX, United States
[3]Biomedical Engineering Department, Houston Methodist Research Institute, Weill Cornell Medicine, Cornell University, TX, United States

Aim: To clarify whether apparently increased specific [^{18}F]AV-1451 binding in areas unlikely to harbor hyperphosphorylated tau, such as the choroid plexus, substantia nigra, globus pallidus and putamen, of older subjects could be related to greater vascular permeability of these regions in older subjects as compared to younger ones.

Methods. In six younger (23±2.1 years of age, three women) and six older (68.8±7.6 years, three women) healthy subjects we measured dynamic [^{18}F]AV-1451 uptake over a three-hour period. Similarly, we obtained dynamic gadolinium concentrations over three hours after a bolus injection of gadolinium by performing a pre-contrast 3D T1 map (five flip angle acquisitions), followed after gadolinium injection by dynamic contrast enhanced (DCE) MRI with fast (3.4 sec frames) 3D T1 mapping for the first 10 minutes and longer (3.7 min) serial 3D T1 maps, with five different flip angle acquisitions, over the next 170 min.

Results. There was greater [^{18}F]AV-1451 uptake in the choroid plexus, nigra region, globus pallidus and putamen of older as compared to younger subjects. Gadolinium concentration on DCE MRI was similar in the cerebellum of younger and older subjects, but it was lower in the lateral temporal cortex of older subjects (two-tailed $t=9.51$, $p<0.001$) and higher in the choroid plexus ($t=2.94$, $p<0.01$), substantia nigra ($t=13.23$, $p<0.001$), globus pallidus ($t=9.21$, $p<0.001$) and putamen ($t=8.16$, $p<0.001$) of older as compared to younger subjects.

Conclusion. Increased capillary permeability in choroid plexus, nigra, pallidum and putamen of healthy older subjects could underlie some of the regional differences in [^{18}F]AV-1451 uptake observed in this age group as compared to healthy younger subjects.

PET imaging of tau deposition in the aging human brain

Samuel Lockhart[1], Michael Schöll[1, 2], Daniel Schonhaut[3], James O'Neil[4], Mustafa Janabi[4], Rik Ossenkoppele[1, 3, 5], Suzanne Baker[4], Jacob Vogel[1], Jamie Faria[4], Henry Schwimmer[1], Gil Rabinovici[1, 3, 4], William Jagust[1, 4]

[1]*Helen Wills Neuroscience Institute, University of California Berkeley, CA, United States*
[2]*MedTech West and the Department of Clinical Neuroscience and Rehabilitation, University of Gothenburg, Sweden*
[3]*Department of Neurology, Memory and Aging Center, University of California, San Francisco, CA, United States*
[4]*Molecular Biophysics and Integrated Bioimaging, Lawrence Berkeley National Laboratory, CA, United States*
[5]*Department of Neurology & Alzheimer Center, Neuroscience Campus Amsterdam, VU University Medical Center, Netherlands*

Objective: Tau deposition can be tracked by 18F-AV-1451 PET in living humans; however, associations with age and β-amyloid (Aβ), and between tau and cognition, in cognitively normal older people, have received limited *in vivo* study.

Methods: Using tau PET agent AV-1451 (80-100 min SUVR, cerebellar grey reference), we examined retention patterns in 33 cognitively normal older adults (OA, aged 64-90), in relation to cognitive performance, age, and Aβ load (measured using PiB PET; DVR 35-90 min, cerebellar grey reference, global cortical target mask). Cross-sectional (n = 33) and longitudinal (n = 30) cognitive factor scores were generated from a larger neuropsychological battery, and included episodic memory, processing speed/executive function, working memory, and a composite global cognition measure. 1.5T MRI scans were used to transform all AV-1451 PET images into common space, which were smoothed and masked to focus analyses on cortical grey matter AV-1451 uptake.

Results: We found that AV-1451 was related to cross-sectional and longitudinal cognitive measures (Figure 1), and that there were differences in the patterns associated with age and Aβ (Figure 2). Older age was related to increased tracer retention in regions of the medial temporal lobe (MTL), which predicted worse cross-sectional and longitudinal episodic memory performance. PET detection of tau in other isocortical regions required the presence of cortical β-amyloid (using a global cortical PiB value), and was associated with decline in global cognition (data not shown).

Conclusions: Our results suggest that tau deposition, especially in MTL, is an important aspect of cognitive aging that may have behavioral consequences. It also suggests a relationship between tau and Aβ with implications for Alzheimer's Disease pathogenesis.

Figure 1: Nonparametric voxelwise regression of AV-1451 on (A) cross-sectional performance and (B) retrospective longitudinal change in episodic memory in older adults.

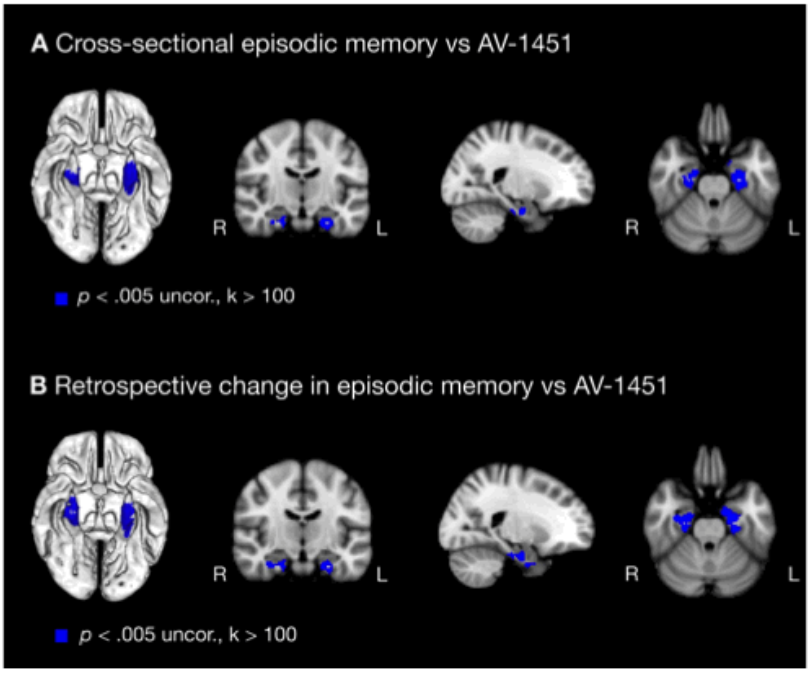

Figure 2: (A) Positive associations (voxelwise nonparametric regression) between age and AV-1451 accumulation in OA (n = 33), controlling for global PiB. (B) Positive associations between PiB DVR and AV-1451 accumulation, controlling for age.

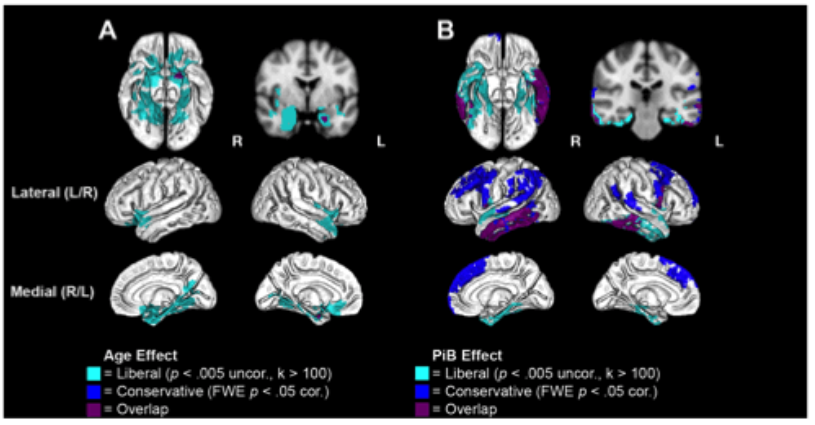

Beta-amyloid deposition, independent of white matter hyperintensities, is associated with altered brain activation in the cognitive control system among clinically normal elderly

Hwamee Oh, Qolamreza Razlighi, Christian Habeck, Yaakov Stern

Department of Neurology and Taub Institute, Columbia University, NY, United States

The accumulation of beta amyloid (Aβ) peptides, a pathological hallmark of Alzheimer's disease (AD), has been associated with functional alterations, often in an episodic memory system with a particular emphasis on medial temporal lobe function. The topography of Aβ deposition, however, largely overlaps with fronto-parietal control (FPC) regions implicated in cognitive control that has been shown to be impaired in early mild AD. To understand the neural mechanism underlying early impairment in cognitive control in the progression of AD, we examined the impact of Aβ deposition on task-evoked FPC activation using functional magnetic resonance imaging (fMRI). Forty-three young and 62 cognitively normal older adults underwent an fMRI session during an executive contextual task in which task difficulty varied: Single (either letter case or vowel/consonant judgment task) vs. dual (switching between letter case and vowel/consonant decisions) task. Older subjects additionally completed 18F-Florbetaben positron emission tomography scans and were grouped into either amyloid positive (Aβ+) or negative (Aβ-). T2-weighted FLAIR images were obtained for older subjects and processed using in-house Matlab-based program procedures to compute white matter hyperintensities (WMH).

Consistent with previous reports, age-related increases in brain activity were found in frontoparietal control regions that were commonly identified across groups. For both task conditions, Aβ-related increases in brain activity were found in comparison to baseline activity. For higher cognitive control load, however, Aβ+ elderly showed reduced task-switching activation in the right inferior frontal cortex, a region important for cognitive control, independent of WMH.

Our results suggest that Aβ deposition, independent of WMH, relates to reduced brain activity in regions important for cognitive control, which may underlie early impairment in executive functions in the progression of AD and serve as an early biomarker reflecting Aβ pathology.

Progression rates from MCI to dementia by biomarker and memory thresholds in ADNI

Warren Barker[1], Maria T Greig[1], Rosemarie Rodriguez[1], David Loewenstein[1, 2], Malek Adjoudai[3], Chunfei LI[3], Gabriel Lizarraga[3], Ranjan Duara[1, 2]

[1]*Wien Center for Alzheimer's Disease and Memory Disorders, Mount Sinai Medical Center, FL, United States*
[2]*Miller School of Medicine, University of Miami, FL, United States*
[3]*Florida International University, FL, United States*

Background: Amyloid load, hippocampal atrophy and memory impairment are risk factors for progression from MCI to dementia. Estimates of the risks conferred by these factors are not readily available to clinicians.

Methods: Data for 497 elderly subjects with a global CDR score of 0.5 was downloaded on 11Nov2015 from the ADNI database. At the baseline amyloid visit, subjects were classified as positive/negative for amyloid (Amy+/-), hippocampal atrophy (HP+/-) and memory impairment (Mem+/-). Thresholds were: Amy+: composite cortical SUVR≥1.1; HP+: hippocampal volume (R+L)/ICV ≤ 0.00476 (Varon et al, 2014); Mem+: Rey Auditory Verbal Learning Test (RAVLT) immediate score <30 (Schmidt et al, 1997). Subjects "progressed" to dementia at the first follow-up visit with a global CDR score of 1 or greater.

Results: 106 subjects progressed to dementia. In multivariate Cox models, all markers (as continuous or dichotomized variables) uniquely predicted progression. The estimated 4-year progression rates to dementia for positive and negative markers were: 55% (44-64%) and 4% (2-9%) for amyloid; 55% (43-66%) and 10% (5-18%) for hippocampal volume; 55% (41-71%) and 25% (17-37%) for memory.

Subjects with concordant positive or negative markers for memory impairment and HP atrophy had a high (75% [51-92%]) or low (6% [3-12%]) likelihood of progression in a 4-year period. The table below shows the additional value of amyloid scans in subjects with discordant markers for memory impairment and HP atrophy.

Progression Rates from MCI to Dementia:
Added value of amyloid imaging to memory testing and MRI imaging

Mem	HP	No Amyloid Scan	Amy+	Amy-
+	-	23% (7-59%)	36% (11-81%)	5% (1-30%)
-	+	41% (27-58%)	56% (31-73%)	2% (-)

Conclusion: Progression from MCI to dementia in a 4-year period ranges from 2% to 75%, based on combinations of markers. Amyloid scans may be especially useful in subjects with discordant findings on MRI and objective cognitive testing.

Statistical methods to measure agreement on the interpretations of beta-amyloid images

Jonathan Mahnken[1, 2], Alvin Beltramo[1]

[1]*The University of Kansas Medical Center, KS, United States*
[2]*The University of Kansas Alzheimer's Disease Center, KS, United States*

New technologies for identifying subjects on a trajectory to develop Alzheimer's disease in a pre-symptomatic state have been developed, including those based on beta-amyloid imaging. However, properly interpreting these images requires special training, and so the level of agreement between independent readers of the same image needs to be better understood.

It is also important to learn which factors drive disagreement between readers, both as they pertain to the characteristics of the reader, such as experience or type of clinical practice, and as they pertain to the patient, such as related clinical history.

We developed a model to evaluate agreement beyond the setting of two raters independently viewing a common set of images to accommodate our research questions and experimental setting.

Some of the statistical challenges in making estimates based on this model, means to overcome these challenges, and the generalizability of this model for other imaging technologies will be presented.

A comparison study of PiB PET in the aspect of mean cortical value and visual read: SUVR, Logan-DVR, and SRTM-DVR

Takashi Kato[1, 2], Ken Fujiwara[2], Yoshitaka Inui[1], Kaori Iwata[2], Naohiko Fukaya[1], Kengo Ito[1, 2], Akinori Nakamura[2], Study Group MULNIAD[2]

[1]Department of Radiology, National Center for Geriatrics and Gerontology, Obu, Japan
[2]Department of Clinical and experimental Neuroimaging, National Center for Geriatrics and Gerontology, Obu, Japan

Background and purpose: The values of SUVR (standard uptake value ratio) and DVR (distribution volume ratio) are generally used for quantitative evaluation of cerebral accumulation of amyloid PET tracers. DVR image is supposed to be superior to SUVR image. In clinical setting for FDA-approved F-18 labeled amyloid tracers, static PET scan image (SUVR-equivalent) is used for visual read. The purpose of this study was to compare the positive/negative discriminating abilities among PiB PET images of SUVR and DVR in the aspect of quantitative values and visual interpretation. DVR image was calculated using Logan graphical plot and SRTM (simplified reference tissue model).

Subjects and method: Subjects selected from in-house studies were 61 CN subjects (age: 69.8±5.7 y.o.), 24 patients with MCI (age: 74.0±6.6), and five patients with AD (age:74.5±7.4). PiB PET scan was performed 0-70 min after the intra-venous injection of PiB (592.2±75.8 (357.0 - 735.4) MBq). SUVR images were made from static scan of 50-70 min. Logan-DVR and SRTM-DVR image was calculated using PMOD software. Mean cortical values of regions of interest werec alculated using Automated anatomical labeling atlas. SUVR, Logan-DVR, and SRTM-DVR images were visually interpreted by two nuclear medicine physician. Cohen's d and Area under the curve (AUC) of ROC analysis were obtained using visual read as gold standard.

Results: The positive/negative visual reads were agreed each other between the SUVR and Logan-DVR in all the cases. In SRTM-Logan, two cases were disagreed and eight cases were undeterminable due to their poor image quality. Cohen's d (2.57-2.62) and AUC (0.979-0.985) were almost identical among the SUVR, Logan-DVR, and SRTM-Logan (except undeterminable cases) images.

Conclusion: The results suggest that SUVR and Logan-DVR of PiB PET are almost equivalent in discriminating the positivity and negativity in visual read and mean cortical value. Further studies are necessary to improve calculation of SRTM-Logan.

FERMT2, CLU and ZCWPW1 are associated with brain amyloidosis

Liana Apostolova[1, 2], Naira Goukasian[1], Triet Do[1], Jonathan Grotts[1], Shannon Risacher[2], Kwangsik Nho[2], David Elashoff[1], Andrew Saykin[2]

[1]*University of California, Los Angeles, CA, United States*
[2]*Indiana University School of Medicine, Indianapolis, IN, United States*

Background: Genome-wide association studies (GWAS) have identified over 20 risk genes for Alzheimer's disease (AD). The precise mechanism through which many of these genes exert their effect on AD remains unknown. We previously found that of the top 20 genes FERMT2 rs17135944, CLU rs11136000, ZCWPW1 rs1476679, MEF2C rs190982 and CASS4 rs3746624 show significant association with mean standard volume uptake ratio (SUVR) in the ADNI-GO/2 cohort.

Objective: To investigate in 3D the pattern of association of these variants and brain amyloidosis.

Methods: Our sample consisted of 248 cognitively normal (NC), 94 subjective memory complaint (SMC), 307 early mild cognitive impairment (EMCI), 202 late MCI (LMCI) and 181 AD subjects from ADNI-GO/2. F18- Florbetapir data was normalized to whole cerebellum yielding SUVR images. Using SPM8 we ran voxel-wise linear regression models with SUVR as the outcome measure and genotypes as predictors while controlling for age, gender and APOE4 status setting the cluster threshold at 50 voxels.

Results: CLU rs11136000 (minor allele OR=0.86) showed significant negative association with anterior and posterior cingulate, precuneus, middle frontal, orbitofrontal and superior parietal SUVR in the pooled sample (Figure 1).

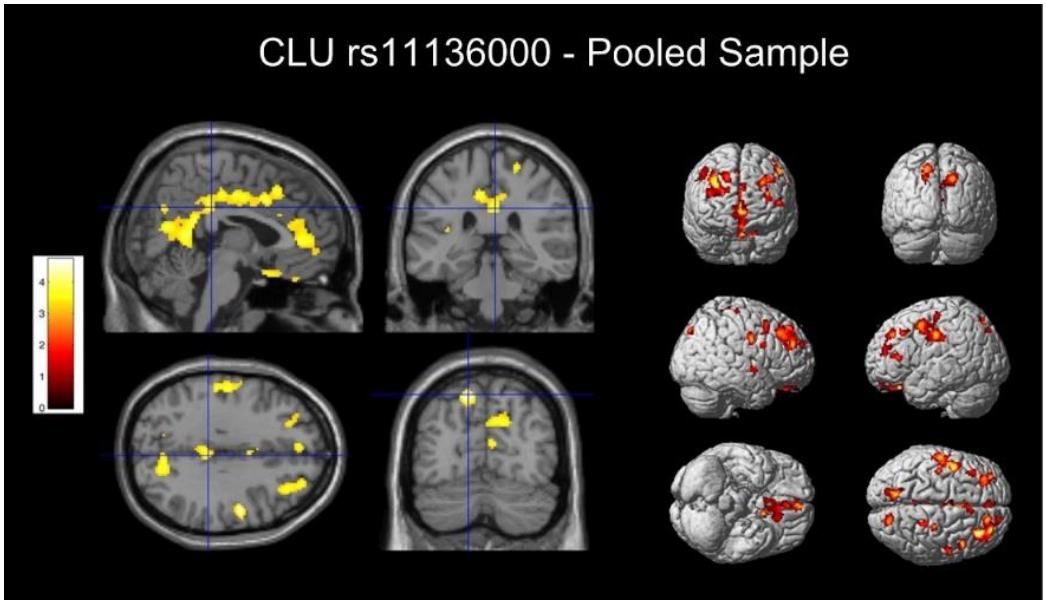

FERMT2 rs17135944 (minor allele OR=1.14) showed a positive effect localized to the medial temporal lobe in the pooled sample and extensive positive SUVR associations in the middle anterior and posterior cingulate, precuneus, lateral parietal, orbitofrontal, inferior and lateral temporal cortices in LMCI and the precuneus in SMC (Figure 2). ZCWPW1 rs1476679 (minor allele OR=0.93) showed a negative association with SUVR in the left lateral temporal and angular gyri in NC only (Figure 3).

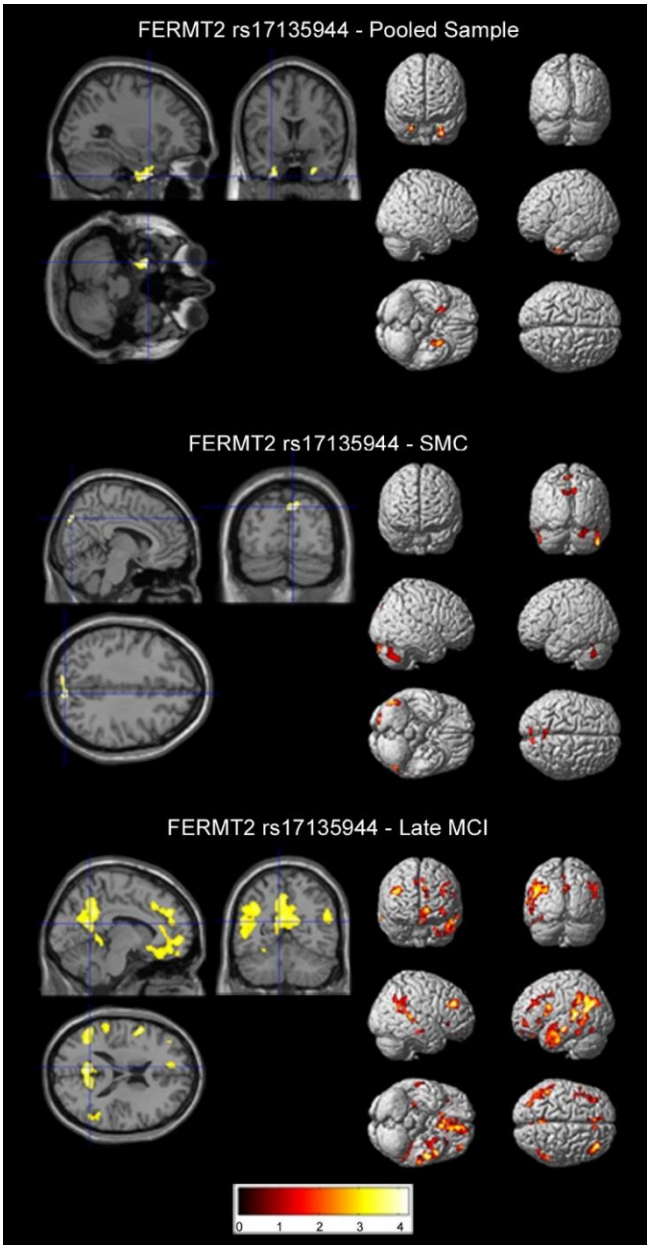

Conclusions: FERMT2, CLU and ZCWPW1 show significant associations with brain amyloidosis in the expected direction. The observed interactions between the effect of FERMT2 and ZCWPW1 and diagnosis indicate that these genes might have a disease-stage specific effect.

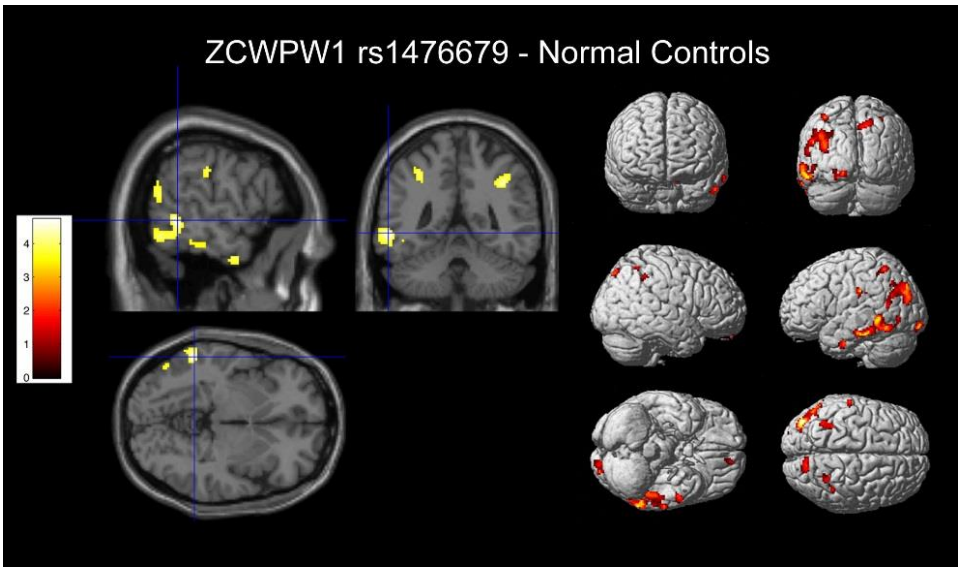

Variability of PiB accumulation in white matter

Val Lowe, Matthew Senjem, Emily Lund, David Jones, Stephen Weigand, David Knopman, Bradley Boeve, Kejal Kantarci, Ronald Petersen, Christopher Schwarz, Clifford Jack

Mayo Clinic, Rochester, MN, United States

Background: C-11 PiB binds to brain white matter (WM) by unclear mechanisms. It is important to understand variability in WM binding to assess WM's suitability as a normalization region. We observed low WM binding in some participants in our ongoing study and therefore evaluated WM PiB binding to assess longitudinal and cross-sectional variability.

Methods: WM PiB uptake in cognitively normal (CN) participants (n=1352 (PiB-positives, n=922 and PiB-negatives, n=430)) was assessed cross-sectionally. Serial WM uptake in participants (n=630; CN, MCI or AD) having at least 2 serial PiB scans were used to evaluate longitudinal WM uptake. WM regions segmented to assess subcortical versus periventricular WM and normalized to cerebellar grey matter (GM) were used (SUVr). PiB GM status was determined by normalization to cerebellar grey matter (GM). Comparisons of regional WM uptake and associations with age were evaluated in CNs. Annual change in WM uptake in the longitudinal group was compared to age, baseline GM uptake and baseline WM uptake.

Results: WM uptake correlated with age in CNs. (Figure 1) The greatest range of SUVr values in WM uptake was seen in PiB- CNs. Modest but significant WM annual change was observed in all regions with mean increases in the range of 0.5% to 1.5% per year ($p<0.001$). (Figure 2) CNs who were GM PiB- tended to have greater rates of accumulation than CN PiB+ participants in the frontal/parietal periventricular, cerebellar, brainstem, and corpus callosum regions. Overall, lower baseline WM values were associated with greater annual WM uptake change ($r=-0.2$ to -0.3, $p<0.001$).

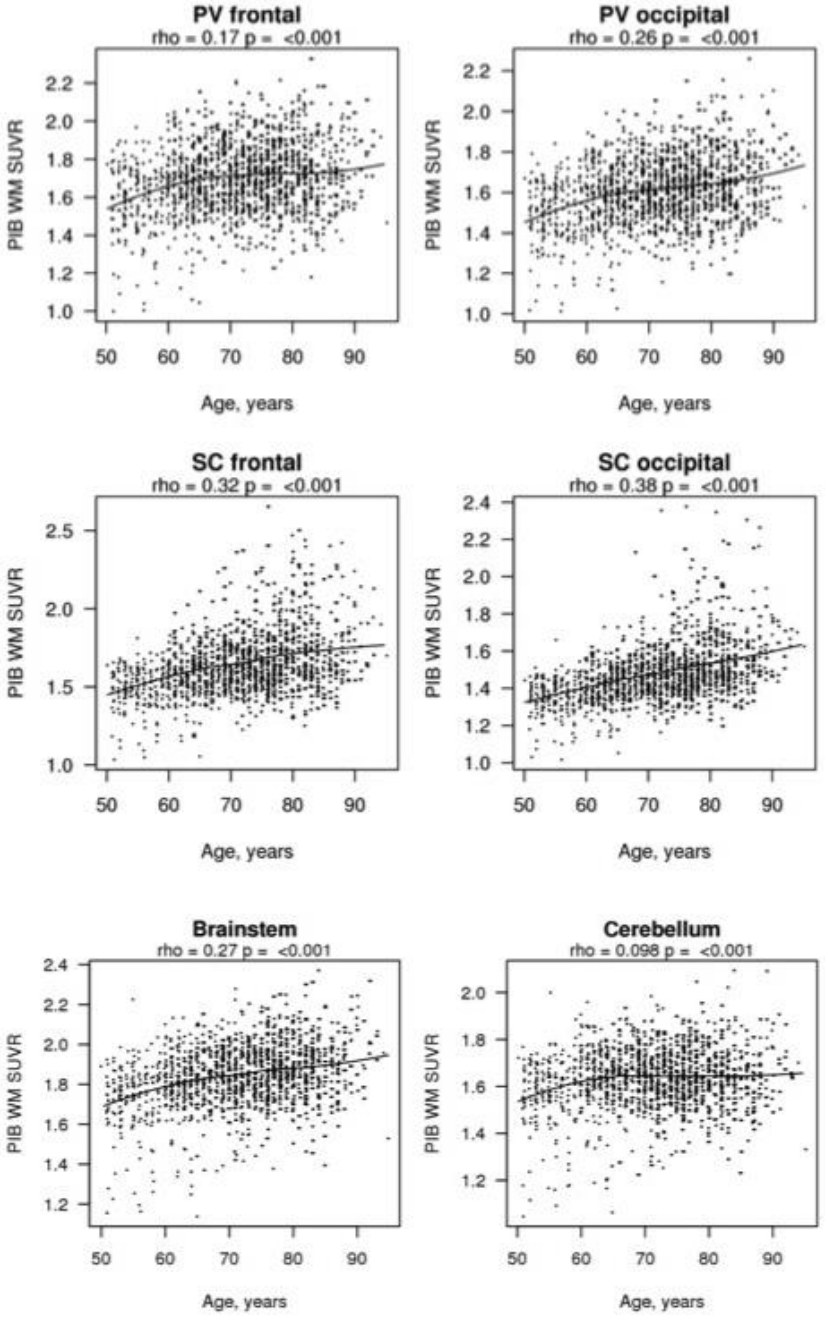

Figure 1: White matter SUVr in frontal and occipital (periventricular/subcortical) and brainstem and cerebellar white matter regions plotted against age. WM SUVr is associated with age in all regions with enchanced association in subcortical regions likely driven by nearby GM signal in PiB+ participants. Cerebellar and brainstem regions with little GM effects also show the association.

Figure2. Annual regional increases in WM PiB uptake in CN participants. Greater annual increases in subcortical WM regions likely reflect adjacent GM influence.

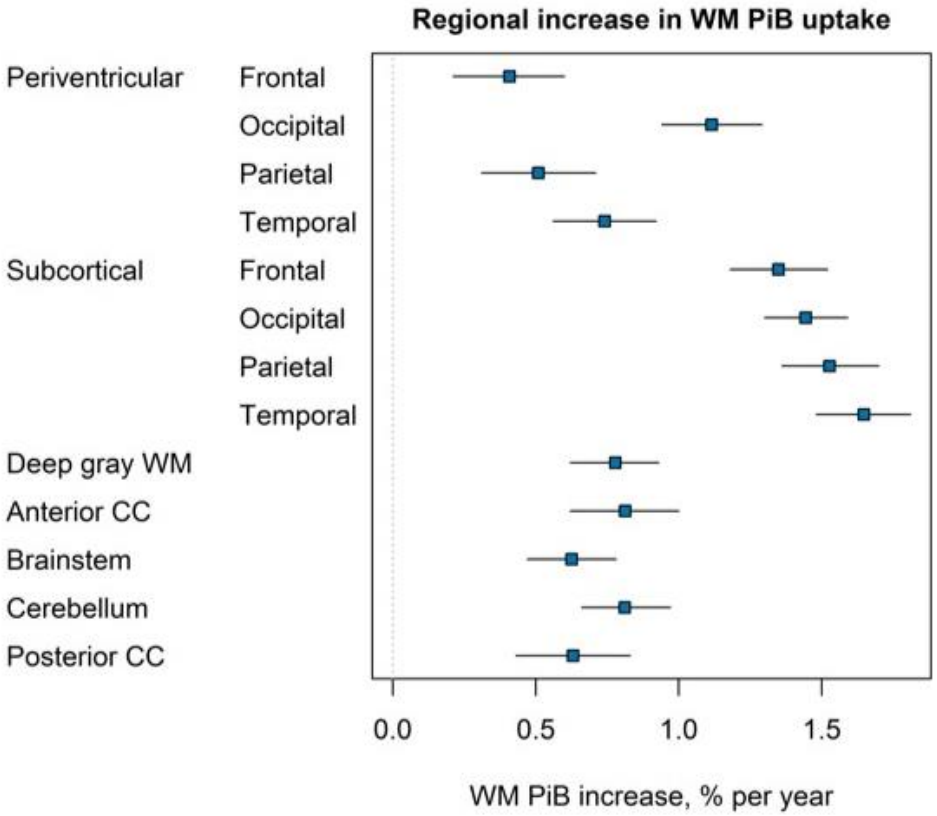

Conclusions: Age and GM PiB status need to be considered when using WM for normalization in cross-sectional analyses. Annual changes in PiB WM uptake are modest and vary with white matter region location and baseline cortical PiB status. These changes need to be considered in longitudinal studies.

Two step hybrid model for predicting clinical progression of dementia

Sulantha Mathotaarachchi[1, 2, 3], Tharick Pascoal[1, 2], Andrea Benedet[1, 2], Min Su Kang[1, 2], Monica Shin[1, 2], Thomas Beaudry[1, 2, 3], Seqian Wang[1, 2], Vladmir Fonov[1, 3], Serge Gauthier[1], Pedro Rosa-Neto[1, 2, 3]

[1]*McGill University, QC, Canada*
[2]*Translational Neuroimaging Laboratory, QC, Canada*
[3]*McConnell Brain Imaging Centre, QC, Canada*

Introduction: Predicting the development of dementia at an early stage has numerous advantages ranging from modified therapeutic interventions to enrichment of clinical trials. Recent advances in machine learning techniques have enabled us to achieve accurate predictions in multiple clinical applications. Present study aims to utilize the Random Forest classifier to predict the development of dementia.

Methods: [18F]Florbetapir images were acquired for 275 MCI individuals from the ADNI cohort and the SUVr maps were generated using cerebellum grey matter and cerebral white matter as reference regions. 70%(192) and 30% of the population were labeled as the training set and the testing set, respectively.

Voxel-wise logistic regression analysis was performed to identify anatomically significant brain regions with highest odds-ratio (OR) to develop dementia with a unit standard deviation of SUVr. A modified Random Forest classifier was trained using 13 features (9 regions based on OR + Global SUVr + Age + Gender + APOE Status) to predict the development of dementia within 24 months based on initial [18F]Florbetapir measurements. Predictor performance was measured against the test set.

Results: Voxel-wise logistic regression analysis indicated that brain regions including Orbitofrontal Cortex, Mid Frontal Sulci, Mid Temporal Sulci, Temporal Occipital junction, PCC, Angular Gyrus, Precuneus, Putamen and the Nucleus Accumbens have the highest OR values for a unit SD increase of [18F]Florbetapir [Figure 1]. Prediction model developed using Random Forest classifier achieved 84% for both average validation accuracy and test accuracy. The Temporal Occipital junction, Mid Temporal Sulci and Mid Frontal Sulci regions indicated the highest contribution in predicting the development of dementia [Figure 2].

Discussion: The developed classifier outperforms the methods developed in previously published literature and can be a utilized as a valuable clinical framework. Regions with the highest contribution can be further investigated to survey regional behavior on the progression of dementia.

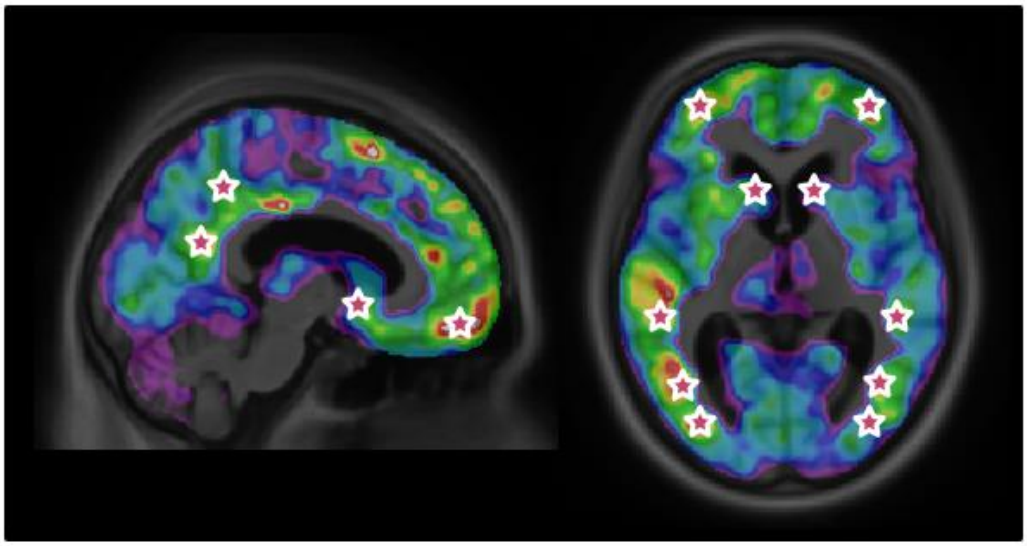

Figure 1: Regions with the highest OR values. Orbitofrontal Cortex, Mid Frontal Sulci, Mid Temporal Sulci, Temporal Occipital junction, PCC, Angular Gyrus, Precuneus, Putamen and the Nucleus Accumbens are indicated.

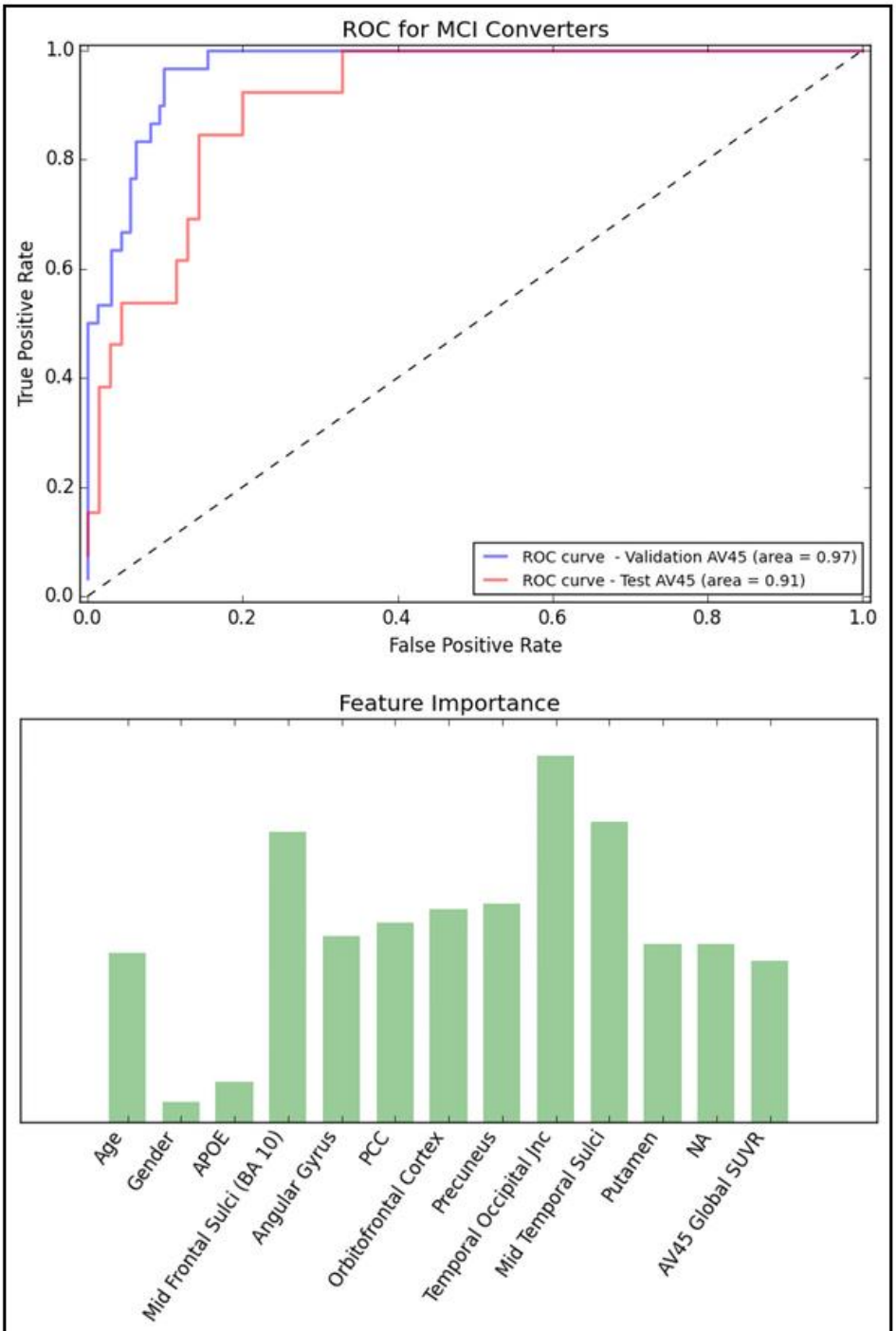

Figure 2: ROC Curve and feature importance graph for the Random Forest classifier in predicting development of dementia. Predictor achieves an AUC of 0.97 for validation and 0.91 for testing. Brain regions such as the Temporal Occipital junction, Mid Temporal Sulci and the Mid Frontal Sulci contribute most to the prediction based on the relative feature importance.

Regional vulnerability associated with the coexistence of brain amyloid-β deposition and hypometabolism

Tharick Pascoal, Sulantha Mathotaarachchi, Sara Mohades, Andrea Benedet, Monica Shin, Min Su Kang, Serge Gauthier, Pedro Rosa-Neto

Translational Neuroimaging Laboratory, The McGill University Research Centre for Studies in Aging, Montreal Canada, QC, Canada

Rationale: A growing body of literature proposes that the coexistence of abnormal amyloid-β deposition (A) and neurodegeneration (N) is determinant to the clinical progression of Alzheimer's disease (AD).

Hypothesis: Here, we tested the hypothesis that the coexistence of these two pathological processes produce specific cognitive signatures according to its regional distribution.

Methods: In order to test this hypothesis, we assessed mild cognitive impairment individuals (n=306) who underwent, at baseline and at two years, [18F]florbetapir and [18F]FDG positron emission tomography (PET) and cognitive assessments (Rey Auditory Verbal Learning Test delay recall (RALVT) (memory), Trail Making Test part B (TMT-B) (executive function) and the Boston Naming Test (BNT) (language)). Individual [18F]florbetapir and [18F]FDG SUVR values were obtained from the regions of interest. For the purpose of the analysis, we divided the participants into four biomarker groups for each region of interest.

Results: We found that A+/N+ individuals segregated based on parahippocampus had significant decline only in RALVT ($P<0.05$), whereas using precuneus or cingulate cortices A+/N+ had significant decline only TMT-B ($P<0.05$). Using the angular gyrus A+/N+ individuals had significant decline in TMT-B and BNT tests ($P<0.05$), while using the medial temporal cortex A+/N+ individuals had significant decline in all neuropsychological functions as compared to other biomarker groups ($P<0.05$). Using occipital lobe A+/N+ individuals did not present neuropsychological declines. The conversion rate to dementia was higher in A+/N+ individuals segregated by the angular gyrus (50%), followed by precuneus (47%), medial temporal lobe (39%), parahippocampus (37%), cingulate (34%) and occipital lobe (16%).

Interpretation: Our results further support the notion that the combination of amyloid-β and neurodegeneration is a valuable strategy to track AD progression. In addition, our results support that evaluating the presence of these pathologies in a regional level may provide complementary information regarding clinical trajectory of individuals.

Amyloid-β and phosphorylated tau synergistic effect drives clinical progression in mild cognitive impairment patients

Tharick Pascoal, Sulantha Mathotaarachchi, Andrea Benedet, Monica Shin, Min Su Kang, Serge Gauthier, Pedro Rosa-Neto

Translational Neuroimaging Laboratory, The McGill University Research Centre for Studies in Aging, Montreal, Canada, QC, Canada

Recent literature suggests that the synergism between amyloid-β and neurodegeneration determines Alzheimer's disease progression. Here, we tested the hypothesis that neuropsychological and clinical decline in mild cognitive impairment individuals is dependent on the synergism between brain amyloid-β deposition and tau hyperphosphorylation. In order to test this hypothesis, we assessed amnestic mild cognitive impairment individuals (n=314) who underwent [18F]florbetapir positron emission tomography, cerebrospinal fluid phosphorylated tau measurements and cognitive testing assessments at baseline and at 2 years. Regression models assessed changes in cognitive tests as a function of baseline imaging and fluid biomarker concentrations. We found that patients with abnormal baseline brain amyloid-β load plus phosphorylated tau had the highest rate of cognitive and clinical decline, as compared with individuals with one or no biomarker abnormalities (P<0.05) (Fig.1). Additionally, regression models revealed that amyloid-β and phosphorylated tau biomarkers' synergistic interaction best predicted cognitive decline and clinical progression to Alzheimer's disease dementia, as compared to the sum of their individual effects (P<0.05). Furthermore, stratified regression analysis showed that the magnitude of amyloid-β and phosphorylated tau biomarkers predicted cognitive decline and clinical progression to dementia only in the presence of abnormal baseline amyloid-β load plus tau phosphorylation (P<0.05). Interestingly, neuropsychological and clinical trajectories did not differ between individuals with mild cognitive impairment having elevated phosphorylated tau but normal amyloid-β deposition (suspected nonamyloid pathology) and biomarker negative individuals.

Together, the present results further support the concept that clinical progression of Alzheimer's disease is driven by a synergism between amyloidosis and neurodegeneration, rather than their respective independent or additive effects. Evidence for the coexistence of abnormal brain amyloid-β deposition and phosphorylated tau might constitute a valuable strategy for population enrichment by including individuals with a higher probability of Alzheimer's disease clinical progression in trials focusing on individuals with amnestic mild cognitive impairment.

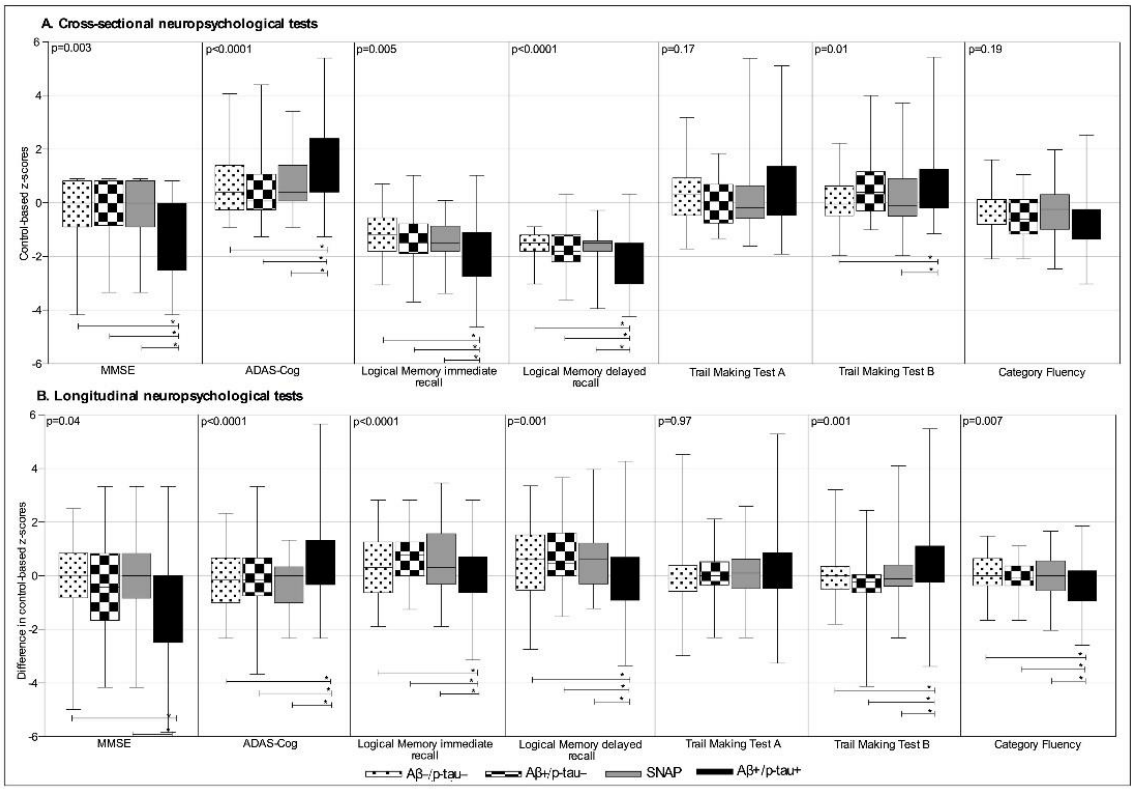

Short-term predictive value of amyloid imaging using NeuroSTAT and subcortical deep search

Richard King, Angela Wang

University of Utah, UT, United States

Objective: Positron emission tomography (PET) using radioligands such as florbetapir (18F-AV-45) has enabled the visualization of b-amyloid, which is a pathologic hallmark of Alzheimer's disease. Processing amyloid-PET data typically involves computing a standardized uptake value (SUV) normalized to a reference region. The purpose of this project is to use a novel method for performing SUV normalization of AV-45 PET imaging data using sterotactic surface projection technology to compute the positive and negative predictive value for symptomatic progression among subject in the Alzheimer's disease neuroimaging initiative (ADNI).

Methods: Baseline AV45 PET Images and demographic data were obtained for 838participants. Using ADNI classifications, the data included 269 normal, 104 significant memory concerns (SMC), 304 early mild cognitive impairment (EMCI), 256 late mild cognitive impairment (LMCI). At the second annual visit, subjects were clinically evaluated as stable or as having converted to a more advanced clinical category. AV45 PET images were analyzed using Neurostat, which extracts regional cortical activity by a three-dimensional stereotactic surface projection (3D-SSP) technique. The algorithm searches for the highest voxel value inward to a depth of 6-pixels (13.5 mm) into the cortex on the anatomically standardized PET image. The peak voxel value is assigned to the predetermined template surface pixel. Cortical uptake values for each region were normalized to the non-specific uptake in the corresponding subcortical white matter. The cutoff amyloid positivity was set at 0.73.

Results: The positive and negative predictive values for each clinical category for conversion at 6 months were as follows; Normal (39 conversion, PPV 0.19, NPV 0.95), SMC (1 conversion), EMCI (17 converters, PPV 0.036, NPV 0.96), LMCI (83 converters, PPV 0.26, NPV 0.83).

Discussion: The prevalence of amyloid positivity increases as clinical symptoms progress. However, the presence of amyloid positivity is not strongly predictive of imminent clinical decline.

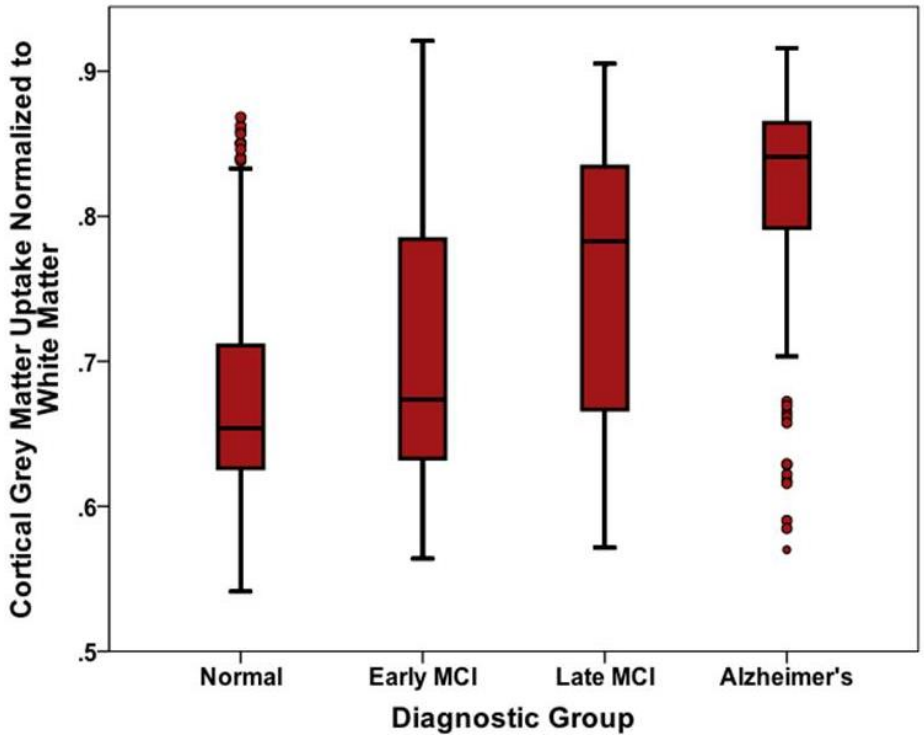

Friday, January 15, 2016 - 10:00 - 11:00am

Podium Presentations

SESSION 8: Tau and Amyloid Biomarker Correlations

Chairs: ***Charles Duyckaerts, Hôpital La Pitié Salpêtrière***
Victor Villemagne, The University of Melbourne

10:00-11:00	**SESSION 8:** **TAU AND AMYLOID BIOMARKER CORRELATIONS**	**CHAIRS:** **Charles Duyckaerts,** Hôpital La Pitié Salpêtrière **Victor Villemagne** University of Melbourne
10:00-10:15	The Tau MeTeR scale for the generation of continuous and categorical measures of tau deposits in the brain: Results from 18F-AV1451 and 18F-THK5351 tau imaging studies	**Victor Villemagne** University of Melbourne
10:15-10:30	Amyloid and tau demonstrate region-specific associations in normal older people	**Samuel Lockhart** University of California, Berkeley
10:30-10:45	Relating cerebrospinal fluid and positron emission tomography measures of tau pathology	**Brian Gordon** Washington University in St. Louis
10:45-11:00	Metabolic efficiency predicts the spatial pattern of Amyloid-β in late life	**Katelyn Arnemann** University of California, Berkeley
11:00-11:40	Discussion	

The Tau MeTeR scale for the generation of continuous and categorical measures of tau deposits in the brain: Results from ^{18}F-AV1451 and ^{18}F-THK5351 tau imaging studies

Victor L Villemagne[1, 2, 3], Vincent Doré[1, 4], Pierrick Bourgeat[4], Tia Cummins[1, 3], Svetlana Pejoska[1], Rachel Mulligan[1], Laura Margison[1], Olivier Salvado[4], Colin L Masters[3], Christopher C Rowe[1, 2]

[1]*Dept of Molecular Imaging & Therapy & Centre for PET, Melbourne, Australia*
[2]*Dept of Medicine, The University of Melbourne, Australia*
[3]*The Florey Institute of Neuroscience and Mental Health, The University of Melbourne, Australia*
[4]*CSIRO Digital Productivity Flagship, The Australian e-Health Research Centre, Brisbane, Australia*

Background: It has been postulated that tau spreads stereotypically from the mesial temporal cortex (MTC) into neocortex and that tau deposition restricted to MTC might be just part of the ageing process, suggesting that both the amount and the location of these tau deposits are likely to be relevant in regards to disease staging, prognosis and progression. We implemented a stereospecific approach to generate both continuous and categorical measures that reflect tau spreading and deposition in order to make results from tau imaging studies clinically relevant and easy to interpret.

Methods: Fifty-nine participants underwent tau and Aβ imaging with ^{18}F-AV1451 and ^{18}F-florbetapir (44-HC, 12-MCI, 4-AD), while 33 received ^{18}F-THK5351 and ^{18}F-flutemetamol (16-HC, 11-MCI, 6-AD). Three tau-masks were constructed: Mesial-temporal (**Me**) comprising entorhinal cortex, hippocampus, parahippocampus and amygdala; Temporoparietal (**Te**) comprising inferior temporal, fusiform, supramarginal and angular gyri, posterior cingulate/precuneus, superior and inferior parietal, and lateral occipital; and Rest of neocortex (**R**) comprising dorsolateral & ventrolateral prefrontal, orbitofrontal, gyrus rectus, superior and middle temporal, and anterior cingulate. A threshold was established for each mask and tracer. A global SUVR was determined by averaging the SUVR of the 3 composite regions. Categorically, a study was deemed "high" when at least 2 of 3 regions showed high tracer retention. The relationship between Aβ and tau was also explored.

Results: A categorical classification using global cut-offs of 1.3-SUVR (^{18}F-AV1451) and 1.8-SUVR (^{18}F-THK5351), yielded similar classification than obtained through the 3 composites. While the sample size is still low, both tracers showed that MTC was high irrespective of Aβ levels, in contrast with the other 2 neocortical regions where high cortical tau was associated with high Aβ.

Conclusions: We have developed a scale that accounts for the particularities of tau deposition, yielding both continuous and categorical measures of tau imaging studies.

Amyloid and tau demonstrate region-specific associations in normal older people

Samuel Lockhart[1], Michael Schöll[1, 2], Taylor Mellinger[1, 3], Kaitlin Swinnerton[1, 3], Rachel Bell[1, 3], Suzanne Baker[1, 3], William Jagust[1, 3]

[1]*Helen Wills Neuroscience Institute, University of California, Berkeley, CA, United States*
[2]*MedTech West and the Department of Clinical Neuroscience and Rehabilitation, University of Gothenburg, Sweden*
[3]*Molecular Biophysics and Integrated Bioimaging, Lawrence Berkeley National Laboratory, CA, United States*

Objectives: To examine local (same region) and nonlocal (different regions) associations between PiB and AV-1451 PET (markers of β-amyloid [Aβ] and tau deposition, respectively) in normal aging.

Methods: 36 cognitively normal older adults (78.4 ± 5.0 y) received AV-1451 and PiB PET and MRI, with all images transformed to a common space. Using biological parametric mapping (BPM) on smoothed (4mm) images, we characterized local cortical PiB—AV-1451 associations. We also calculated mean AV-1451 and PiB values within 87 regions of interest (ROI), and a global cortical PiB value, for each subject. We examined PiB—AV-1451 correlations for all pairwise ROIs for strength and significance to identify PiB—AV-1451 association patterns, and explored relationships between pairwise correlation strength and mean PET signal.

Results: BPM revealed local association patterns and their relation with increases in AV-1451 or PiB PET signal (Figure 1). Pairwise ROI analysis demonstrated positive and negative PiB—AV-1451 associations (Figure 2). Importantly, strong ($p < .001$) positive correlations were identified between AV-1451 in temporal lobes and PIB in numerous temporal and extra-temporal ROIs. We additionally found less frequent but strong positive associations of regional PiB with frontoparietal AV-1451. Further, we found that significant positive pairwise correlations were driven by elevated regional values of PiB and AV-1451 (relative to non-significant correlations).

Conclusions: Aβ and tau pathology, measured using PET, show significant associations among cognitively normal elderly. These associations exist locally, as shown by BPM, but critically they also exist nonlocally. In particular, increased Aβ both within and outside the temporal lobes is correlated with tau in the temporal lobes. Further, significant positive PET correlations appeared to be driven by pathology reaching critical thresholds, with a certain burden of Aβ and tau pathology necessary for the pathologies to be correlated.

Figure 1: (A) Significant BPM PiB—AV-1451 associations ($p < .001$, cov. age and sex), clusters labeled by median smoothed PET signal. (B) Median smoothed PiB and AV-1451 signal in each significant cluster (k-means labeling of clusters).

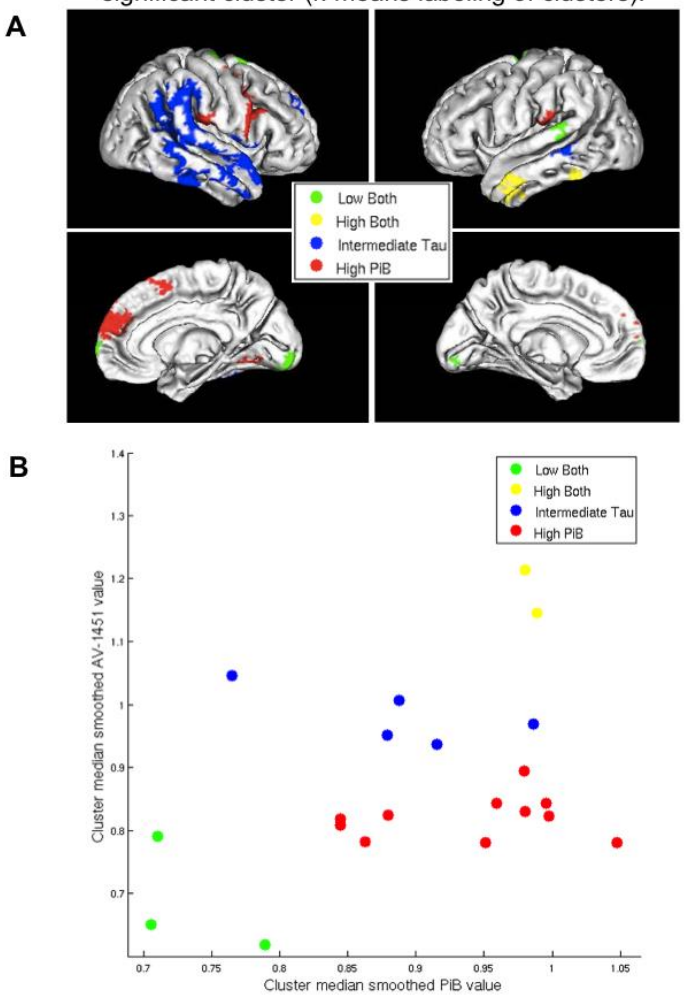

Figure 2: Correlation matrix for 87 regions and a global cortical PiB value, thresholded at $p < .001$, collapsed by hemisphere and lobe.

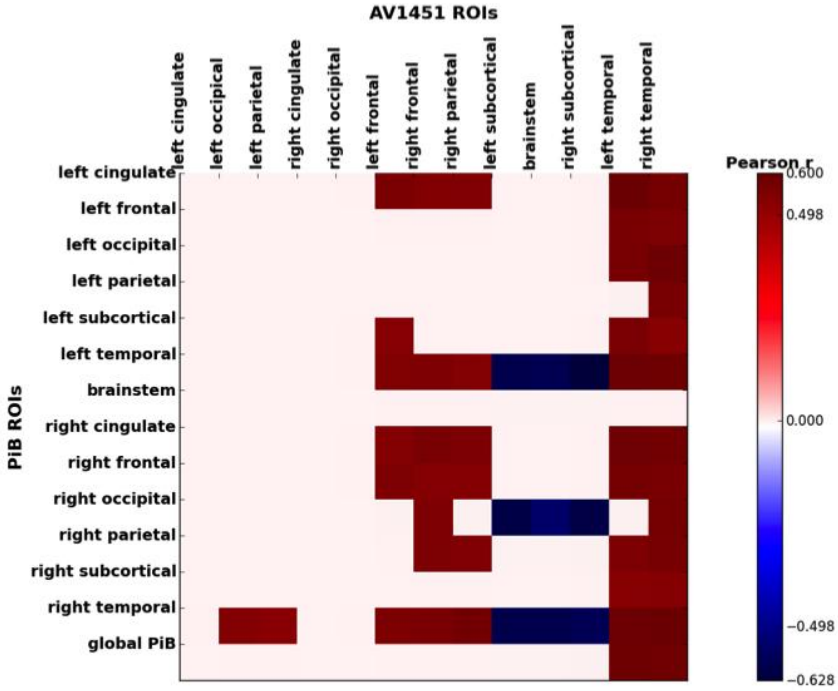

Relating cerebrospinal fluid and positron emission tomography measures of tau pathology

Brian Gordon[1, 2], Karl Friedrichsen[1], Matthew Brier[3], Tyler Blazey[4], Yi Su[1], Jon Christensen[1], Patricia Aldea[1], Jonathan McConathy[1], David Holtzman[2, 3, 4, 5], Nigel Cairns[2, 3, 4], John Morris[2, 3], Anne Fagan[2, 3, 4], Beau Ances[2, 3, 4], Tammie Benzinger[1, 2, 6]

[1]*Washington University in St. Louis, Department of Radiology, MO, United States*
[2]*Knight Alzheimer's Disease Research Center, MO, United States*
[3]*Washington University in St. Louis, Department of Neurology, MO, United States*
[4]*Washington University in St. Louis, Division of Biology and Biomedical Sciences, MO, United States*
[5]*The Hope Center for Neurological Disorders, MO, United States*
[6]*Washington University in St. Louis, Department of Neurological Surgery, MO, United States*

Background: The two primary pathologies in Alzheimer disease are the aggregation of beta-amyloid into plaques and of tau into neurofibrillary tangles. Quantifications of these pathologies in vivo have been restricted to cerebrospinal fluid (CSF) assays, and positron emission tomography (PET) using amyloid tracers. The recent addition of PET tau tracers provides a valuable tool, although the relationships of this tracer to other Alzheimer biomarkers are still unknown.

Methods: We examined the radioactive [F-18]- AV-1451 positron emission tomography (PET) tracer, a tau ligand, in a population of 41 cognitively normal and 9 demented older adults. All participants underwent a lumbar puncture to assess CSF levels of total tau, p-tau181 and Aβ42. Statistics were run at a voxel-wise level using nonparametric permutation testing to examine patterns of elevated tau deposition associated with cognitive impairment as well as levels of CSF biomarkers. All analyses controlled for age and gender. Analyses examining the relationships between PET and CSF measures included the time between imaging and lumbar puncture assessments as an additional covariate.

Results: Cognitive impaired individuals (Clinical Dementia Rating >0) had elevated levels of PET tau deposition. This elevation was most prominent in the medial temporal lobe and temporoparietal junction, but extended more broadly into parietal and frontal cortices. In the entire cohort, there were significant relationships between all CSF biomarkers and PET tau deposition, but the strongest relationships were for CSF tau-related markers. Within the cognitively normal cohort (CDR=0) levels of CSF Aβ42, but not t-tau or p-tau181, were associated with elevated PET tau deposition confined primarily to the medial temporal lobe and adjacent neocortical regions.

Conclusions: In cognitively normal individuals, AD pathology is associated with focal tau pathology when measured with [F-18]- AV-1451. Tau deposition is elevated in cognitively impaired individuals, and this deposition is highly correlated with CSF measures of tauopathy.

Figure 1

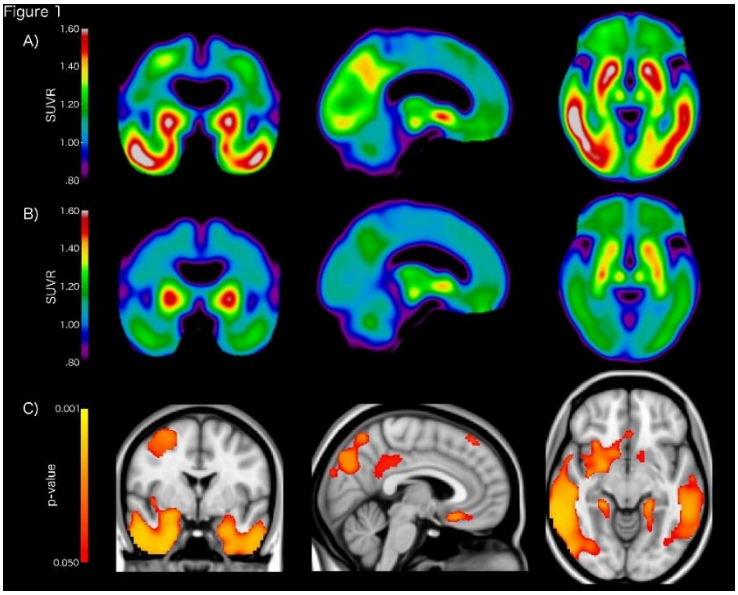

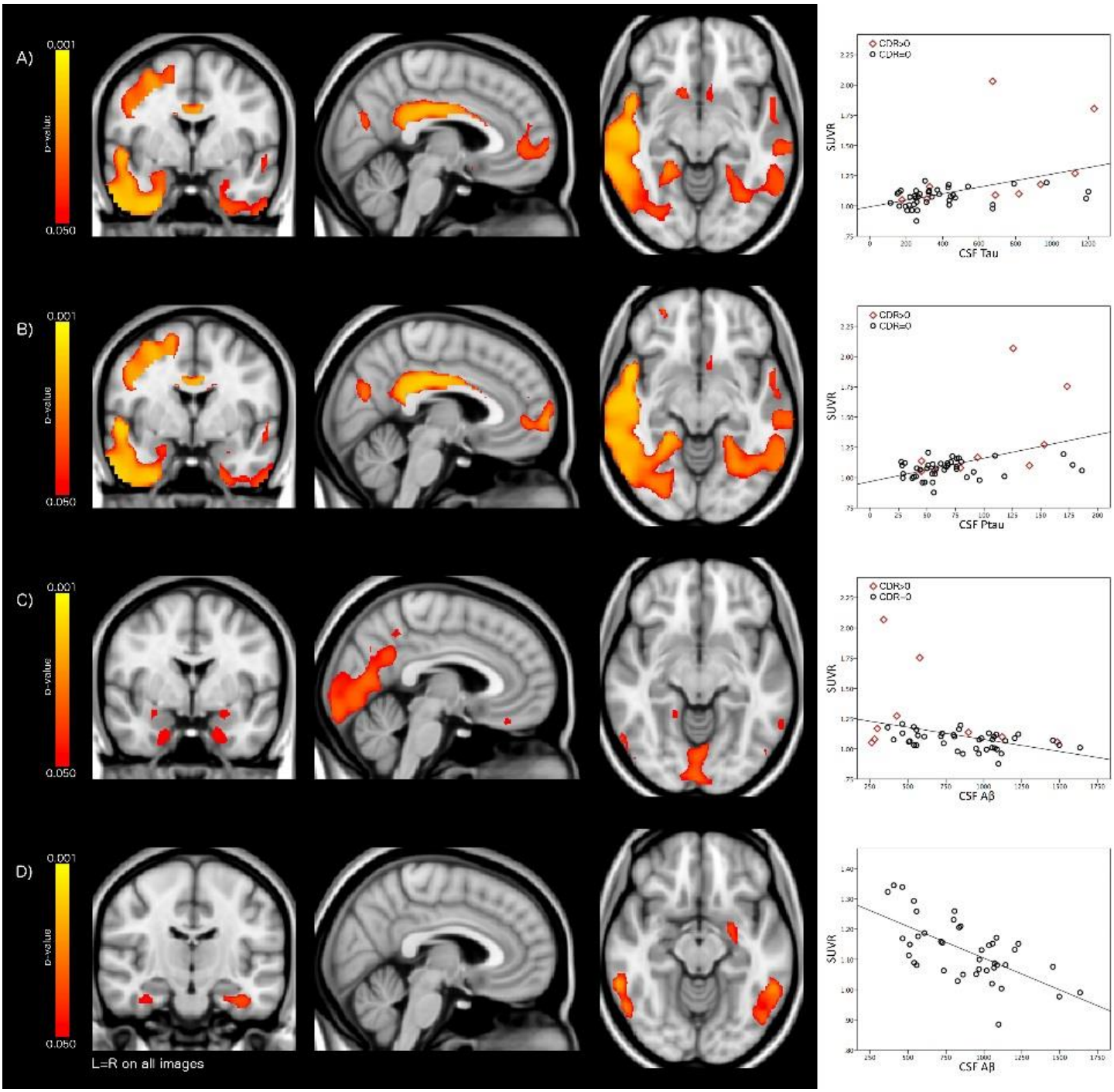
A)
B)
C)
D)
0.001
p-value
0.050
L=R on all images
CDR>0
CDR=0
SUVR
CSF Tau
CSF Ptau
CSF Aβ
CSF Aβ

Metabolic efficiency predicts the spatial pattern of amyloid-β in late life

Katelyn Arnemann, Leonardino Digma, Sharada Narayan, Ollie Peng, William Jagust

University of California, Berkeley, CA, United States

Amyloid-β (Aβ) exhibits a stereotyped spatial pattern of deposition across the brain. We hypothesized that spatial patterns of Aβ would relate to network centrality (i.e. "hubness"), glucose metabolism, and a novel measure that combines the two which we call metabolic efficiency. We used measures derived from young adults, centrality from resting-state fMRI (N=62, age=23±2.8) and glucose metabolism from FDG-PET (N=13, age=23±2.0), to predict the location of Aβ deposition from PIB-PET in cognitively normal older adults (N=135, age=76.4±5.8, PIB DVR=1.04±0.1). We first examined the interrelationships between multiple metrics of centrality and their relationship to metabolism in order to define redundance among centrality metrics. We then used the centrality measures to model metabolism via multiple linear regression, using the residual as a novel metric "metabolic efficiency", which identified brain regions with lower (more efficient) or higher (less efficient) metabolism than predicted by the region's centrality. We found that brain regions with low metabolic efficiency in youth accumulated more Aβ in older people (p=0.00006), and that metabolic efficiency was more strongly correlated with the spatial pattern of Aβ deposition (R=0.48, p=0.00001) than was metabolism (R=0.26, p=0.02) or the most strongly correlated measures of centrality (participation coefficient: R=0.38, p=0.0007 and betweenness centrality: R=-0.35, p=0.001). Interestingly, degree, betweenness centrality, and within-module degree demonstrated the opposite relationship with metabolism and Aβ deposition than participation coefficient, such that the former were positively correlated with metabolism and negatively correlated with Aβ, whereas the latter was negatively correlated with metabolism and positively correlated with Aβ. Although centrality and metabolism covary, this work suggests that low metabolic efficiency in brain regions that are more metabolic than predicted by their network connectivity leads to Aβ pathology. While the cause of this vulnerability remains to be determined, reduced efficiency may reflect more neural activity that leads to greater Aβ secretion.

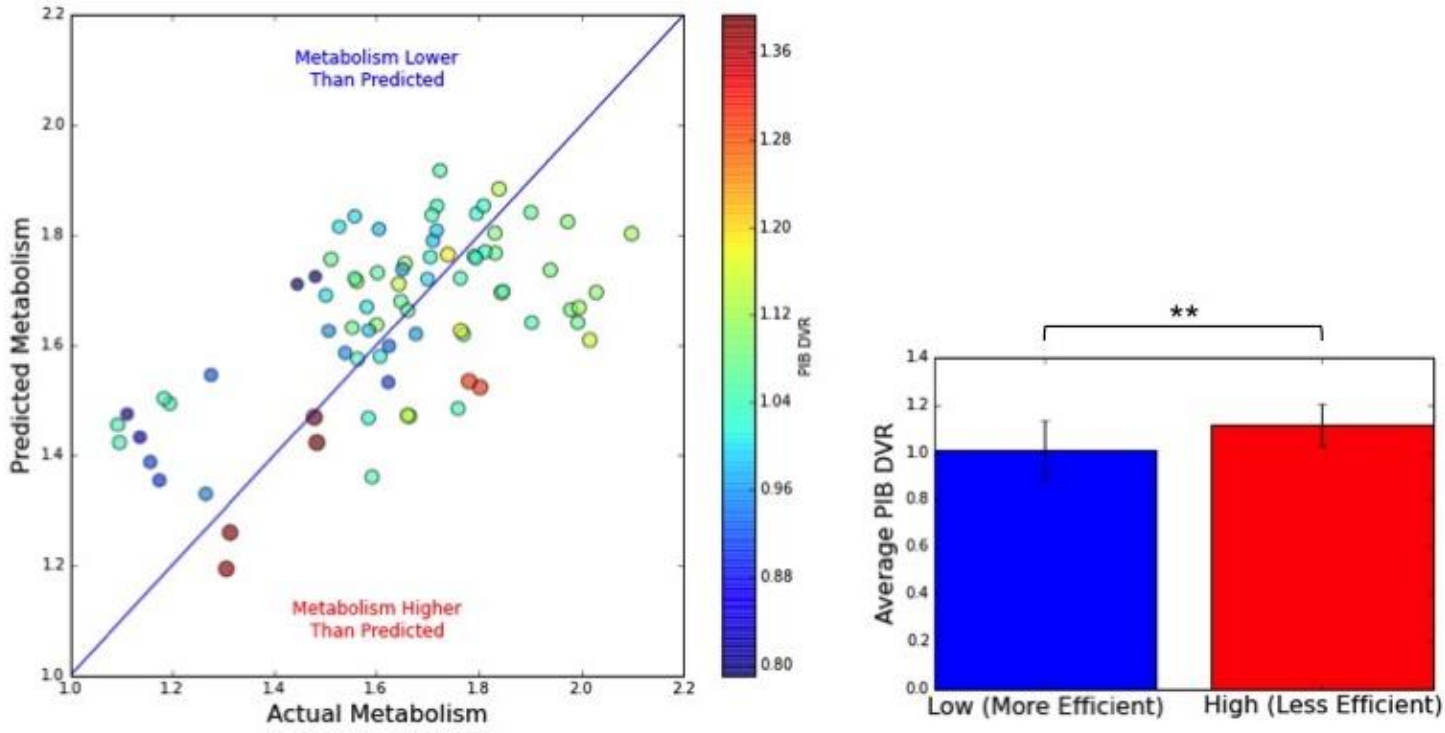

Figure 1: (Left) Regional measures of actual metabolism versus metabolism predicted by multiple linear regression of metabolism on hubness (FDG = β_1+dcen + β_2-dcen + β_3+pc + β_4-pc + β_5+wd + β_6-wd + β_7+bcen; R^2=0.37) in young subjects, colored by average regional PIB DVR in older subjects **(Right)** Comparison of average PIB DVR in regions with **(blue)** metabolism lower than predicted (i.e. more metabolically efficient) and **(red)** less metabolism than predicted (i.e. less metabolically efficient) from the regression model of metabolism on hubness. ** p>0.00006

Friday, January 15, 2016 - 11:40 - 12:10pm

Keynote Lecture

Synergy of Aβ and tau pathologies, neuropathological data

Charles Duyckaerts

Laboratoire de Neuropathologie Raymond Escourolle, Groupe Hospitalier Pitie-Salpetrière-Charles Foix, ICM, UPMC, Paris, France

Two components – tau intraneuronal aggregation and Aβ extracellular accumulation- characterize Alzheimer disease. Genetic data and animal models point to a disturbance of production or of clearance of Aβ peptide as the primary pathogenic mechanism. At first sight, however, the neuropathological data contradict the hypothesis. In two well-known systems of connections –entorhino-dentate and subiculo-fornico-mammillary – the first visible changes are tau positive axons. Aβ deposits appear secondarily while axons degenerate. In the same way, tau immunoreactivity may appear first in subcortical nuclei, such as the raphe nuclei, the locus coeruleus and the nucleus basalis of Meynert, that project directly to cerebral cortex, still free of Aβ deposits. The secondary appearance of Aβ deposits in the distal synaptic fields of tau positive neurons is thus a common morphological feature. It is tempting to consider that such observation indicates that tau positive neurons secrete Aβ that accumulates and form senile plaques. Alternatively, if a change in Aβ metabolism is to be taken as the primary pathogenic mechanism preceding tau pathology, that change is clearly invisible with current morphological methods. The visible accumulation of Aβ in senile plaques is then to be considered as a late by-product that occurs, however, in the specific areas where the initial alteration took place. If, indeed, the first Aβ alterations are only visible through their consequence on tau aggregation, it is inadequate to isolate from the Alzheimer continuum cases with initial tau positive changes as has been done with the concept of "primary age-related tauopathy" (PART). Progression of both Aβ and tau pathologies has been mimicked experimentally in a manner suggestive of a prion-like transmission. In the Human, contacts between tau positive neurons, clearly visible at the microscopic level, evokes an invasion of the connective network independent of Aβ pathology: the chronology and the distribution of Aβ accumulation, however, coincides in many aspects with tau progression from distal synapses of the initially affected neuron to dendrites of the secondarily involved one. Aβ seems to favor or, even, to permit progression of tau pathology through synapses. Alzheimer disease is, from the symptomatic point of view, a tauopathy related to a primary, still badly understood, alteration in Aβ metabolism.

Friday, January 15, 2016 - 1:50 - 2:50pm

Podium Presentations

SESSION 9: Translation to Clinical Populations and Genetic Factors

Chairs: ***Christopher Rowe, The University of Melbourne***
Andrew Saykin, Indiana University

1:50-2:50	**SESSION 9:** **TRANSLATION TO CLINICAL POPULATIONS AND GENETIC FACTORS**	**CHAIR:** **Christopher Rowe** The University of Melbourne **Andrew Saykin** Indiana University
1:50-2:05	Appraisal of the utility of the AIT appropriate use criteria of the Amyloid-PET	**Marina Boccardi** IRCCS Centro San Giovanni di Dio Fatebenefratelli
2:05-2:20	[11C]PiB imaging in the Down syndrome population: A closer investigation of amyloid burden in the striatum	**Patrick Lao** University of Wisconsin–Madison
2:20-2:35	APOE epsilon 2 genotype associates with reduced amyloid load but does not affect brain structure or function in non-demented older individuals	**Michel Grothe** German Center for Neurodegenerative Diseases
2:35-2:50	Association between [11C]PIB PET and CSF Aβ1-42 in a multicentre European memory clinic population	**Antoine Leuzy** Karolinska Institutet
2:50-3:30	Discussion	

Appraisal of the utility of the AIT appropriate use criteria of the amyloid-PET

Marina Boccardi[1], Daniele Altomare[1], Ugo Guerra[2], Michela Pievani[1], Emiliano Albanese[3], Cristina Festari[1], Luigi Antelmi[4], Patrizio Pasqualetti[5], Cristina Muscio[1, 6], Flavio Nobili[7], Alessandro Padovani[8], Giovanni Frisoni[1, 4, 9]

[1]*Laboratory of Alzheimer's Neuroimaging and Epidemiology, IRCCS Centro San Giovanni di Dio Fatebenefratelli, Brescia, Italy*
[2]*Department of Nuclear Medicine, Poliambulanza Foundation, Brescia, Italy*
[3]*Department of Mental Health and Psychiatry, University Hospital of Geneva, Switzerland*
[4]*LANVIE - Laboratory of Neuroimaging of Aging, University Hospitals of Geneva, Switzerland*
[5]*Fatebenefratelli Hospital of Isola Tiberina, Roma, Italy*
[6]*European Foundation Biomedical Research (FERB), Center of Excellence Alzheimer, Ospedale Briolini of Gazzaniga, Bergamo, Italy*
[7]*Clinical Neurology, Department of Neuroscience (DINOGMI), University of Genoa, Italy*
[8]*Centre for Neurodegenerative Disorders, Neurology Unit, University of Brescia and Spedali Civili of Brescia, Italy*
[9]*Memory Clinic, University Hospitals and University of Geneva, Switzerland*

Background: Appropriate Use Criteria (AUC) for the prescription of amyloid-PET were published by the Amyloid Imaging Task force (Johnson et al., 2013) before the availability of studies assessing the impact of the exam. The aim of this work is to test the hypothesis that prescription of the amyloid-PET according to AUC (AUC-like) is associated with greater clinical utility than inappropriate prescription (Non-AUC-like).

Methods: From a study on the impact of the amyloid-PET on patients with cognitive impairment, we aimed to select 2 groups of patients: AUC-like and Non-AUC-like. The AUC were operationalized as reported in Figure 1. The clinical utility was evaluated as follows.

Figure 1. Algorithm for the definition of AUC-like and Non-AUC-like groups.

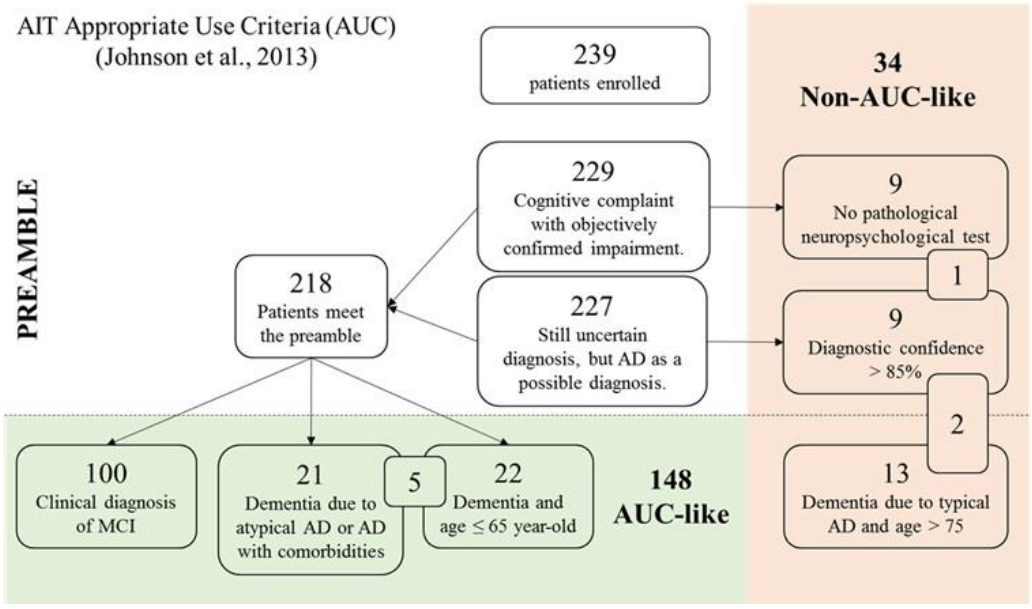

- Consistent diagnostic change: from AD to Non-AD after negative amyloid-PET, or from Non-AD to AD after positive amyloid-PET in patients aged ≤ 65 y/o.

- Consistent therapeutic change in cognition-specific medications (i.e. acetylcholinesterase inhibitor (AChEI) and memantine): reduced after negative amyloid-PET, or increased after positive amyloid-PET.

- Consistent therapeutic change in cognition-non-specific medications (i.e. anxiolytic, hypnotic, antidepressants, antipsychotics and anticonvulsants): increased after negative amyloid-PET, or reduced after positive amyloid-PET.

- Overall consistent change in diagnosis or medications.

- Increase in diagnostic confidence after the amyloid-PET independently from diagnosis and scan result.

We compared frequencies of patients showing clinical utility in AUC- and Non-AUC- like groups by Fisher's Exact Test and assessed the increase in diagnostic confidence by Mann-Whitney Test (W).

Results: We extracted 148 AUC-like and 34 Non-AUC-like patients. We found no difference between AUC-like and Non-AUC-like in the evaluated outcomes (Table 1).

Table 1. Consistent diagnostic and therapeutic changes in patients AUC-like and Non-AUC-like.

Amyloid-PET utility	AUC-like (N = 148)	Non-AUC-like (N = 34)	Between-group comparisons*
Consistent diagnostic change	26% (38)	21% (8)	$p = 1$
Consistent therapeutic change in cognition-specific medications	30% (45)	21% (8)	$p = 0.53$
Consistent therapeutic change in cognition-non-specific medications	7% (10)	12% (4)	$p = 0.30$
Overall consistent change (in diagnosis or medications)	57% (84)	47% (16)	$p = 0.34$
Increase in diagnostic confidence	+10.5% (13.8)	+6.2% (14.4)	$p = 0.14$ $r = 0.11$

Conclusion: AUC-like prescription does not correspond to greater clinical utility. Future investigation may improve the AUC based on the evidence that current studies on amyloid-PET are collecting.

[^{11}C]PiB imaging in the Down syndrome population: A closer investigation of amyloid burden in the striatum

Patrick Lao[1], Tobey Betthauser[1], Julie Price[2], William Klunk[2], Peter Bulova[2], Sigan Hartley[1], Regina Hardison[2], Rameshwari Tumuluru[2], Dhanabalan Murali[1], Chester Mathis[2], Ann Cohen[2], Todd Barnhart[1], Darlynne Devenny[3], Sterling Johnson[1], Benjamin Handen[2], Bradley Christian[1]

[1]*University of Wisconsin-Madison, Departments of Medical Physics, Psychiatry, Mechinie-Geriatrics and Waisman Center, WI, United States*
[2]*University of Pittsburgh, Department of Psychiatry, Medicine, Radiology, and Epidemiology Data Center, PA, United States*
[3]*New York State Institute for Basic Research in Developmental Disabilities, NY, United States*

Background: Amyloid PET imaging in genetically predisposed populations such as APP, PS1, and PS2 mutation carriers as well as individuals with Down syndrome (DS), has revealed early accumulation of fibrillar amyloid-β plaques in striatal regions. The goal of this work was to investigate the patterns of elevated PiB binding in striatal regions, prior to that in cortical regions, for individuals with DS.

Methods: In an ongoing longitudinal [^{11}C]PiB PET study of young DS participants (n=72, age=30-53), parametric SUVR images of the baseline scans were generated from data 50-70 min post-injection using a cerebellar gray matter reference region. ROIs were defined in standard space and PiB positivity was determined based on the mean SUVR in the anterior cingulate, frontal cortex, parietal cortex, precuneus, striatum, or temporal cortex exceeding a ROI specific PiB positivity threshold established by k-means clustering. Therefore the classification of a subject as PiB+ can arise from one, several, or all ROIs exceeding their PiB positivity threshold. The striatum was further divided into caudate (head and body), putamen, and nucleus accumbens.

Results: Of the 28% (20/72) of subjects that were classified as PiB+, the striatum demonstrated supra-threshold binding in almost all cases (19/20).

20% (4/20) were positive in striatum only and 55% (11/20) were positive in all six ROIs.

Within the striatum, the mean PiB SUVR in putamen was highest, followed by that in caudate (body>head) and in nucleus accumbens.

	PiB+ Pattern					
Subject Number(s)	AC	FC	P	PC	S	TC
1-11	+	+	+	+	+	+
12	+	+	-	+	+	+
13	-	-	+	+	+	-
14	+	+	-	+	+	+
15	-	-	-	+	+	-
16	-	-	+	+	-	+
17-20	-	-	-	-	+	-
21-72	-	-	-	-	-	-

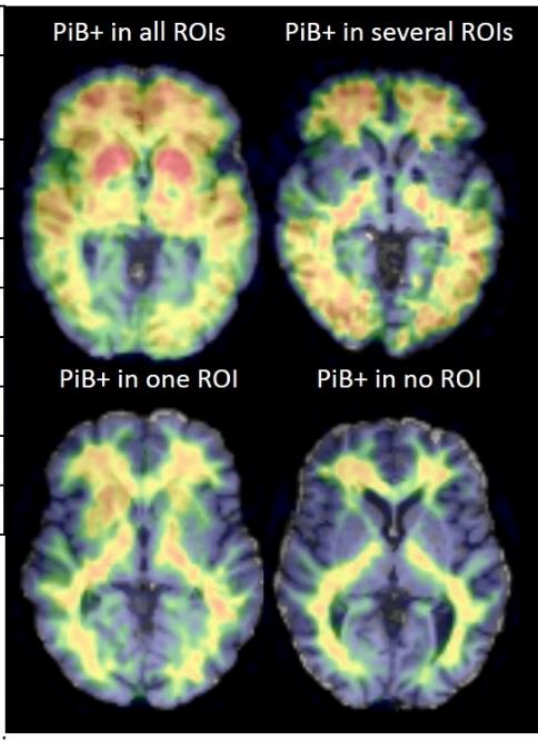

Figure 1. PiB positivity shown by subject and region of interest (ROI). A positive symbol indicates a mean PiB standard uptake value ratio (SUVR) exceeding the PiB positivity threshold for that ROI. PiB SUVR images were PiB+ in all, several, one, or no ROIs. ROIs include the anterior cingulate (AC), frontal cortex (FC), precuneus (P), parietal cortex (PC), striatum (S), and temporal cortex (TC).

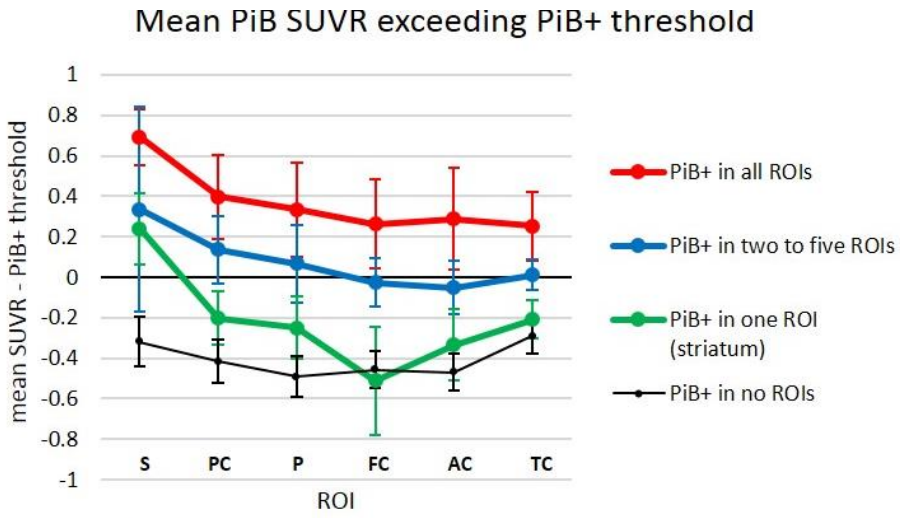

Figure 2. Mean PiB standard uptake value ratio (SUVR) in 6 regions of interest (ROI; S=Striatum, PC=Parietal Cortex, P=Precuneus, FC=Frontal cortex, AC=Anterior cingulate, TC=Temporal cortex) by PiB positivity pattern suggesting that fibrillar amyloid-β accumulates across all ROIs in striatum-dominant manner as disease neuropathogenesis progresses.

Conclusion: Based upon this cross-sectional analysis of the baseline studies, PiB binding in younger subjects is equally low throughout the brain, but gradually accumulates in a striatum dominant pattern that is present in nearly all individuals with DS. The putamen and caudate are most likely equally affected, but the proximity of the caudate head to the ventricle space introduces partial volume effects that reduce the mean PiB SUVR.

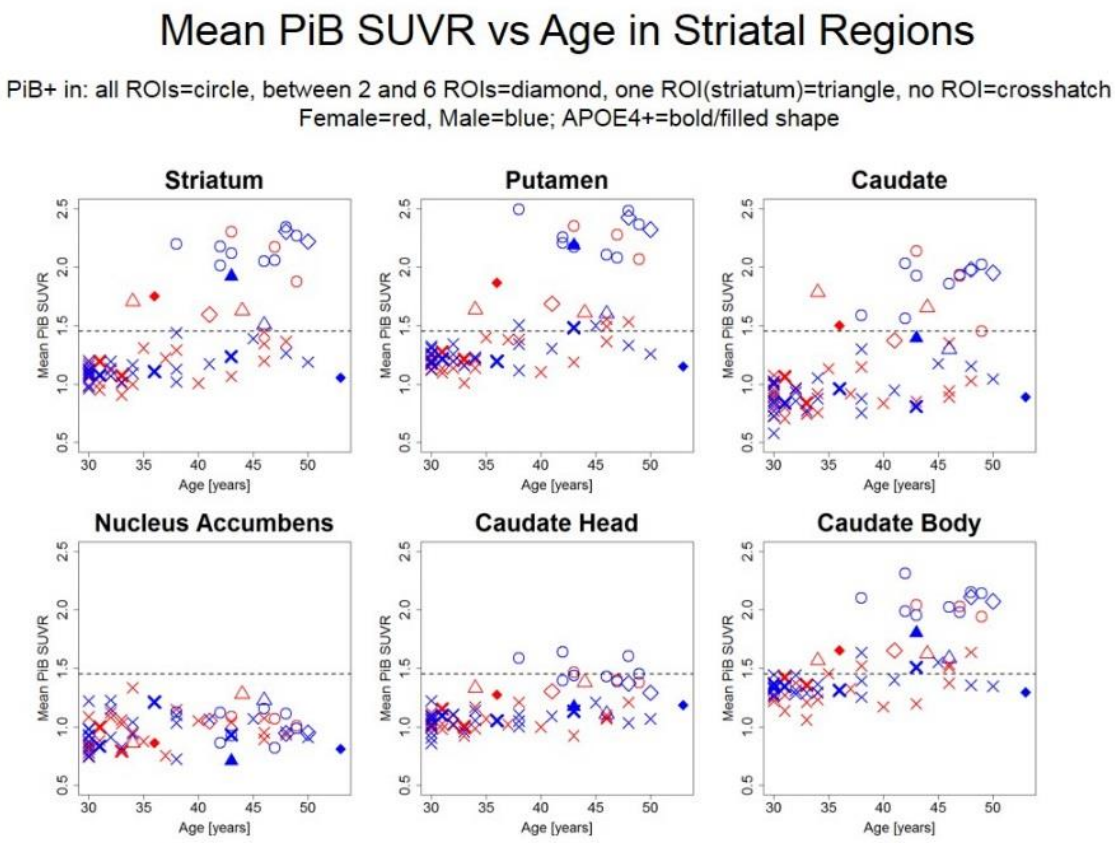

Figure 3. Mean PiB standard uptake value ratio (SUVR) plot against age for the striatum as a whole; the putamen, caudate, and nucleus accumbens; and the caudate head and body. Also represented are PiB positivity threshold, PiB positivity pattern, sex, and APOE4 allele status. Mean PiB SUVR is negligible in the nucleus accumbens, but elevated in the caudate and putamen. Further inspection of the caudate reveals mostly negligible binding in the head, but elevated binding in the body.

APOE epsilon 2 genotype associates with reduced amyloid load but does not affect brain structure or function in non-demented older individuals

Michel Grothe[1], Sylvia Villeneuve[2, 3], Martin Dyrba[1], David Bartrés-Faz[4], Miranka Wirth[5]

[1]*German Center for Neurodegenerative Diseases (DZNE), Rostock, Germany*
[2]*Douglas Mental Health University Institute, Research Centre, Verdun, QC, Canada*
[3]*Department of Psychiatry, McGill University, Montreal, QC, Canada*
[4]*Department of Psychiatry and Clinical Psychobiology, Faculty of Medicine, University of Barcelona, Spain*
[5]*NeuroCure Clinical Research Center, and Department of Neurology, Charité – Universitätsmedizin Berlin, Germany*

Background: The epsilon-2 allele of the APOE gene (APOE2) has been shown to reduce the risk for late-onset (sporadic) Alzheimer's disease (AD) dementia. Little is known about APOE2-related brain changes that may underlie this protective effect.

Methods: We used multimodal neuroimaging data to examine potential protective brain effects of the APOE2 genotype compared to the risk-neutral homozygous APOE3 genotype in a large sample of non-demented older individuals (cognitively normal subjects and those with mild cognitive impairment). Imaging data was obtained from a total of 572 individuals from the ADNI cohort and included assessments of regional amyloid load using AV45-PET, glucose metabolism using FDG-PET, and gray matter volume using structural MRI. Group differences in imaging markers were assessed using region-of-interest (ROI) and voxel-based analyses, controlled for age, sex, education, and clinical diagnosis. Additional linear regression models examined genotype-specific effects of age on the distinct imaging markers. In secondary analyses, cerebrospinal fluid (CSF) markers of amyloid and tau pathology were examined to assess the reproducibility of the main imaging findings using fluid biomarkers.

Results: ROI-based analysis showed that APOE2 carriers had significantly less precuneal amyloid pathology ($p = 0.009$) and did not show the typical age-related increase in amyloid load ($\beta = 0.10$, $p = 0.49$). By contrast, temporoparietal metabolism and hippocampal volume did not differ between APOE2 and APOE3 genotypes, and both groups showed comparable negative effects of age on these markers (Figure 1). The specificity of APOE2-related brain changes for amyloid pathology was corroborated in spatially unbiased voxel-wise analyses (Figure 2), as well as by a significant APOE2 effect on CSF markers of amyloid ($p = 0.02$), but not tau, pathology.

Conclusions: APOE2-related changes in the aged brain are relatively specific for cortical amyloid pathology as opposed to a more general neuroprotective effect on brain structure and function.

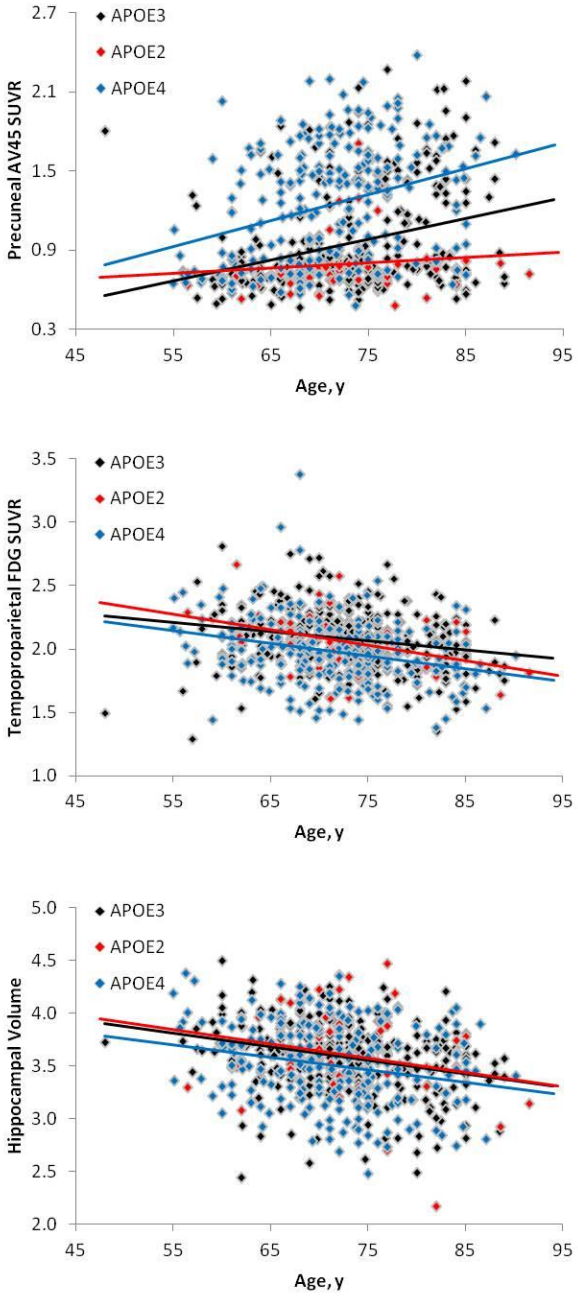

Figure 1. Effects of age and APOE genotype on multimodal imaging markers. Precuneal AV45-SUVR (top), temporoparietal FDG-SUVR (middle), and hippocampal volume (bottom) are plotted against age for APOE3 (black) and APOE2 (red) genotypic groups. APOE4 carriers (blue) are included for comparison. Separate linear regression lines are fitted for each group.

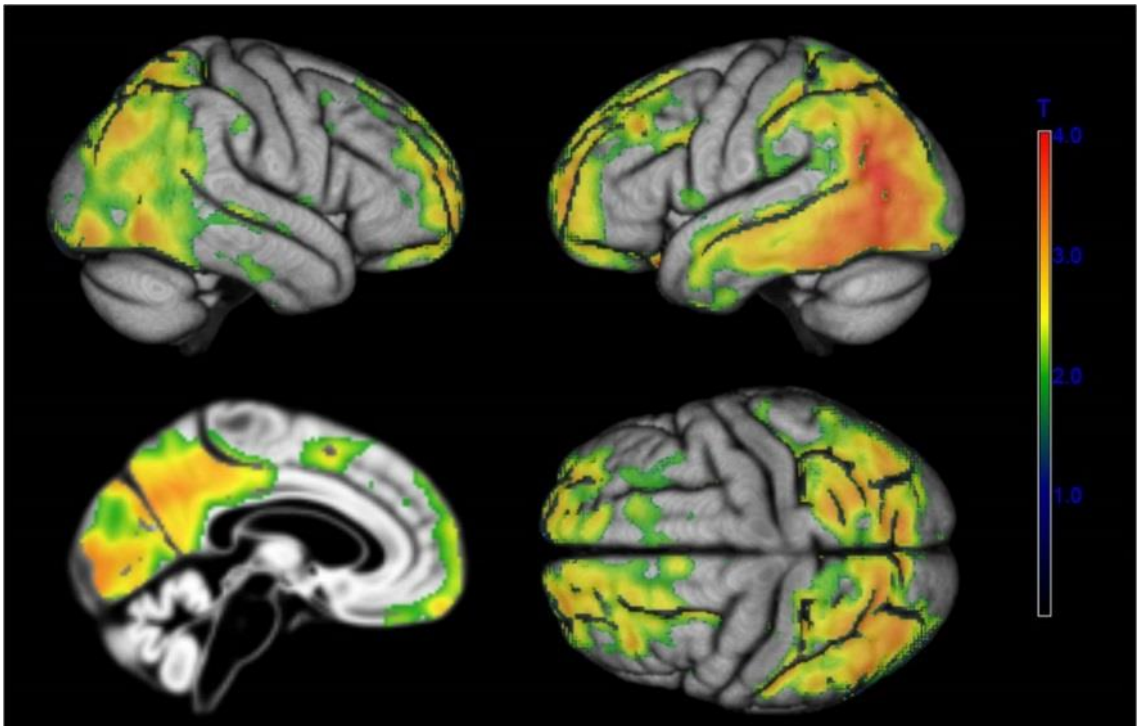

Figure 2. Voxel-wise analysis of reduced amyloid load in non-demented older APOE2 carriers
Significant effects of a voxel-wise two-sample t-test assessing reduced AV45-SUVR in APOE2 carriers compared to the APOE3 control group, controlled for age, gender, education, and clinical diagnosis. Statistical map was thresholded at p(FDR) < 0.05. Analogous analyses for FDG-SUVR or gray matter volume did not reveal any significant effects

Association between [^{11}C]PIB PET and CSF A$\beta_{1\text{-}42}$ in a multicentre European memory clinic population

Antoine Leuzy[1], Konstantinos Chiotis[1], Josef Pannee[2], Steen Hasselbalch[3], Juha Rinne[4], Alexander de Mendonça[5], Miguel Castelo-Branco[6], Isabel Santana[7], Alberto Lléo Bisa[8], Jarrko Johansson[4], Sarah Anderl-Straub[9], Markus Otto[9], Erik Portelius[2], Henrik Zetterberg[2], Kaj Blennow[2], Agneta Nordberg[1, 10]

[1]*Department of NVS, Centre for Alzheimer Research, Division of Translational Alzheimer Neurobiology, Karolinska Institutet, Stockholm, Sweden*
[2]*Department of Psychiatry and Neurochemistry, The Sahlgrenska Academy at University of Gothenburg, Sahlgrenska University Hospital, Mölndal, Sweden*
[3]*Danish Dementia Research Centre, Copenhagen University Hospital, Rigshospitalet, Copenhagen, Denmark*
[4]*Turku PET Centre and Department of Neurology, University of Turku and Turku University Hospital, Finland*
[5]*Department of Neurology and Laboratory of Neurosciences, Faculty of Medicine, University of Lisbon, Portugal*
[6]*Institute for Nuclear Sciences Applied to Health (ICNAS), Institute for Biomedical Imaging and Life Sciences (IBILI), and Brain Imaging Network of Portugal, Faculty of Medicine, University of Coimbra, Portugal*
[7]*Department of Neurology, Coimbra University Hospital, Coimbra, Portugal*
[8]*Department of Neurology, Institut d'Investigacions Biomèdiques, Hospital de Sant Pau, Barcelona, Spain*
[9]*Department of Neurology, Ulm University Hospital, Ulm, Germany*
[10]*Department of Geriatric Medicine, Karolinska University Hospital Huddinge, Stockholm, Sweden*

Introduction: Though an inverse relationship has generally been found between CSF Aβ1-42 and amyloid PET, a subset of cases show discordant results. Few studies addressing agreement between CSF Aβ1-42 and amyloid PET, however, have been conducted in subjects representative of memory clinic populations.

Aims: To assess agreement between CSF Aβ1-42 and [11C]PIB PET in a mixed memory clinic sample drawn from seven European research centres. Given the established between centre variability in ELISA derived CSF Aβ1-42 values, we likewise aimed to determine whether concordance would be improved by centralized CSF reanalysis. Moreover, we examined the hypothesis that discordance between amyloid biomarkers may be due to interindividual differences in total Aβ production, by adjusting Aβ1-42 levels for those of Aβ1-40.

Methods: Our study population consisted of 395 subjects from seven centres, including HC, MCI, AD, FTLD, and VaD—for whom CSF Aβ1-42 and [11C]PIB PET data were available. A total of 243 CSF samples across all subject groups were reanalyzed using Meso Scale Discovery (MSD) ELISA (Aβ1-40, Aβ1-42) and a novel, antibody-independent, mass spectrometry (MS) based assay (Aβ1-40, Aβ1-42). [11C]PIB images were assessed visually and quantitatively. Given different scanning windows, [11C]PIB SUVR results were scaled using the Centiloid method (CL).

Results: Relative to Innotest ELISA using local cutoffs, results using MSD and MS (Aβ1-42 and Aβ1-42/Aβ1-40) reduced discordance in MCI and AD. Discordance, however, varied among HC, FTLD, and VaD. Discordance in non-AD groups was higher relative to MCI and AD subjects. Agreement between visual ratings and CL scores was high (>90%), with concordance improved when using CL.

Conclusion: Despite improved results using reanalyzed CSF, a minority of subjects showed discordance. Our results reinforce the parallel use of amyloid PET and CSF Aβ1-42 in clinical contexts and indicate that the CL method can be successfully implemented in multicentric studies.

Friday, January 15, 2016 - 4:25 - 5:10pm

Podium Presentations

SESSION 10: Multiple Molecular Imaging Biomarkers

Chairs: *Gaël Chételat, INSERM, Université de Caen*
Susan Landau, University of California, Berkeley

4:25-5:10	**SESSION 10:** **MULTIPLE MOLECULAR IMAGING BIOMARKERS**	**CHAIRS:** **Gaël Chételat** INSERM, Université de Caen **Susan Landau** University of California, Berkeley
4:25-4:40	Rates of transition between amyloid and neurodegeneration biomarker states and to dementia among non-demented individuals in a longitudinal population-based cohort study	**Clifford Jack, Jr.** Mayo Clinic, Rochester
4:40-4:55	Do midlife vascular risk factors contribute to brain amyloid? The ARIC-PET amyloid imaging study	**Rebecca Gottesman** Johns Hopkins University
4:55-5:10	The clinical significance of increasing amyloid in cognitively normal, amyloid negative individuals	**Susan Landau** University of California, Berkeley
5:10-5:40	Discussion	

Rates of transition between amyloid and neurodegeneration biomarker states and to dementia among non-demented individuals in: A longitudinal population-based cohort study

Clifford Jack, Jr., Terry Therneau, Heather Wiste, Stephen Weigand, David Knopman, Val Lowe, Michelle Mielke, Prashanthi Vemuri, Rosebud Roberts, Mary Machulda, Matthew Senjem, Jeffrey Gunter, Walter Rocca, Ronald Petersen

Mayo Clinic, Rochester, MN, United States

Background: We previously observed in a cross-sectional analysis (Lancet Neurology 2014) that frequencies of amyloid and neurodegeneration biomarker states varied greatly by age among clinically normal participants, suggesting dynamic within-person processes. Our objective in this longitudinal study was to estimate rates of transitioning from a less- to a more-abnormal biomarker state by age among non-demented individuals, as well as rates of transitioning to dementia by biomarker state.

Methods: All participants (n=4049) were non-demented at baseline (age range 50 to 90 years). A subset of 1541 underwent multi-modality imaging. Amyloid PET was used to classify individuals as amyloid positive (A+) or negative (A−). FDG PET and MRI were used to classify individuals as neurodegeneration positive (N+) or negative (N−). All observations from the 4049 individuals were used in a multi-state model to estimate four different age-specific biomarker state transition rates among non-demented individuals: A−N− to A+N−; A−N− to A−N+ (SNAP); A+N− to A+N+; A−N+ (SNAP) to A+N+. We also estimated two age-specific rates to dementia: A+N+ to dementia; and A−N+ (SNAP) to dementia.

Results: All transition rates were low at age 50 and (with one exception) were well-characterized by an exponential increase with age. The one exception to an exponential rate increase with age was the transition rate from A−N− to A+N− which increased from 4.0 transitions per 100 person-years at age 65 to 7 transitions per 100 person-years in the 70s and then plateaued beyond that age.

Discussion: Our transition rates suggest that brain aging can be conceptualized as a nearly inevitable *acceleration* toward worse biomarker and clinical states. The one exception was that transition to amyloidosis without neurodegeneration was most dynamic from age 60 to 70 and then plateaued beyond that age. We found that simple transition rates can explain complex, highly interdependent biomarker state frequencies in our sample.

Do midlife vascular risk factors contribute to brain amyloid? The ARIC-PET amyloid imaging study

Rebecca Gottesman[1], Andrea Schneider[1], Josef Coresh[1], Edward Green[2], Naresh Gupta[5], David Knopman[4], Akiva Mintz[3], Arman Rahmim[1], A. Richey Sharrett[1], Lynne Wagenknecht[3], Dean Wong[1], Yun Zhou[1], Thomas Mosley[2]

[1]*Johns Hopkins University, MD, United States*
[2]*University of Mississippi Medical Center, MS, United States*
[3]*Wake Forest School of Medicine, NC, United States*
[4]*Mayo Clinic, MN, United States*
[5]*Hagerstown Imaging, MD, United States*

Objective: To determine if midlife vascular risk factors are associated with late-life brain amyloid deposition, measured using florbetapir PET in the Atherosclerosis Risk in Communities (ARIC)-PET Amyloid Imaging Study.

Methods: The ARIC study recruited participants from four US communities in 1987-1989, with detailed evaluation of vascular risk factors and markers. In 2011-2013, 347 ARIC participants without dementia from Washington County, MD, Forsyth County, MD, and Jackson, MS underwent florbetapir PET imaging. Standardized Uptake Value Ratios (SUVR) were calculated, using the cerebellum as the reference region. Associations between elevated mean global cortical florbetapir (defined at the sample median, SUVR>1.2) and vascular risk factors at ARIC baseline (ages 45-64) were explored in multivariable models including adjustment for age, sex, race, APOE genotype, and educational level.

Results: In 322 participants without dementia and with nonmissing midlife vascular risk factors (43% black, 58% female), neither body mass index (BMI), smoking status, hypertension, diabetes, or hyperlipidemia in midlife nor in late-life were associated with elevated SUVR. In stratified models, relationships between vascular risk factors and florbetapir did not differ by race. In the presence of 1 or 2 APOE ε4 alleles, however, each SD increase in midlife BMI was associated with elevated SUVR (OR 2.48, 95% CI 1.26-4.88, vs 1.11, 95% CI 0.85-1.44 in persons without an e4 allele; p-interaction=0.09), and virtually all risk factors were noted to have higher effect sizes, although nonsignificantly so, for florbetapir positivity in ε4 carriers (figure).

Discussion: In this biracial cohort representing three US communities, midlife and late-life vascular risk factors were generally not associated with late-life brain amyloid by PET. However, data suggested higher odds of elevated amyloid among persons with both elevated vascular risk and an APOE ε4 allele, supportive of a two-hit hypothesis of vascular disease and neurodegeneration contributing to AD development.

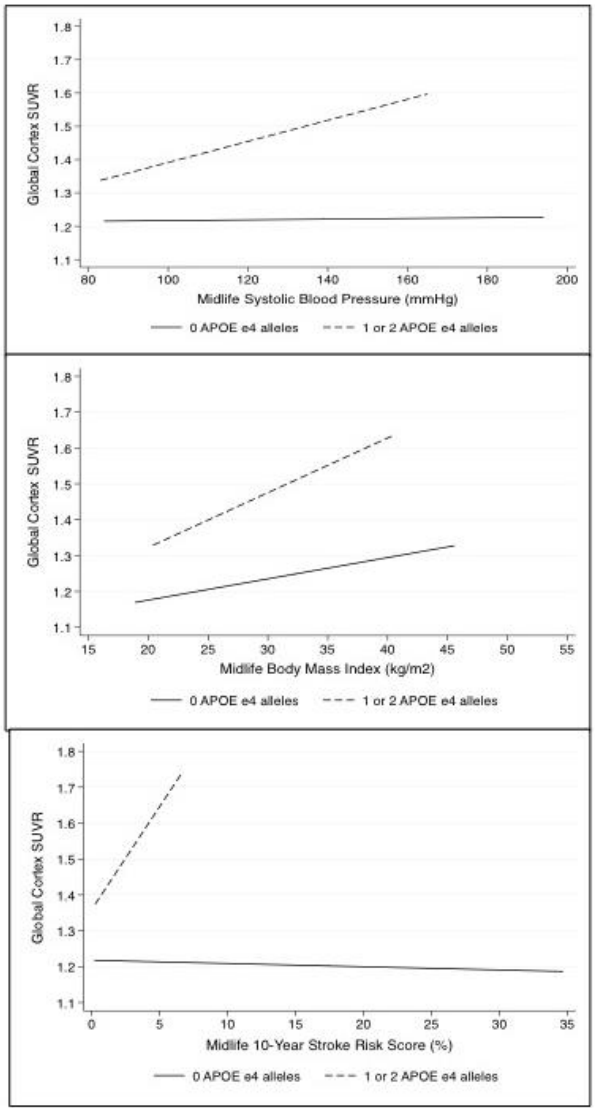

Figure: Systolic blood pressure (panel A), body mass index (panel B), and a composite stroke risk score (panel C), all from midlife, in associated with late-life global cortical SUVR level, among participants with 0 versus 1 or 2 APOE ε4 alleles.

The clinical significance of increasing amyloid in cognitively normal, amyloid negative individuals

Susan Landau, Andy Horng, William Jagust

University of California, Berkeley, CA, United States

Beta-amyloid (Aβ) positivity has been associated with neurodegeneration and cognitive decline, but little is known about the transition from Aβ negative to positive status or the point at which Aβ accumulation becomes clinically significant. To investigate these questions, we examined Aβ accumulation in Aβ-negative, cognitively normal ADNI subjects and its association with concurrent neurodegenerative and cognitive change.

In 136 Aβ-negative normals, cortical florbetapir SUVR change over a 2.0+/-0.3yr period (2 florbetapir-PET scans) was not associated with any longitudinal cognitive or biomarker measurements (episodic memory, CSF, FDG-PET and hippocampal volume). When we considered 35 Aβ-negative normals with longer followup (3 florbetapir-PET scans over 4.0+/-0.2yrs), increasing Aβ over the 4yr period was associated with decline on episodic memory, but not executive function (p=0.03; figure), decreasing CSF Aβ (p=0.03), increasing CSF p-tau (p=0.04), and marginally, hippocampal atrophy.

The Aβ-negative normals who increased on Aβ over the followup period (14/35; 40%) were more likely to be ApoE4+ (p<0.01), but otherwise they did not differ on any other baseline cognitive or biomarker measurements (CSF-Aβ, t-tau, p-tau; FDG-PET and hippocampal volume). Despite their declining memory performance, Aβ-negative but increasing normals had the same rate of conversion to MCI or AD (20%) as non-increasing negative normals (19%). However, 5 of the 14 (36%) Aβ-negative increasing normals became Aβ-positive by the end of the followup period (figure).

Increasing florbetapir over 4yrs in Aβ-negative normals (some of whom transition to Aβ-positivity) is related to memory decline and neurodegeneration during the same time period. Importantly, these relationships not apparent with 2yrs of followup data despite a considerably larger dataset, suggesting that the clinical consequences of amyloid accumulation in Aβ-negatives are detectable only over a relatively long time period and/or that additional timpoints reduce measurement noise in longitudinal data.

Figure. Florbetapir change over 4yrs in baseline Aβ- normals is associated with cognitive decline and hippocampal atrophy

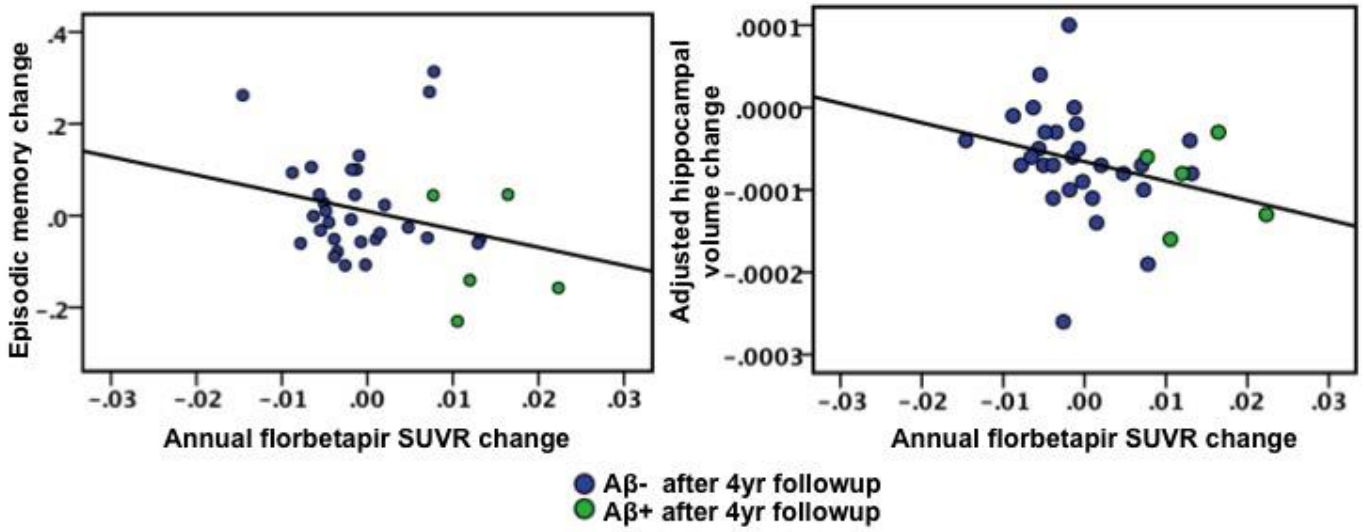

Funding for this conference was made possible in part by grant R13 AG042201 from the National Institute on Aging and the National Institute of Biomedical Imaging and Bioengineering.

The 10h Human Amyloid Imaging Conference is supported through educational grants from:

PLATINUM

Lilly

For further information
concerning Lilly grant funding
visit www.lillygrantoffice.com

GOLD

GE Healthcare

Biogen

Silver

janssen

Roche

Bronze

MERCK

BIOCLINICA™